Energy coupling of metabolite transport in Saccharomyces cerevisiae

de Valk, S.C.

DOI
10.4233/uuid:035865fb-2ba6-4088-9c3e-cb2e2e5fd2c1

Publication date
2022

Document Version
Final published version

Citation (APA)
de Valk, S. C. (2022). *Energy coupling of metabolite transport in Saccharomyces cerevisiae*. [Dissertation (TU Delft), Delft University of Technology]. https://doi.org/10.4233/uuid:035865fb-2ba6-4088-9c3e-cb2e2e5fd2c1

Important note
To cite this publication, please use the final published version (if applicable).
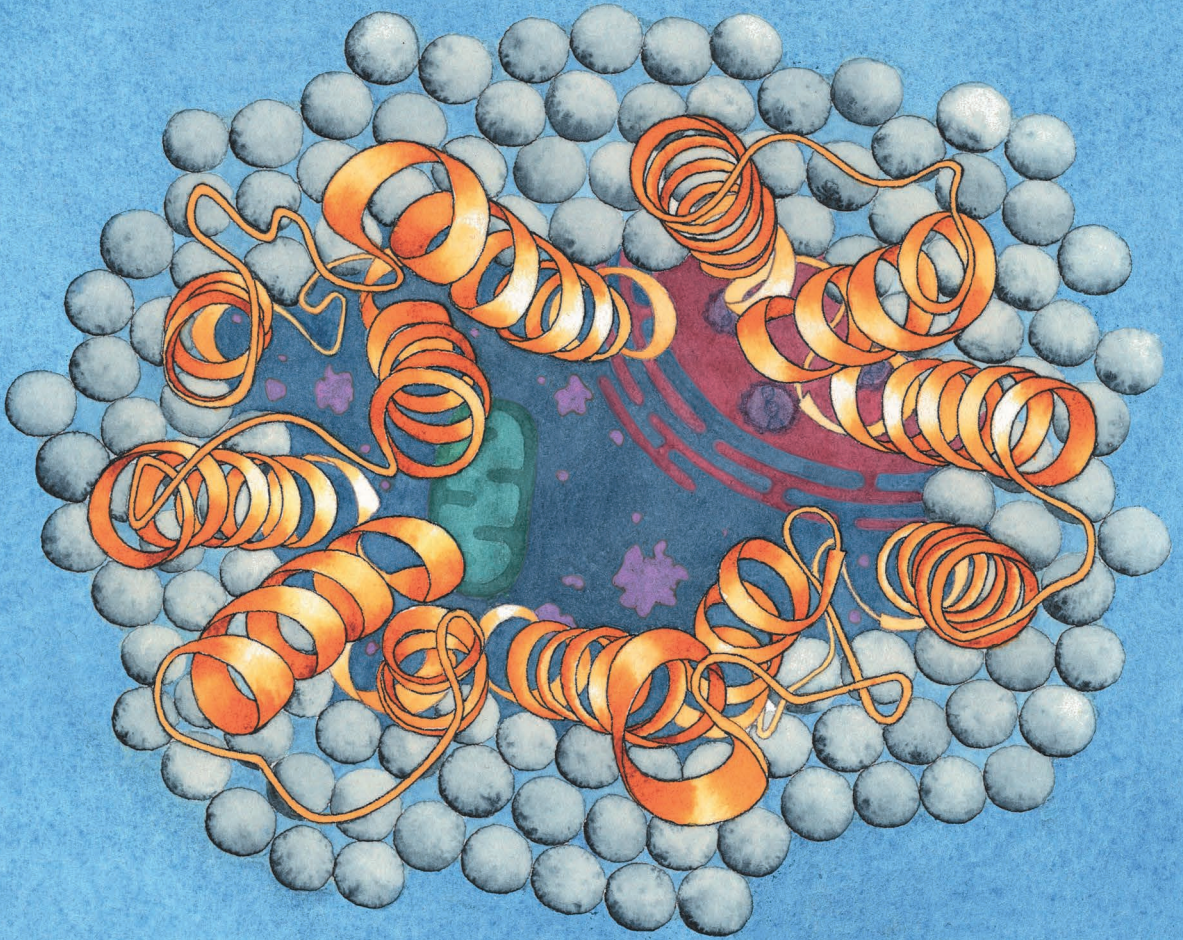Please check the document version above.

Energy coupling of metabolite transport

in *Saccharomyces cerevisiae*

Sophie C. de Valk

Energy coupling of metabolite transport in *Saccharomyces cerevisiae*

Dissertation

for the purpose of obtaining the degree of doctor
at Delft University of Technology
by the authority of the Rector Magnificus prof. dr. ir. T.H.J.J. van der Hagen,
Chair of the Board for Doctorates
to be defended publicly on
Friday 24 June 2022 at
12:30 o'clock

by

Sophie Claire DE VALK

Master of Science in Life Science & Technology
Delft University of Technology, The Netherlands
born in Vlaardingen, The Netherlands

This dissertation has been approved by the promotors.

Composition of the doctoral committee:

Rector Magnificus	Chairperson
prof. dr. J. T. Pronk	Delft University of Technology, promotor
dr. ir. R. Mans	Delft University of Technology, copromotor

Independent members:

prof. dr. ir. H. Noorman	Delft University of Technology
prof. dr. F. J. Bruggeman	Free University of Amsterdam
prof. dr. I. Borodina	Technical University of Denmark
dr. S. K. Billerbeck	University of Groningen

Reserve member:

prof. dr. F. Hollman	Delft University of Technology

Other member:

prof. dr. B. Poolman	University of Groningen

The research presented in this thesis was performed at the Industrial Microbiology Section, Department of Biotechnology, Faculty of Applied Sciences, Delft University of Technology, The Netherlands.

Table of contents

Summary

In living cells, transport proteins allow for the translocation of molecules across biological membranes that are otherwise impermeable to charged and polar solutes. These membrane-associated proteins play an essential role in the uptake of substrate molecules and export of metabolic products, as well as in the maintenance of electrochemical gradients across membranes, which are exploited energy stores by all living cells. Over the course of evolution, a variety of transport proteins have emerged, with diverse substrate specificities, kinetics and mechanisms. To study the transport function of proteins, the yeast *Saccharomyces cerevisiae* has been widely used as a model organism for the expression and functional characterization of heterologous genes encoding these transport proteins. Aside from numerous advantageous traits that facilitate its cultivation and genetic modification, another benefit of using this yeast as a model is that there is already a vast collection of knowledge available in the scientific literature on its native complement of transport proteins. Besides studying the diversity of transporters already present in nature, (targeted) changes to transport proteins can be introduced that can alter their biological function.

Engineering of transport proteins is interesting from a fundamental perspective, but can also be a highly relevant strategy for the improvement of microbial strains for application in industrial biotechnology. *S. cerevisiae* is also a popular microbial host in industry and has been engineered for the optimization of productivity and yields of both native and non-native products via metabolic engineering, mutagenesis and selection and adaptive laboratory evolution. Engineering strategies focused on transport proteins have, for instance, enabled the uptake of non-native substrates, increased substrate-uptake rates, decreased inhibition of uptake by other molecules and, by improving product export, increased product titers. Whereas many of these strategies are focused on engineering the specificity and kinetics of transporters, the mechanism of transport can also be a highly relevant target for engineering.

Transport mediated by proteins with a facilitated diffusion mechanism is merely driven by the concentration gradient of the transported solute, whereas in active transport, another form of metabolic energy, such as ATP or the proton motive force, contributes to the driving force of transport. In *S. cerevisiae*, metabolic energy is acquired via the dissimilation of sugars, which are used as carbon and energy source in most yeast-based industrial processes. The ATP that is formed in sugar dissimilation is used for energy-requiring processes, such as cellular maintenance and the formation of new biomass from sugar (growth). Whether or not transport processes require a net input of energy can have a substantial effect on the net ATP yield that

can be achieved in dissimilation and thus on how sugar is distributed over energy-yielding and energy-requiring processes. Depending on the nature of the desired product, the product yield on substrate can benefit from either increasing or decreasing this ATP yield, for instance by engineering the mechanisms of transport processes involved in susbtrate uptake and/or product export.

Yeast biomass and other products whose synthesis from substrate requires the input of ATP are often produced under aerobic conditions, so that ATP can be obtained via respiratory dissimilation of (part of) the substrate. If the ATP-efficiency of this dissimilatory route can be increased, less substrate has to be respired to supply the required ATP and thus more substrate is available for product formation. On the other hand, yields of products whose formation from substrate results in a net synthesis of ATP, such as ethanol in *S. cerevisiae*, may benefit from a decreased ATP-yield. If the ATP production rate via the product pathway is sufficient to meet maintenance energy-requirements, other dissimilatory pathways for ATP generation (such as respiration) are obsolete, and such products can often be made under anaerobic conditions. If the ATP yield of such a pathway is decreased, more substrate has to be allocated to product formation to supply the ATP required for biomass synthesis. Consequently, the product yield on sugar is increased, whereas the yield of biomass (which is often considered a by-product in industrial fermentations) on sugar is decreased.

The research described in this thesis focused on the development and application of strain engineering strategies that target metabolite transporters of *S. cerevisiae* and studies their impact on strain physiology in *S. cerevisiae*.

Uptake of the disaccharides sucrose and maltose by *S. cerevisiae* is mediated by proton-symporters such as Mal11, with a sugar/H$^+$ stoichiometry of 1. Previous work showed that three acidic amino-acid residues in Mal11 are responsible for coupling transport of these sugars to the translocation of a proton. Their substitution by neutral residues resulted in an uncoupled version of the protein that only facilitates sugar transport down the concentration gradient (facilitated diffusion). These uncoupled mutant transporter variants could be highly relevant to increase the efficiency of substrate dissimilation in sucrose-based industrial processes. In **Chapter 2** these mutated *MAL11* alleles were expressed as the sole disaccharide transporter gene in *S. cerevisiae,* which allowed for growth in media with sucrose as the sole carbon source. However, the specific growth rates of the resulting strains were very low. Therefore, three different strains engineered with the various Mal11 transporter variants were evolved in a total of six independent evolution experiments to increase the growth rate of these strains on sucrose. Analysis of the *MAL11* sequence in the evolved strains led to the identification of additional mutations in the *MAL11* open-reading frame, which upon reverse engineering were found to be responsible for the improved growth rate on sucrose. In four evolution lines, these additional mutations led to the emergence of an acidic residue in the central cavity of the protein, which was found to restore proton-coupling in the protein. Whereas two of these amino-acid changes were in the same position as the acidic residues in wild-type Mal11, the others occurred in new positions, indicating flexibility in the location of acidic residues that mediate the binding of protons. Whereas the final two Mal11 variants also contained additional mutations that originated from the evolution, these did not generate acidic residues and were therefore selected for further analysis. These transporter variants were then expressed in a strain harboring sucrose phosphorylase, in which uncoupled transport should theoretically increase the anaerobic biomass yield on sucrose by 25% relative to that of a strain relying on proton-coupled transport. However, when grown in anaerobic, sucrose-limited chemostats,

the biomass yield of a strain expressing one of the uncoupled transporter-encoding *MAL11* alleles was only 9% higher than that of a wild-type (proton-coupled) *MAL11*-expressing strain. This lower-than-expected biomass yield could be explained by other physiological changes in the strain with uncoupled Mal11, which resulted in allocation of sucrose to processes other than dissimilation and biomass synthesis. When changes in biomass composition, glycerol production rate and formation of extracellular glucose-1-phosphate were taken into account, the efficiency of sucrose dissimilation appeared 21% higher compared to the reference strain, which is close to the expected 25% increase. Finally, based on the analysis of the location of the mutations in a structural model of Mal11, a mechanistic model was proposed of proton-coupled sugar transport by wildtype Mal11 and uncoupled transport by the mutated variants.

The research on Mal11 in **Chapter 2** was aimed at increasing the energetic efficiency of substrate uptake. From an industrial perspective, this research could be especially relevant for molecules whose formation from sugar does not provide or require any ATP. One such pathway is the formation of lactic acid in engineered *S. cerevisiae* strains. An increase of the ATP yield of lactic acid fermentation would enable anaerobic production of lactic acid with *S. cerevisiae*. This could either be achieved by increasing the ATP conservation from the intracellular formation of lactate from sugar, or by decreasing the energy requirements of lactate export. Hitherto, the complete set of genes involved in the lactic acid export system in *S. cerevisiae* remained elusive, but on the other hand, two genes have been described to be involved in the uptake of lactic acid: *JEN1* and *ADY2*. In **Chapter 3**, the search for genes involved in lactic acid transport was continued by prolonged incubation of a *jen1Δ ady2Δ* strain in medium with lactic acid as the sole carbon source, which led to the emergence of mutations in *ATO2* and *ATO3*. Reverse engineering of these mutations confirmed that the mutated Ato2 and Ato3 transporter variants catalyzed the uptake of lactic acid and enabled growth in lactic-acid-based medium up to a specific rate of 0.15 h^{-1}. A comparison between (evolved) sequences and homology models of these proteins led to the hypothesis that the mutations resulted in a widening of the narrowest hydrophobic constriction in the anion channel of Ato2 and Ato3, thereby improving lactic acid transport. Although this study did not lead to the identification of the export mechanism of lactic acid in *S. cerevisiae*, its results increase the understanding of the structural requirements of transport proteins for enabling lactic acid transport, which could potentially narrow the search for lactic acid exporters within the yeast transportome.

Chapter 2 and **3** focused on strategies for increasing the energetic efficiency of substrate dissimilation and product export to reduce or eliminate the need for respiratory dissimilation. In contrast, the formation of ethanol from sugar in *S. cerevisiae* yields ATP and therefore, industrial production of ethanol is performed under anaerobic conditions. Ethanol is produced at large scale (99 billion liters in 2020) in yeast-based processes, and therefore even small improvements of performance indicators can have large economic impact. Ethanol formation provides the yeast with ATP that is used for biomass formation, and the resulting conversion of sugar into biomass competes for carbon with the production of ethanol. In addition, the formation of biomass from sugar results in net reduction of NAD$^+$ to NADH, which, in anaerobically grown *S. cerevisiae*, can only be re-oxidized via the formation of glycerol from sugar. Pathway engineering strategies that have been developed for the improvement of bioethanol yield on sugar by focusing on altering the ratio between ethanol, biomass and glycerol are reviewed in **Chapter 4**. Conditions of yeast fermentations can be altered in favor of the product yield, for instance by promoting cellular maintenance energy requirements. By increasing ATP expenditure, less ATP is available for biomass synthesis, so more substrate

is allocated to ethanol production. Such increased ATP expenditure can also be promoted via strain engineering, for instance by introduction of futile cycles or energy-requiring transport processes. Glycerol formation can be decreased by engineering redox-cofactor coupling in carbon and nitrogen metabolism, to either decrease the surplus of NADH that is formed during biomass synthesis or even utilize these electrons for the formation of additional ethanol. For industrial application of these strategies, it is important to consider whether the beneficial effects observed in controlled, laboratory-scale conditions may readily translate to dynamic industrial conditions. Additionally, other performance indicators such as productivity or strain robustness should not be compromised by the increased ethanol yield, whereas in many studies, decreased specific growth rates of engineered strains have been reported. Therefore, translation of these proof-of-concepts to industrial fermentations may require additional and process-specific strain optimization.

One of the strategies for increasing the ethanol yield on sugar in *S. cerevisiae* that was described in **Chapter 4** is based on the replacement of the facilitated diffusion mechanism for hexose uptake by hexose-proton symport. In **Chapter 5**, two glucose- and two fructose-proton symporter-encoding genes were introduced in an *S. cerevisiae* strain devoid of all native hexose transporters. The resulting strains were able to grow on their corresponding hexose sugar under aerobic conditions and, after applying evolutionary engineering, under anaerobic conditions. When tested in anaerobic, glucose- or fructose-limited chemostats, the biomass yield of these strains was 44-48% lower than that of an isogenic reference strain that expressed the hexose uniporter gene *HXT5*. Concurrently, the ethanol yield was increased by up to 17.2%. To apply this strategy to increase the ethanol yield on sucrose, a platform strain was then constructed in which a combination of all genes encoding hexose transporters, disaccharide transporters and disaccharide hydrolases were deleted. The resulting 'sugar-negative' strain, which contained a total number of 32 gene deletions, was unable to grow on any of the sugar substrates that are consumed by wild-type *S. cerevisiae*. Subsequently, a combination of a glucose-proton symporter gene (*HGT1* from *Kluyveromyces marxianus*), fructose-proton symporter gene (*FSY1* from *Saccharomyces eubayanus*) and *S. cerevisiae SUC2,* responsible for the extracellular hydrolysis of sucrose to glucose and fructose, were introduced. After evolution for anaerobic growth, the resulting strain exhibited a 16.6% higher anaerobic ethanol yield and a 46.6% lower biomass yield on sucrose in anaerobic sucrose-limited chemostats, which was close to the theoretically predicted values (+16.2% and -50%, respectively).

The sugar-negative platform strain constructed in **Chapter 5**, which is devoid of all sugar transporters and disaccharide hydrolases, could act as a valuable starting point for future studies on sugar transport. The absence of native sugar transporters allows for growth complementation-based functional characterization of predicated transporter genes, as well as assaying the uptake of radio-labelled sugars in the absence of 'background signal' that would otherwise be caused by the presence of endogenous transporters. In addition, this platform strain can be applied for evolutionary engineering of specific transport proteins, especially for those that transport multiple sugar substrates. In **Chapter 6**, this strain was used to test a new evolutionary engineering strategy for altering the substrate specificity of Mal11 from *S. cerevisiae*. This strategy was based on the principle that the proton-motive force driven accumulation of sucrose in the absence of a sucrose hydrolase could lead to toxic intracellular accumulation. *MAL11* was therefore introduced in the sugar-negative platform strain, after which the resulting strain was evolved in glucose-limited continuous cultures that were subjected to pulse-wise addition of sucrose at an increasing frequency. Over time,

mutants were enriched that were less sensitive to the presence of sucrose than their parental strain. Sequence analysis showed that in each of the two independent evolution lines three mutations emerged in the *MAL11* sequence that resulted in two overlapping and one unique amino acid substitution(s). Growth of parental, evolved and reverse-engineered strains was then investigated in medium with glucose and different concentrations of sucrose or maltose. The evolved strains performed better in the presence of disaccharides than the parental strain, whereas the growth rate on glucose in the absence of disaccharides was not negatively affected. Growth performance of the reverse engineered strains indicated that the mutations in *MAL11* were indeed responsible for the evolved phenotype, suggesting that the evolved Mal11 variants had a decreased affinity for disaccharides. The identified mutations can provide valuable hints towards the role of these specific amino acid residues in determining the specificity of the protein. Combined, these results demonstrate the potential to harness solute toxicity due to intracellular accumulation in a novel approach to engineer substrate specificity of transport proteins via evolutionary engineering.

Samenvatting

Transporteiwitten maken het mogelijk om moleculen te verplaatsen door biologische membranen, die anders impermeabel zijn voor geladen en polaire verbindingen. Deze membraangebonden eiwitten spelen een essentiële rol in de opname van substraatmoleculen, de export van metabole producten en in het onderhouden van de elektrochemische gradiënten over membranen, die voor levende cellen een vorm van energie vertegenwoordigen. In de loop van de evolutie is er een variëteit aan transporteiwitten ontstaan, met verschillende substraatspecificiteiten, kinetische eigenschappen en mechanismen. Om de transportfunctie van eiwitten in kaart te brengen wordt de gist *Saccharomyces cerevisiae* veel gebruikt als een modelorganisme voor de expressie van heterologe genen die coderen voor deze transporteiwitten. Los van vele voordelige eigenschappen die het makkelijk maken om deze gist te kweken en genetisch te modificeren, is er ook al een uitgebreide verzameling kennis over transporteiwitten in *S. cerevisiae* beschikbaar in de wetenschappelijke literatuur, wat voordelig is voor het gebruik van deze gist als modelorganisme. Het sleutelen aan transporteiwitten is niet alleen interessant vanuit een fundamenteel perspectief, maar kan ook worden ingezet om microbiële stammen te verbeteren voor toepassing in industriële biotechnologie. *S. cerevisiae* is een populair micro-organisme in de industrie en is aangepast voor het maximaliseren van productiviteit en opbrengst van producten door het toepassen van gerichte genetische modificatie, mutagenese en selectie en laboratoriumevolutie. Strategieën voor het verbeteren van stammen die zijn gericht op transporteiwitten hebben bijvoorbeeld de opname van substraten mogelijk gemaakt die niet van nature door *S. cerevisiae* gebruikt worden, maar ook verhoogde substraatopnamesnelheden, verminderde remming door andere moleculen en, door verbeterde productexport, verhoogde productconcentraties. Hoewel veel van deze strategieën zijn gefocust op specificiteit en kinetiek van transporters, is ook het transportmechanisme een relevant doelwit voor de verbetering van industriële stammen.

Zogenaamde 'gefaciliteerde diffusie' wordt enkel gedreven door de concentratiegradiënt van de getransporteerde verbinding, terwijl er bij actief transport een andere vorm van metabole energie, zoals ATP of de proton motive force, bijdraagt aan de drijvende kracht voor transport. In *S. cerevisiae* wordt metabole energie verkregen door de dissimilatie van suikers, welke vaak als koolstof- en energiebron worden gebruikt in industriële toepassingen van deze gist. De ATP die wordt gevormd tijdens de dissimilatie van suiker wordt gebruikt voor processen in de cel die energie nodig hebben, zoals cellulair onderhoud en het vormen van nieuwe biomassa uit suiker (groei). De energiekosten van een transportproces kunnen een sterk effect hebben op de netto ATP-opbrengst die behaald kan worden tijdens dissimilatie, en daarom ook op hoe

geconsumeerd suiker wordt verdeeld over verschillende processen die energie opleveren en energie kosten. Afhankelijk van het soort product kan een verhoging of juist een verlaging van die ATP-opbrengst voordelig zijn voor de opbrengst van het product. Een dergelijke verandering van de efficiëntie van suikerdissimilatie kan onder andere bewerkstelligd worden door het mechanisme van een van de betrokken transportprocessen aan te passen.

Gistbiomassa en andere producten waarvan de vorming uit substraat energie kost worden vaak geproduceerd onder aerobe omstandigheden, zodat ATP gevormd kan worden door een deel van het substraat te dissimileren via ademhaling. Als de ATP-efficiëntie van deze dissimilatieroute kan worden verhoogd, dan hoeft er minder substraat te worden verademd om de benodigde ATP te leveren, en is er dus meer substraat beschikbaar voor de vorming van het gewenste product. Het verlagen van de ATP-opbrengst kan daarentegen voordelig zijn voor de opbrengst van producten waarvan de synthese uit substraat ATP oplevert, zoals ethanol in *S. cerevisiae*. Zolang de ATP-productiesnelheid voldoende is om aan energiebehoeften voor cellulair onderhoud te kunnen voldoen, zijn andere dissimilatieroutes (zoals ademhaling) overbodig en kunnen dergelijke producten onder anaerobe omstandigheden worden gemaakt. Wanneer de ATP-opbrengst van een dergelijke productroute wordt verlaagd, moet er meer substraat worden omgezet in product om aan de ATP-behoefte voor cellulair onderhoud en groei te voldoen. De opbrengst van product op suiker neemt daardoor toe, terwijl de opbrengst van biomassa (wat vaak als bijproduct wordt beschouwd in industriële fermentaties) op suiker afneemt. Het onderzoek dat wordt beschreven in dit proefschrift was gefocust op de ontwikkeling en toepassing van strategieën voor de verbetering van stammen, gericht op het transport van metabolieten in *S. cerevisiae* en de impact ervan op de fysiologie van stammen.

In *S. cerevisiae* worden de disachariden sacharose en maltose opgenomen door proton symporters zoals Mal11, met een suiker/H^+-stoichiometrie van 1. In eerder onderzoek is aangetoond dat er drie zure aminozuurresiduen verantwoordelijk zijn voor de koppeling tussen proton- en suikertransport. Wanneer deze drie zure residuen worden vervangen door neutrale residuen wordt deze koppeling opgeheven en kan transport van suiker alleen nog plaatsvinden van hoge naar lage suikerconcentraties (gefaciliteerde diffusie). Deze gemuteerde, ontkoppelde varianten van de transporter kunnen relevant zijn om de efficiëntie van substraatdissimilatie te verhogen in industriële processen die gebaseerd zijn op sacharose als koolstof- en energiebron. In **Hoofdstuk 2** werd aangetoond dat de expressie van dergelijke gemuteerde *MAL11* allelen als enige disacharidetransportergen ervoor zorgt dat de resulterende stammen kunnen groeien in medium met sacharose als enige koolstofbron, maar de groeisnelheden van de resulterende stammen waren echter erg laag. Door het toepassen van laboratoriumevolutie kon de groeisnelheid van drie verschillende stammen, met diverse Mal11 varianten, worden verhoogd in (in totaal) zes onafhankelijke experimenten. In de geëvolueerde stammen werden extra mutaties gevonden in de sequentie van *MAL11*, waarvan werd aangetoond dat deze ten grondslag lagen aan de verhoogde groeisnelheid op sacharose van de geëvolueerde stammen. In vier van de zes evolutielijnen leidde de mutatie tot de herintroductie van een zuur aminozuurresidu in de centrale holte van het eiwit, waardoor het transport weer proton-gekoppeld werd. Terwijl de positie van twee van deze mutaties overeenkwamen met die van zure residuen in het wild-type eiwit, waren de andere mutaties in een andere locatie. Deze observatie wijst op de flexibiliteit van de locatie van zure residuen die zorgen voor de binding van protonen in een proton-gekoppelde transporter. De laatste twee Mal11 varianten bevatten ook extra mutaties die voortkwamen

uit de evolutie, maar deze resulteerden niet in de introductie van zure aminozuurresiduen. Deze varianten werden daarom tot expressie gebracht in een stam met een sacharose fosforylasegen. In deze stam zou onkoppeld sacharosetransport in theorie leiden tot een 25% toename van de biomassaopbrengst vergeleken met protongekoppeld transport. In anaerobe, sacharose-gelimiteerde chemostaatcultures was de biomassaopbrengst van een stam met een van de ontkoppelde Mal11 varianten echter slechts 9% hoger dan die van een stam met (proton-gekoppelde) wild-type Mal11. Dat deze biomassaopbrengst lager was dan verwacht, werd toegeschreven aan de andere fysiologische veranderingen in de stam met de ontkoppelde Mal11-transporter, die ervoor zorgden dat sacharose werd gebruikt voor andere processen dan dissimilatie en biomassasynthese. Wanneer er rekening werd gehouden met veranderingen in de compositie van biomassa, glycerolproductiesnelheid en de vorming van extracellular glucose-1-fosfaat, bleek dat de efficiëntie van sacharosedissimilatie 21% hoger was dan die van de referentiestam, en daarmee dichter bij de verwachte 25% lag. Verder werd, om meer te weten te komen over hoe verschillende aminozuurresiduen betrokken zijn bij het mechanisme van protongekoppeld suikertransport, de locatie van de gevonden mutaties in een structuurmodel van Mal11 bestudeerd.

Het onderzoek in **Hoofdstuk 2** was gericht op het verhogen van de energetische efficiëntie van substraatopname. Vanuit een industrieel perspectief kan dit onderzoek relevant zijn voor productie van moleculen waarvan de vorming uit substraat geen ATP kost of oplevert. Een dergelijk proces is de vorming van melkzuur door genetisch gemodificeerde *S. cerevisiae*-stammen. Een toename van de ATP-opbrengst van melkzuurfermentatie zou het mogelijk maken om melkzuur onder anaerobe omstandigheden te produceren met *S. cerevisiae*. Dit zou bereikt kunnen worden door de hoeveelheid ATP die geconserveerd wordt via de intracellulaire vorming van melkzuur uit suiker te verhogen, of door de energiebehoefte van melkzuurexport te verlagen. Tot nu toe zijn nog niet alle genen die betrokken zijn bij het exportsysteem voor melkzuur in *S. cerevisiae* geïdentificeerd, maar er zijn wel twee genen beschreven die betrokken zijn bij de opname van melkzuur: *JEN1* en *ADY2*. In **Hoofdstuk 3** werd de zoektocht naar genen die betrokken zijn bij melkzuurtransport voortgezet door de langdurige incubatie van een *jen1Δ ady2Δ*-stam in medium met melkzuur als enige koolstofbron, wat leidde tot het ontstaan van mutaties in *ATO2* en *ATO3*. Door het karakteriseren van ongeëvolueerde stammen waarin deze gemuteerde allelen tot overexpressie waren gebracht werd aangetoond dat de gemuteerde Ato2- en Ato3-varianten de opname van melkzuur katalyseerden. Deze stammen groeiden op medium met melkzuur als enige koolstofbron met een specifieke snelheid tot 0.15 h^{-1}. Uit een vergelijking van (geëvolueerde) sequenties en homologie-modellen van deze eiwitten volgde de hypothese dat de mutaties zorgden voor een verbreding van de nauwste hydrofobe doorgang in het anionkanaal van Ato2 en Ato3, waardoor melkzuurtransport werd verbeterd. Hoewel het mechanisme voor melkzuurexport in *S. cerevisiae* in dit onderzoek niet werd geïdentificeerd, dragen de resultaten wel bij aan het begrip van de structurele benodigdheden van melkzuurtransporters, waardoor de zoektocht naar melkzuurexporters in het transportoom van *S. cerevisiae* kan worden verfijnd.

Hoofdstuk 2 en **3** focussen zich op het verhogen van de energetische efficiëntie van substraatdissimilatie en productexport, om zo de behoefte voor ademhaling te reduceren of te elimineren. In tegenstelling tot de vorming van melkzuur levert de vorming van ethanol uit suiker in *S. cerevisiae* wel ATP op, daarom wordt industriële productie van ethanol onder anaerobe omstandigheden uitgevoerd. Doordat ethanol op grote schaal wordt geproduceerd (99 miljard liter in 2020) kunnen zelfs kleine procesverbeteringen grote economische

gevolgen hebben. De ATP die gevormd wordt tijdens alcoholische gisting wordt gebruikt om nieuwe biomassa te vormen uit suiker, waardoor er competitie is voor koolstof tussen biomassavorming en de productie van ethanol. Daarnaast leidt de vorming van biomassa uit suiker tot een netto reductie van NAD^+ naar NADH, wat onder zuurstofloze omstandigheden wordt geoxideerd via de vorming van glycerol uit suiker. In **Hoofdstuk 4** worden strategieën omschreven die zijn ontwikkeld om de opbrengst van ethanol op suiker te verbeteren door te focussen op het aanpassen van de verhouding tussen ethanol-, biomassa- en glycerolproductie. De omstandigheden tijdens industriële fermentaties kunnen aangepast worden om de productopbrengst te verhogen, bijvoorbeeld door de energiebehoefte voor cellulair onderhoud te stimuleren. Door het gebruik van ATP te verhogen is er minder ATP beschikbaar voor de synthese van biomassa en wordt er dus meer substraat in ethanol omgezet. Een dergelijke verhoging van het ATP-gebruik kan ook worden bereikt via genetische modificatie, bijvoorbeeld door combinaties van genen tot expressie te brengen die leiden tot futiele cycli of de introductie van een energiegedreven transportproces. Glycerolvorming kan worden verminderd door de koppeling van redox-cofactoren in koolstof- en stikstofmetabolisme aan te passen. Hierdoor kan het NADH-overschot dat ontstaat tijdens biomassasynthese worden verminderd, of zelfs worden gebruikt om extra ethanol te vormen. Voor de industriële toepassing van deze strategieën is het van belang om na te gaan of de voordelige effecten die in gecontroleerde omstandigheden in laboratoriumexperimenten worden geobserveerd ook van toepassing zijn in dynamische, industriële omstandigheden. Daarnaast mag deze verhoogde ethanolopbrengst niet ten koste gaan van andere relevante eigenschappen, zoals productiviteit en robuustheid van stammen. Veel onderzoeken demonstreren dat de genetisch gemodificeerde stammen een lagere groeisnelheid hebben dan de bijbehorende referentiestam. Vertaling van deze 'proof-of-concepts' naar industriële fermentaties kan daarom extra, proces-specifieke optimalisatie vereisen.

Een van de strategieën voor het verhogen van de opbrengst van ethanol op suiker in *S. cerevisiae* die wordt beschreven in **Hoofdstuk 4**, is gebaseerd op het vervangen van de gefaciliteerde diffusie van hexoses door hexose-proton symport. In **Hoofdstuk 5** werden twee glucose- en twee fructose-proton symportergenen geïntroduceerd in een *S. cerevisiae*-stam waarin alle oorspronkelijke hexosetransporters uitgeschakeld zijn. De resulterende stammen waren in staat in medium met hun bijbehorende suiker (glucose of fructose) te groeien onder aerobe omstandigheden en, na toepassing van laboratoriumevolutie, ook onder anaerobe omstandigheden. In anaerobe, glucose- of fructosegelimiteerde chemostaatcultures bleken deze stammen een 44-48% lagere biomassaopbrengst op suiker te hebben dan een isogene stam die het gen *HXT5*, coderend voor een hexose uniporter, tot expressie bracht. Daarnaast was de opbrengst van ethanol op suiker met 17.2% verhoogd. Om een soortgelijke strategie toe te kunnen passen om de opbrengst van ethanol op sacharose te verhogen, werd een stam geconstrueerd waarin alle genen die coderen voor hexose transporters, disacharide transporters en disacharide hydrolases waren uitgeschakeld. De resulterende 'suiker-negatieve' stam, welke in totaal 32 gendeleties bevatte, was niet in staat om te groeien op de suikersubstraten die door wild-type *S. cerevisiae* worden geconsumeerd. Vervolgens werd een combinatie van een glucose-proton symportergen (*HGT1* uit *Kluyveromyces marxianus*), een fructose-proton symportergen (*FSY1* uit *Saccharomyces eubayanus*) en *S. cerevisiae* *SUC2*, verantwoordelijk voor de extracellulaire hydrolyse van sacharose, geïntroduceerd. Na evolutie voor groei onder anaerobe omstandigheden bleek de resulterende stam een 16.6% hogere ethanolopbrengst en een 46.6% lagere biomassaopbrengst op sacharose te hebben in anaerobe sacharose-gelimiteerde chemostaatcultures. Deze resultaten benaderden de

verwachte waarden van respectievelijk +16.2% en -50%.

De suiker-negatieve platformstam die in **Hoofdstuk 5** werd geconstrueerd, waarin alle suikertransporters en disacharide hydrolases zijn uitgeschakeld, kan een waardevol startpunt zijn voor toekomstig onderzoek naar suikertransport. De afwezigheid van endogene suikertransporters zorgt ervoor dat de functie van genen die vermoedelijk coderen voor suikertransporters kan worden gekarakteriseerd aan de hand van groeicomplementatie. In dergelijke stammen kan ook de opname van radioactief gelabelde suikers worden gevolgd in de afwezigheid van een 'achtergrondsignaal' dat anders wordt veroorzaakt door endogene transporters. Daarnaast kan deze platformstam worden toegepast voor laboratoriumevolutie van specifieke suikertransporters, vooral voor degene met een breed substraatspectrum. In **Hoofdstuk 6** werd deze stam gebruikt om via evolutie de substraatspecificiteit van Mal11 in *S. cerevisiae* aan te passen. De hiervoor gebruikte nieuwe strategie was gebaseerd op het principe dat proton-motive forcegedreven accumulatie van sacharose in de afwezigheid van disacharide hydrolase zou kunnen leiden tot toxische intracellulaire accumulatie. *MAL11* werd daarom geïntroduceerd in de suiker-negatieve stam, waarna de resulterende stam werd geëvolueerd in glucose-gelimiteerde continuculturen waaraan met toenemende frequentie pulsen van een geconcentreerde sacharoseoplossing werden toegevoegd. Tijdens deze evolutie-experimenten werden mutanten verrijkt die minder gevoelig waren voor de aanwezigheid van sacharose dan hun moederstam. Uit analyse van de sequentie van *MAL11* bleek dat geëvolueerde stammen uit twee onafhankelijke evolutielijnen drie mutaties hadden verkregen in dit transportergen, welke resulteerden in twee overlappende en een unieke aminozuursubstitutie(s) in het Mal11 eiwit. De gemuteerde *MAL11* allelen werden geïntroduceerd in de ongeëvolueerde suiker-negatieve stam, om vervolgens groei van de resulterende stam in medium met glucose en toevoeging van verschillende concentraties sacharose of maltose te bestuderen. Hieruit bleek dat de geëvolueerde stammen hogere groeisnelheden bereikten in de aanwezigheid van disacchariden, en dat de mutaties in *MAL11* inderdaad verantwoordelijk waren voor dit geëvolueerde fenotype. Deze mutaties kunnen waardevolle aanwijzingen geven voor de functie van deze specifieke aminozuurresiduen voor het bepalen van de specificiteit van dit eiwit. Gecombineerd demonstreren deze resultaten de mogelijkheid om de toxiciteit van een verbinding als gevolg van intracellulaire accumulatie te gebruiken in een nieuwe methode voor het aanpassen van de substraatspecificiteit van transporteiwitten via laboratoriumevolutie.
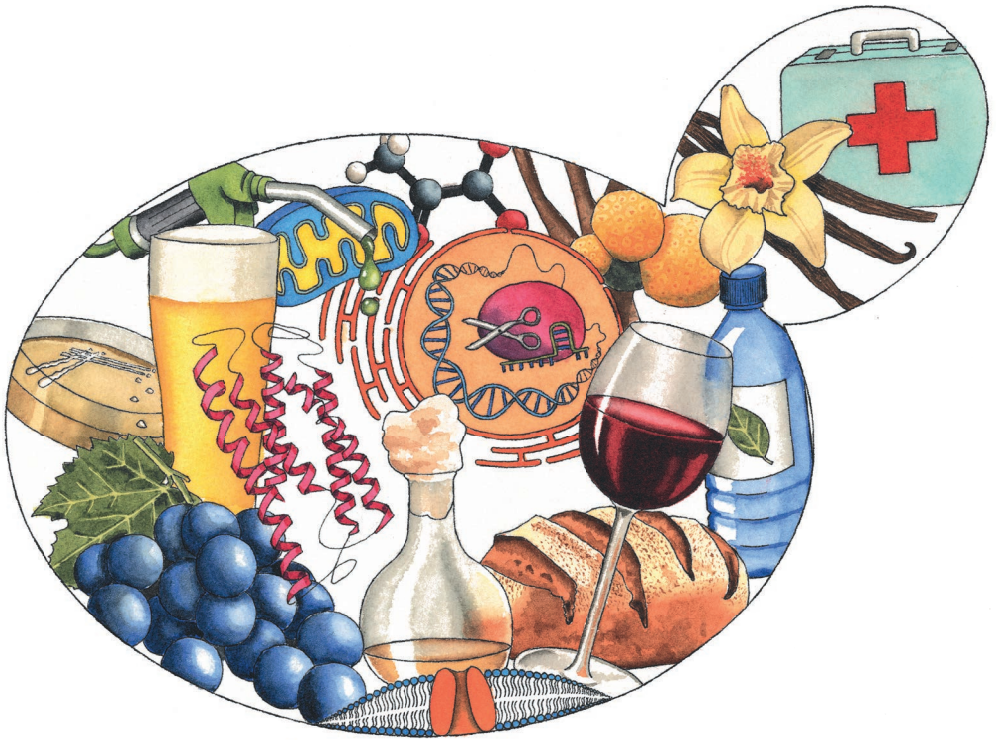
Chapter 1

General Introduction

1.1 Biological membranes

Biological membranes are essential structural elements of living cells in all domains of life (Monnard and Deamer, 2010). A biological membrane forms the border between the cell and its environment and encapsulates intracellular macromolecules such as DNA, RNA and proteins. This border provides protection from changes in the extracellular environment, thus allowing cells to maintain stable intracellular concentrations (homeostasis) even when extracellular conditions are highly dynamic. In addition, especially in eukaryotic cells, biological membranes also define the borders of intracellular compartments (organelles) such as mitochondria, chloroplasts and vacuoles.

Although different species show diversity in the chemical composition of their biological membranes, most membranes are structurally similar and have lipids with a polar head group and an apolar tail, as important constituents (Yeagle, 2016). In aqueous environments, the apolar lipid tails assemble to form a hydrophobic layer that is shielded from the water phase by the polar heads (Figure 1.1). The resulting lipid bilayer is poorly or not permeable to charged and/or polar molecules. However, what would a living cell be if it could not interact with its environment? In fact, living cells continuously exchange compounds with their environment by taking up nutrients and excreting products. It is speculated that in the earliest forms of life, temporal disruptions in membrane structure allowed for passage of compounds that would otherwise not be able to cross (Deamer and Bramhall, 1986; Nagle and Scott, 1978). Such 'leakage' of molecules would have allowed for some interaction with the environment, but the kinetics of this type of transfer would have made life very slow (Monnard and Deamer, 2010; Pohorille et al., 2005). Transport-limited growth rates would have caused a strong selective pressure for evolution of specialized transport systems that allow for fast and specific uptake and export of molecules across biological membranes.
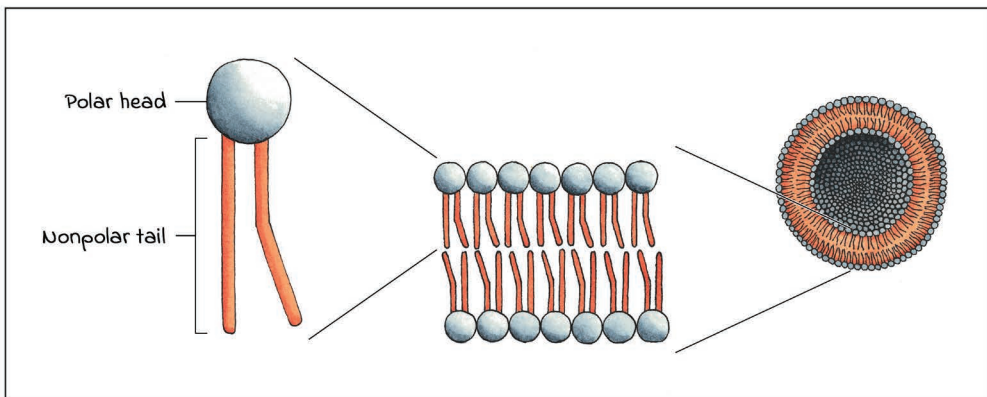
Figure 1.1: Schematic representation of the typical lipid-bilayer structure of biological membranes. Membranes are largely composed of lipids, which contain a polar head and an apolar tail (left). In aqueous solutions, these lipids assemble in lipid bilayers so that the apolar tails are shielded from the water phase by the polar heads (middle). If lipid bilayers form elliptical shapes (such as in living cells), all apolar tails are shielded from the water phase (right, showing a cross-section of a membrane vesicle).

1.2 Role of cellular membranes in energy metabolism

The impermeability of cellular membranes to polar compounds is essential to define the boundaries of living cells and organelles. In addition, it plays a central role in conserving and utilizing free energy. Via a process known as chemiosmotic coupling, prokaryotes use their cytoplasmic membrane to store energy, while eukaryotes utilize the specialized membranes of dedicated organelles (mitochondria, hydrogenosomes and chloroplasts) for this purpose.

In aerobic, respiring organotrophic organisms, high-energy electrons derived from the oxidation of organic compounds are transferred along a series of electron carriers embedded in the plasma membrane (prokaryotes) or inner mitochondrial membrane (eukaryotes), to finally reduce oxygen to water (respiration, Figure 1.2). In plants, high-energy electrons are obtained from water by chlorophyll and sunlight and transferred along a series of electron carriers embedded in the thylakoid membrane of chloroplasts (photosynthesis). The energy that is released during the step-wise transfer of electrons from a high-energy state (low electrical potential) to a low-energy state (high electrical potential) is used to drive the translocation of protons across the corresponding (organelle) membrane. The resulting electrochemical gradient, the so-called proton-motive force (pmf), represents a key 'currency' of cellular energy and is maintained at near-constant values under dynamic conditions (Mitchell, 1966). When protons flow back along their electrochemical gradient, free energy is released, which can be used to drive the synthesis of adenosine triphosphate (ATP) from adenosine diphosphate (ADP) and inorganic phosphate (P_i) via the action of F-type ATP synthases (Figure 1.2). These protein complexes are embedded in the cytoplasmic membrane of bacteria, the inner mitochondrial membrane of eukaryotes and the thylakoid membrane of chloroplasts in plants. Under physiological conditions, the free energy that is released by hydrolysis of ATP to ADP and P_i (approximately -45 kJ mol^{-1}) can subsequently be used to drive cellular reactions that would otherwise be thermodynamically unfavorable (Canelas *et al.*, 2011; de Kok *et al.*, 2012a). Depending on the magnitude of the pmf, the ratio of intracellular ATP, ADP and P_i concentrations and H$^+$/ATP stoichiometry, ATP synthases (or ATPases) can also operate in the opposite direction, thereby 'pumping' protons against chemiosmotic potential difference while hydrolyzing ATP. In eukaryotes, P-type ATPases that are embedded in the plasma membrane often operate in this 'ATP-hydrolyzing' direction to maintain a relatively stable intracellular pH. This proton-pumping role of ATP-ases enables respiration-independent build-up and maintenance of a proton-motive force across cellular membranes that do not harbor a functional respiratory chain, such as the plasma membrane of eukaryotes and the cytoplasmic membrane of obligatory fermentative organisms. This pmf can then be employed to drive transport of other solutes across these membranes.

The proton-motive force consists of two components, which can individually or together contribute to the thermodynamic driving force of transport: a chemical potential difference (-zΔpH, in which z corresponds to ln10 R·T/F, which follows from the Nernst equation (Mitchell, 1961)), which arises due to the difference in proton concentrations on each side of the membrane, and an electrical potential difference ($\Delta\psi$), due to the difference in charge on each side of the membrane. Thus, the pmf (in mV) can be described as:

pmf = $\Delta\psi$ – zΔpH   (1.1)
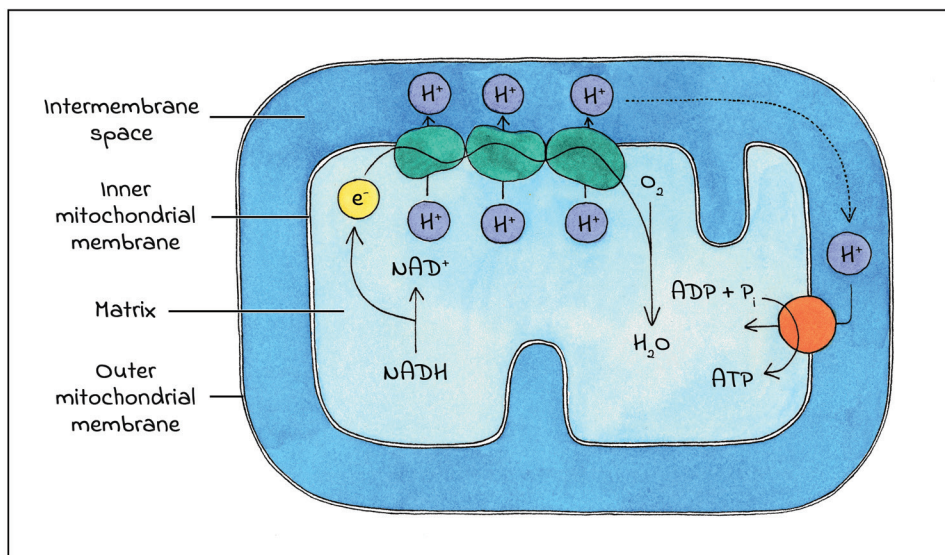
Figure 1.2: Schematic representation of chemiosmotic coupling in mitochondria. High-energy electrons are obtained by oxidation of electron donors such as NADH ($E^{0\prime}$=-0.32 V for NAD$^+$/NADH (Madigan *et al.*, 2011)). These electrons are then transferred along a series of electron carriers embedded in the inner mitochondrial membrane before reducing oxygen to water ($E^{0\prime}$=+0.82 V for ½O$_2$/H$_2$O (Madigan *et al.*, 2011)). The free energy released by this transfer of electrons is used to translocate protons from the mitochondrial matrix to the intermembrane space, resulting in a proton motive force. The free energy that is released when protons subsequently flow back into the mitochondrial matrix along their electrochemical potential difference via an ATP-synthase complex is used to drive the synthesis of ATP from ADP and P$_i$.

Depending on the solute and the mechanism of transport, one, both or none of the components of the pmf can contribute to the driving force of solute transport (see below). Under some conditions, such as in extreme alkaline environments, electrochemical gradients of other ions are an advantageous alternative to a pmf. Some alkaliphiles have adapted to low extracellular proton concentrations by utilizing an electrochemical gradient of sodium (sodium-motive force), which is established via primary Na$^+$ pumps and Na$^+$-dependent F-type ATPases (Mulkidjanian *et al.*, 2008).

1.3 Transport proteins

All currently living cells contain numerous proteins that mediate the transport of specific compounds across membranes. On average, about one third of the genes present in living cells encode membrane-associated proteins, and of those membrane proteins, about one third mediate solute transport (Paulsen *et al.*, 1998b; Wallin and von Heijne, 1998). Transport proteins often consist of multiple transmembrane domains that each contain 18-22 hydrophobic amino acid residues, which allow their embedment in the hydrophobic center of the lipid bilayer (Möller *et al.*, 2001). Multiple hydrophobic transmembrane domains can together form a channel through the membrane. The amino acid composition and relative positioning of the inward-facing amino acid residues of these domains allow for binding and passage of specific substrates (Pohorille *et al.*, 2005). Even very simple, small peptides have been shown to form bundles of transmembrane segments that function as trans-membrane channels (Duff and

Ashley, 1992; Lear *et al.*, 1988). This observation may reflect how the earliest forms of transport proteins arose (Pohorille *et al.*, 2005; Saier, 2016). Once the genetic information encoding such peptides was present in the DNA, intragenic duplications may have led to the expansion of the number of transmembrane domains within one protein, giving rise to ever more complex transport proteins (Lam *et al.*, 2011; Nikaido, 2003; Saier, 2001). In addition, gene duplication and subsequent local mutations could have led to the emergence of a diverse range of transport proteins with varying structures, substrate specificities and transport mechanisms (Voordeckers and Verstrepen, 2011).

Two main types of transport proteins can be distinguished: channels and carriers. Channels are pores that can be accessed from both sides of the membrane and transport solutes down their concentration gradient. They are generally responsible for transport of ions and small molecules and are often regulated (also called 'gated') by chemical and physical signals, such as electrostatic membrane potential or membrane tension (Gadsby, 2009). In contrast to channels, carriers (also called transporters or permeases) bind their substrate on one side of the membrane, then undergo a series of conformational changes, to subsequently release the substrate on the other side of the membrane (Forrest *et al.*, 2011; Shi, 2013).

1.4 Characterization of transport proteins

The typical structure of membrane proteins, in which hydrophobic transmembrane regions are alternated by hydrophilic regions, is easily distinguished from that of soluble proteins by comparing their amino acid sequences. Prediction of membrane localization of proteins from genome sequence data is therefore relatively straightforward (Ikeda *et al.*, 2002; Mishra *et al.*, 2014; Möller *et al.*, 2001). However, the functional characterization of predicted transporter proteins by analyzing their substrate specificity, kinetics and regulation can be considerably more challenging. Transport can, for instance, be studied by monitoring the intra- and extracellular concentration of radiolabeled solutes over time (Chen *et al.*, 2015; Jarvis, 2000; Weusthuis *et al.*, 1994). However, in many organisms, multiple transport proteins translocate the same substrate(s). This functional redundancy impedes characterization of a single transporter without interference of other transporters with the same or overlapping substrate specificity (Abbott *et al.*, 2009b; Haferkamp and Linka, 2012). Furthermore, subsequent metabolism of the labelled substrate can interfere with accurate determination of its uptake and accumulation inside the cell (Weusthuis *et al.*, 1994). To circumvent problems associated with *in vivo* transport studies, specific membrane proteins can be purified from host cells and integrated into lipid vesicles (liposomes) (Jarvis, 2000; van der Rest *et al.*, 1995). Subsequent analysis of transport using these vesicles has the advantage that metabolic reactions in these vesicles are (mostly) absent. When sufficient amounts of pure transport protein to perform such studies cannot be obtained (Haferkamp and Linka, 2012), the responsible structural gene can be expressed in model organisms to facilitate purification of the corresponding protein and improve its yield (Dreyer *et al.*, 1999; Haferkamp and Linka, 2012).

To study transport proteins in their native biological context without the aforementioned interference of (redundant) transport proteins, for example to investigate their impact on growth energetics, *in vitro* studies do not suffice. When all transporters with the same transport function in an organism, or in a closely related model organism, are known, their corresponding genes can be deleted prior to introduction of genes encoding the transporters of interest. This approach enables analysis of the studied transporter in a near-natural context with minimized

'background' transport (Dreyer *et al.*, 1999). Furthermore, if transport of the (predicted) substrate can be made essential for growth or survival of the model organism under certain cultivation conditions, the (rate of) growth of the expression host can be used as a direct read-out of *in vivo* transporter activity. Functional heterologous expression of transport proteins can be challenging, especially for evolutionary distant organisms (Abbott *et al.*, 2009b; Lazar *et al.*, 2017; Liang *et al.*, 2018; Young *et al.*, 2011). However, when this hurdle can be overcome, heterologous expression in 'transporter-negative' tester strains can be a powerful strategy for fast, parallel functional analysis of multiple orthologous genes that are known or predicted to encode transporters with overlapping substrate specificities.

1.5 *Saccharomyces cerevisiae* as model organism for studying metabolite transport

Saccharomyces cerevisiae (baker's yeast) is widely used as a model organism for characterization of eukaryotic transport proteins (Karathia *et al.*, 2011; Mustacchi *et al.*, 2006). This yeast has numerous advantageous traits for functional analysis studies (Mustacchi *et al.*, 2006), including ease of cultivation, excellent genetic accessibility, early availability of its full genomic sequence (*S. cerevisiae* was the first eukaryote to have its genome fully sequenced (Goffeau *et al.*, 1996)) and a strong preference for homologous recombination (HR) over non-homologous end-joining (NHEJ) as a DNA-repair mechanism. The latter property allows for the design of DNA fragments that can be faithfully assembled into large genetic constructs (Gibson *et al.*, 2008). This approach recently enabled one-step *in vivo* assembly of up to 44 transformed DNA fragments (Postma *et al.*, 2021). The discovery of CRISPR systems as tools for genetic modification further accelerated genetic modification of *S. cerevisiae*. Using this genome-editing technique, multiple double-strand DNA breaks can be simultaneously introduced at different, defined locations in the genome. Subsequent repair of these double-strand breaks by HR, using carefully designed synthetic DNA fragments, enables high-fidelity introduction of gene deletions and site-directed mutations as well as genomic integration of clusters of gene expression cassettes (DiCarlo *et al.*, 2013; Mans *et al.*, 2015). A specific advantage of *S. cerevisiae* for functional analysis of transport proteins is that the genetics and functional characteristics of its native complement of transport proteins are extensively described in the scientific literature (Paulsen *et al.*, 1998a). This knowledge base is exemplified by studies on transport of sugars (Diderich *et al.*, 1999; Lagunas, 1993; Reifenberger *et al.*, 2004), amino acids (Bianchi *et al.*, 2019), glycerol (Klein *et al.*, 2017), carboxylic acids (Casal *et al.*, 2016; Mans *et al.*, 2017), small ions like potassium and sodium (Yenush, 2016), protons (Uchida *et al.*, 1988), water (Laizé *et al.*, 2000; Petterson *et al.*, 2006), ammonium (Marini *et al.*, 1997), phosphate (Persson *et al.*, 2003), sulfate (Samyn and Persson, 2016) and metal ions (Eide, 1998). Especially for functional analysis of eukaryotic sugar transporters, *S. cerevisiae* remains an invaluable experimental platform. Its popularity as a platform for sugar-transport studies is illustrated by the extensive use of the hexose transporter-deficient strain EBY.VW4000, in which all genes encoding hexose transporters have been deleted (Wieczorke *et al.*, 1999). Since its construction in 1999, the article describing this strain has been cited 613 times to date, with 56 citations in 2021 (Google Scholar).

1.6 *S. cerevisiae* as a platform organism in microbial biotechnology

S. cerevisiae is not only used as a eukaryotic model organism, but also as an indispensable workhorse in industrial biotechnology. Its innate capacity for fast alcoholic fermentation lies

at the basis of the long history of use of *S. cerevisiae* in bread making and the production of alcoholic beverages, which started long before the discovery of yeasts and other microorganisms (McGovern *et al.*, 2004; Pasteur, 1857; Pasteur, 1860; van Leeuwenhoek, 1680). Nowadays, *S. cerevisiae* is used for the large-scale industrial production of bioethanol as a renewable transport fuel (Renewable Fuels Association, 2021). In addition to formation of this natural fermentation product, (over)production of a variety of native and non-native products, including lactic acid, succinic acid, isobutanol, resveratrol, farnesene, β-carotene, artemisinic acid, naringenin and vanillin was enabled by application of genetic engineering techniques (Borodina and Nielsen, 2014; Dai *et al.*, 2015).

Microbial production can often provide a more stable and cheap supply of chemical compounds than would be possible using natural sources. Additionally, microbial products can be a more sustainable alternative to products that would otherwise be produced by the petrochemical industry, as the carbon sources used in industrial cultivation media generally consist of sugars originating from renewable plant biomass. The challenge for these biotechnological processes is that they have to be economically competitive with their (petro)chemical counterparts. Microbial fermentation processes are always conducted in aqueous solutions, which can make product recovery in downstream processing challenging (Hatti-Kaul, 2010). It is therefore desirable to achieve high product concentrations (titers), along with high production rates and high product yields on substrate in industrial fermentations.

In addition to optimization of process conditions, strain improvement programs can be used to improve performance indicators of yeast-based industrial processes, for example by metabolic engineering, which encompasses the use of recombinant-DNA technology to improve cellular properties by modifying specific biochemical reactions or introducing new ones (Lian *et al.*, 2018; Nielsen, 2001). When identification of targets for metabolic engineering is challenging, classical strain improvement techniques can be applied, which are based on random mutagenesis followed by selection of mutants with a desired phenotype (Nevoigt, 2008). Alternatively, mutants with a desired phenotype can be obtained via adaptive laboratory evolution ('evolutionary engineering') (Dragosits and Mattanovich, 2018; Mans *et al.*, 2018). In this approach, strains are grown for prolonged periods under conditions that are carefully designed to confer a selective benefit to spontaneous or induced mutants with a desired phenotype. Adaptive laboratory evolution thereby circumvents the need to screen large numbers of individual random mutants. For example, mutants with increased maximum specific growth rates on an industrially relevant substrate can often be easily enriched via serial transfer of shake flask cultures or sequential batch reactors. After evolution, comparison of the genomic sequence of evolved and parental strains allows for the identification of potential causal mutations that underlie the evolved phenotype. To distinguish between causal and non-causal mutations that occurred during laboratory evolution, the effect of reintroducing mutations into the genome of an unevolved strain background can be studied (reverse engineering) (Oud *et al.*, 2011).

1.7 Engineering of transport for strain improvement

Transport proteins are often important targets in strain improvement programs, since they affect the rate and specificity for uptake of substrate(s) and export of product(s). For instance, numerous studies showed how transporter engineering led to improved uptake of pentose sugars that occur in lignocellulosic hydrolysates of agricultural residues and are not naturally

consumed by *S. cerevisiae*. These studies contributed to improved productivities and yields of ethanol on such feedstocks (Nijland and Driessen, 2020). Strategies used include the introduction of heterologous transporters from organisms that naturally assimilate pentose sugars (Bracher *et al.*, 2018; Subtil and Boles, 2011; Young *et al.*, 2011), rational engineering of endogenous transporters (Gonçalves *et al.*, 2014; Nijland *et al.*, 2017), including the targeted modification of specific amino acid residues (protein engineering) (Nijland *et al.*, 2016), and evolutionary engineering (Apel *et al.*, 2016; Reznicek *et al.*, 2015; Sanchez *et al.*, 2010; Verhoeven *et al.*, 2018). The latter strategy is readily applicable for improving the uptake of sugars, as mutants with improved uptake kinetics often grow faster than their unevolved parental strains and can thus be easily selected.

Engineering of export proteins has been shown to improve production of, for instance, malic acid (Zelle *et al.*, 2008), succinic acid (Darbani *et al.*, 2019; Jansen *et al.*, 2017b), short branched-chain fatty acids (Yu *et al.*, 2016), fumaric acid (Xu *et al.*, 2012), fatty alcohol (Hu *et al.*, 2018) and β-carotene (Bu *et al.*, 2020). Moreover, engineering of product export can contribute to a reduced toxicity of products and, thereby, to higher product titers, as well as generate an increased driving force for product formation (Lian *et al.*, 2018; Soares-Silva *et al.*, 2020).

1.8 Energetics of solute transport across biological membranes

Transport proteins not only show a broad diversity of substrate specificities and kinetic properties, but they also exhibit different modes of energy coupling of substrate translocation. When transport via a carrier is solely driven by the concentration gradient of a single uncharged solute (diffusion via so-called uniporters or facilitators), transport of solutes can only occur down their concentration gradient, as is also the case with channels (Figure 1.3). Other carriers mediate 'active transport', which allows transport of solutes against their concentration gradients at the cost of a form of metabolic energy. Active transport can, for instance, play a crucial role in uptake of substrates when extracellular concentrations are low and in export of toxic compounds from the cytosol (Kschischo *et al.*, 2016). So-called primary active transporters, such as transporters belonging to the ATP-binding-cassette (ABC) family (Higgins, 1992), directly couple ATP hydrolysis to solute translocation. Alternatively, energy stored in the form of an electrochemical gradient, such as the proton-motive force, can be used to drive transport (secondary active transport). If transport of a solute is coupled to the translocation of protons along their electrochemical gradient, both the chemical and electrical potential difference of the pmf contribute to the driving force of transport, which may enable thermodynamically favorable transport of the solute against its concentration gradient. In such coupled transport systems, symport refers to a situation in which the two molecules are transported in the same direction, whereas coupled transport in opposite directions is defined as antiport (Figure 1.3). When a uniporter translocates a single, charged compound through a membrane across which an electrical potential difference exists, $\Delta\psi$ contributes to the driving force for solute translocation and the resulting transport process is characterized as secondary active transport (Figure 1.3).

1.9 Effects of energy coupling of transport reactions on growth and product formation

In microbial cultures, the mode of energy coupling of the transport of substrate and product
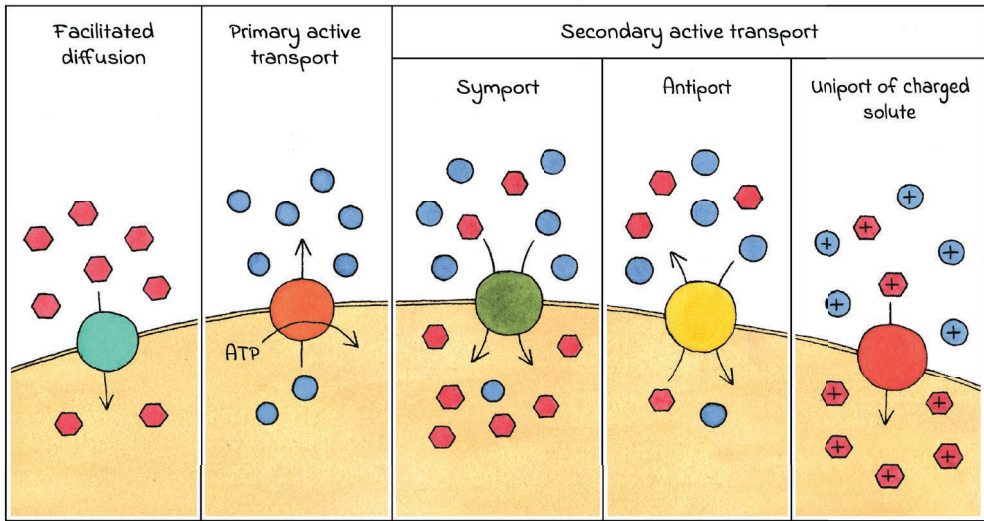
Figure 1.3: Mechanisms for metabolite transport via carriers. Facilitated diffusion: Transport is only driven by the concentration gradient of the solute. Primary active transport: Transport is directly driven by hydrolysis of ATP. Symport: The (electro)chemical gradient of one solute (blue circles) contributes to the driving force of transport of another solute (red hexagons), in the same direction. Antiport: The (electro)chemical gradient of one solute (blue circles) contributes to the driving force of transport of another solute (red hexagons), in the opposite direction. Uniport of charged solute: The electrical potential difference ($\Delta\psi$) of a charged solute that is not co-transported (blue circles) contributes to the driving force of transport of another charged solute (pink hexagons).

can affect the yield of product on substrate in different ways, depending on the nature of the substrate and the product. In microbial biotechnology, a distinction is made between two types of products: dissimilatory products and assimilatory products. Dissimilatory products are molecules whose formation from substrate results in the net production of ATP. Ethanol, produced in anaerobic cultures of *S. cerevisiae*, is an example of a dissimilatory product. In *S. cerevisiae*, intracellular glucose is dissimilated via the classical Embden-Meyerhof-Parnas glycolysis, yielding 2 moles of pyruvate, 2 moles of ATP and 2 moles of NADH per mol of glucose. Under anaerobic conditions, the NADH is re-oxidized via alcoholic fermentation, converting the pyruvate into 2 moles of CO_2 and ethanol, so the overall conversion of glucose to ethanol has a net yield of 2 moles of ATP per mol of glucose via substrate-level phosphorylation (Figure 1.4A). Alternatively, *S. cerevisiae* can achieve a substantially higher ATP yield by respiring glucose with oxygen as electron acceptor. In aerobic, fully respiratory cultures, pyruvate is oxidized to CO_2 (in this case the only dissimilatory product) via the pyruvate-dehydrogenase complex and TCA cycle, resulting in 2 moles of GTP (energetically equivalent to ATP), 8 moles of NADH and 2 moles of $FADH_2$ per mol of glucose. These reduced cofactors, as well as the 2 moles of NADH formed in glycolysis, are re-oxidized via the mitochondrial respiratory chain to generate ATP via the mitochondrial ATP synthase (Figure 1.4B). In *S. cerevisiae*, this oxidative phosphorylation process yields approximately 1 ATP per oxidized NADH or $FADH_2$. Complete oxidation of a glucose molecule to CO_2 by *S. cerevisiae* therefore results in the synthesis of approximately 16 ATP equivalents (including those derived from substrate-level phosphorylation) (Pronk *et al.*, 1994; Verduyn *et al.*, 1991).

ATP formed in dissimilatory reactions is used for the formation of new biomass (growth) and
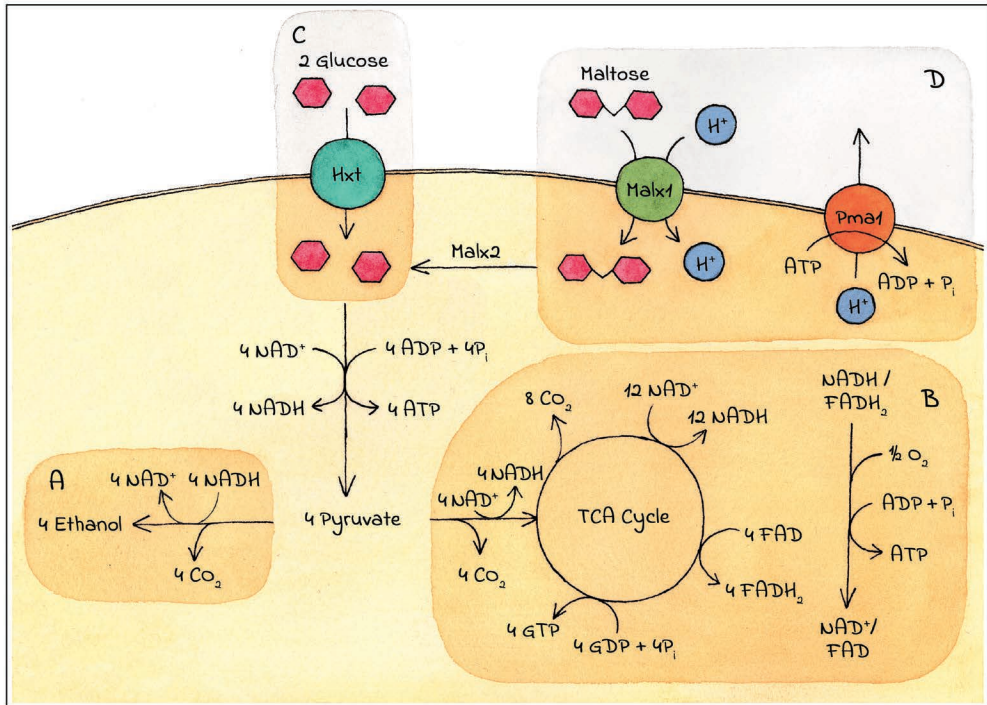
Figure 1.4: Simplified schematic representation of sugar dissimilation in *S. cerevisiae*. A: Through alcoholic fermentation NADH is re-oxidized in the conversion of pyruvate to ethanol. B: In respiration, full oxidation of pyruvate occurs in the TCA cycle and re-oxidation of reduced cofactors NADH and $FADH_2$ via the mitochondrial respiratory chain. C: Facilitated diffusion of glucose via transporters encoded by the *HXT* gene family. D: Proton-coupled uptake of maltose via transporters encoded by *MALX1* and subsequent extrusion of protons via the plasma membrane ATPase Pma1.

for energy-dependent cellular processes that do not lead to production of new cell material (maintenance) (Figure 1.5). Maintenance-related processes include (but are not limited to) macromolecule turnover, maintenance of concentration gradients across membranes and defense against oxygen stress. Initially, these maintenance requirements, which require dissimilation of substrate, were assumed to be independent of the growth rate. Based on this assumption, distribution of an energy substrate over growth (requiring both assimilation and dissimilation of substrate) and maintenance (requiring only dissimilation of substrate) could, under energy-limited cultivation conditions, be described by the Pirt equation (Pirt, 1965):

$$q_s = \mu / Y_{xs}^{max} + m_s \qquad (1.2)$$

In equation 1.2, q_s is the specific substrate consumption rate, μ the specific growth rate, Y_{xs}^{max} the (theoretical) biomass yield in the absence of maintenance and m_s the maintenance coefficient. This relation implies that, as the specific growth rate is decreased, an ever larger fraction of the consumed substrate has to be dissimilated to meet maintenance energy requirements. In addition to growth and maintenance, ATP can be used for the production of so-called assimilatory products, which are molecules whose formation from substrate requires a net input of ATP (Figure 1.5). The amount of ATP that can be produced via substrate dissimilation and the amount of ATP that is required for growth, maintenance and assimilatory product
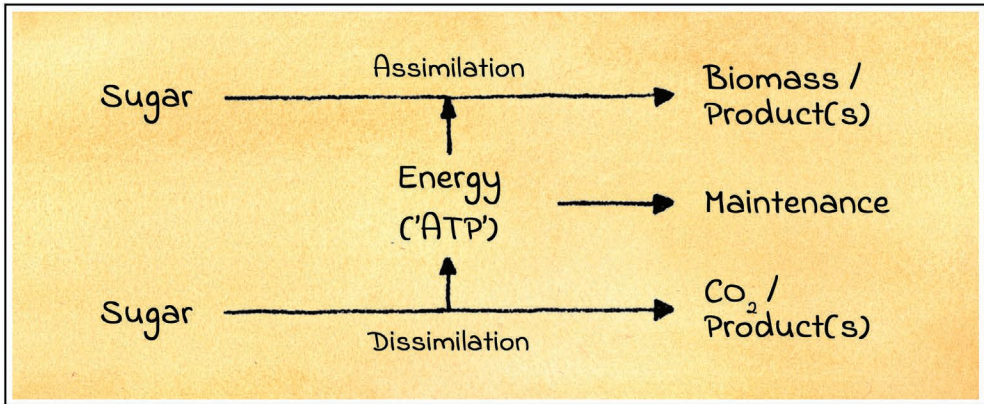
Figure 1.5: Allocation of consumed sugar in heterotrophic, organotrophic organisms. Sugar is dissimilated to supply energy (ATP), resulting in the production of CO_2 and (potentially) other dissimilatory products. The ATP produced in dissimilation is required for cellular maintenance and for the assimilation of sugar into new biomass (growth) and assimilatory products.

formation play a major role in defining how substrate (often a sugar in case of industrial processes that employ *S. cerevisiae*) is distributed over these different processes. The energy requirements of transport associated with substrate dissimilation and/or product formation can therefore have a significant effect on the yields of biomass and products on sugar that can be achieved in microbial cultures (Weusthuis *et al.*, 1994), and are a relevant target for engineering strains with improved product yields (de Kok *et al.*, 2012a).

Depending on the nature of the desired product, optimization of product yield on substrate can either require an increase or a decrease of the energetic efficiency (ATP yield) of substrate dissimilation. Increasing the ATP yield of substrate dissimilation can be a very relevant aspect for optimization of industrial processes focused on the production of biomass, protein or other assimilatory products. Yeast biomass and other products whose synthesis from substrate requires a net input of ATP are generally produced in aerobic processes, so that the required ATP can be obtained via respiration. In that case, it is advantageous to maximize the ATP yield from substrate dissimilation, for instance by exchanging an active transport system for uptake of the carbon and energy substrate by a facilitated diffusion system. By circumventing an energy requirement for substrate uptake, less substrate is 'lost' to dissimilation and more substrate can be used to form additional product. Moreover, in aerobic processes, a higher ATP stoichiometry of substrate dissimilation can reduce process costs due to a lower oxygen demand and associated heat production, which decreases energy requirements for stirring, aeration and cooling (Cueto-Rojas et al., 2015; Weusthuis et al., 2011).

Increasing the efficiency of substrate dissimilation is also relevant for the production of compounds that are produced via energy-neutral pathways, i.e. pathways that do not yield or require ATP. Any increase in the ATP yield would turn such a zero-ATP pathway into an ATP-yielding, dissimilatory pathway, and thereby eliminate the need to divert the carbon substrate to other dissimilatory pathways. Under the condition that the ATP production rate via such a product-generating dissimilatory pathway exceeds the ATP requirement for maintenance processes (m_{ATP}; in *S. cerevisiae* corresponding to approximately 1 mmol ATP per gram yeast

1

biomass per hour (Boender *et al.*, 2009)), turning a zero-ATP pathway into an ATP-positive pathway would allow for anaerobic process conditions, since respiration is not required. Ideally, such anaerobic product-coupled dissimilation pathways can conserve all available electrons from the dissimilated substrate in the desired final product, which benefits product yield. Furthermore, in such engineered strains, the formation of product and biomass become coupled by the production and requirement of ATP, which facilitates selection of fast-producing mutants by evolutionary engineering for increased growth rate (de Kok *et al.*, 2012a; Dragosits and Mattanovich, 2018; Mans *et al.*, 2018).

Production of lactic acid by engineered strains of *S. cerevisiae* is an example of an energy-neutral pathway. The combined overexpression of a (heterologous) lactate dehydrogenase gene (*ldh*) and deletion of the three *S. cerevisiae* genes encoding pyruvate decarboxylase (*PDC1*, *PDC5* and *PDC6*) yields strains in which the formation of ethanol from pyruvate is replaced by the formation of lactate from pyruvate (Porro et al., 1995). Formation of 2 moles of (intracellular) lactate from glucose is redox-neutral and results in the production of 2 moles of ATP. However, export of one mole of lactic acid requires one mole of ATP due to the involvement of an as yet unidentified export mechanism (Abbott *et al.*, 2009a; Mans *et al.*, 2017; van Maris *et al.*, 2004). Therefore, production of extracellular lactic acid from glucose is ATP-neutral, which results in an inability of engineered homo-fermentative lactic-acid-producing *S. cerevisiae* strains to grow anaerobically. To enable anaerobic production of lactic acid with *S. cerevisiae*, more ATP should be conserved from the formation of intracellular lactate from substrate, or the ATP requirement of lactate export should be identified and eliminated by metabolic engineering.

For dissimilatory products such as ethanol, whose formation from substrate results in a net synthesis of ATP, it is advantageous for product yield to minimize ATP formation. If the ATP yield of dissimilation is decreased, more substrate has to be dissimilated to supply the energy required for formation of the same amount of biomass. Therefore, higher dissimilatory product yields can be obtained, while formation of biomass, which can be considered an undesirable by-product of many industrial fermentation processes, is reduced. An important constraint in strategies to accomplish this goal is that the rate of ATP generation should not decrease below cellular maintenance-energy requirements.

1.10 Mechanisms of sugar transport in *S. cerevisiae*

Since sugars are used as carbon and energy substrates in most yeast-based industrial processes, altering the efficiency of sugar dissimilation by targeting their uptake is a relevant engineering strategy to improve industrial productions. In *S. cerevisiae*, 20 genes belonging to the *HXT* family encode transporters which mediate the facilitated diffusion of hexoses such as glucose, fructose and galactose. This set includes transporters with diverse uptake kinetics and transcriptional regulation. For instance, *HXT1* and *HXT3* encode low-affinity transporters (K_M 100 and 60 mM, respectively) that are transcribed in the presence of high (40 g L^{-1}) glucose concentrations. Conversely, *HXT2*, *HXT6* and *HXT7* encode high-affinity transporters (K_M 1-2 mM) and are transcribed at low (1 g L^{-1}) glucose concentrations (Boles and Hollenberg, 1997; Özcan and Johnston, 1995; Reifenberger *et al.*, 2004). This transcriptional regulation, in combination with the removal and inactivation of transport proteins in response to varying glucose concentrations and modulation of transporter affinity (as observed for Hxt2 (Reifenberger *et al.*, 2004)), allows *S. cerevisiae* to optimize hexose-transport capacity in response to varying extracellular sugar concentrations (Boles and Hollenberg, 1997). Additionally, some Hxt

transporters have a broad substrate specificity and play a role in the uptake of non-sugar substrates. This diversity is exemplified by the ability of Hxt13, Hxt15, Hxt16 and Hxt17 to take up polyols (Jordan *et al.*, 2016). The high uptake capacity in the presence of varying sugar concentrations and affinity for additional substrates may have contributed to fitness of *S. cerevisiae* in natural environments. Such an evolutionary advantage may explain why so many genes with overlapping functions were retained over the course of evolution of this yeast species (Ciriacy and Reifenberger, 1997; Kruckeberg, 1996). After their uptake, (fast) activity of hexose-phosphorylating enzymes (hexokinase, glucokinase or galactokinase) 'traps' the hexoses intracellularly in their phosphorylated form. This mechanism led to a now refuted hypothesis that uptake and phosphorylation of monosaccharides in *S. cerevisiae* are coupled at the molecular level (Lagunas, 1993).

In contrast to the Hxt-mediated facilitated diffusion of monosaccharides, transport of the disaccharides sucrose, maltose and trehalose in *S. cerevisiae* is mediated by proton symporters, encoded by *MALX1* genes (Santos *et al.*, 1982; Serrano, 1977; Stambuk *et al.*, 2000; Stambuk *et al.*, 1999; Stambuk and de Araujo, 2001; Stambuk *et al.*, 1996). The resulting coupling of disaccharide uptake to the proton motive force can theoretically, at thermodynamic equilibrium, support intracellular accumulation of these sugars to concentrations that are up to 1000-fold higher than their extracellular concentrations (de Kok *et al.*, 2012a). In cultivation media containing 20 g L^{-1} sugar, which is a typical concentration used in laboratory growth studies, the osmotic pressure caused by a 1000-fold accumulation would lead to cell death. It is therefore imperative that proton symport of disaccharides and their subsequent intracellular hydrolysis rates are tightly regulated. The importance of such coordinated expression is demonstrated by the observation that, after prolonged growth of *S. cerevisiae* under maltose-limited conditions, a sudden switch to maltose excess conditions causes a significant fraction of cells to burst, a phenomenon known as 'substrate-accelerated cell death' (Jansen *et al.*, 2004; Postma *et al.*, 1990).

The impact of the mechanism of sugar uptake on cellular physiology and biomass yield of *S. cerevisiae* can be illustrated by a comparison of anaerobic fermentation of glucose and maltose in this yeast. As previously discussed, in anaerobic *S. cerevisiae* cultures, intracellular glucose is fermented to ethanol and CO_2, yielding 2 moles of ATP per mol of glucose via substrate-level phosphorylation (Figure 1.4). Since neither the uptake of glucose by facilitated diffusion nor export of these fermentation products requires an input of ATP (Figure 1.4A), the net ATP yield of anaerobic glucose dissimilation by *S. cerevisiae* is 2 moles of ATP per mol of glucose. Maltose, a disaccharide consisting of two glucose monomers, is taken up via proton symport with a maltose/H$^+$ stoichiometry of 1 (Van Leeuwen *et al.*, 1992) (Figure 1.4D). The resulting maltose-associated import of protons should be compensated by proton expulsion in order to prevent intracellular acidification and dissipation of the proton-motive force across the plasma membrane. In *S. cerevisiae*, proton export occurs via the plasma-membrane ATPase, Pma1, at the cost of 1 ATP per proton (Carmelo *et al.*, 1996; Serrano, 1977). As a consequence, the net ATP yield of anaerobic, fermentative maltose dissimilation in this yeast is only 3 moles of ATP per mol of maltose, or 1.5 moles of ATP per mol of glucose equivalent (Weusthuis *et al.*, 1993).

In sugar-limited cultures, biomass yield on sugar can be used as a read-out for the efficiency of substrate dissimilation in the absence of other major assimilatory products. The rate at which *S. cerevisiae* uses ATP for cellular maintenance is essentially growth-rate independent (Boender *et al.*, 2009; Pirt, 1965; Tännler *et al.*, 2008; Vos *et al.*, 2015). As a consequence, more sugar is

allocated towards dissimilation to meet maintenance energy requirements at lower growth rates (Equation 1.2). Therefore, to compare the impact of different transport mechanisms on the overall efficiency of substrate dissimilation, comparisons of growth substrates or yeast strains should ideally be made at identical growth rates. This can be accomplished in steady-state chemostat cultures, in which the specific growth rate is equal to the dilution rate (ratio of the outflow rate of spent medium and the constant liquid volume of the culture). To assess the impact of the difference in energy coupling of glucose and maltose transport on the biomass yield, *S. cerevisiae* was grown in anaerobic chemostat cultures that were either glucose- or maltose-limited, both at a dilution rate of 0.10 h^{-1} (Weusthuis *et al.*, 1993). The 25% lower ATP yield of maltose fermentation implies that for each gram of biomass formed, an additional 33% of substrate should be dissimilated to supply the required energy. Consistent with this prediction, the biomass yield of *S. cerevisiae* in anaerobic maltose-limited chemostat cultures was 25% lower (0.077 gram biomass per gram maltose monohydrate) than the corresponding biomass yield on glucose (0.103 gram biomass per gram glucose) (Weusthuis *et al.*, 1993). Also in line with theoretical predictions, the lower biomass yield on maltose was accompanied by a 16% higher yield of ethanol on substrate (Weusthuis *et al.*, 1993). This result provides a powerful demonstration of the sometimes counterintuitive fact that a less ATP-efficient dissimilation pathway can result in higher product yields of microbial fermentation processes.

The low biomass yield and high ethanol yield observed in anaerobic maltose-limited cultures is not observed in corresponding cultures of wild-type *S. cerevisiae* grown on sucrose (Basso *et al.*, 2011b). This difference is due to the fact that sucrose is predominantly hydrolyzed extracellularly by invertase (*SUC2*) (Gascón and Lampen, 1968), after which the resulting monosaccharides (glucose and fructose) are taken up via facilitated diffusion, with neither sucrose hydrolysis nor monosaccharide uptake requiring a net input of free energy (Figure 1.6A).

The effect of active transport on physiology is generally less apparent in aerobic, respiring cultures than in anaerobic, fermentative cultures. As previously mentioned, in aerobic, fully respiratory cultures, complete oxidation of a glucose molecule to CO_2 results in the synthesis of approximately 16 ATP equivalents (Pronk *et al.*, 1994; Verduyn *et al.*, 1991). The different ATP yields from respiratory and fermentative sugar metabolism are also reflected by the biomass yields reported for aerobic and anaerobic, glucose-limited chemostat cultures (~0.5 gram biomass per gram glucose and ~0.1 gram biomass per gram glucose, respectively, at a dilution rate of 0.1 h^{-1} (Postma *et al.*, 1989; Verduyn *et al.*, 1990b)). When comparing the effects of glucose and maltose transport on the aerobic biomass yield, a net requirement of 1 ATP for maltose uptake would result in a mere 3% reduction of the ATP yield from respiratory dissimilation (31 instead of 32 moles of ATP per mol of maltose). For these reasons, quantification of the energetic impact of metabolite transport with biomass yield as a readout is best tested under anaerobic conditions.

1.11 Engineering energy coupling of transport

Due to the potential benefits of altering the energetic efficiency of substrate conversion that were discussed above, energy coupling of cellular transport systems has been an important optimization target for metabolic engineering studies. Inspired by the study of Weusthuis *et al.* (1993) on maltose metabolism, a dedicated metabolic engineering study focused on decreasing the ATP yield of sucrose fermentation in order to increase the yield of ethanol on
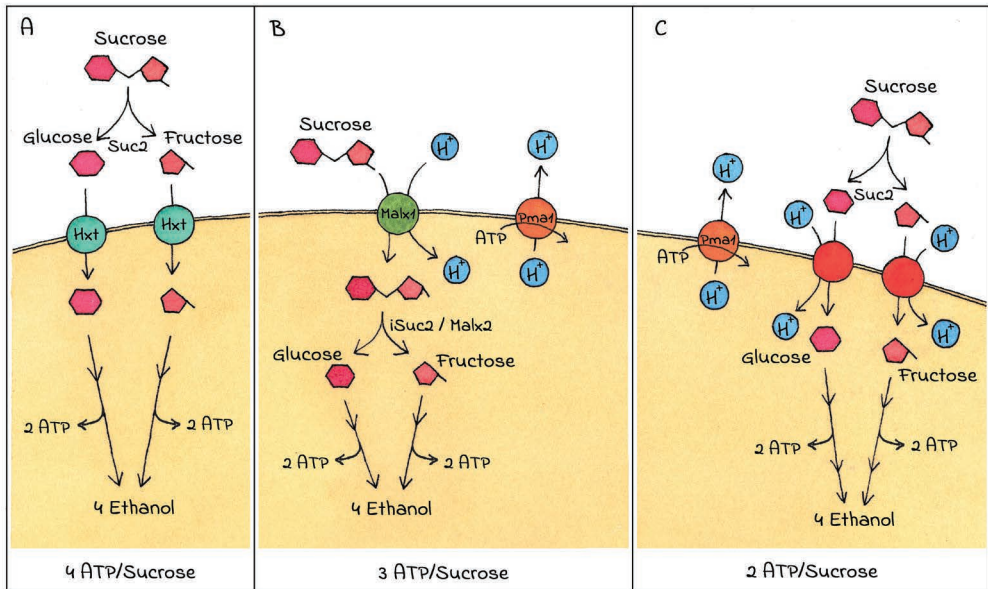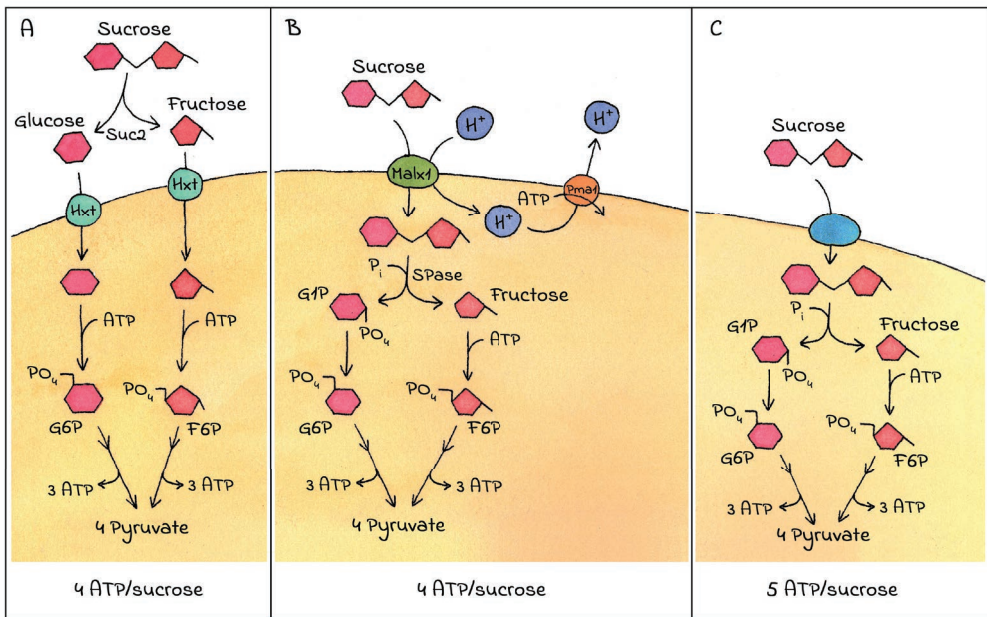
Figure 1.6: Strategies to decrease the ATP yield of sucrose fermentation. A: In wild-type *S. cerevisiae*, sucrose is predominantly hydrolyzed extracellularly by Suc2 (invertase). The resulting monosaccharides are taken up via facilitated diffusion (Hxt), after which they are further metabolized via the Embden-Meyerhof glycolysis and alcoholic fermentation. The net ATP yield of this route is 4 ATP per sucrose. B: By removing extracellular hydrolysis activity, consumption of sucrose is initiated by its Malx1-mediated proton symport. Import of the associated proton is counteracted by the plasma membrane ATPase (Pma1), which exports a proton at the cost of 1 ATP. Intracellularly, sucrose can be hydrolyzed by intracellularly targeted invertase (iSuc2) or hydrolases (Malx2). The net ATP yield of this route is 3 ATP per sucrose. C: Extracellular hydrolysis of sucrose combined with proton-coupled uptake of the resulting monosaccharides would further decrease the net ATP yield to 2 ATP per sucrose (Chapter 5).

sucrose (Basso *et al.*, 2011b). Sucrose, the main carbohydrate in cane sugar, beet sugar and molasses, is widely used as a carbon and energy source for large-scale industrial fermentation processes (Marques *et al.*, 2018a; Marques *et al.*, 2015). As mentioned in section 1.10, wild-type *S. cerevisiae* strains predominantly hydrolyze sucrose extracellularly, using the enzyme invertase (Suc2). Subsequently, the resulting fructose and glucose molecules are taken up by facilitated diffusion mediated by Hxt transporters (Figure 1.6A). Anaerobic dissimilation of sucrose via this route yields 4 moles of ATP per mole of sucrose. In an alternative route, which in wild-type strains accounts only for a minute fraction of metabolized sucrose, this disaccharide is taken up via proton symport, mediated by Malx1 transporters, and subsequently hydrolyzed by intracellular maltases (encoded by *MALX2*) and invertase (encoded by *SUC2*) (Batista *et al.*, 2004; Santos *et al.*, 1982; Stambuk *et al.*, 2000). The first 60 base pairs of the *SUC2* open-reading frame encode an extracellular localization signal, which is followed by a second start codon (Carlson and Botstein, 1982). Initiation of transcription at this second start codon results in the synthesis of a functional, intracellularly retained Suc2 protein. Basso *et al.* (2011) removed the extracellular localization sequence of *SUC2* (the 5'-truncated gene was called '*iSUC2*'), resulting in a predominantly intracellular localization of invertase. Similar to the situation with maltose, the proton-coupled uptake of sucrose that precedes intracellular hydrolysis indirectly results in the hydrolysis of 1 mol of ATP per mol of sucrose, so this strategy decreased the ATP yield of sucrose fermentation from 4 to 3 moles of ATP per mol of sucrose (Figure 1.6B). After laboratory evolution to increase the capacity of Mal11-mediated sucrose import, the *iSUC2*-expressing

strain exhibited a 30% lower biomass yield and an 11% higher ethanol yield in anaerobic, sucrose-limited chemostat cultures (Basso *et al.*, 2011b). This result clearly demonstrated the potential of metabolic engineering strategies based on decreasing the ATP yield for improved dissimilatory product formation.

Other studies were focused on increasing rather than decreasing the ATP yield of sucrose dissimilation, with the ultimate goal to improve yields of products whose formation from glucose does not result in a net positive yield of ATP. As a first step, sucrose hydrolysis was replaced by intracellular phosphorolysis by a heterologously expressed sucrose phosphorylase (Figure 1.7B). In contrast to hydrolysis of sucrose, which dissipates the energy contained in the glucose-fructose bond, sucrose phosphorolysis conserves this energy by yielding fructose and glucose-1-phosphate. In combination with the enzyme phosphoglucomutase, which converts glucose-1-phosphate into glucose-6-phosphate, sucrose phosphorolysis circumvents the ATP-dependent phosphorylation of glucose by hexokinase (Figure 1.7B) (Marques *et al.*, 2018a). Although this replacement saves one ATP, the net ATP yield per hexose unit is still the same as that of glucose fermentation, since sucrose uptake in the engineered strains occurs

Figure 1.7: Strategies for increasing the ATP yield of anaerobic sucrose dissimilation in *S. cerevisiae*. A: In wildtype strains, sucrose is predominantly hydrolyzed extracellularly by Suc2 (invertase). The resulting monosaccharides are taken up via facilitated diffusion (Hxt transporters), after which each monosaccharide is phosphorylated at the cost of ATP, resulting in glucose-6-phosphate (G6P) and fructose-6-phosphate (F6P), which are further metabolized in the Embden-Meyerhof glycolytic pathway. The net ATP yield of this route is 4 ATP per sucrose. B: The combined action of a heterologous, intracellular sucrose phosphorylase (SPase), which cleaves sucrose into glucose-1-phosphate (G1P) and fructose, and phosphoglucomutase (Pgm2), which converts G1P into G6P, saves one ATP that would otherwise be required for a hexokinase reaction. The uptake of sucrose indirectly results in hydrolysis of 1 ATP by the plasma membrane ATPase (Pma1), which exports a proton at the cost of 1 ATP to counteract the import of protons via sucrose-proton symport (Malx1). The net ATP yield of this route is 4 ATP per sucrose. C: Combined expression of an intracellular sucrose phosphorylase and a sucrose uniporter would increase the net ATP yield to 5 ATP per sucrose.

via proton symport rather than by facilitated diffusion (Lagunas, 1993; Santos *et al.*, 1982). To further increase the ATP yield from sucrose fermentation, all endogenous sucrose-transporter genes were deleted and replaced by a heterologous sucrose transporter gene from the plant *Phaseolus vulgaris* (*PvSUF1*) that was predicted to encode a sucrose facilitator (Zhou *et al.*, 2007). Compared to an isogenic strain that expressed an endogenous sucrose-proton symporter, the *PvSUF1*-expressing strain was expected to exhibit a 25% higher anaerobic biomass yield, as the ATP yield of sucrose dissimilation should be increased from 4 to 5 moles of ATP per mol of sucrose (Figure 1.7C). However, in anaerobic, sucrose-limited chemostats, its biomass yield was only 8% higher than that of such a reference strain and it was determined that, when *PvSUF1* was expressed in *S. cerevisiae*, sucrose transport remained at least partly proton coupled (Marques *et al.*, 2018a).

The large scale at which bioethanol is currently produced (99 billion liters in 2020) (Renewable Fuels Association, 2021) and the increasing demand for bio-based food, feed, fuels, chemicals and polymers (Bos and Broeze, 2020) provide strong incentives to further improve product yields of engineered *S. cerevisiae* strains. Increasing the understanding of transport mechanisms that are associated with the conversion of substrate into desired products and, based on such understanding, the development of metabolic engineering strategies to alter the ATP yield of substrate dissimilation, can contribute to improved performance of microbial fermentation processes.

1.12 Scope of this thesis

This thesis explores engineering strategies involving different transport systems in *S. cerevisiae*, with the aim to quantify and control their impact on energy metabolism and, consequently, on the stoichiometry and kinetics of growth and product formation under industrially relevant conditions.

The combined expression of a sucrose phosphorylase gene and a sucrose uniporter gene has the potential to increase the energetic efficiency of sucrose dissimilation by 1 ATP. However, sucrose uniporters are not widely described or characterized in fungi and previous attempts to express heterologous plant transporters did not result in fully uncoupled transport of sucrose (Marques *et al.*, 2018a; Marques *et al.*, 2018b). In **Chapter 2**, a combination of rational protein engineering and evolutionary engineering was used to convert the endogenous *S. cerevisiae* sucrose-proton symporter Mal11 into a sucrose uniporter. The resulting modified transporters were functionally characterized by sugar transport assays and their impact on strain physiology was analyzed in anaerobic, sucrose-limited chemostats.

Increasing the efficiency of substrate dissimilation could theoretically be applied to enable anaerobic production of lactic acid in *S. cerevisiae*. In addition to strategies focused on substrate uptake, strain engineering could target the energy requirement of lactate export, but the identity of the *S. cerevisiae* transport protein(s) responsible for lactic acid export remains elusive (Mans *et al.*, 2017). In **Chapter 3**, a laboratory evolution approach was applied to identify two genes that, after acquiring point mutations, enabled lactic acid transport by an *S. cerevisiae* strain in which genes encoding known uptake systems for this organic acid had been deleted. The evolved transporters were structurally investigated via homology modeling to gain insight into the mechanism by which the observed mutations enabled lactic acid transport. While this study did not resolve the lactic acid export enigma in yeast, its results provide a clear illustration

of the evolutionary plasticity of the yeast 'transportome', and increase the understanding of the structural requirements for lactate uptake by monocarboxylate transporters.

In terms of research target, **Chapter 4 and 5** represent a mirror image of the work presented in Chapter 2. As discussed above, metabolic engineering interventions that reduce the ATP yield of sugar fermentation have the potential to lead to increased yields of dissimilatory products such as ethanol. **Chapter 4** reviews metabolic engineering strategies described in the scientific literature that were aimed at improving the yield of bioethanol on sugar in anaerobic *S. cerevisiae* cultures. In addition to strategies that were primarily focused on decreasing the ATP yield from sugar fermentation, this chapter also reviews strategies aimed at decreasing the formation of the by-product glycerol by redox-cofactor engineering strategies.

One of the metabolic engineering approaches that leads to a decreased ATP yield on sugar is the replacement of facilitated diffusion of sugar by energy-dependent transport mechanisms. In **Chapter 5**, the hexose-transport system in *S. cerevisiae*, which exclusively relies on hexose uptake by facilitated diffusion, was replaced by hexose-proton symporters to increase the ethanol yield on the hexose sugars glucose and fructose. Subsequently, glucose- and fructose-proton symporters were combined in a strain that exclusively relied on extracellular invertase for the hydrolysis of sucrose, with the goal to also increase the yield of ethanol on sucrose (Figure 1.6C). To this end, a novel platform strain was constructed, in which all hexose transporters, disaccharide transporters and disaccharide hydrolases were deleted. The resulting '*sugar*^{0} strain' was unable to grow on any of the tested sugar substrates and provides a valuable platform for functional analysis studies on native and heterologous sugar transporters.

In **Chapter 6,** the *sugar*^{0} platform strain was applied to explore a novel evolutionary engineering strategy that was specifically designed to select for mutant strains with an altered substrate specificity of proton symporters. As a model, Chapter 6 focuses on the Mal11 disaccharide-proton symporter, which also has a low capacity for glucose transport. In the absence of disaccharide hydrolases, the presence of *MAL11* renders cells highly sensitive to the presence of sucrose or maltose. Evolution in glucose-limited chemostats that were, at an increasing frequency, subjected to pulse-wise addition of a concentrated sucrose solution, enabled selection of cells with mutations in the *MAL11* open reading frame. Reverse engineering of these mutated *MAL11* alleles into an unevolved *sugar*^{0} strain showed that they led to a decreased sensitivity towards both sucrose and maltose without negatively affecting the maximum specific growth rate on medium with glucose as the sole carbon source.
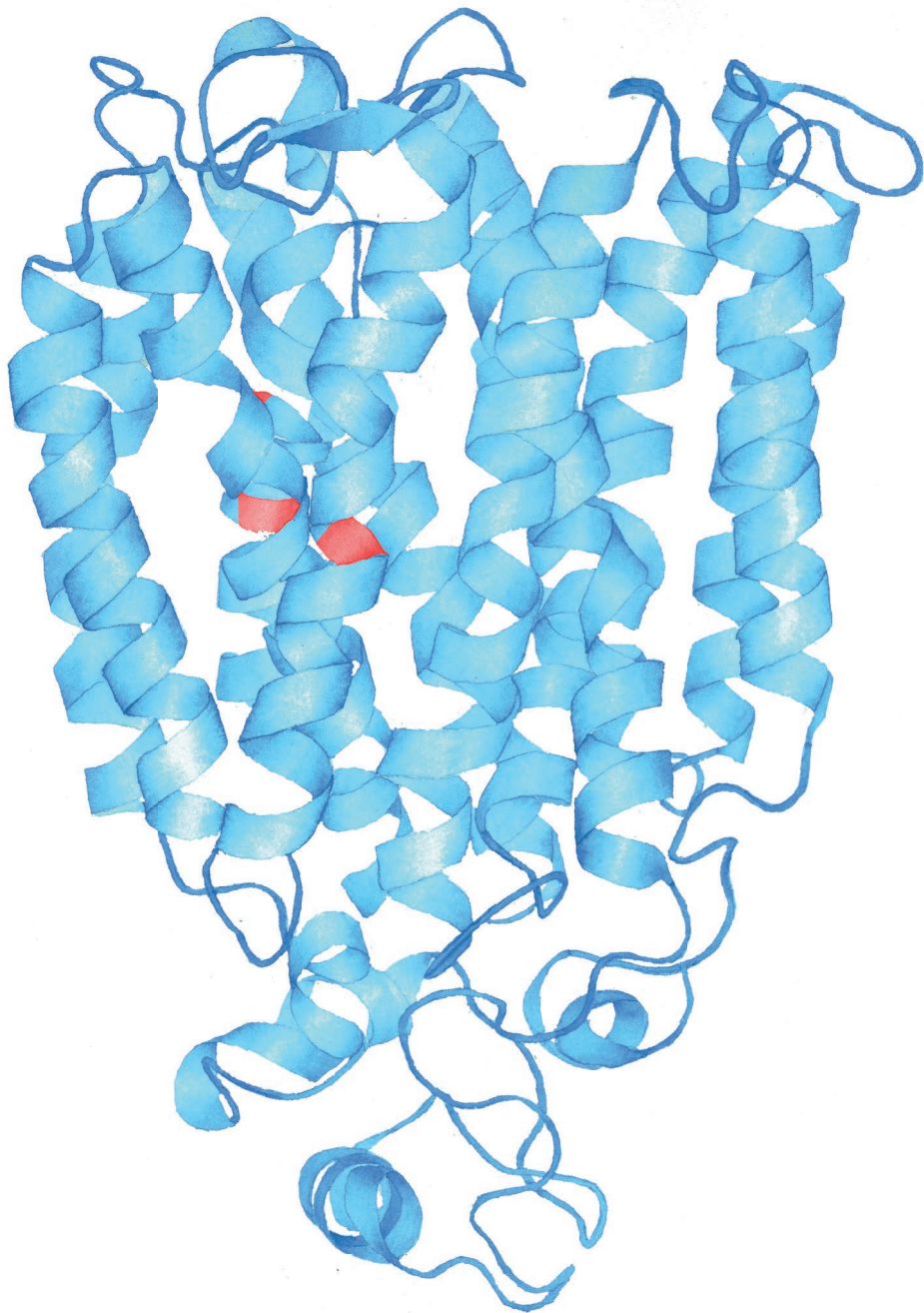
Chapter 2

Energy coupling of membrane transport and efficiency of sucrose dissimilation in yeast

Ryan K. Henderson*, Sophie C. de Valk*, Bert Poolman and Robert Mans

*These authors contributed equally to this work.

Abstract

Proton coupled transport of α-glucosides via Mal11 into *Saccharomyces cerevisiae* costs one ATP per imported molecule. Targeted mutation of all three acidic residues in the active site resulted in sugar uniport, but expression of these mutant transporters in yeast did not enable growth on sucrose. We then isolated six unique transporter variants of these mutants by directed evolution of yeast for growth on sucrose. In three variants, new acidic residues emerged near the active site that restored proton-coupled sucrose transport, whereas the other evolved transporters still catalysed sucrose uniport. The localization of mutations and transport properties of the mutants enabled us to propose a mechanistic model of proton-coupled sugar transport by Mal11. Cultivation of yeast strains expressing one of the sucrose uniporters in anaerobic, sucrose-limited chemostat cultures indicated an increase in the efficiency of sucrose dissimilation by 21% when additional changes in strain physiology were taken into account. We thus show that a combination of directed and evolutionary engineering results in more energy efficient sucrose transport, as a starting point to engineer yeast strains with increased yields for industrially relevant products.

2

2.1 Introduction

In heterotrophic microorganisms, an important determinant of the maximal product yield is the amount of energy (ATP) conserved by substrate dissimilation and the energy requirements of assimilatory reactions, as this coupling determines the distribution of substrate over biomass and product formation. Therefore, the energy metabolism in microbial production hosts is an important optimization target to obtain high product yields, which is essential for the production of bulk chemicals where the carbon feedstock can make up 70% of the total variable costs of industrial processes (Borodina and Nielsen, 2014; de Kok *et al.*, 2012a; Pfromm *et al.*, 2010). An increase of the energetic efficiency of substrate dissimilation could decrease the costly oxygen demand of compounds whose formation require the input of ATP (like biomass, proteins or complex chemicals) or even enable anaerobic production of compounds with an ATP neutral production pathway, such as lactic acid in engineered *S. cerevisiae* strains (van Maris *et al.*, 2004).

Metabolic engineering strategies have been developed to increase energetic efficiency, for instance by altering the route for cytosolic acetyl-CoA supply and increasing the efficiency of the respiratory chain and the H^+-ATPase (de Kok *et al.*, 2012a). In the yeast *Saccharomyces cerevisiae*, it has previously been shown that the ATP yield of dissimilation of the disaccharides maltose and sucrose could be increased by substituting intracellular hydrolysis by phosphorolysis (de Kok *et al.*, 2011). Whereas transport of monosaccharides occurs predominantly through uniport, all known disaccharide transporters are proton-coupled symporters belonging to the Major Facilitator Superfamily (MFS) (Horák, 2013; Serrano, 1977; Van Leeuwen *et al.*, 1992). As proton export via the plasma membrane ATPase comes at a net cost of 1 ATP per proton in *S. cerevisiae*, the energetic efficiency of these engineered strains did not exceed that of regular glucose metabolism. For the complete conversion of extracellular substrate to extracellular product, energetic requirements for substrate import and/or product export can be a major contributor to the total energy costs. In an attempt to increase the ATP yield of sucrose dissimilation, the expression of a sucrose phosphorylase was combined with expression of a heterologous transporter gene from *Phaseolus vulgaris* (*PvSUF1*), that was described to facilitate sucrose uniport (Marques *et al.*, 2018a). However, the experimental data indicated that, in contrast to what was suggested in previous research (Zhou *et al.*, 2007), the transport of sucrose by PvSUF1 in *S. cerevisiae* was (at least partially) proton coupled.

In *S. cerevisiae*, the α-glucoside transporter Mal11 catalyses proton-coupled import of a wide range of sugars, including maltose, sucrose and maltotriose (Han *et al.*, 1995; Pao *et al.*, 1998; Serrano, 1977; Stambuk and de Araujo, 2001; Van Leeuwen *et al.*, 1992; Yan, 2015) and has been an engineering target to modulate cellular energetics (Basso *et al.*, 2011b). The acidic residues involved in proton coupling in Mal11 are Glu-120, Asp-123 and Glu-167 (Henderson and Poolman, 2017). In previous work, mutation of one or two of these acidic residues to neutral residues created a "leak" pathway in the transport cycle, which allowed some of the sugar substrate to be transported in the absence of a proton (Henderson *et al.*, 2019b; Lolkema and Poolman, 1995). Mutation of all three residues completely abolished proton-coupled transport but still enabled facilitated diffusion of the substrate.

In this work, we investigated the ability of uncoupled Glu-120/Asp-123/Glu-167 triple Mal11 mutants to enable growth of *S. cerevisiae* in medium containing sucrose as the sole carbon source. Parallel directed evolution experiments were then applied to acquire a series of

second-site suppressor mutations, which were able to restore the transport function of the mutated Mal11 transporters. We found that for some of the evolved acidic residue mutants, proton coupling was restored, whereas the other transporters still catalyzed sugar uniport. We characterized the physiology of reverse-engineered strains expressing the evolved mutated sucrose transporters in sucrose-limited anaerobic chemostats to investigate the impact of the mutations in Mal11 on the energetic efficiency of sucrose dissimilation. In addition, the properties of the identified mutations and corresponding transporter variants were used to propose a model of the transport mechanism of Mal11, which has the potential to be applied for the design of targeted engineering strategies to change the mechanism of other MFS transporters.

2.2 Materials and methods

Strains and maintenance

All *S. cerevisiae* strains used in this study (Table S2.1) are derived from the CEN.PK lineage (Entian and Kötter, 2007; Salazar *et al.*, 2017) and *Escherichia coli* strains MC1061 and XL1 blue were used to store and amplify plasmids. To prepare stock cultures, glycerol was added to growing cultures to a final concentration of 30% (v/v) and 1 mL aliquots were stored at -80 °C. *S. cerevisiae* transformations were performed as described previously (Gietz and Woods, 2002) using 1 μg of DNA, unless specified otherwise. All plasmids and their sources and primers are listed in Table S2.2 and S2.3.

Media and cultivation

E. coli was cultivated in LB medium, using 100 μg mL^{-1} ampicillin for selection and maintenance of plasmids. *S. cerevisiae* strains were cultivated in YPD (1% (w/v) yeast extract, 2% (w/v) peptone, 2% (w/v) glucose, pH 6.0), in synthetic complete media (SC) (0.67% (w/v) yeast nitrogen base without amino acids) (YNB, Formedium, UK) or synthetic medium (SM) (pH 6.0 when used in shake flasks) prepared as described previously (Verduyn *et al.*, 1992). When needed, SC was supplemented with a Kaiser amino acid mixture lacking leucine, uracil, or both (Formedium, UK). For growth characterization in shake flasks, SM with 2.3 g L^{-1} urea (pH 6.0) as the sole nitrogen source was used (Luttik *et al.*, 2000). SM used in bioreactors was supplemented with autoclaved (20 min at 121 °C) Antifoam Emulsion C to a final concentration of 0.2 g L^{-1}.

Aerobic shake flask cultures were grown in an Innova incubator shaker at 30 °C and 200 rpm using 500 mL round-bottom shake flasks containing 100 mL medium. Anaerobic shake flask cultures were grown at 30 °C in a Bactron anaerobic chamber with an atmosphere of 5% (v/v) H$_2$, 6% (v/v) CO$_2$ and 89% (v/v) N$_2$, on a IKA KS 260 basic shaker at 200 rpm, using 50 mL shake flasks containing 30 mL medium.

Bioreactor cultivations were performed in 2-L laboratory bioreactors (Applikon Biotechnology, Delft, The Netherlands) with a working volume of 1 L. Cultures were stirred at 800 rpm and sparged with 500 mL N$_2$ min^{-1} (<5 ppm O$_2$). The medium vessels were sparged with N$_2$ as well. The pH of the culture was maintained at 5.0 by automated addition of 2 M KOH and the temperature was controlled at 30 °C. The reactors were inoculated with *S. cerevisiae* strains to obtain an initial optical density (OD$_{660}$) of approximately 0.15. After the batch phase, the medium pump was switched on to obtain a constant flowrate. The working volume was kept

constant using an effluent pump controlled by an electric level sensor. Chemostat cultures were assumed to be in steady state when, after five volume changes, the culture dry weight, extracellular concentrations of sucrose, ethanol and glycerol and CO_2 production rate varied by less than 2% over at least 2 more volume changes. At the end of each experiment, the actual dilution rate and carbon recovery were determined (Table S2.4).

For plate-based growth assays, *S. cerevisiae* strains cultivated for at least two days in SC with 1% (v/v) ethanol to an OD_{600} of roughly 0.5. Cells were then diluted in 1x SC to an OD_{600} between 0.1 and 0.4, and, subsequently, the cells were dispensed in 60 µL aliquots into microplate wells and mixed with 30 µL of 2x SC plus 30 µL of 2x carbon source. 96-well flat-bottom microplates (CELLSTAR, Greiner Bio-One) were used and sealed with a Breath-Easy membrane (Sigma-Aldrich). OD_{600} measurements were made at 10 minute intervals using a PowerWave 340 spectrophotometer (BioTek) and cells were maintained at 30 °C with shaking at variable speed in between measurements. All growth assays included blank wells (SC and carbon source) for each carbon source, the values of which were subtracted from all measurements as background.

Directed evolution of *Mal11* triple mutants

S. cerevisiae strains R250 (Mal11$_{QAQ}$), R252 (Mal11$_{ANA}$), and R254 (Mal11$_{QNA}$) were grown on SD/-AA and each diluted to an OD_{600} of 0.1 in 50 mL SCM containing 2 % (w/v) and 8% (w/v) sucrose in 250 mL flasks. When an OD_{600} greater than 1 was reached, the culture was diluted in fresh media to an OD_{600} of 0.1. This process was repeated at least two more times for each culture until the time between dilutions was 24 - 48 h, at which point samples were sequenced and glycerol stocks were made. Evolution lines growing rapidly in SCM with 8% (w/v) sucrose were then diluted in 50 mL SCM with 2% (w/v) sucrose and the above evolution protocol was repeated.

Evolved plasmids from single colonies were isolated and transformed into *E. coli* for amplification and then sequencing of *MAL11*. These plasmids were subsequently introduced into IMZ630, resulting in strains R265 (Mal11$_{QAQ/A384D}$), R267 (Mal11$_{QNA/A515D}$), R270 (Mal11$_{QAQ/R504C}$) and R274 (Mal11$_{ANA/W376S}$).

At the end of the chemostat cultures single colonies were isolated, resulting in IMS0960 (evolved R270) and IMS0962 (evolved R267). From both single cell lines, plasmids were isolated, renamed pUDE862 (from IMS0960) and pUDE864 (from IMS0962) and introduced into IMZ630, resulting in IME441 and IME442, respectively.

Analytical methods

Growth was monitored by optical density (OD) measurements at a wavelength of 660 nm. For biomass dry weight measurements, 10 mL culture was filtered over a pre-weighed nitrocellulose filter with pore size 0.45 µm. Subsequently, the filters were washed with demineralized water and dried for 20 min at 360 W in a microwave oven, after which they were weighed again. Concentrations of sucrose, ethanol and glycerol in culture supernatants were measured via HPLC analysis on an Agilent 1260 HPLC, equipped with a Bio-Rad HPX 87H column. Detection was performed by means of an Agilent refractive index detector and an Agilent 1260 VWD detector. Off gas concentrations of CO_2 and O_2 were measured using an NGA 2000 analyser.

Glucose-1-phosphate concentrations in culture supernatant were enzymatically determined by measuring the reduction of $NADP^+$ by glucose-6-phosphate dehydrogenase before and after addition of phosphoglucomutase. Cellular protein content was determined as described previously (Verduyn *et al.*, 1990b) with the exception that 1 M NaOH was used instead of 1 M KOH and the absorbance was measured at 510 nm instead of 550 nm.

Transport assays using radiolabeled sugars

Sugar transport was measured in whole yeast cells essentially as previously described (Henderson and Poolman, 2017). *S. cerevisiae* strains were pre-grown on SE/-AA or SE/-Leu, as appropriate, before harvesting in early exponential phase of growth by centrifugation at 3,000 g for 5 minutes at 4 °C. After washing twice in 3 mL assay buffer (potassium-citrate-phosphate (KCP) + 10 mM galactose), cells were resuspended in assay buffer and stored on ice for no more than four hours. Initially, cells at an OD_{600} of 12 or 24 were incubated for ten minutes at 30 °C to increase the adenylate energy charge (Guimarães and Londesborough, 2008), followed by addition of approximately 48,100 Bq mL^{-1} [U-^{14}C]maltose or [U-^{14}C]sucrose (both 600 mCi $mmol^{-1}$; American Radiolabeled Chemicals, Inc.) to start the reaction. Measurements were taken by addition of a reaction sample to 2 mL ice-cold KCP and rapid filtration on 0.45 μm pore-size cellulose-nitrate filters (GE-Healthcare, Little Chalfont, UK), which were pre-soaked in KCP plus 1 mM sugar. Filters were then washed with an additional 2 mL KCP, dissolved in 2 mL scintillation solution (Emulsifier^{plus}, PerkinElmer, Waltham, MA, USA), and the radioactivity quantified in a Tri-Carb 2800TR liquid scintillation analyzer (PerkinElmer). The amount of intracellular maltose or sucrose was normalized to 10^6 cells by counting the number of cells in samples of 20 μL at OD_{600} of 0.4 in an Accuri C6 flow cytometer (BD Biosciences, Durham, USA). The intracellular concentration of sugar was calculated using an estimated 60 fL internal volume per cell. Purity of radiolabeled substrates was checked by TLC and generally better than 99%, aliquots were stored in the freezer and used within one year.

Statistical analysis

Mean values and mean deviations were calculated from the data obtained from two independent experiments. Significance was assessed by performing a two-sided unpaired Student's t-test. Differences were considered to be significant if a p-value < 0.05 was obtained.

Biomass yield calculations

Glycerol formation

Differences in biomass-specific glycerol production rates ($\Delta q_{glycerol}$, in mol g_x^{-1} h^{-1}) between reference strain R249 (wt Mal11) and R270 (Mal11$_{QAQ/R504C}$) or R267 (Mal11$_{QNA/A515D}$) (Figure 2.3B) were used to calculate the effect on the steady-state concentration of glycerol ($\Delta C_{glycerol}$, in mol L^{-1}) for a reactor with biomass concentration C_x (in g_x L^{-1}) and dilution rate D (in h^{-1}) via Equation 2.1:

$$\Delta C_{glycerol} = \Delta q_{glycerol} \cdot C_x / D \qquad\qquad (2.1)$$

Biosynthesis of 1 mol glycerol requires 0.25 mol sucrose and 0.75 mol ATP (Figure 2.3A). For R270 (Mal11$_{QAQ/R504C}$) sucrose uniport was assumed (Figure 2.2b), resulting in 5 mol ATP formed in anaerobic dissimilation of 1 mol sucrose. Therefore, sucrose consumed by R270 for additional

glycerol formation ($\Delta C_{s,glycerol}{}^{R270}$ in mol L^{-1}) was calculated via Equation 2.2:

$$\Delta C_{s,glycerol}{}^{R270} = 0.25 \cdot \Delta C_{glycerol} + 0.75 \cdot 0.2 \cdot \Delta C_{glycerol} \qquad (2.2)$$

For R267 (Mal11$_{QNA/A515D}$) sucrose proton symport was assumed (Figure 2.2B), resulting in the requirement of an additional 0.25 mol ATP per glycerol and 4 ATP formed in anaerobic dissimilation of 1 mol sucrose. Sucrose consumed by R267 for additional glycerol formation ($\Delta C_{s,glycerol}{}^{R267}$) was calculated via Equation 2.3:

$$\Delta C_{s,glycerol}{}^{R267} = 0.25 \cdot \Delta C_{glycerol} + 1 \cdot 0.25 \cdot \Delta C_{glycerol} \qquad (2.3)$$

To calculate the corrected biomass yields of R270 and R267 in the absence of increased glycerol formation ($Y_{xs}{}^{corr,glycerol}$), sucrose that was used for additional glycerol formation ($\Delta C_{s,glycerol}$) was subtracted from the total consumed sucrose ($C_{s,medium} - C_{s,residual}$) and biomass yields were calculated by Equation 2.4:

$$Y_{xs}{}^{corr,glycerol} = C_x / (C_{s,medium} - C_{s,residual} - \Delta C_{s,glycerol}) \qquad (2.4)$$

Extracellular glucose-1-phosphate formation

Extracellular sucrose phosphorylation and subsequent uptake and anaerobic dissimilation of the resulting fructose results in a net yield of 2 mol ATP per mol phosphorylated sucrose. The ATP 'lost' in the form of unused extracellular glucose-1-phosphate (G1P) can be represented in the form of sucrose not contributing to biomass formation ($\Delta C_{s,G1P}$). For R270 and R267, 1 mol of G1P formed is equivalent to 0.6 (3 out of 5 ATP lost) and 0.5 (2 out of 4 ATP lost) respectively, resulting in Equations 2.5 and 2.6:

$$\Delta C_{s,G1P}{}^{R270} = 0.6 \cdot C_{G1P} \qquad (2.5)$$

$$\Delta C_{s,G1P}{}^{R267} = 0.5 \cdot C_{G1P} \qquad (2.6)$$

To calculate the corrected biomass yields of R270 and R267 in the absence of extracellular sucrose phosphorolysis ($Y_{xs}{}^{corr,G1P}$), the calculated 'sucrose equivalent' that did not contribute to biomass formation ($\Delta C_{s,G1P}$ in mol L^{-1}) was subtracted from the total consumed sucrose ($C_{s,medium} - C_{s,residual}$) and biomass yields were calculated by Equation 2.7:

$$Y_{xs}{}^{corr,G1P} = C_x / (C_{s,medium} - C_{s,residual} - \Delta C_{s,G1P})$$

Protein content

To quantify the impact of increased protein content in R270 and R267 compared to R249 (wt Mal11), an estimation of the ATP requirements for biomass formation of the three strains was made, based on a previous analysis of macromolecular composition and the corresponding energy requirements of yeast biomass (Table S2.5 and S2.6) (Lange and Heijnen, 2001; Stouthamer, 1973).

Variations in the protein content were observed between the strains used in this study, and we assumed that the ratio of the other (non-protein) macromolecules remained the same as was previously determined (Lange and Heijnen, 2001), although their fraction of the total biomass

decreased due to the increased protein content (Table S2.6).

The ATP requirement for each component (ATP_i for component i in mmol g^{-1} component) (Table S2.5) was then multiplied by the weight fraction of the corresponding component (γ_i in g g^{-1} biomass) to determine the total ATP requirement for biomass formation of each strain (ATP_x in mmol g$_x^{-1}$), including ATP requirements for mRNA turnover (ATP_{mRNA} in mmol g$_x^{-1}$) and transport of nutrients ($ATP_{transport}$ in mmol g$_x^{-1}$) via Equation 2.8:

$$ATP_x = \Sigma(ATP_i \cdot \gamma_i) + ATP_{mRNA} + ATP_{transport} \qquad (2.8)$$

To calculate the corrected biomass yields of R270 and R267 in a scenario in which their energetic cost of biomass synthesis would have been identical to R249 ($Y_{xs}^{corr,BioComp}$), the biomass yield of R270 was multiplied by the ratio of the ATP requirement of biomass synthesis of R270 (ATP_x^{R270}) or R267 (ATP_x^{R267}) over that of R249 (ATP_x^{R249}) Equation 2.9:

$$Y_{xs}^{corr,BioComp} = C_x / (C_{s,medium} - C_{s,residual}) \cdot (ATP_x^{(R270\ or\ R267)} / ATP_x^{R249}) \qquad (2.9)$$

Final corrected biomass yields

To calculate the corrected biomass yields of R270 and R267 in the absence of additional glycerol and extracellular glucose-1-phosphate formation and with an identical protein content to R249, the equations 4,7 and 9 were combined in Equation 2.10:

$$Y_{xs}^{corr} = C_x / (C_{s,medium} - C_{s,residual} - \Delta C_{s,glycerol} - \Delta C_{s,G1P}) \cdot (ATP_x^{(R270\ or\ R267)} / ATP_x^{R249}) \quad (2.10)$$

More details on materials and methods are given in Supplementary Materials and Methods.

2.3 Results

Mal11 triple mutants are unable to facilitate rapid growth on sucrose

Previously constructed Mal11 triple mutant transport proteins were able to catalyze rapid, coupled or uncoupled maltose transport in radiolabeled sugar transport assays (Henderson and Poolman, 2017). To study the transport of sucrose by these mutated Mal11 proteins *in vivo*, wildtype Mal11 and the three variants Glu-120-Gln/Asp-123-Ala/Glu-167-Gln (Mal11$_{QAQ}$), Glu-120-Ala/Asp-123Asn/Glu-167-Ala (Mal11$_{ANA}$), and Glu-120-Gln/Asp-123-Asn/Glu-167-Ala (Mal11$_{QNA}$) were expressed in *S. cerevisiae* strain IMZ630 using episomal plasmids. IMZ630 carries deletions of genes encoding all native disaccharide transporters and hydrolysis enzymes (suc$^-$) and overexpresses an integrated copy of sucrose phosphorylase from *Leuconostoc mesenteroides* (LmSPase) (Marques *et al.*, 2018a). We then tested the ability of the resulting strains to grow aerobically in medium containing 20, 40 or 80 g L^{-1} sucrose as the sole carbon source using YNB medium in 96-well plates. Within 30 hours, growth of the strain expressing wildtype Mal11 was observed in each of the cultures, whereas none of the triple mutants grew in media containing 20 or 40 g L^{-1} sucrose after 90 hours. However, in the cultures containing 80 g L^{-1} sucrose, the triple mutants exhibited growth after three days (Figure 2.1A).

Second-site suppressor mutations enable faster growth on sucrose

Next, we evolved the yeast strains carrying the three triple mutants by selecting for faster
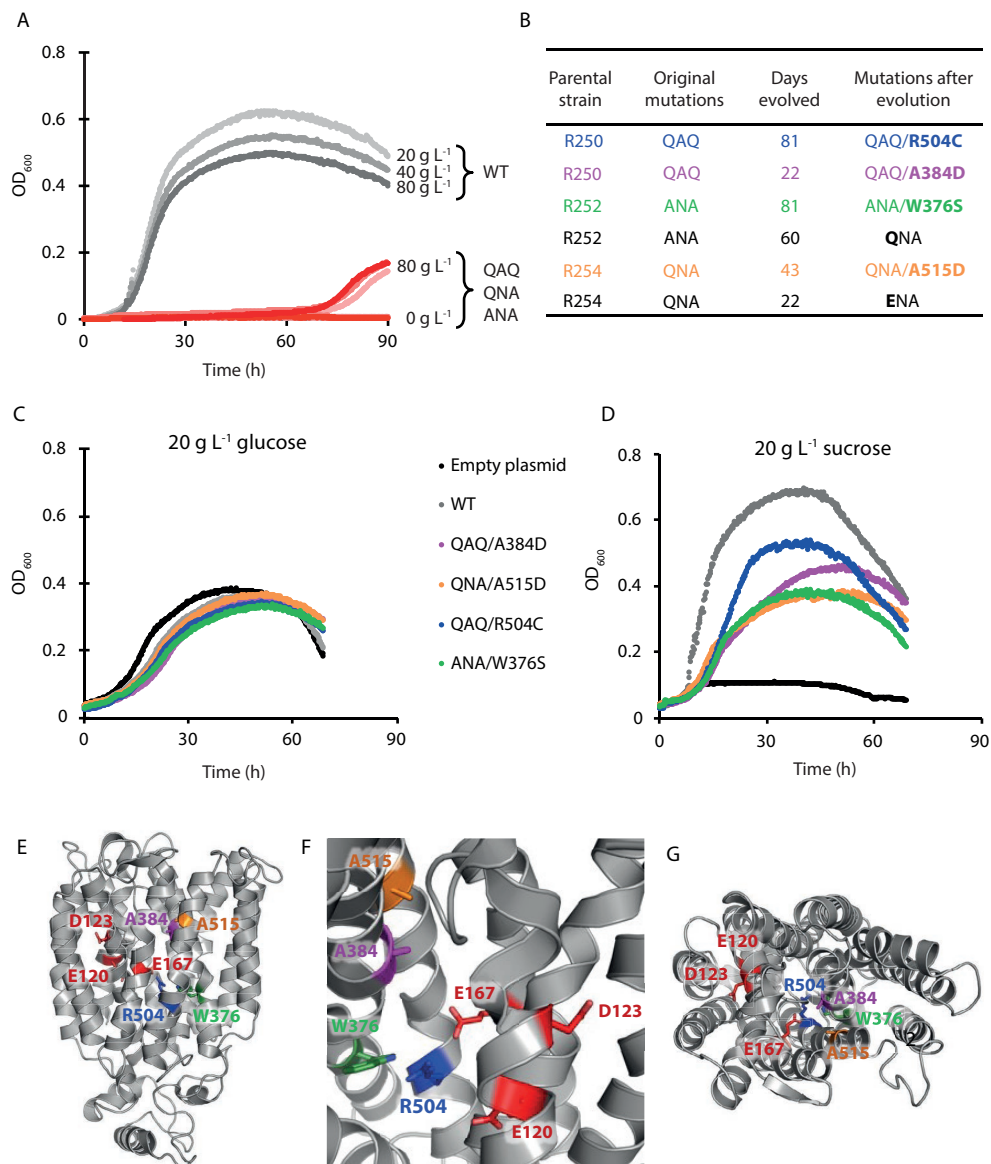
Figure 2.1: Directed evolution of triple Mal11 mutants. A: Growth of unevolved IMZ630 strains expressing wildtype or triple mutated versions of Mal11 in 96-well plates with SC containing 0, 20, 40 or 80 g L^{-1} sucrose as sole carbon source. For each strain, one representative dataset of two independent experiments is shown. B: Mutations that occurred in Mal11 during directed evolution of Mal11 triple mutants. Strains were grown on 20 or 80 g L^{-1} sucrose until rapid growth occurred. Strains that could rapidly grow on 80 g L^{-1} sucrose were transferred to 20 g L^{-1} sucrose until rapid growth resumed. Mutations that were not present in the unevolved parental strain are represented in bold. C, D: Growth of IMZ630 strains expressing evolved versions of Mal11 in 96-well plates with SC containing 20 g L^{-1} glucose (C) or 20 g L^{-1} sucrose (D). For each strain, one representative dataset of two independent experiments is shown. E, F, G: Structural model of Mal11 (Henderson and Poolman, 2017) highlighting the location of the introduced mutations and the evolved mutations during construction and directed evolution of triple mutants on sucrose.

growth on sucrose, using sequential batch cultivation in shake flasks with synthetic complete media (SC) and 80 g L^{-1} sucrose as the sole carbon source (Mans *et al.*, 2018). When the cultures with 80 g L^{-1} sucrose were able to reach a high cell density within 2-3 days after dilution, they were transferred to SC medium with 20 g L^{-1} sucrose for further evolution. Within three months, all six evolution cultures were able to grow within two days in medium with 20 g L^{-1} sucrose. Single colonies were then isolated and the evolved *MAL11* genes were amplified and sequenced (Figure 2.1B).

The *MAL11* expression plasmids were purified from the evolved single colony isolates and introduced into the unevolved IMZ630 (suc$^-$, *LmSPase*) background. All strains displayed wildtype-like growth in medium containing 20 g L^{-1} glucose (Figure 2.1C) and were able to grow well on medium containing 20 g L^{-1} sucrose (Figure 2.1D), showing that the suppressor mutations in Mal11 are responsible for the gain of function.

Mapping of the additional mutations that arose during evolution onto a homology model of Mal11 (Henderson and Poolman, 2017) uncovered that, although the two residues Ala-384-Asp (TM7) and Ala-515-Asp (TM11) are located on different helices, they are both found in the central cavity of the protein, on helix faces oriented inwardly, and are at the same height along the transport pathway. Importantly, they are also all in close proximity to the three mutated acidic residues E120 (TM1), D123 (TM1), and E167 (TM4) (Figure S2.4): Using E167 as a central reference point, the distance to A384 and A515 are 7.6 Å and 9.7 Å, respectively. The other two mutations, Arg-504-Cys (TM11) and Trp-376-Ser (TM7), are located at the bottom of the central cavity, on adjacent helices in the structure, facing inwardly, and are at the same height along the transport pathway (Figure 2.1E-G, Figure S2.4). Notably, Arg-504 is the only basic residue in the transmembrane region of Mal11 and is the only charged residue remaining in the central cavity of the uncoupled triple mutants.

Coupling mechanism of evolved Mal11 mutants

To investigate whether the additional mutations altered the transport mechanism of the mutants, each Mal11 protein was tagged with fluorescent YPet and overexpressed in strain IMK291, using the inducible *GAL1* promotor on a multicopy plasmid. IMK291 lacks all native disaccharide transporters and hydrolysis enzymes (suc$^-$) and has been used previously to study the mechanism of disaccharide transport (Marques *et al.*, 2018a). Visualisation of galactose-induced cells with fluorescence microscopy showed that all Mal11-YPet variants are properly localised to the periphery of the cell (Figure 2.2A).

Flow cytometry analysis indicated a roughly five-fold lower average fluorescence intensity of the fluorescent population of Mal11$_{QNA/A515D}$ compared to wildtype Mal11 (Figure S2.1). Apparently, the A515D mutation destabilized the Mal11 protein resulting in increased turnover in the yeast plasma membrane.

Next, the ability of the IMK291-derived strains for substrate uptake in the presence 1 mM radiolabelled maltose or sucrose was tested and the ratio between intra- and extracellular sugar concentrations (accumulation ratio) was determined. The results indicate that the transporters that evolved a new acidic residue in the central cavity (Mal11$_{QAQ/A384D}$ and Mal11$_{QNA/A515D}$) could accumulate both sugars inside the cell (accumulation ratio >1), suggesting a restored proton-coupled transport mechanism (Figure 2.2B). The second group of mutants (Mal11$_{QAQ/R504C}$ and Mal11$_{ANA/W376S}$) could not accumulate either sugar within 45 minutes, which
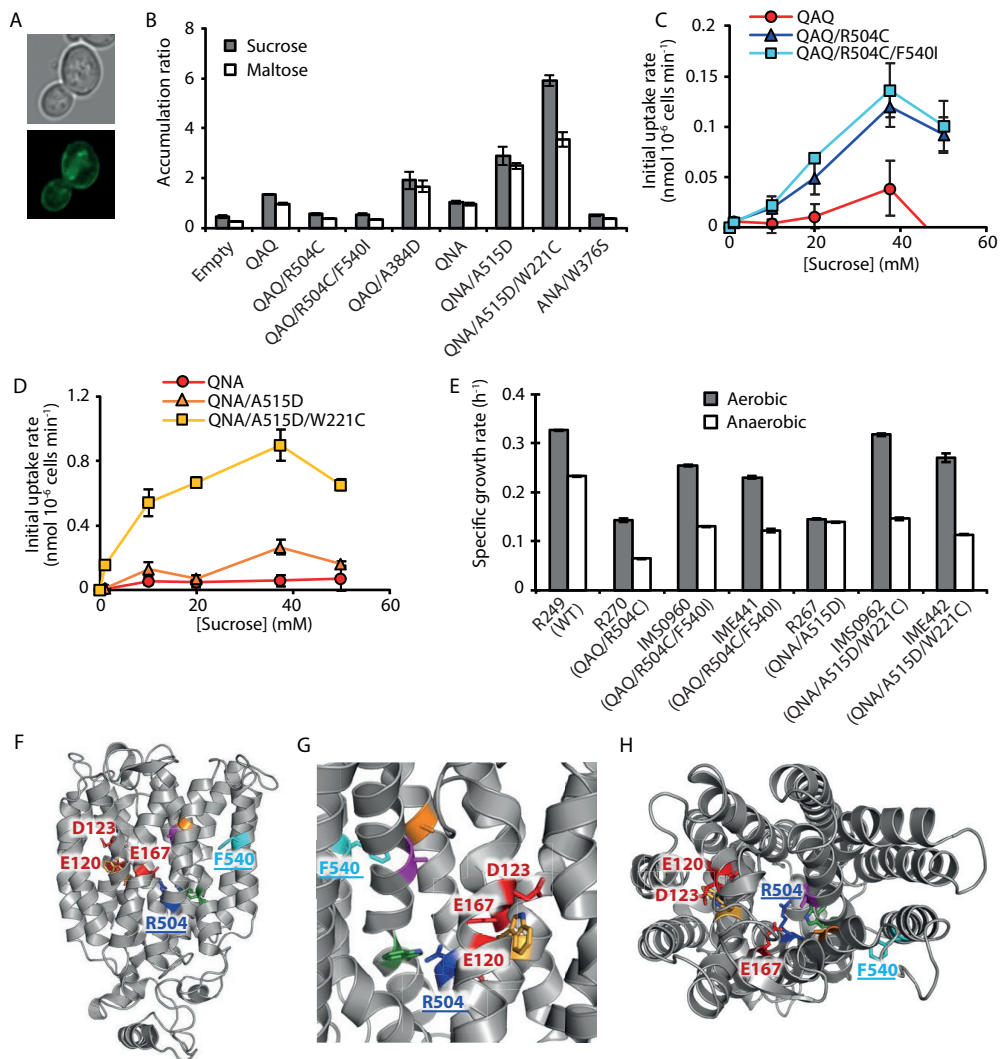
Figure 2.2: Transport characteristics of evolved and unevolved Mal11 triple mutants. A: Representative confocal fluorescence microscopy image of IMK291 strains expressing wildtype and mutant Mal11-YPet from the *GAL1* promoter on pRHA00L-based plasmids, including brightfield (top) and fluorescence (bottom) image. B: Uptake of 1 mM ^{14}C-maltose and 1mM ^{14}C-sucrose after 30 min. Bars and error bars represent the average and standard deviation, respectively, of triplicate measurements. C, D: Concentration dependence of sucrose transport by unevolved and evolved Mal11 transporters. Cells were equilibrated at 30 °C for 10 minutes before addition of 1, 5, 25, 37.5, and 50 mM ^{14}C-sucrose. After 1 or 2 min of incubation, cells were filtered and the amount of intracellular radioactivity was determined to calculate the initial transport rate. Points and error bars represent the background-subtracted average and standard deviation, respectively, of triplicate measurements. E: Aerobic and anaerobic specific growth rates of strains carrying variants of Mal11, including single colony isolates from anaerobic chemostats (IMS0960 and IMS0962) and their corresponding reverse engineered strains (IME441 and IME442) in shake flasks containing SM with 20 g L^{-1} sucrose. Growth rates were calculated from optical density measurements from at least five data points in the exponential phase. Data represent average values and mean deviations of duplicate experiments. F, G, H: Structural model of Mal11 (Henderson and Poolman, 2017) highlighting the location of the introduced and evolved mutations of the QAQ/R504C/F540I mutant. A structural model with the location of mutations in QNA/A515D/W221C is shown in Figure S2.5.

could be an indication of a very low transport rate at low substrate concentrations or energy-independent sugar import. From each group of mutants, the initial rates of transport of the Mal11 mutants derived from a fast-growing strain (Mal11$_{QAQ/R504C}$ and Mal11$_{QNA/A515D}$) (Figure 2.1D) at a range of sucrose concentrations were compared to that of their corresponding unevolved triple mutant. Transport measurements with ≥50 mM sucrose were obscured by the background signal, and therefore kinetic parameters K_M and V_{max} could not be estimated. However, important trends are visible in the data obtained at lower sucrose concentrations. While at 1 mM sucrose there was little difference in the initial rates between the strains expressing no Mal11 (negative control), Mal11$_{QAQ}$ and Mal11$_{QAQ/R504C}$, at 20 mM sucrose, the rate of transport of strains expressing Mal11$_{QAQ/R504C}$ (0.069 ± 0.016 nmol 10^{-6} cells min^{-1}) was six-fold higher (p-value < 0.05) than that of Mal11$_{QAQ}$ (0.011 ± 0.012 nmol 10^{-6} cells min^{-1}) (Figure 2.2C). The increased uptake rate of sucrose at higher concentrations is most likely the result of the selection for mutants able to catalyse fast transport under high-substrate conditions. Similarly, initial transport rates of strains expressing unevolved Mal11$_{QNA}$ were low compared to those of strains expressing Mal11$_{QNA/A515D}$ (Figure 2.2D).

Consequences of uncoupled transport on cellular energetics

Strains in which sucrose transport is proton coupled require subsequent extrusion of the proton via the plasma membrane H$^+$-ATPase (Pma1), resulting in a net expense of 1 ATP per transported sucrose (Figure 2.3A). To analyse the effect of the energy coupling mechanism on cellular energetics and strain physiology, a fast-growing uncoupled mutant, R270 (Mal11$_{QAQ/R504C}$) and proton-coupled mutant, R267 (Mal11$_{QNA/A515D}$) (Figure 2.1D) were selected for further analysis with respect to their impact on the energetic efficiency of sucrose dissimilation. For this purpose, the strains are preferentially grown under anaerobic conditions, where the theoretical difference in the energetic efficiency of sucrose dissimilation between sucrose-proton symport and uniport would be 25% (increase from 4 ATP to 5 ATP per sucrose) and result in a 25% increased biomass yield.

To avoid growth-rate dependent effects, the strains were characterized in anaerobic steady-state chemostat cultures. In the preceding batch phase, the maximum specific growth rates were 0.33 ± 0.00 h^{-1} for R249 (wildtype Mal11), 0.09 ± 0.00 h^{-1} for R270 (Mal11$_{QAQ/R504C}$) and 0.17 ± 0.00 h^{-1} for R267 (Mal11$_{QNA/A515D}$) (Figure S2.2). Based on these growth rates, we decided to operate the chemostats at a constant dilution rate of 0.07 h^{-1} and samples were taken once steady state conditions were reached. In steady state, the biomass yield of R270 (Mal11$_{QAQ/R504C}$) was 0.095 ± 0.002 g biomass g sucrose^{-1}, which is ~9% higher (p-value = 0.09) than that of the reference strain R249 (Mal11, 0.087 ± 0.002 g biomass g sucrose^{-1}). Surprisingly, the biomass yield of R267 (Mal11$_{QNA/A515D}$, 0.060 g biomass g sucrose^{-1}) was ~31% lower than that of R249 (Figure 2.3B). These apparent differences in energetic efficiency are reflected in the biomass specific rates of sucrose uptake and ethanol plus CO_2 production, as the energetic efficiency of sugar dissimilation dictates the rate of sucrose dissimilation to ethanol and CO_2 to provide ATP for biomass formation at identical growth rates. Overall, the data suggest that the energetic efficiency of R270 (Mal11$_{QAQ/R504C}$) is increased and that of R267 (Mal11$_{QNA/A515D}$) is decreased compared to R249 (wildtype Mal11).

We then investigated the basis for the lower than expected increase in biomass yield (9 versus 25%) of R270. To this end, we first determined the extracellular concentration of glucose-1-phosphate, which could be formed when sucrose phosphorylase (LmSPase) is released from the cells. Extracellular sucrose phosphorolysis would lead to extracellular glucose-
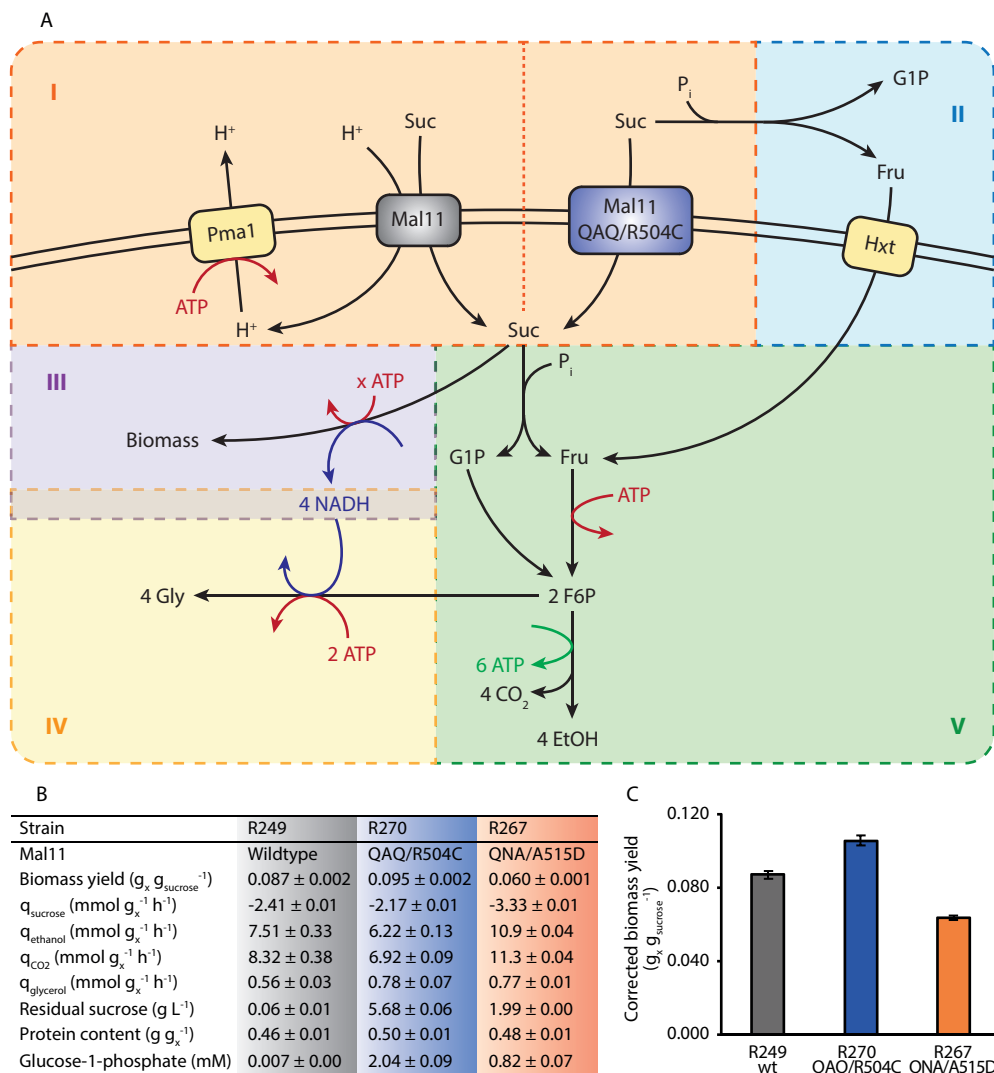
Figure 2.3: Energetic efficiency of sucrose metabolism. A: Schematic representation of sucrose metabolism in R249, R270 and R267. I: Proton-coupled sucrose transport requires the expense of one ATP per sucrose for extrusion of the co-transported proton by Pma1. II: Extracellular sucrose phosphorylase activity leads to extracellular formation of G1P, which cannot be imported, and fructose, imported by Hxt transporters, resulting in an overall yield of 2 ATP per sucrose. III: Biomass formation requires biomass-composition-dependent investment of ATP. IV: Glycerol formation to re-oxidize NADH from biosynthesis requires sucrose for carbon (0.25 mol Suc mol Gly^{-1}) and ATP (depending on Suc transport mechanism, either 1 or 0.75 mol ATP mol Gly^{-1}). V: Intracellular sucrose dissimilation to ethanol by sucrose phosphorylase and glycolysis, yielding 5 ATP per sucrose. Suc = sucrose, Fru = fructose, G1P = glucose-1-phosphate, F6P = Fructose-6-phosphate, Gly = glycerol, EtOH = ethanol. B: Growth characteristics of R249, R270 and R267 in sucrose-limited anaerobic chemostat cultures at a dilution rate of 0.07 h^{-1}. Biomass-specific production and consumption rates are depicted as q$_{metabolite}$. The data represent average values and mean deviations obtained from duplicate experiments. C: Biomass yields after correction for 1) increased glycerol production, 2) extracellular sucrose phosphorylase and 3) increased protein content. R249 (wt Mal11) was used as reference for the corrections, hence the corrected biomass yield of this strain is identical to the measured biomass yield. Bars and error bars represent the average and mean deviations of the corrected biomass yields calculated for each duplicate experiment.

1-phosphate accumulation and fructose uptake, resulting in an overall yield of only 2 ATP per sucrose (Figure 2.3A). High glucose-1-phosphate concentrations were measured in the cultures of R270 (Mal11$_{QAQ/R504C}$, 2.04 ± 0.09 mM) and R267 (Mal11$_{QNA/A515D}$, 0.82 ± 0.07 mM) but were negligible for R249 (wildtype Mal11) (Figure 2.3B). Most likely, the higher residual sucrose concentrations observed for R270 and R267 compared to R249 (Figure 2.3B) allowed for the increased extracellular sucrose phosphorolysis rate.

Next, we quantified the effect of increased glycerol formation on the biomass yield. In anaerobic *S. cerevisiae* cultures, glycerol is formed to re-oxidize NADH generated in biosynthetic reactions (van Dijken and Scheffers, 1986). We found that the biomass specific glycerol production rates of both R267 and R270 are ~38% higher than for the reference strain (Figure 2.3B). Formation of glycerol from sucrose requires the investment of substrate in the form of carbon as well as energy (Figure 2.3A), and therefore negatively affects the biomass yield. Furthermore, the increased specific glycerol production rate at identical growth rates indicates an increased oxidation state of the biomass and a change in biomass composition. Since the protein fraction of biomass accounts for the majority of the energetic costs of biosynthesis, we determined the protein content in each of the steady-state chemostat cultures. We found that the protein content of R270 (0.50 ± 0.01 g g biomass^{-1}) and R267 (0.48 ± 0.01 g g biomass^{-1}) were increased by 10 and 5% relative to R249 (0.46 ± 0.01 g g biomass^{-1}) (Figure 2.3B). This suggests that on top of extracellular sucrose phosphorolysis and increased glycerol formation, R270 and R267, carrying engineered Mal11, also have an increased energetic cost of biomass formation.

Additional mutations in Mal11 enable fast anaerobic growth

In the anaerobic pre-cultures grown on sucrose used to inoculate the bioreactors, we observed a ~90h lag phase prior to exponential growth of strain R267 (Mal11$_{QNA/A515D}$) (data not shown), which prompted us to search for additional mutations in the *MAL11* gene of strains grown in anaerobic chemostat cultures and sampled at the end of the experiment. In addition to the four mutations in Mal11 that were initially present, R270 had gained a Phe-540-Ile mutation (Mal11$_{QAQ/R504C/F540I}$) and R267 had gained a Trp-221-Cys mutation (Mal11$_{QNA/A515D/W221C}$). Single colonies of these double-evolved cultures of R270 and R267 were isolated and named IMS0960 and IMS0962, respectively. When tested under aerobic conditions, the specific growth rates of both IMS0960 (0.25 ± 0.00 h^{-1}) and IMS0962 (0.32 ± 0.00 h^{-1}) were higher than the parental strains R270 (0.14 ± 0.00 h^{-1}) and R267 (0.15 ± 0.00 h^{-1}) (Figure 2.2E). Under anaerobic conditions, the growth rate of IMS0960 (Mal11$_{QAQ/R504C/F540I}$) was also higher (0.13 ± 0.00 h^{-1}) than its parent R270 (0.06 ± 0.00 h^{-1}), whereas the growth rates of IMS0962 (0.15 ± 0.00 h^{-1}) and R267 (0.14 ± 0.00 h^{-1}) were similar.

Next, the *MAL11*-carrying plasmids of IMS0960 and IMS0962 were introduced into the unevolved background strain IMZ630 and the growth rates under aerobic and anaerobic conditions were determined (Figure 2.2E). From the observed growth rates, it is evident that the F540I mutation in *MAL11* is solely responsible for the higher aerobic and anaerobic growth rate of IMS0960, whereas the W221C mutation decreased the lag phase in IMS0962 (Figure S2.3). Most likely, IMS0962 contains another (genomic) mutation responsible for the increased anaerobic growth rate compared to IME442.

To examine whether the additional F540I and W221C mutations changed the transport mechanism, genes encoding Mal11$_{QAQ/R504C/F540I}$ and Mal11$_{QNA/A515D/W221C}$ were also expressed in IMK291 and the ability of the resulting strains to accumulate maltose or sucrose was

investigated using radiolabelled substrates (Figure 2.2B). Mal11$_{QNA/A515D/W221C}$ was able to accumulate both sugars and no sugar accumulation was observed in the strains expressing Mal11$_{QAQ/R504C/F540I}$, which indicates that the transport mechanism of both transporters was not altered by the acquisition of the fifth mutation. The initial transport rates of Mal11$_{QAQ/R504C/F540I}$ at 1 and 20 mM sucrose were comparable to that of Mal11$_{QAQ/R504C}$ (Figure 2.2C), whereas the W221C mutation improved the transport rates compared to Mal11$_{QNA/A515D}$ (Figure 2.2D). Flow cytometry analysis indicated that unlike Mal11$_{QNA/A515D}$, the average fluorescence intensity of the fluorescent population expressing Mal11$_{QNA/A515D/W221C}$ was similar to that of the mutants (Figure S2.1). Apparently, the W221C mutation resolved the issue of Mal11 protein expression or instability in the membrane that resulted from the A515D mutation. The increased influx of sucrose by this stabilized Mal11 variant could also explain the reduced lag phase when cells are transferred from aerobic to anaerobic conditions. A low expression level would not be expected to affect steady-state accumulation levels of sucrose in the IMK291 background but would impact initial uptake rates, which is in accordance with the results shown in Figure 2.2D.

2.4 Discussion

In previous work, the proton relay network of Mal11 consisting of Glu-120, Asp-123, and Glu-167 was studied and mutants with an uncoupled transport mechanism were characterized (Henderson and Poolman, 2017). Here, we have expanded on that work by discovering a number of second-site suppressor mutations in Mal11 required for efficient growth of *S. cerevisiae* on sucrose. We identified three suppressor mutants that regained sugar-proton symport activity and two mutants that were still uncoupled. The effect of one coupled and one uncoupled variant of Mal11 on the energetic efficiency of yeast was investigated in anaerobic chemostats. We show that proton-decoupled transport of sucrose allows this yeast to dissimilate sucrose in an energetically more efficient way, but the engineered proteins come with additional phenotypic effects, resulting in an altered biomass composition and extracellular metabolite profile.

Suppressor analysis yields two classes of mutants

Analysis of second-site suppressors arising from evolution studies is a powerful tool for biochemists to study the relationship between protein sequence and function and has a long history of use in transporters, because structural information is directly linked to functional data (Arastu-Kapur *et al.*, 2005; Jessen-Marshall *et al.*, 1997; Pazdernik *et al.*, 1997; Pi *et al.*, 2002; Saraceni-Richards and Levy, 2000). The evolution experiment under aerobic conditions gave rise to two types of mutants. One type contained mutations in which a new acidic residue replaced a neutral residue in the upper portion of the central cavity (A384D, A515D) and in the other type a mutation to a residue below the binding site occurred (W376S, R504C) (Figure 2.1B, E-G). The new acidic aspartate residues in the evolved transporters are all located one helix-turn above Glu-167, at the top of the central cavity (Figure 2.1E-G), and all three Mal11 variants are capable of active sucrose uptake (Figure 2.2B). Apparently, proton coupling in the uncoupled triple mutants can be restored via the introduction of a single acidic residue in the vicinity of the sugar-binding cavity and there is flexibility in terms of the exact position of the residue.

The second class of mutants (W376S, R504C) hints at a cytoplasmic gate of the transporter that alternately seals and opens the central cavity from the cytoplasm and thereby controls

the release of substrate, a molecular mechanism previously suggested for Major Facilitator Superfamily transporters based on the amassed body of crystal structures (Quistgaard *et al.*, 2016). Such a gate could potentially involve Arg-504, which is located in close proximity to Glu-167 at the bottom of the central cavity.

Modelling of the data: class I mutants

Based on the localization and transport properties of the acidic residue mutants and the evolved second-site suppressors, we propose a model of proton-coupled sugar transport by Mal11 (Figure 2.4A). Although there is insufficient evidence to suggest whether sugar and proton binding is ordered, we propose the following mechanism: Glu-167 becomes protonated and sugar binds to outward-facing Mal11 and induces closure of the extracellular gate; Arg-504 is then released from the inter-domain salt-bridge with Glu-167 and is free to swing away from the transport path to interact with Trp-376, opening the cytoplasmic side of the protein; the inward-facing transporter then releases the sugar and proton, at which point Glu-167 and Arg-504 are available for interaction with each other and the inward-to-outward switch is once again permitted.

This model can be used to explain the phenotypes of the *S. cerevisiae* strains expressing mutated transporters. The unevolved triple mutants lack Glu-167, meaning no salt bridge can form with Arg-504, which makes the outward-facing conformation less favorable compared to the inward-facing state (Figure 2.4B). With the conformational probability shifted towards the inward-facing state, there is an unchanged or increased likelihood of sugar binding at the intracellular face of Mal11. Such a mechanism explains why the triple mutants have slow sugar influx (Figure 2.2C, D) but demonstrate wildtype-like efflux and exchange (Henderson and Poolman, 2017).

The evolved Asp residues one helix-turn above Gln- or Ala-167 may serve to facilitate closure of the extracellular gate upon substrate binding and may even bind substrate due to their position at the top of the central cavity (Figure 2.4C). Arg-504 is likely too far away from the evolved Asp for salt-bridge formation, so the outward-facing conformation remains unfavorable compared to the wildtype. Protonation and interaction of the evolved acidic residue with the substrate would stabilize the outward-facing conformation and promote closure of the top of the transporter.

Protonation-based closure of the transporter would provide a mechanism for leaky proton coupling and may even create an EH-leak (proton leak) pathway (Henderson *et al.*, 2019b; Lolkema and Poolman, 1995). In a cellular context, such a proton leak pathway would result in a net energetic cost of 1 ATP per proton and could contribute to the low biomass yield of R267 (Mal11$_{QNA/A515D}$), which was ~31% lower than the well coupled wildtype Mal11-expressing strain R249 (Figure 2.3B). The anaerobic cultivation of R267 led to mutation of a central cavity residue, W221C. An isogenic population carrying this additional mutation (IMS0961) exhibited a ~79% reduced lag phase under anaerobic conditions (Figure S2.3). From fluorescence measurements of YPet-tagged constructs, the W221C mutation appeared to vastly increase the protein abundance level of transporter in the membrane (Figure S2.1) and doubled the accumulation level of the sugar (Figure 2.2B). The additional mutation may play a predominantly structural, rather than catalytic, role.
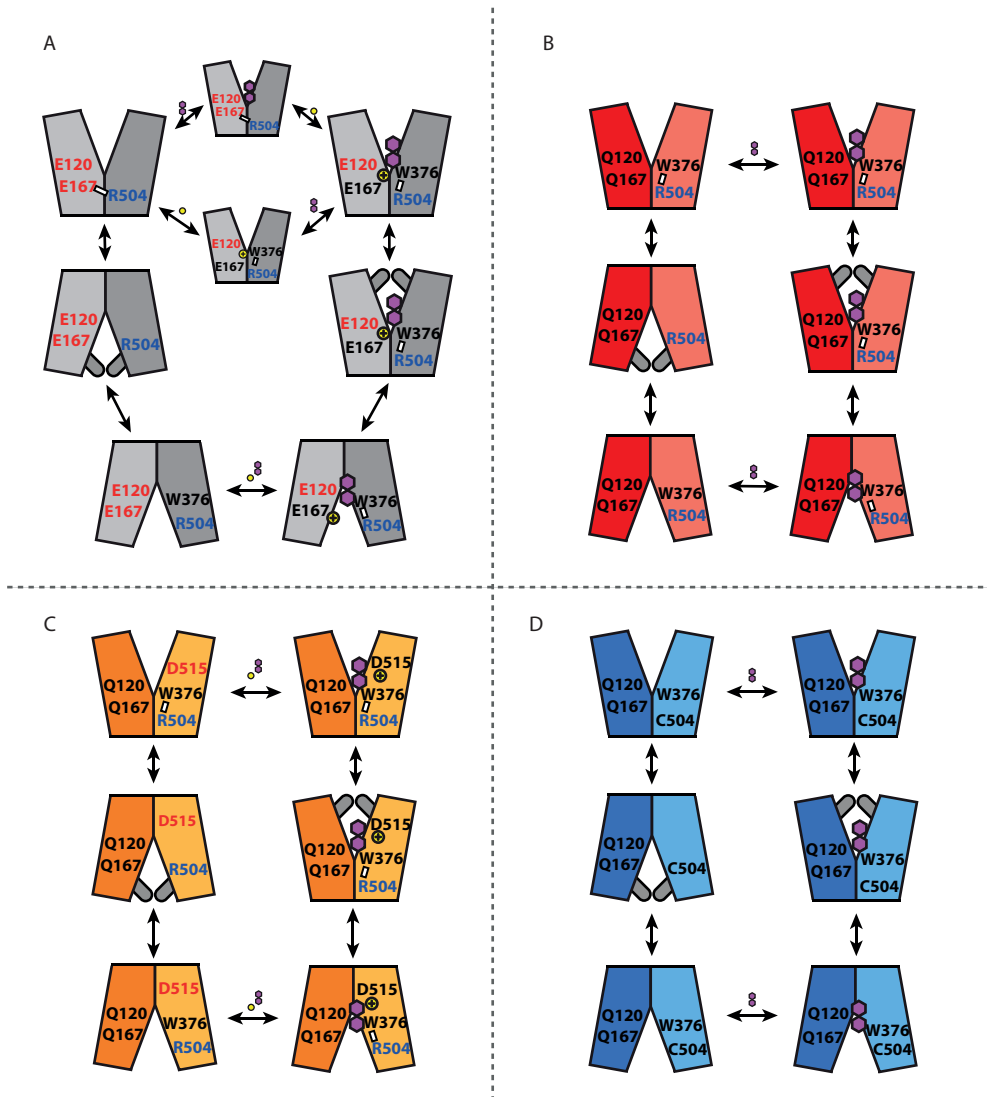
Figure 2.4: Model of proton-coupled transport by Mal11. A: In the wildtype transporter, the cycle of conformational changes is regulated by the alternate interactions of Arg-504 with Glu-167 or Trp-376. In the outward-facing conformation, binding of a proton (yellow circle) to Glu-167 releases Arg-504 and permits interaction with Trp-376. Binding of sugar (pink hexagons) causes the extracellular gate to close around the substrate. With both sugar and proton bound, the transporter switches to an inward-facing conformation and releases its substrates before returning to an outward-facing conformation. B: In the triple mutant transporters (only Mal11$_{QAQ}$ is shown), the salt-bridge between Glu-167 and Arg-504 can no longer form, and without transmembrane acidic residues the transporters are no longer proton-coupled. Thus, only sugar is transported via uniport. C: In the triple mutants with an evolved aspartate residue (Mal11$_{QAQ/A384D}$, and Mal11$_{QNA/A515D}$), the acidic residue facilitates closure of the extracellular gate of the protein. This makes the conformational transitions occur more rapidly than in the triple mutants. However, with the evolution of a central cavity acidic residue comes (partial) restoration of proton-coupled transport. D: The evolved triple mutants with a mutation at the bottom of the central cavity (Mal11$_{QAQ/R504C}$ and Mal11$_{ANA/W376S}$; only Mal11$_{QAQ/R504C}$ is shown), both interactions (Glu-167 with Arg-504 and Trp-376 with Arg-504) governing proton-coupled conformational changes are disrupted and thus conformational changes may be more flexible. Without a protonatable residue in the central cavity, proton binding cannot occur and thus the transporter is uncoupled, as in the triple mutants.

Modelling of the data: class II mutants

In the second class of evolved mutants (Mal11$_{QAQ/R504C}$ and Mal11$_{ANA/W376S}$), both interactions that mediate proton coupling in the wildtype transporter have been disrupted (Figure 2.4D). Without the interaction between Arg-504 and Trp-376, the inward-facing conformation becomes less favourable than in the unevolved triple mutants, which increases the likelihood of the outward-facing conformation. This could result in an increased opportunity for extracellular sucrose binding and transport in Mal11 variants unable to bind and transport protons, due to a lack of acidic residues in the central cavity. Sucrose uptake studies indicated that both Mal11$_{QAQ/R504C}$ and Mal11$_{ANA/W376S}$ appear to be fully uncoupled (Figure 2.2B) and behave as sugar uniporters, which is in accordance with the transport model presented here.

After anaerobic cultivation, an additional mutation arose, F540I, which was located at a helix-helix interface away from the central cavity. While this mutation did not have any distinct effect on the accumulation level (Figure 2.2B), initial transport rates (Figure 2.2C) or expression level (Figure S2.1), the *S. cerevisiae* strain expressing Mal11$_{QAQ/R504C/F540I}$ grew significantly faster than the Mal11$_{QAQ/R504C}$ mutant (Figure 2.2E). We speculate that the F540I mutation may have increased the protein stability (less protein turnover), therefore resulting in improved overall growth performance.

Biomass yield and energetic efficiency

Expression of the uncoupled Mal11$_{QAQ/R504C}$ in a sucrose-phosphorylase-expressing strain was expected to result in a 25% increase in biomass yield compared to a strain expressing the proton-coupled wildtype Mal11, corresponding to an increase in energetic efficiency of 4 to 5 ATP per sucrose (Marques *et al.*, 2018a). However, in steady-state chemostat cultures the biomass yield of R270 (Mal11$_{QAQ/R504C}$) was increased by only 9% (p=0.09) compared to the reference strain (wildtype Mal11). Three possible contributors to this lower-than-expected biomass yield were identified: (i) increased extracellular sucrose phosphorolysis; (ii) increased specific glycerol formation rates; and (iii) an increased biomass protein content (Figure 2.3A). The increased glycerol production is most likely linked to the increased protein content, as synthesis of amino acids from sugars is the major NADH yielding process in *S. cerevisiae* cells (Verduyn *et al.*, 1990b).

To determine whether these observed effects could fully explain the low yield, we estimated the biomass yields that would have been achieved by R270 if it would display a similar growth phenotype as the control strain R249 (wildtype Mal11) (see Biomass yield calculations in Material and methods section). With these assumptions, the 'corrected' biomass yield of R270 would be 0.106 ± 0.03 g g^{-1} sucrose, which is a $21.3 \pm 2.9\%$ increase relative to R249 and close to the predicted value of 25% (p-value < 0.05) (Figure 2.3C). A fourth factor that could explain the remaining 5% is increased cellular maintenance due to increased protein turnover as a result of a higher protein content (Canelas *et al.*, 2010; Hong *et al.*, 2012; van Bodegom, 2007). Finally, we cannot rule out the possibility that proton-leakage through the uncoupled Mal11$_{QAQ/R504C}$ transporter causes additional consumption of ATP, and thus leads to a lower biomass yield in this strain.

Application of engineered transporters for industrial strains

The data and analysis of energy coupling mechanisms in metabolite transport presented in this

work can be applied for future design of other energy-efficient transporters to improve product yields and volumetric productivity in the biotechnological industry. When we account for increased glycerol formation, extracellular phosphorolysis of sucrose and a change in biomass composition, Mal11$_{QAQ/R504C}$ has increased the energetic efficiency of sucrose dissimilation by 21%. For industrial application of this engineered transporter, the aforementioned factors that limit its beneficial impact on final product yields will have to be addressed. Although we have not identified clear metabolic engineering targets to resolve the increased protein content, glycerol production and extracellular phosphorolysis, we propose a directed evolution strategy for further optimization of yeast strains expressing Mal11$_{QAQ/R504C}$ as a next step. To avoid the emergence of new acidic residues that restore proton coupling, it is essential that a selective pressure on ATP-independent sucrose transport is maintained. Since combined use of a sucrose uniporter and phosphorylase theoretically increases the ATP yield of anaerobic sucrose dissimilation (to ethanol) to 2.5 ATP per hexose equivalent, which is higher than the 2 ATP obtained from anaerobic dissimilation of glucose, a strain design resulting in a 'zero ATP pathway' on glucose could be used to enable such an evolutionary strategy. This strategy could for example be achieved in an engineered homo-fermentative lactic acid producing *S. cerevisiae* strain, where the conversion of sucrose to lactic acid only conserves ATP when energy-independent sucrose transport is maintained (van Maris *et al.*, 2004).

The design and construction of yeast strains able to catalyze energetically efficient uptake and conversion of polysaccharides has the potential to improve industrial production of energy requiring (assimilatory) products. Furthermore, by exceeding the energetic efficiency (per hexose equivalent) of glucose utilization, energy-efficient polysaccharide utilization could also enable anaerobic production of products whose biosynthetic pathway from glucose does not provide ATP for cellular maintenance and growth (van Maris *et al.*, 2004; van Rossum *et al.*, 2016; Zelle *et al.*, 2008). While we focused on sucrose, an important industrial sugar predominantly derived from sugarcane (Marques *et al.*, 2015), we hypothesize that our proposed model could be applied in the design of improved cell factories on other carbon substrates. For example, for other oligosaccharides, such as maltose, cellobiose, trehalose, cellodextrin and lactose, phosphorylases have already been described (Alexander, 1968; Belocopitow and Maréchal, 1970; de Groeve *et al.*, 2009; de Kok *et al.*, 2011; Sadie *et al.*, 2011; Sheth and Alexander, 1967), whereas a uniporter has only been described for cellobiose (Kim *et al.*, 2014). In addition, even when future research leads to the identification of additional polysaccharide uniporters in other organisms, expression of heterologous transporters in microbial cell factories remains a significant challenge (Marques *et al.*, 2018a; Marques *et al.*, 2018b). Therefore, a combination of rational engineering, for which our model could act as a starting point, and evolutionary engineering of endogenous transporters could be a valuable alternative strategy to obtain improved transporters. For example, de Kok *et al.* (2011) proposed a strategy for trisaccharide utilization which could yield even more ATP per hexose unit (2.67 ATP), requiring a maltotriose uniporter and a maltose and maltotriose phosphorylase (de Kok *et al.*, 2011). While a maltotriose uniporter has thus far not been identified in nature, a recent evolution study revealed that a maltotriose transporter could evolve by combination of multiple maltose transporters in *Saccharomyces eubayanus* (Brouwers *et al.*, 2018). Since the resulting chimeric transporter has a high sequence similarity to *S. cerevisiae MAL11*, our evolved Mal11$_{QAQ/R504C}$ transporter provides valuable insights that can be applied to engineer the coupling mechanism of the chimeric maltotriose transporter.

Conclusion

We show that proton coupling in sugar transport by Mal11 requires a single acidic residue but the protein tolerates various locations for these residues around the sugar-binding site. On the basis of our mutant analysis and functional studies, and building on previous structural studies, we propose a model for energy coupling in the *S. cerevisiae* Mal11 disaccharide transporter. Furthermore, we demonstrate that a combination of targeted protein engineering and subsequent evolutionary engineering results in a sucrose facilitator, as a starting point to engineer energy-efficient yeast strains with increased yields of industrially relevant products.

2.5 Acknowledgements

2.6 Supplementary information
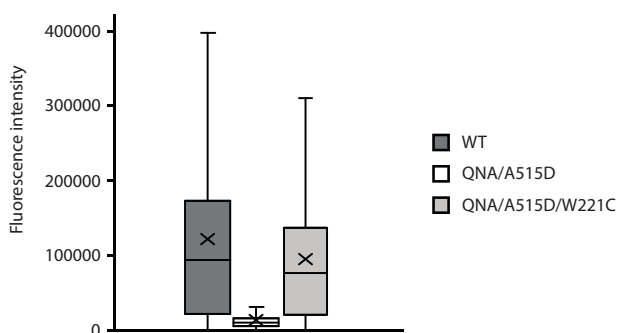
Figure S2.1: Flow cytometry analysis of cells expressing YPet-tagged variants of Mal11. Values lower than 3 times the average fluorescence intensity of IMK291 with an empty vector were disregarded to filter out non-fluorescent cells.
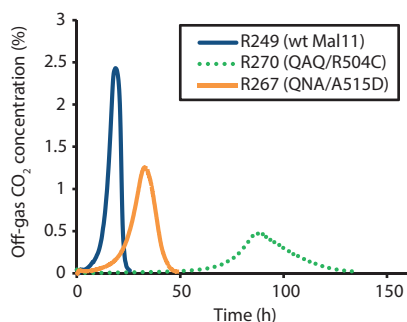
Figure S2.2: CO_2 concentration in the off-gas of reactors during anaerobic batch cultivation of strains carrying different variants of Mal11. Strains were grown on synthetic medium with 25 g L^{-1} sucrose. Data show one representative trace from two independent duplicate experiments. Increased 'tailing' towards the end of the batch phase was observed for R267 and R270, indicating a decreasing growth rate at the end of the batch phase. This effect is most likely caused by the low affinity for sucrose by R267 and R270 compared to the reference strain R249, causing a decreased growth rate at the low sucrose concentrations at the end of the batch phase.
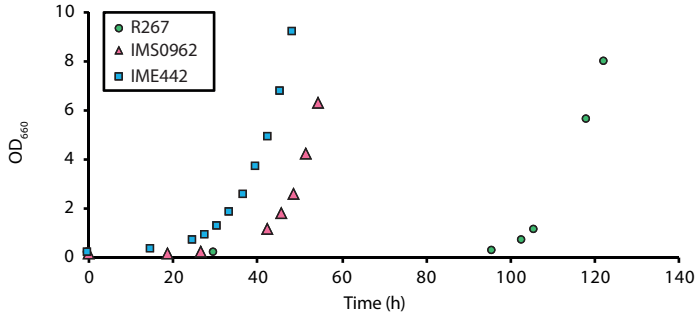
Figure S2.3: Anaerobic growth of *S. cerevisiae* carrying Mal11$_{QNA/A515D}$ (R267) and Mal11$_{QNA/A515D/W221C}$ (single colony isolate from anaerobic chemostat culture: IMS0962; reverse engineered: IME442). Cells were grown in shake flasks containing synthetic medium with 20 g L^{-1} sucrose as the sole carbon source. One representative dataset of two independent duplicate experiments is shown.
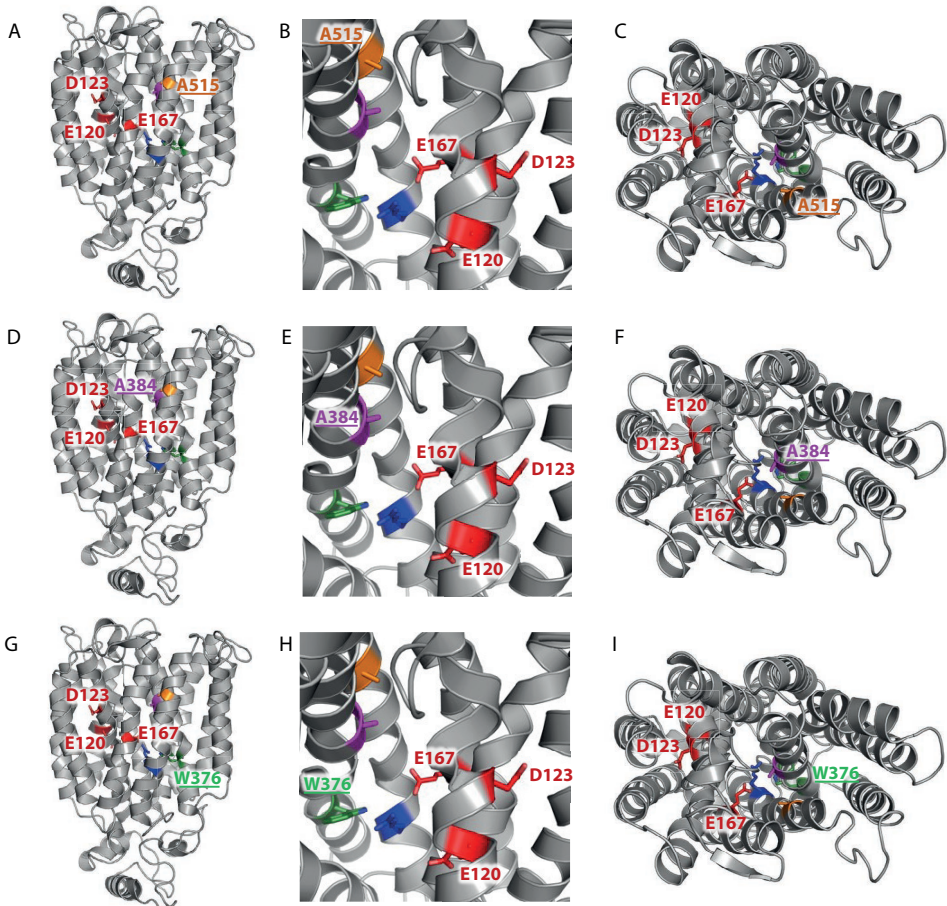
Figure S2.4: Structural model of Mal11 (Henderson and Poolman, 2017) highlighting the location of the introduced mutations and the evolved mutations during construction of triple mutants and directed evolution on sucrose, showing mutants QNA/A515D (A-C), QAQ/A384D (D-F) and ANA/W376S (G-I).
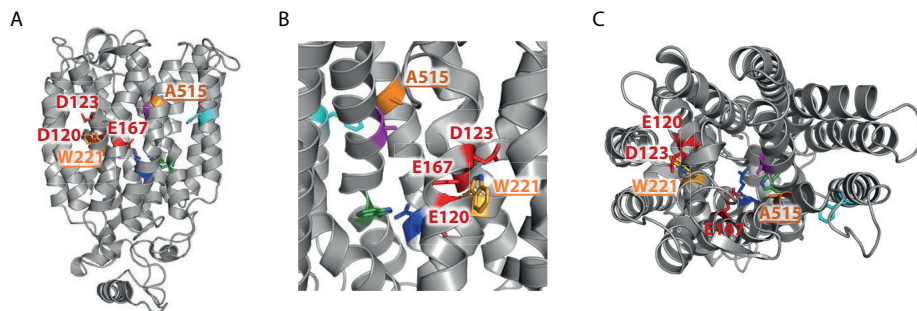
Figure S2.5: Structural model of Mal11 (Henderson and Poolman, 2017) highlighting the location of the introduced mutations and the evolved mutations during construction of triple mutants, directed evolution on sucrose and anaerobic growth, showing mutant QNA/A515D/W221C.

Table S2.1: Strains used in this study

Name	Relevant genotype	Parental strain	Origin
IMZ627	*MATa ura3-52 LEU2 MAL2-8C malΔ mphΔ suc2Δ ima1Δ ima2Δ ima3Δ ima4Δ ima5Δ sga1Δ:: MAL12*	IMZ616	(Marques *et al.*, 2018a)
IMZ630	*MATa ura3-52 LEU2 MAL2-8C malΔ mphΔ suc2Δ ima1Δ ima2Δ ima3Δ ima4Δ ima5Δ sga1Δ:: LmSPase*	IMZ616	(Marques *et al.*, 2018a)
IMK291	*MATa leu2-112 ura3-52 MAL2-8C malΔ mphΔ suc2Δ*	IMK289	(Marques *et al.*, 2017)
R248	IMZ630 pR240 (*URA3*)	IMZ630	This study
R249	IMZ630 pUDE496 (*URA3 PGM2 MAL11*)	IMZ630	This study
R250	IMZ630 pR242 (*URA3 PGM2 MAL11*$_{QAQ}$)	IMZ630	This study
R252	IMZ630 pR244 (*URA3 PGM2 MAL11*$_{ANA}$)	IMZ630	This study
R254	IMZ630 pR246 (*URA3 PGM2 MAL11*$_{QNA}$)	IMZ630	This study
R265	IMZ630 pR250E05-1(evolved plasmid; *URA3 PGM2 MAL11*$_{QAQ/A384D}$)	IMZ630	This study
R267	IMZ630 pR254L04-1 (evolved plasmid; *URA3 PGM2 MAL11*$_{QNA/A515D}$)	IMZ630	This study
R270	IMZ630 pR250L041-3 (evolved plasmid; *URA3 PGM2 MAL11*$_{QAQ/R504C}$)	IMZ630	This study
R274	IMZ630 pR252L03-2 (evolved plasmid; *URA3 PGM2 MAL11*$_{ANA/W376S}$)	IMZ630	This study
IMS0960	*MATa ura3-52 LEU2 MAL2-8C malΔ mphΔ suc2Δ ima1Δ ima2Δ ima3Δ ima4Δ ima5Δ sga1Δ:: LmSPase* pR250L041-3 (*URA3 PGM2 MAL11*$_{QAQ/R504C/F540I}$) (single colony isolate from evolution)	R270	This study
IMS0962	*MATa ura3-52 LEU2 MAL2-8C malΔ mphΔ suc2Δ ima1Δ ima2Δ ima3Δ ima4Δ ima5Δ sga1Δ:: LmSPase* pR252L03-2 (*URA3 PGM2 MAL11*$_{QNA/A515D/W221C}$) (single colony isolate from evolution)	R267	This study
IME441	IMZ630 pUDE862 (*URA3 PGM2 MAL11*$_{QAQ/R504C/F540I}$)	IMZ630	This study
IME442	IMZ630 pUDE864 (*URA3 PGM2 MAL11*$_{QNA/A515D/W221C}$)	IMZ630	This study
IMX1090	IMZ627 pUDE466 (*URA3 MAL11*$_{QNQ}$-YPet)	IMZ627	This study
R275	IMK291 pR275 (*LEU2 MAL11*$_{QAQ/A384D}$-YPet)	IMK291	This study
R276	IMK291 pR276 (*LEU2 MAL11*$_{QNA/A515D}$-YPet)	IMK291	This study
R277	IMK291 pR277 (*LEU2 MAL11*$_{QAQ/R504C}$-YPet)	IMK291	This study
R278	IMK291 pR278 (*LEU2 MAL11*$_{ANA/W376S}$-YPet)	IMK291	This study
R285	IMK291 pR285 (*LEU2 MAL11*$_{QAQ/R504C/F540I}$-YPet)	IMK291	This study
R286	IMK291 pR286 (*LEU2 MAL11*$_{QNA/A515D/W221C}$-YPet)	IMK291	This study
R300	IMK291 pRHA00L (*LEU2 MAL11-YPet*)	IMK291	This study
R301	IMK291 pRHA00L0 (*LEU2*)	IMK291	This study
R302	IMK291 pR113 (*LEU2 MAL11*$_{QAQ}$-YPet)	IMK291	This study
R303	IMK291 pR118 (*LEU2 MAL11*$_{QNA}$-YPet)	IMK291	This study

2

Table S2.2: Plasmids used in this study

Plasmid	Relevant characteristics	Source
pUDE496	2µm *URA3 pTEF1-MAL11-tCYC1 pTPI1-PGM2-tTEF1*	(Marques *et al.*, 2018a)
pR170	2µm *URA3 pTEF1-MAL11$_{QNQ}$-YPet-tCYC1*	This study
pR119	2µm *URA3 pTEF1-MAL11$_{QNQ}$-TEV-YPet-his-tCYC1*	(Henderson and Poolman, 2017)
pUDE379	2µm *amdSYM pTEF1-MAL11-tCYC1*	(Marques *et al.*, 2018a)
pRHA00L	2µm *LEU2 pGAL1-MAL11-TEV-YPet-his-tCYC1*	(Henderson and Poolman, 2017)
pRHA00L0	2µm *LEU2*	(Henderson and Poolman, 2017)
pUDE466	2µm *URA3 pTEF1-MAL11$_{QNQ}$-tCYC1*	This study
pUDE453	2µm *URA3 pTEF1-MAL11-YPet-tCYC1*	(Marques *et al.*, 2018a)
pUDE862	2µm *URA3 pTEF1-MAL11$_{QAQ/R504C/F540I}$-tCYC1 pTPI1-PGM2-tTEF1*	This study
pUDE864	2µm *URA3 pTEF1-MAL11$_{QNA/A515D/W221C}$-tCYC1 pTPI1-PGM2-tTEF1*	This study
pR226	2µm *LEU2 pGAL1-MAL11$_{QAQ}$-TEV-his-tCYC1*	(Henderson and Poolman, 2017)
pR228	2µm *LEU2 pGAL1-MAL11$_{ANA}$-TEV-his-tCYC1*	This study
pR230	2µm *LEU2 pGAL1-MAL11$_{QNA}$-TEV-his-tCYC1*	(Henderson and Poolman, 2017)
pR242	2µm *URA3 pTEF1-MAL11$_{QAQ}$-tCYC1 pTPI1-PGM2-tTEF1*	This study
pR244	2µm *URA3 pTEF1-MAL11$_{ANA}$-tCYC1 pTPI1-PGM2-tTEF1*	This study
pR246	2µm *URA3 pTEF1-MAL11$_{QNA}$-tCYC1 pTPI1-PGM2-tTEF1*	This study
pR250E05-1	2µm *URA3 pTEF1-MAL11$_{QAQ/A384D}$-tCYC1 pTPI1-PGM2-tTEF1 PGM2*	This study
pR254L04-1	2µm *URA3 pTEF1-MAL11$_{QNA/A515D}$-tCYC1 pTPI1-PGM2-tTEF1 PGM2*	This study
pR250L041-3	2µm *URA3 pTEF1-MAL11$_{QAQ/R504C}$-tCYC1 pTPI1-PGM2-tTEF1 PGM2*	This study
pR252L03-2	2µm *URA3 pTEF1-MAL11$_{ANA/W376S}$-tCYC1 pTPI1-PGM2-tTEF1 PGM2*	This study
pR275	2µm *LEU2 pGAL1-MAL11$_{QAQ/A384D}$-YPet-tCYC1*	This study
pR276	2µm *LEU2 pGAL1-MAL11$_{QNA/A515D}$-YPet-tCYC1*	This study
pR277	2µm *LEU2 pGAL1-MAL11$_{QAQ/R504C}$-YPet-tCYC1*	This study
pR278	2µm *LEU2 pGAL1-MAL11$_{ANA/W376S}$-YPet-tCYC1*	This study
pR285	2µm *LEU2 pGAL1-MAL11$_{QAQ/R504C/F540I}$-YPet-tCYC1*	This study
pR286	2µm *LEU2 pGAL1-MAL11$_{QNA/A515D/W221C}$-YPet-tCYC1*	This study
pR113	2µm *LEU2 pGAL1-MAL11$_{QAQ}$-YPet-tCYC1*	(Henderson and Poolman, 2017)
pR118	2µm *LEU2 pGAL1-MAL11$_{QNA}$-YPet-tCYC1*	(Henderson and Poolman, 2017)

Table S2.3: Primers used in this study

Primer	Sequence
580	GAATGTAAGCGTGACATAAC
1642	TTTCCCAGTCACGACGTTG
4114	GGGACCTAGACTTCAGGTTGTC
4938	TTTCGGTTAGAGCGGATGTGG
4995	AATTAACCCTCACTAAAGGG
5271	CAAGGAGAAAAAACCCCGGATTCTAGAACTAGTGGATCCCCCATGAAAAATATCATTTCATTGGTAAG
5272	GAATAATTCTTCACCTTTAGAACCTTGAAAATATAAATTTTCCCCTCCACATTTATCAGCTGCATTTAATTC
5273	GGAGGGGAAAATTTATATTTTCAAGGTTC
5274	GGGGGATCCACTAGTTCTAGAATC
5921	AAAACTTAGATTAGATTGCTATGCTTTCTTTCTAATGAGC
5959	AGGGGAAAATTTATATTTTCAAGG
5960	CATTTTGGGATCCACTAGTTCTAG

5961	TCTAGAACTAGTGGATCCCAAAATGAAAAATATCATTTCATTGG
6324	TTGTTCCCTTTAGTGAGGG
6717	CTCATTAGAAAGAAAGCATAGCAATC
7476	ATGAAAAATATCATTTCATTGGTAAGC
7477	AGTTAGACAACCTGAAGTCTAGG
7478	TACCAATGAAATGATATTTTTCATGGATCCACTAGTTCTAG
7812	TCATGTAATTAGTTATGTCACGCTTACATTC

Table S2.4: Growth characteristics of R249, R270 and R267 in sucrose-limited anaerobic chemostat cultures at a dilution rate of 0.07 h^{-1}. Biomass specific production and consumption rates are depicted as q$_{metabolite}$. The data represent average values and standard deviations obtained from duplicate experiments.

Strain	R249	R270	R267
Transporter	Wildtype Mal11	Mal11$_{QAQ/R504C}$	MAL11$_{QNA/A515D}$
Biomass yield (g$_x$ g$_{sucrose}$$^{-1}$)	0.087 ± 0.002	0.095 ± 0.002	0.060 ± 0.001
q$_{sucrose}$ (mmol g$_x$$^{-1}$ h^{-1})	-2.41 ± 0.01	-2.17 ± 0.01	-3.33 ± 0.01
q$_{ethanol}$ (mmol g$_x$$^{-1}$ h^{-1})	7.51 ± 0.33	6.22 ± 0.13	10.9 ± 0.04
q$_{CO2}$ (mmol g$_x$$^{-1}$ h^{-1})	8.32 ± 0.38	6.92 ± 0.09	11.3 ± 0.04
q$_{glycerol}$ (mmol g$_x$$^{-1}$ h^{-1})	0.56 ± 0.03	0.78 ± 0.07	0.77 ± 0.01
Protein content (g g$_x$$^{-1}$)	0.46 ± 0.01	0.50 ± 0.01	0.48 ± 0.01
Residual sucrose (g L^{-1})	0.058 ± 0.01	5.68 ± 0.06	1.99 ± 0.00
Glucose-1-phosphate (mM)	0.007 ± 0.00	2.04 ± 0.09	0.82 ± 0.07
Carbon recovery (%)	97.6 ± 0.05	98.1 ± 0.10	97.8 ± 0.03
Actual dilution rate (h^{-1})	0.072 ± 0.00	0.070 ± 0.00	0.068 ± 0.00

Table S2.5: ATP requirement for the formation of microbial cells from glucose and inorganic salts. Adapted from previously estimated values (Stouthamer, 1973).

Component	Content (g g^{-1} biomass)	ATP requirement (mmol g^{-1} biomass)	ATP requirement (mmol g^{-1} component)
Polysaccharide	0.17	2.05	12.36
Protein	0.52	20.50	39.11
Lipid	0.09	0.14	1.49
RNA	0.16	4.37	27.83
DNA	0.03	1.06	33.00
mRNA turnover	N.A.	1.39	N.A.
Transport	N.A.	5.21	N.A.

N.A. = Not applicable

Table S2.6: Estimation of the biomass composition of R249 (wt Mal11), R270 (Mal11$_{QAQ/R504C}$) and R267 (Mal11$_{QNA/A515D}$). Based on measured protein content and macromolecular composition of microbial biomass as previously determined (Lange and Heijnen, 2001).

Component	Content in R249 (g g^{-1} biomass)	Content in R270 (g g^{-1} biomass)	Content in R267 (g g^{-1} biomass)
Polysaccharide	0.36	0.35	0.36
Protein	0.46	0.50	0.48
Lipid	0.07	0.06	0.07
RNA	0.05	0.05	0.05
DNA	0.04	0.04	0.04

Supplementary Materials and methods

Strains and maintenance

All *Saccharomyces cerevisiae* strains used in this study (Table S2.1) are derived from the CEN. PK lineage (Entian and Kötter, 2007; Salazar *et al.*, 2017) and *Escherichia coli* strains MC1061 and XL1 blue were used to store and amplify plasmids. To prepare stock cultures, glycerol was added to growing cultures to a final concentration of 30% v/v and 1 mL aliquots were stored at -80°C.

Molecular biology techniques

Diagnostic PCR was performed using Dreamtaq PCR mastermix (Thermo Fisher Scientific, Waltman, MA), according to the manufacturer's protocol. For cloning and sequencing purposes, PCR amplification was performed with Phusion High-Fidelity DNA polymerase (Thermo Fisher Scientific), also according to the manufacturer's instructions. Primers were purchased from Sigma-Aldrich (St. Louis, MO) and were PAGE-purified for cloning purposes, or desalted for diagnostic PCR reactions. Separation of DNA fragments was performed using a 1% agarose gel in TAE buffer (40 mM Tris-Acetate pH 8.0 and 1 mM EDTA), which was run for 30 min at 100 V. DNA fragments were isolated from gel using the Zymoclean Gel DNA Recovery kit (Zymo Research, Irivine, CA). Plasmids were transformed into *E. coli* for storage and amplification according to the NEBuilder HiFi DNA Assembly Chemical Transformation Protocol (New England Biolabs, Ipswich, MA, USA) and isolated from *E. coli* using the GenElute HP Plasmid Miniprep Kit (Sigma-Aldrich) according to the manufacturer's instructions. For isolation of plasmids from *S. cerevisiae* strains, the Zymoprep Yeast Plasmid Miniprep II kit (Zymo Research) was used according to the manufacturer's protocol. Genomic DNA was isolated from yeast as described previously (Lõoke *et al.*, 2011).

The PCR products for sequencing of *MAL11* were obtained using the *MAL11* expression plasmids that were extracted from yeast as a template with primers 1642 and 4938 and Sanger sequenced at BaseClear BV (Leiden, The Netherlands). For whole genome sequencing, genomic DNA was isolated from stationary *S. cerevisiae* cultures using the QIAGEN Blood & Cell Culture DNA Kit with 100/G Genomics-tips (Qiagen, Hilden, Germany) according to the manufacturer's protocol. Whole-genome sequencing of these DNA samples was performed by Novogene (Bejing, China). 350 bp insert libraries were constructed, which were paired-end sequenced (150 bp reads) with an Illumina HiSeq X sequencer. The data analysis was performed as described previously (van den Broek *et al.*, 2015).

Media and cultivation

E. coli was cultivated in LB medium (1%(w/v) tryptone, 0.5% (w/v) yeast extract, 1% (w/v) NaCl), using 100 µg mL^{-1} ampicillin for selection and maintenance of plasmids.

S. cerevisiae strains were cultivated in YPD (1% (w/v) yeast extract, 2% (w/v) peptone, 2% (w/v) glucose), in synthetic complete media (SC) (0.67% (w/v) yeast nitrogen base without amino acids (YNB, Formedium, UK) and 2 % (w/v) glucose, maltose, sucrose, or 1% (v/v) ethanol) or synthetic medium (SM) as previously described (Verduyn *et al.*, 1990b). When needed, SC was supplemented with a Kaiser amino acid mixture lacking leucine, uracil, or both (Formedium, UK).

For shake flasks cultures, the pH was adjusted to 6.0 using a 2 M KOH solution. SM was autoclaved for 20 min at 121 °C, after which separately filter-sterilized vitamin and sucrose solutions were added. For anaerobic cultivation, 336 g L^{-1} Tween 80 (Merck, Darmstadt, Germany) and 8 g L^{-1} ergosterol (Sigma-Aldrich) were dissolved in ethanol and added to the media to a final concentration of 0.42 g L^{-1} Tween 80 and 10 mg L^{-1} ergosterol. For growth characterization in shake flasks, SM with 2.3 g L^{-1} urea as the sole nitrogen source was used instead of ammonium to prevent extensive acidification of the medium(Luttik *et al.*, 2000). In this medium, 6.6 g L^{-1} K_2SO_4 was added to obtain the same final SO_4^{2-} concentration as present in SM. SM used in bioreactors was supplemented with autoclaved (20 min at 121 °C) Antifoam Emulsion C (Sigma-Aldrich) to a final concentration of 0.2 g L^{-1}.

Aerobic shake flask cultures were grown in an Innova incubator shaker at 30 °C and 200 rpm using 500 mL round-bottom shake flasks containing 100 mL medium. Anaerobic shake flask cultures were grown at 30°C in a Bactron anaerobic chamber with an atmosphere of 5% H_2, 6% CO_2 and 89% N_2, on a IKA KS 260 basic shaker at 200 rpm, using 50 mL shake flasks containing 30 mL medium.

Bioreactor cultivations were performed in 2-L laboratory bioreactors (Applikon Biotechnology, Delft, The Netherlands) with a working volume of 1 L. Cultures were stirred at 800 rpm and sparged with 500 mL N_2 min^{-1} (<5 ppm O_2) to maintain anaerobic conditions. To prevent entry of oxygen into the culture via the ingoing medium, the medium vessels were sparged with N_2 as well. The pH of the culture was maintained at 5.0 by automated addition of 2 M KOH and the temperature was controlled at 30 °C. The reactors were inoculated with *S. cerevisiae* strains to obtain an initial optical density (OD_{660}) of approximately 0.15. After the batch phase, the medium pump was switched on, resulting in continuous addition of medium to the cultures at a constant flowrate. To maintain a constant dilution rate, the working volume was kept constant using an effluent pump controlled by an electric level sensor. The exact working volume was measured at the end of each experiment. Chemostat cultures were assumed to be in steady state when, after five volume changes, the culture dry weight, extracellular concentrations of sucrose, ethanol and glycerol and CO_2 production rate varied by less than 2% over at least 2 more volume changes.

Pre-cultures were inoculated using frozen stock cultures and in the late-exponential phase, an aliquot from the pre-culture was transferred to a second pre-culture to obtain an OD_{660} of approximately 0.15. In the late-exponential growth phase, these second pre-cultures were used to inoculate flasks or bioreactors for physiological growth characterization. To prevent excessive acidification of the pre-culture medium, aliquots were transferred before the OD_{660} of the culture exceeded 6.0.

For plate-based growth assays, *S. cerevisiae* strains were grown from glycerol stocks in synthetic complete glucose media without amino acids (SD/-AA) and then cultivated for at least two days in synthetic complete ethanol medium without amino acids (SE/-AA) to an OD_{600} of roughly 0.5. Cells were then diluted in 1x YNB without amino acids to an OD_{600} between 0.1 and 0.4, and, subsequently, the cells were dispensed in 60 μL aliquots into microplate wells and mixed with 30 μL of 2x YNB plus 30 μL of 2x carbon source. 96-well flat-bottom microplates (CELLSTAR, Greiner Bio-One) were used to cultivate 120 μL liquid yeast cultures and were sealed with a Breath-Easy membrane (Sigma-Aldrich). OD_{600} measurements were made at 10 minute intervals using a PowerWave 340 spectrophotometer (BioTek) and cells were maintained at 30

°C with shaking at variable speed in between measurements. All growth assays included blank wells (YNB and carbon source) for each carbon source, the values of which were subtracted from all measurements as background, and wells with no carbon source (YNB and cells only) for each yeast strain.

Plasmid and strain construction

S. cerevisiae transformations were performed as described previously (Gietz and Woods, 2002) using 1 μg of DNA, unless specified otherwise. Transformants were selected on solid medium plates with SM with 20 g L^{-1} glucose and 2% (w/v) agar. All plasmids and their sources and primers are listed in Table S2.2 and S2.3. Wildtype and variants of *MAL11* ORF were amplified from pRHA37 (wildtype), pR226 (Mal11$_{QAQ}$), pR228 (Mal11$_{ANA}$) and pR230 (Mal11$_{QNA}$) using primers 7476 and 4114 and the backbone of plasmid pUDE496 (Marques *et al.*, 2018a) was amplified using primers 7477 and 7478, such that the *MAL11* and backbone fragments were overlapping. Plasmids were then constructed by Gibson assembly, transformed into *E. coli* and sequenced. A plasmid lacking *MAL11* (pR240) was constructed by digestion of pUDE496 with *BssH*II (New England Biolabs, USA), ligation with T4 ligase (New England Biolabs, USA), and transformation into *E. coli*. Plasmids were then isolated from *E. coli*, the open reading frames sequenced, and transformed into IMZ630, resulting in R249, R250, R252, R254 and R248 (Table S2.1).

Plasmid pR170 was constructed by Gibson assembly of three overlapping PCR-amplified fragments: 1) the open reading frame from pR119 (Henderson and Poolman, 2017), coding for YPet-tagged Mal11-E120Q/D123N/E167Q (*MAL11$_{QNQ}$-YPet*), with primers 5961 and 5272; 2) P_{TEF1} from pUDE379 with primers 4995 and 5960; and 3) the backbone of pRHA00L with primers 5959 and 6324. To construct plasmid pUDE466, Gibson assembly of two overlapping PCR fragments was performed: 1) *MAL11$_{QNQ}$* from pR170 with primers 6717 and 580; and 2) the backbone of pUDE453 (Marques *et al.*, 2018a) using primers 5921 and 7812. The assembled pUDE466 was introduced into *E. coli*, purified, and transformed into IMZ627, resulting in strain IMX1090. For construction of pR275, pR276, pR277, pR278, pR285 and pR286, the ORF of pR250E05-1, pR254L04-1, pR250L041-3, pR252L03-2, pUDE862 and pUDE864 respectively was amplified using primers 5271 and 5272. The plasmids were assembled in vivo by introduction of the PCR fragment containing the YPet-tagged ORF into IMK291, along with the backbone of pRHA00L which was amplified using primers 5273 and 5274.

Directed evolution of *Mal11* triple mutants

S. cerevisiae strains R250 (Mal11$_{QAQ}$), R252 (Mal11$_{ANA}$), and R254 (Mal11$_{QNA}$) were grown on SD/-AA from glycerol stocks and each diluted to an OD$_{600}$ of 0.1 in 50 mL synthetic complete media containing 2% (w/v) and 8% (w/v) sucrose (SC2S/-AA and SC8S/-AA, respectively) in sterile 250 mL flasks. Cells were incubated in a room heated to 30 °C on an open-air shaker at 200 rpm. 1 mL samples were periodically taken to check the densities of the cultures until an OD$_{600}$ greater than 1 was reached, at which point the culture was diluted in fresh media to an OD$_{600}$ of 0.1. This process was repeated at least two more times for each culture until the time between dilutions was 24 - 48 h, at which point samples were sequenced and glycerol stocks were made. Evolution lines growing rapidly in SC8S/-AA were then diluted in 50 mL SC2S/-AA and the above evolution protocol was repeated.

After all evolution lines reached an endpoint, several single colonies of each line were isolated

from glycerol stocks by plating on SD/-AA agar plates. Evolved plasmids from these single colonies were isolated and transformed into *E. coli* for amplification and then sequencing of *MAL11*. These plasmids were subsequently introduced into IMZ630, resulting in strains R265 (Mal11$_{QAQ/A384D}$), R267 (Mal11$_{QNA/A515D}$), R270 (Mal11$_{QAQ/R504C}$) and R274 (Mal11$_{ANA/W376S}$).

To obtain single colony isolates from chemostat cultures, cells were plated on agar plates with SM with 20 g L^{-1} sucrose as sole carbon source. Colonies were restreaked three times on fresh plates to obtain single cell lines, which resulted in IMS0960 (evolved R270) and IMS0962 (evolved R267). From both single cell lines, plasmids were isolated, renamed pUDE862 (from IMS0960) and pUDE864 (from IMS0962) and introduced into IMZ630, resulting in IME441 and IME442, respectively.

Analytical methods

Growth was monitored by optical density (OD) measurement at a wavelength of 660 nm using a Jenway 7200 spectrophotometer. For biomass dry weight measurements, 10 mL culture was filtered over a pre-weighed nitrocellulose filter with pore size 0.45 µm. Subsequently, the filters were washed with demineralized water and dried for 20 min at 360 W in a microwave oven, after which they were weighted again. Culture supernatants were obtained via centrifugation at 13,000 g for 3 min. Concentrations of sucrose, ethanol and glycerol in these culture supernatants were measured via high-performance liquid chromatography (HPLC) analysis on an Agilent 1260 HPLC, equipped with a Bio-Rad HPX 87H column. The column was eluted at 60 °C with 0.5 g L^{-1} H$_2$SO$_4$ at a flowrate of 0.6 mL min^{-1}. Detection was performed by means of an Agilent refractive index detector and an Agilent 1260 VWD detector. Off gas concentrations of CO$_2$ and O$_2$ were measured using an NGA 2000 analyser, after the gas was cooled by a condenser at 4 °C and dried with a permapure type MD-110-48P-4 dryer.

Glucose-1-phosphate concentrations in culture supernatant were enzymatically determined by measuring the absorbance at 340 nm in a 1 mL reaction mixture containing 200 mM potassium phosphate buffer (pH 7.0), 1 mM EDTA, 10 mM MgCl, 10 µM α-D-glucose-1,6-bisphosphate, 2 mM NADP$^+$, 2 U glucose-6-phosphate dehydrogenase and 20-100 µL culture supernatant, before and after addition of 2 U phosphoglucomutase. Cellular protein content was determined as described previously (Verduyn *et al.*, 1990b) with the exception that 1 M NaOH was used instead of 1 M KOH and the absorbance was measured at 510 nm instead of 550 nm.

Radiolabelled sugar transport

Sugar transport was measured in whole yeast cells essentially as previously described (Henderson and Poolman, 2017). *S. cerevisiae* strains were pre-cultured on SE/-AA or SE/-Leu, as appropriate, for at least two days before harvesting in early exponential phase of growth (OD$_{600}$ = 0.3-0.7) by centrifugation at 3,000 g for 5 minutes at 4 °C. After washing twice by resuspending the cells in 3 mL assay buffer (potassium-citrate-phosphate (KCP) + 10 mM galactose) and centrifugation, cells were resuspended in assay buffer and stored on ice for no more than four hours. Initially, cells at an OD$_{600}$ of 12 or 24 were incubated for ten minutes at 30 °C to increase the adenylate energy charge (Guimarães and Londesborough, 2008), followed by addition of approximately 48,100 Bq mL^{-1} [U-^{14}C]maltose (600 mCi mmol^{-1}; American Radiolabeled Chemicals, Inc.) or [U-^{14}C]sucrose (600 mCi mmol^{-1}; American Radiolabeled Chemicals, Inc.) to start the reaction (final sugar concentration as indicated). The reactions were incubated

with stirring for up to 45 min, depending on the experiment, and measurements were taken by addition of a reaction sample to 2 mL ice-cold KCP and rapid filtration on 0.45 μm pore-size cellulose-nitrate filters (GE-Healthcare, Little Chalfont, UK), which were pre-soaked in KCP plus 1 mM sugar to block non-specific adsorption of the radiolabelled material. These measurements were made in triplicate and averaged, as indicated. Filters were then washed with an additional 2 mL KCP, dissolved in 2 mL scintillation solution (Emulsifier[plus], PerkinElmer, Waltham, MA, USA), and the radioactivity quantified in a Tri-Carb 2800TR liquid scintillation analyzer (PerkinElmer). The amount of intracellular maltose or sucrose was normalized to 10^6 cells by counting the number of cells in samples of 20 μL at OD_{600} of 0.4 in an Accuri C6 flow cytometer (BD Biosciences, Durham, USA). The intracellular concentration of sugar was calculated using an estimated 60 fL internal volume per cell.

2

Lactic acid

Ato2

jen1Δ
ady2Δ

Ato3

SM +
Lactic acid

Ato2^{L218S}

Ato3^{F95S}
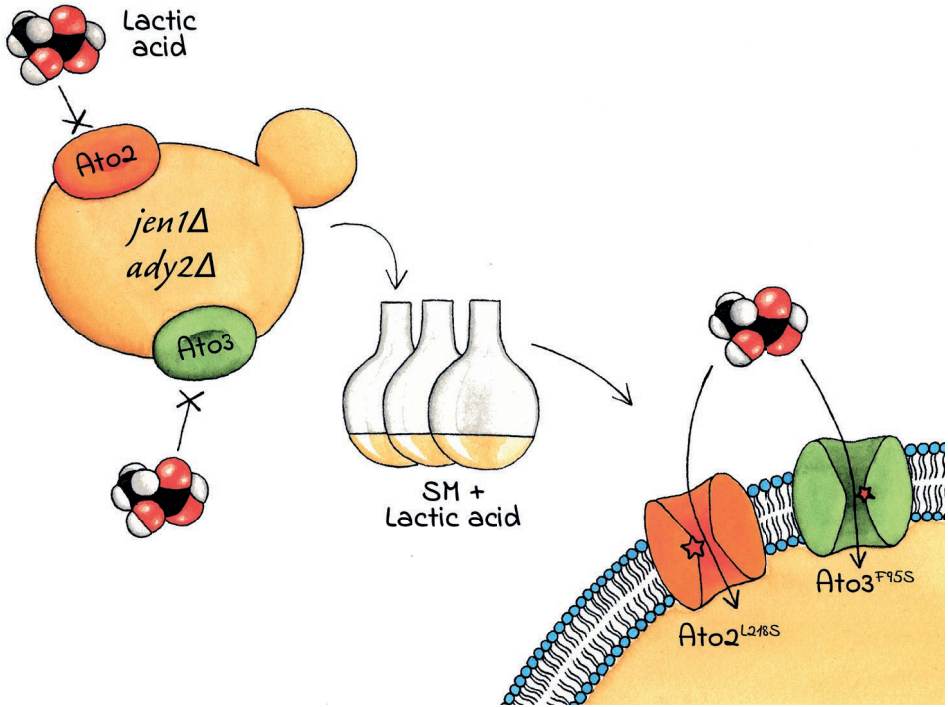
Chapter 3

Evolutionary engineering reveals amino acid substitutions in Ato2 and Ato3 that allow improved growth of *Saccharomyces cerevisia*e on lactic acid

Nicolò Baldi*, Sophie C. de Valk*, Maria Sousa-Silva, Margarida Casal, Isabel Soares-Silva & Robert Mans

* These authors contributed equally to this work.

Abstract

In *Saccharomyces cerevisiae*, the complete set of proteins involved in transport of lactic acid across the cell membrane has not been determined. In this study we aimed to identify transport proteins not previously described to be involved in lactic acid transport via a combination of directed evolution, whole-genome resequencing and reverse engineering. Evolution of a strain lacking all known lactic acid transporters on lactate led to the discovery of mutated Ato2 and Ato3 as two novel lactic acid transport proteins. When compared to previously identified *S. cerevisiae* genes involved in lactic acid transport, expression of $ATO3^{T284C}$ allowed the highest growth rate (0.15 ± 0.01 h^{-1}) on this carbon source. A comparison between (evolved) sequences and 3D models of the transport proteins showed that most of the identified mutations resulted in a widening of the narrowest hydrophobic constriction of the anion channel. We hypothesize that this observation, sometimes in combination with an increased binding affinity of lactic acid to the sites adjacent to this constriction, is responsible for the improved lactic acid transport in the evolved proteins.

3

3.1 Introduction

The yeast *Saccharomyces cerevisiae* is able to utilize a variety of compounds as carbon and energy source, including monosaccharides, disaccharides, monocarboxylic acids, amino acids and polyols (Kruckeberg and Dickinson, 2004; Lagunas, 1993). Assimilation and dissimilation of these compounds inside cells is preceded by their transport across the plasma membrane. A lot of research has been dedicated to the elucidation of structure, function and mechanism of action of proteins involved in uptake, both to understand cellular response to different conditions as well as for the application of metabolic engineering strategies to increase the efficiency of substrate usage and broaden the substrate range of industrial cell factories (Agrimi and Steiger, 2021).

This research field has tremendously benefitted from engineered 'platform strains', in which all transporters for a certain substrate have been knocked out. One of the most applied platform strains is the so called 'hxt^0 strain', in which the uptake of hexoses is completely abolished by the knockout of all 21 genes involved in the uptake of hexoses (Wieczorke *et al.*, 1999). This hxt^0 strain has been indispensable for studies where both endogenous and heterologous proteins were characterized for their ability to catalyze the uptake of various hexose and pentose sugars (Anjos *et al.*, 2013; Bueno *et al.*, 2020; Chattopadhyay *et al.*, 2020; Gao *et al.*, 2019; Huang *et al.*, 2020; Li *et al.*, 2015; Morii *et al.*, 2020). The absence of all hexose transporters in this strain renders it unable to grow on media in which a monosaccharide is the sole carbon source, and therefore allows for screening of growth phenotypes that are linked to the expression of an investigated transport protein. The application of the hxt^0 strain is also preferred for *in vivo* transport assays in which the intracellular accumulation of substrates is measured, since background signal caused by other transporters is minimized (Nogueira *et al.*, 2020; Paulsen *et al.*, 2019; Schmidl *et al.*, 2021). In addition, it has often been used as background strain in directed evolution of (heterologous) transport proteins, for which selection is based on growth on the transported substrate (Colabardini *et al.*, 2014; Li *et al.*, 2016; Nijland and Driessen, 2020; Sloothaak *et al.*, 2016; Wang *et al.*, 2013; Zhang *et al.*, 2015). The benefit of a platform strain in an evolutionary engineering approach is that the presence of other genes that could (upon mutation) provide a selective advantage is minimized, and thus allows for improved selection of mutants of the gene under investigation. Similar platform strains have been constructed to study disaccharide transporters (Riesmeier *et al.*, 1992) and ABC transporters (Suzuki *et al.*, 2011).

Transport of monocarboxylic acids across the yeast plasma membrane remains enigmatic (Borodina, 2019) and therefore the establishment of specialized platform strains to study transport of specific monocarboxylic acids could be an important next step to further our understanding. Whereas the undissociated, protonated form of carboxylic acids can cross biological membranes by passive diffusion, the charged anionic form that is predominant in pH conditions well above the pK_a of the acid requires (a) protein(s) to mediate rapid transport across the membrane (Gabba *et al.*, 2020). These monocarboxylic acid transport proteins play an important role in, for instance, food preservation, weak organic acid tolerance in second generation bioethanol production, metabolic engineering strategies for industrial production of carboxylic acids and in development of cancer therapies (Pinheiro *et al.*, 2012; Soares-Silva *et al.*, 2020). Two genes encoding permeases for monocarboxylic acids have been identified so far in *S. cerevisiae*: *JEN1* and *ADY2* (Casal *et al.*, 2016). Jen1 is a member of the Major Facilitator Superfamily which enables uptake of lactic, acetic and pyruvic acid (Casal *et al.*, 1999). Ady2 is

3

an acetate transporter that belongs to the AceTr family, for which two homologs have been described in *S. cerevisiae*, Ato2 and Ato3 (Paiva *et al.*, 2004; Ribas *et al.*, 2019). A powerful strategy to identify more genes involved in a specific physiological function is the use of adaptive laboratory evolution. Application of a selective pressure is used to enrich for mutants with the phenotype of interest, which can subsequently be analyzed by whole genome sequencing to identify mutated genes related to the evolved phenotype (Mans *et al.*, 2018). This concept was demonstrated in a previous study, in which laboratory evolution of a *jen1Δ* strain in culture medium with lactic acid as sole carbon source led to the identification of mutated *ADY2* alleles that had an increased uptake capacity for lactic acid (de Kok *et al.*, 2012b). Lactic acid, which is produced on industrial scale using biotechnological processes, is used as preservative in the dairy industry and as a precursor for the production of bioplastic, with a demand of 1.220.000 tons in 2016 that is expected to further increase by 16.2% before 2025 (Singhvi *et al.*, 2018).

In this study, we use adaptive laboratory evolution to identify additional transporters, which upon mutation can efficiently catalyze lactic acid uptake in *S. cerevisiae*. Subsequently, we overexpress the complete suite of native and evolved lactic acid transporters in a strain background devoid of all (putative) organic acid transporters, characterize the ability of the resulting strains to grow on monocarboxylic acids and assess the uptake of labelled lactate and acetate by the evolved transporters. Finally, we identify specific amino acid residues playing a key role in the transport of lactic acid and provide a mechanistic explanation using three-dimensional structure predictions combined with molecular docking analysis.

3.2 Materials and methods

Strains and maintenance

The *S. cerevisiae* strains used in this study (Table 3.2) share the CEN.PK113-7D or the CEN. PK2-1C genetic backgrounds (Entian and Kötter, 2007). Stock cultures of *S. cerevisiae* were grown aerobically in 500 mL round-bottom shake flasks containing 100 mL synthetic medium (SM) (Verduyn *et al.*, 1992) or YP medium (10 g L^{-1} Bacto yeast extract, 20 g L^{-1} Bacto peptone) supplemented with 20 g L^{-1} glucose. When needed, auxotrophic requirements were complemented via addition of 150 mg L^{-1} uracil, 100 mg L^{-1} histidine, 500 mg L^{-1} leucine and/or 75 mg L^{-1} tryptophan (Pronk, 2002). For plate cultivation, 2% (w/v) agar was added to the medium prior to heat sterilization. Stock cultures of *E. coli* XL1-Blue Subcloning Grade Competent Cells (Agilent, Santa Clara, CA, USA) that were used for plasmid propagation were grown in LB medium (5 g L^{-1} Bacto yeast extract, 10 g L^{-1} Bacto tryptone, 10 g L^{-1} NaCl) supplemented with 100 mg L^{-1} ampicillin. Media were autoclaved at 121 °C for 20 min and supplements and antibiotics were filter sterilized and added to the media prior to use. Frozen culture stocks were prepared by addition of sterile glycerol (to a final concentration of 30% v/v) to exponentially growing shake flask cultures of *S. cerevisiae* or overnight cultures of *E. coli* and 1 mL aliquots were stored at -80 °C.

Molecular biology techniques

Phusion High-Fidelity DNA Polymerase (Thermo Fisher Scientific, Waltham, MA, USA) was used for PCR amplification for cloning purposes. Diagnostic PCRs were performed using DreamTaq PCR Master Mix (2X) (Thermo Fisher Scientific). In both cases, the manufacturer's protocol was followed, with the exception of the use of lower primer concentrations (0.2 μM each). Desalted

(DST) oligonucleotide primers were used, except for primers binding to coding regions, which were PAGE purified. Primers were purchased from Sigma Aldrich (Saint Louis, MO, USA), with the exception of primers 17453 and 17453, which were purchased from Ella Biotech (Planegg, Germany). For diagnostic PCR, yeast genomic DNA was isolated as described by Lõoke *et al*. (2011). Commercial kits for DNA extraction and purification were used for plasmid DNA isolation (Sigma Aldrich), PCR cleanup (Sigma Aldrich), and gel extraction (Zymo Research, Irvine, CA, USA). Restriction analysis of constructed plasmids was performed using FastDigest restriction enzymes (Thermo Scientific). Gibson assembly of linear DNA fragments was performed using NEBuilder HiFi DNA Assembly Master Mix (New England Biolabs, Ipswich, MA, USA) in a total reaction volume of 5 μL. Transformation of chemically competent *E. coli* XL1-Blue (Agilent) was performed according to the manufacturer's protocol.

Plasmid construction

The plasmids and oligonucleotide primers used in this study are listed in Table 3.1 and Table S3.1, respectively. All plasmids were constructed by Gibson assembly of two linear fragments. With the exception of the fragments used for the construction of plasmid pUDR420, all fragments were PCR-amplified from either a template plasmid or from genomic DNA.

Plasmid pUDR405 was constructed by Gibson assembly of two linear fragments, both obtained via PCR amplification of plasmid pROS13 using primers 8664 and 6262 (for the *JEN1*-gRNA_2μ_ *ADY2*-gRNA insert) and 6005 (for the plasmid backbone), as previously described (Mans et al., 2015). Plasmid pUDR420 was constructed by Gibson assembly of a double-stranded DNA fragment, obtained by annealing the complementary single-stranded oligonucleotides 8691 and 13552, and a vector backbone amplified from plasmid pMEL13 using primers 6005 and 6006. Plasmid pUDR767 was constructed by Gibson assembly of two linear fragments, both obtained via PCR amplification of plasmid pROS10 using primers 8688 (for the *ATO2*-gRNA_2μ_*ATO2*-gRNA insert) and 6005 (for the plasmid backbone). For construction of pUDE813, the linear p426-TEF plasmid backbone was amplified from plasmid p426-TEF using primers 5921 and 10547 and the *ATO3* open reading frame (ORF) was amplified from yeast strain CEN.PK113-7D genomic DNA using primers 13513 and 13514. Subsequently, Gibson assembly of the linear p426-TEF plasmid backbone and the *ATO3* insert yielded pUDE813. pUDE814, pUDE1001, pUDE1002, pUDE1003, pUDE1004, pUDE1021 and pUDE1022 were constructed similar to pUDE813, using primers 5921 and 10547 to amplify the linear p426-TEF plasmid backbone. The inserts were amplified from genomic DNA of strain CEN.PK113-7D (for wildtype genes) or from genomic DNA of the corresponding evolved strain (for mutated genes) using primers 13513 and 13514 (pUDE814), 17170 and 17171 (pUDE1001), 17168 and 17169 (pUDE1002, pUDE1003 and pUDE1004) or 17452 and 17453 (pUDE1021 and pUDE1022). For construction of pUDC319, plasmid p426-TEF was amplified using primers 2949 and 17741 and the CEN6 origin of replication was amplified from pUDC156 using primers 17742 and 17743. Subsequently, Gibson assembly of the linear p426-TEF plasmid fragment and the CEN6 fragment yielded pUDC319. pUDC320, pUDC321, pUDC322, pUDC323, pUDC324, pUDC325, pUDC326 and pUDC327 were constructed in a similar way using the same primers, but the linear plasmid fragment was amplified from pUDE813, pUDE814, pUDE1001, pUDE1002, pUDE1003, pUDE1004, pUDE1021 and pUDE1022, respectively.

3

Table 3.1: Plasmids used in this study.

Name	Relevant characteristic	Origin
pROS13	2μm ampR *kanMX* gRNA-*CAN1* gRNA-*ADE2*	(Mans *et al.*, 2015)
pROS10	2μm ampR *URA3* gRNA-*CAN1* gRNA-*ADE2*	(Mans *et al.*, 2015)
pMEL13	*2μm* ampR *kanMX* gRNA-*CAN1*	(Mans *et al.*, 2015)
pUDR405	2μm ampR *kan*MX gRNA-*JEN1* gRNA-*ADY2*	This study
pUDR420	2μm ampR *kanMX* gRNA-*ATO3*	This study
pUDR767	2μm ampR *URA3* gRNA-*ATO2*	This study
p426-TEF	*2μm URA3 pTEF1-tCYC1*	(Mumberg *et al.*, 1995)
pUDE813	*2μm URA3 pTEF1-ATO3-tCYC1*	This study
pUDE814	*2μm URA3 pTEF1-ATO3^{T284C}-tCYC1*	This study
pUDE1001	*2μm URA3 pTEF1-JEN1-tCYC1*	This study
pUDE1002	*2μm URA3 pTEF1-ADY2-tCYC1*	This study
pUDE1003	*2μm URA3 pTEF1- ADY2^{C755G} -tCYC1*	This study
pUDE1004	*2μm URA3 pTEF1- ADY2^{C655G}-tCYC1*	This study
pUDE1021	*2μm URA3 pTEF1-ATO2-tCYC1*	This study
pUDE1022	*2μm URA3 pTEF1-ATO2^{T653C}-tCYC1*	This study
pUDC156	*CEN6 URA3 pTEF-CAS9-tCYC1*	(Marques *et al.*, 2017)
pUDC319	*CEN6 URA3 pTEF-tCYC1*	This study
pUDC320	*CEN6 URA3 pTEF1-ATO3-tCYC1*	This study
pUDC321	*CEN6 URA3 pTEF1-ATO3^{T284C}-tCYC1*	This study
pUDC322	*CEN6 URA3 pTEF1-JEN1-tCYC1*	This study
pUDC323	*CEN6 URA3 pTEF1-ADY2-tCYC1*	This study
pUDC324	*CEN6 URA3 pTEF1- ADY2^{C755G} -tCYC1*	This study
pUDC325	*CEN6 URA3 pTEF1- ADY2^{C655G}-tCYC1*	This study
pUDC326	*CEN6 URA3 pTEF1-ATO2-tCYC1*	This study
pUDC327	*CEN6 URA3 pTEF1-ATO2^{T653C}-tCYC1*	This study

3

Strain construction

S. cerevisiae strains were transformed with the LiAc/ssDNA method (Gietz and Woods, 2002). For transformations with a dominant marker, the transformation mixture was plated on YP plates, containing glucose (20 g L^{-1}) as carbon source, and supplemented with 200 mg L^{-1} G418 (Invitrogen, Carlsbad, CA, USA). Gene deletions were performed as previously described (Mans *et al.*, 2015). For transformation of plasmids harboring an auxotrophic marker, transformed cells were plated on SM medium with glucose (20 g L^{-1}) as a carbon source and when needed, appropriate auxotrophic requirements were supplemented.

The tryptophan auxotrophy of IMX1000 was the result of a single point mutation in the *TRP1* gene (*trp1-289*) (Botstein *et al.*, 1979) and was spontaneously reverted by plating the strain on SM medium supplemented with uracil, histidine and leucine, and picking a tryptophan prototrophic colony, yielding strain IMX2486. Strain IMX2487 was constructed by transforming IMX2486 with a linear fragment, obtained by PCR amplification of the *LEU2* gene from CEN. PK113-7D, using primers 1742 and 1743. Strain IMX2488 was constructed by transforming IMX2487 with a linear fragment, obtained by PCR amplification of the *HIS3* gene from CEN. PK113-7D, using primers 1738 and 3755. Strain IMK875 was constructed by transforming the Cas9-expressing strain IMX585 with plasmid pUDR405 and two double stranded repair oligonucleotides obtained by annealing oligonucleotides 8597 to 8598 and 8665 to 8666.

Strain IMK876 was constructed by transforming the Cas9-expressing strain IMX581 with plasmid pUDR405 and two double stranded repair oligonucleotides obtained by annealing oligonucleotides 8597 to 8598 and 8665 to 8666. Strains IMK882 and IMK883 were obtained by transforming strains IMK875 and IMK876, respectively, with plasmid pUDR420 and a double stranded repair oligonucleotide obtained by annealing oligonucleotides 14120 and 14121. Strain IMK982 was constructed by transforming strain IMK883 with plasmid pUDR767 and a double stranded repair oligonucleotide obtained by annealing oligonucleotides 8689 and 8690. Plasmids p426-TEF, pUDE813, pUDE814, pUDE1001, pUDE1002, pUDE1003, pUDE1004, pUDE1021, pUDE1022, pUDC319, pUDC320, pUDC321, pUDC322, pUDC323, pUDC324, pUDC325, pUDC326 and pUDC327 were transformed in strain IMX2488, yielding IME581, IME582, IME583, IME584, IME585, IME586, IME587, IME588, IME589, IMC164, IMC165, IMC166, IMC167, IMC168, IMC169, IMC170, IMC171 and IMC172, respectively.

Evolution of IMK341 and IMK882 was performed by inoculating duplicate shake flasks with 20 mL synthetic medium with lactic acid as the sole carbon source (SML, see section 2.5 'Media and cultivation') with these strains to obtain a starting optical density at 660 nm (OD_{660}) of 0.1. Once the cultures grew and stationary phase was reached, a 1 mL aliquot of each culture was transferred to 20 mL fresh SML and grown until stationary phase again (in total approximately 14 generations for IMK341 and 7 generations for IMK882). Single colony isolates from these evolution cultures ('IMS'-strains) were obtained by plating the cultures using an inoculation loop (~10 μL) on solid SML and restreaking a grown colony to a fresh plate three consecutive times, after which one colony was grown in liquid SML and stocked.

Table 3.2: *Saccharomyces cerevisiae* strains used in this study

Strain name	Relevant genotype	Origin
CEN.PK113-7D	Prototrophic reference, *MAT*a	(Entian and Kötter, 2007)
IMX581	*MAT*a *ura3-52 can1::cas9-natNT2*	(Mans *et al.*, 2015)
IMX585	*MATa can1::cas9-natNT2*	(Mans *et al.*, 2015)
IMK341	*MAT*a *ura3::loxP ady2::loxP-hphNT1-loxP jen1::loxP*	(de Kok *et al.*, 2012b)
IMW004	*MATa URA3 ADY2^{C755G} jen1::loxP-KanMX4-loxP*	(de Kok *et al.*, 2012b)
IMW005	*MATa URA3 ADY2^{C655G} jen1::loxP-KanMX4-loxP*	(de Kok *et al.*, 2012b)
IMX1000	*MATa ura3-52 trp1-289 leu2-3112 his3Δ can1Δ::cas9-natNT2 mch1Δ mch2Δ mch5Δ aqy1Δ itr1Δ pdr12Δ mch3Δ mch4Δ yil166cΔ hxt1Δ jen1Δ ady2Δ aqr1Δ thi73Δ fps1Δ aqy2Δ yll053cΔ ato2Δ ato3Δ aqy3Δ tpo2Δ yro2Δ azr1Δ yhl008cΔ tpo3Δ*	(Mans *et al.*, 2017)
IMK875	*MATa can1::cas9-natNT2 jen1Δ ady2Δ*	This study
IMK876	*MATa can1::cas9-natNT2 ura3-52 jen1Δ ady2Δ*	This study
IMK882	*MATa can1::cas9-natNT2 jen1Δ ady2Δ ato3Δ*	This study
IMK883	*MATa can1::cas9-natNT2 ura3-52 jen1Δ ady2Δ ato3Δ*	This study
IMK982	*MATa can1::cas9-natNT2 ura3-52 jen1Δ ady2Δ ato3Δ ato2Δ*	This study
IMS807	IMK341 evolved for growth on lactate, evolution line A	This study
IMS808	IMK341 evolved for growth on lactate, evolution line A	This study
IMS809	IMK341 evolved for growth on lactate, evolution line A	This study
IMS810	IMK341 evolved for growth on lactate, evolution line B	This study
IMS811	IMK341 evolved for growth on lactate, evolution line B	This study
IMS1122	IMK882 evolved for growth on lactate	This study
IMS1123	IMK882 evolved for growth on lactate	This study

3

IMS1130	IMK882 evolved for growth on lactate	This study
IMX2486	IMX1000 *ura3-52 TRP1, leu2-3112, his3Δ*	This study
IMX2487	IMX1000 *ura3-52 TRP1, LEU2, his3Δ*	This study
IMX2488	IMX1000 *ura3-52 TRP1, LEU2, HIS3*	This study
IME581	IMX2488 p426-TEF (2μm)	This study
IME582	IMX2488 pUDE813 (2μm *ATO3*)	This study
IME583	IMX2488 pUDE814 (2μm *ATO3*[T284C])	This study
IME584	IMX2488 pUDE1001 (2μm *JEN1*)	This study
IME585	IMX2488 pUDE1002 (2μm *ADY2*)	This study
IME586	IMX2488 pUDE1003 (2μm *ADY2*[C755G])	This study
IME587	IMX2488 pUDE1004 (2μm *ADY2*[C655G])	This study
IME588	IMX2488 pUDE1021 (2μm *ATO2*)	This study
IME589	IMX2488 pUDE1022 (2μm *ATO2*[T653C])	This study
IMC164	IMX2488 pUDC319 (*CEN6*)	This study
IMC165	IMX2488 pUDC320 (*CEN6 ATO3*)	This study
IMC166	IMX2488 pUDC321 (*CEN6 ATO3*[T284C])	This study
IMC167	IMX2488 pUDC322 (*CEN6 JEN1*)	This study
IMC168	IMX2488 pUDC323 (*CEN6 ADY2*)	This study
IMC169	IMX2488 pUDC324 (*CEN6 ADY2*[C755G])	This study
IMC170	IMX2488 pUDC325 (*CEN6 ADY2*[C655G])	This study
IMC171	IMX2488 pUDC326 (*CEN6 ATO2*)	This study
IMC172	IMX2488 pUDC327 (*CEN6 ATO2*[T653C])	This study

Media and cultivation

Evolution experiments were performed in 500 mL shake-flask cultures containing 100 mL synthetic medium (Verduyn *et al.*, 1992) with 84 mM L-lactic acid as sole carbon source. The pH of the medium was set at 5.0 and the cultures were incubated at 30 °C in an Innova incubator shaker (New Brunswick Scientific, Edison, NJ, USA) set at 200 rpm. Auxotrophic requirements were supplemented as needed.

Strains were characterized in SM supplemented with different carbon sources. To achieve an initial carbon concentration of 250 mM, the culture media contained either 42 mM D-glucose, 83 mM L-lactic acid, 125 mM acetic acid or 83 mM pyruvic acid. The characterization was performed in a Growth-Profiler system (EnzyScreen, Heemstede, The Netherlands) equipped with 96-well plates in a culture volume of 250 μL, set at 250 rpm and 30 °C. The measurement interval was set at 30 minutes. Raw green values were corrected for well-to-well variation using measurements of a 96-well plate containing a culture with an externally determined optical density of 3.75 in all wells. Optical densities were calculated by converting green values (corrected for well-to-well variation) using a calibration curve that was determined by fitting a third-degree polynomial through 22 measurements of cultures with known OD_{660} values between 0.1 and 20. Growth rates were calculated using the calculated optical densities of at least 15 points in the exponential phase. Exponential growth was assumed when an exponential curve could be fitted with an R^2 of at least 0.985.

Analytical methods

Culture optical density at 660 nm was measured with a Libra S11 spectrophotometer (Biochrom,

Cambridge, United Kingdom). In order to measure within the linear range of the instrument (OD between 0.1 and 0.3), cultures were diluted in an appropriate amount of demineralized water. Metabolite concentrations in culture supernatants and media were analyzed using an Agilent 1260 Infinity HPLC system equipped with a Bio-rad Aminex HPX-87H ion exchange column, operated at 60 °C with 5 mM H_2SO_4 as mobile phase at a flow rate of 0.600 mL min^{-1}.

DNA extraction and whole genome sequencing

Strain IMK341 and the evolved single colony isolates (IMS-strains) were grown in 500 mL shake flasks containing 100 mL YP medium supplemented with glucose (20 g L^{-1}) as a carbon source. The cultures were incubated at 30 °C until the strains reached stationary phase and genomic DNA was isolated using the Qiagen 100/G kit (Qiagen, Hilden, Germany) according to the manufacturer's instructions and quantified using a Qubit® Fluorometer 2.0 (Thermo Fisher Scientific). The isolated DNA was sequenced in-house on a MiSeq (Illumina, San Diego, CA, USA) with 300 bp paired-end reads using TruSeq PCR-free library preparation (Illumina). For all strains, the reads were mapped onto the *S. cerevisiae* CEN.PK113-7D genome (Salazar *et al.*, 2017) using the Burrows–Wheeler Alignment tool (BWA) and further processed using SAMtools and Pilon for variant calling (Li and Durbin, 2010; Li *et al.*, 2009; Walker *et al.*, 2014).

Transport assays

The uptake of labelled carboxylic acids was assessed as previously described by Ribas *et al.*, (2017), using [1-^{14}C] acetic acid (Perkin Elmer, Massachusetts, USA) and [U-^{14}C] L-lactic acid (Perkin Helmer, Massachusetts, USA) with a specific activity of 2000 dpm/nmol. The data shown are mean values of at least three independent experiments.

3D modelling and molecular docking of Ady2, Ato2 and Ato3

The three-dimensional modelling analysis was performed for the protein sequences of Ady2, Ady2[L219V], Ady2[A252G], Ato2, Ato2[L218S], Ato3 and Ato3[F95S]. The amino acid sequences were retrieved from the *Saccharomyces* Genome Database (Cherry *et al.*, 2012). To determine the predicted transporter 3D structures, the amino acid sequences were threaded through the PDB library using LOMETS (Local Meta-Threading-Server). The *Citrobacter koseri* succinate acetate permease (CkSatP, PDB 5YS3) was the top ranked template threading identified in LOMETS for Ato1, Ato2 and Ato3 (Qui *et al.*, 2018). Since the CkSatP three-dimensional structure obtained the best score as template for protein structure prediction, it was further considered for molecular docking analysis. CkSatP presents a protein identity of 35% with Ady2, 34% with Ato2 and 28% with Ato3 and similarity of 0.566, 0.548 and 0.515, respectively. Molecular docking simulations were performed as described by Ribas *et al.* (2017). Ligand structures of acetic, lactic and pyruvic acid for all target proteins in the study were downloaded from the Zinc database (Sterling and Irwin, 2015). Structures used for docking were all confirmed in Maestro v11.2 before ligand-protein simulations were performed using AutoDock Vina in the PyRx software (Trott and Olson, 2010). The docking studies were performed with the dissociated forms of each carboxylic acid. The protonation states were adjusted to match a pH of 5.0-6.0 and exported in the mol2 format. Docking was performed with four docking-boxes for each protein, containing top, bottom and middle-structure parts for a more robust use of Autodock Vina. The exhaustiveness parameter was set up for 1000 calculations for each of the grid-zones defined for docking. The generated docking scores and 2-3D pose views were evaluated for the establishment of molecular interactions and ligand binding affinities.

3

3.3 Results

**Laboratory evolution on lactic acid leads to point mutations in Ato2 or Ato3**

In an attempt to identify additional transporters able to catalyze the uptake of lactic acid after gaining point mutations, we incubated strains IMK341 and IMX1000 in duplicate shake flasks cultures containing synthetic medium with lactic acid as the sole carbon source. In IMK341 the known carboxylic acid transporters *JEN1* and *ADY2* are knocked out (*jen1Δ*, *ady2Δ*), whereas in IMX1000 a further 23 genes encoding putative lactic acid transport proteins are deleted (Table 3.2) (Mans *et al.*, 2017). After 9 weeks, growth was observed in both cultures of IMK341 whereas no growth was observed after 12 weeks of incubation of IMX1000. Whole-genome sequencing of evolved IMK341 (*jen1Δ*, *ady2Δ*) cell lines, named IMS807-811 which were isolated after a transfer to fresh medium, revealed three to seven non-synonymous SNPs in each mutant and no chromosomal duplications or rearrangements (Table 3.3). Strikingly, all evolved isolates shared an identical mutation in *ATO3* (*ATO3^{T284C}*). To investigate the role of *ATO3* in lactic acid uptake, we overexpressed both the native and evolved *ATO3* in IMK883 (*jen1Δ*, *ady2Δ*, *ato3Δ*) and tested the resulting strains for growth on SM lactic acid plates. After 5 days, only the reference strain CEN.PK113-7D and the strain carrying the *ATO3^{T284C}* allele were able to grow (Figure S3.1), indicating that the T284C mutation in *ATO3* was responsible for the evolved phenotype. We then combined the deletion of *JEN1*, *ADY2* and *ATO3* in strain IMK882 (*jen1Δ, ady2Δ, ato3Δ*) and repeated the evolution. After 5 and 12 days, growth was observed in two independent cultures from which evolved strains IMS1122 and IMS1123 were isolated after transfer to a flask with fresh medium. In both single colony isolates, five SNPs were present (Table 3.3), including a common mutation in *ATO2*, (*ATO2^{T653C}*), which has been described as an ammonium transporter together with *ATO3* and *ADY2* (Palková *et al.*, 2002). Finally, the evolution was repeated with IMK982 (*jen1Δ, ady2Δ, ato3Δ, ato2Δ*), but no growth was observed after 12 weeks of incubation.

Table 3.3: Amino acid changes identified by whole-genome sequencing of single colony isolates evolved for growth in medium containing lactic acid as sole carbon source. Isolates IMS807 to IMS811 are derived from IMK341 (*jen1Δ, ady2Δ*) and IMS1122 and IMS1123 are derived from IMK882 (*jen1Δ, ady2Δ, ato3Δ*). IMS807, IM808 and IMS809 are isolates from evolution line #1 and IMS810 and IMS811 are isolates from evolution line #2. The mutation Sip5^{*490Q} indicates loss of the stop codon.

IMK341 evolution #1			IMK341 evolution #2		IMK822 evolution #1	IMK822 evolution #2
IMS807	IMS808	IMS809	IMS810	IMS811	IMS1122	IMS1123
Ato3^{F95S}	Ato3^{F95S}	Ato3^{F95S}	Ato3^{F95S}	Ato3^{F95S}	Ato2^{L218S}	Ato2^{L218S}
Mms2^{Y58C}	Mms2^{Y58C}	Mms2^{Y58C}	Sip5^{*490Q}	Sip5^{*490Q}	Lrg1^{H979N}	Whi2^{E119*}
Pih1^{D147Y}	Pih1^{D147Y}	Pih1^{D147Y}	Ssn2^{M1280R}	Lip5^{R4L}	Ykr051w^{Y285H}	Ykr051w^{Y285H}
Uba1^{L952F}		Drn1^{P213L}			Jjj1^{H356Q}	Jjj1^{H356Q}
Stv1^{L275F}					Trm10^{A49V}	Trm10^{A49V}
Whi2^{E187*}						
Vba4^{P198L}						

Overexpression of mutated transporters enables rapid growth in liquid medium with lactic acid as sole carbon source

Strikingly, the evolved transporters able to catalyze the uptake of lactic acid (*ATO2* and *ATO3* in this study, and *ADY2* in work by de Kok *et al.*, 2012) represent all members of the *S. cerevisiae* Acetate Uptake Transporter Family (TCDB 2.A.96). To characterize the impact of the mutations
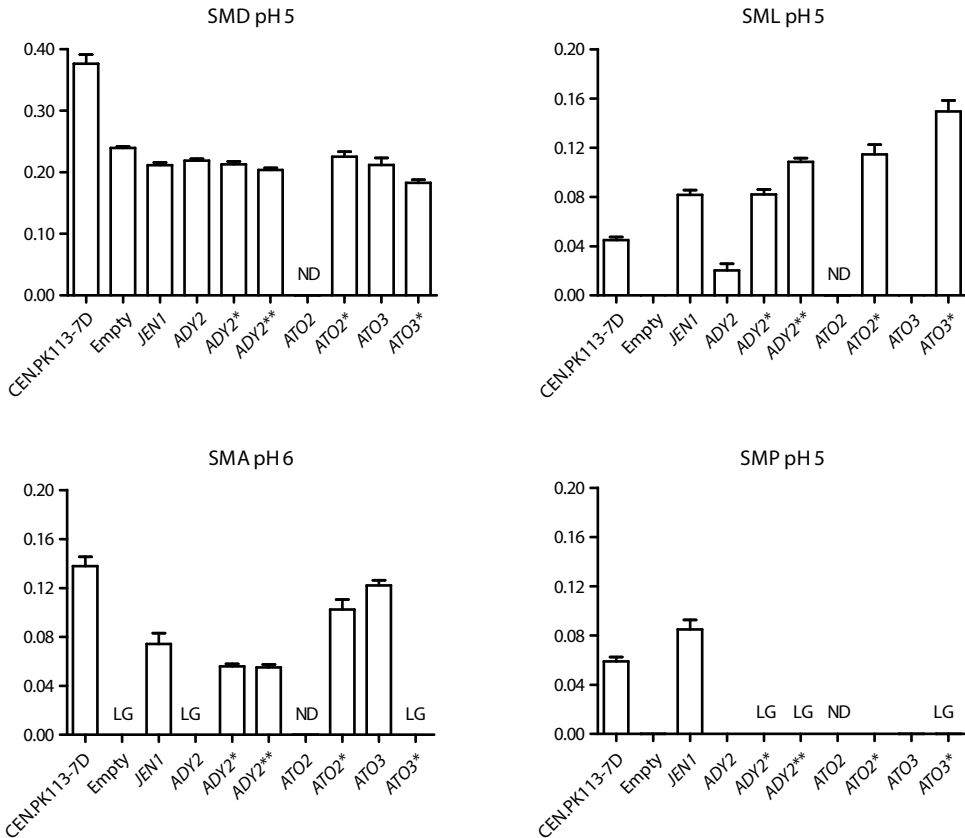
Figure 3.1: Growth rates on different sole carbon sources of *S. cerevisiae* reference strain CEN.PK113-7D and the 25-transporter deletion strain IMX2488 expressing an empty vector or a vector carrying the indicated organic acid transporter. Bars and error bars represent the average and standard deviation of three independent experiments. SMD: synthetic medium with 42 mM glucose. SML: synthetic medium with 83 mM lactic acid. SMA: synthetic medium with 125 mM acetic acid. SMP: synthetic medium with 83 mM pyruvic acid. Empty: empty plasmid. *ADY2**: *ADY2*^C755G allele. *ADY2***: *ADY2*^C655G allele. *ATO2**: *ATO2*^T653C allele. *ATO3**: *ATO3*^T284C allele. For some experiments, a linear increase in optical density was observed, which impeded the determination of an exponential growth rate (indicated by L.G. for Linear Growth). N.D.: not determined.

on the transport of organic acids, cellular growth was evaluated in strains individually expressing *JEN1, ADY2, ATO2* and *ATO3* and their mutated alleles under control of the strong *TEF1* promotor (Mumberg *et al.*, 1995), via centromeric vectors in IMX2488, which is a strain background in which 25 (putative) organic acid transporters were deleted (Table 3.2). No viable cultures could be obtained with strains overexpressing wildtype *ATO2*, which suggests a severe toxic effect of the overexpression of *ATO2* on cellular physiology, and for this reason no growth rate could be reported. All other IMX2488-derived transporter-expressing strains had similar growth rates in liquid medium with 42 mM glucose as carbon source compared to the empty vector control (IMC164), indicating no major physiological effects caused by the overexpression of the transporters when grown on glucose (Figure 3.1, top left panel). Overexpression of the transporter variants from multicopy vectors resulted in a growth rate reduction of up to 66% compared to the empty vector reference when grown on glucose.
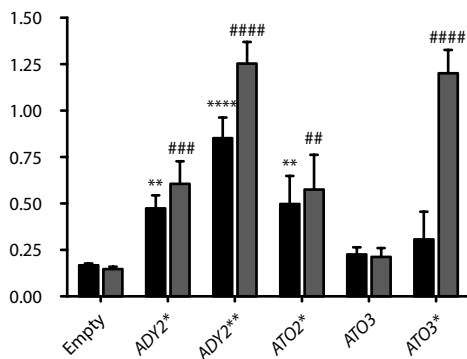
Figure 3.2: Transport of acetate and lactate in *S. cerevisiae* IMX1000 cells expressing native and evolved *ADY2*, *ATO2* and *ATO3*. Black bars: uptake of 5 mM of ¹⁴C-acetic acid (pH 6.0). Grey bars: uptake of ¹⁴C-lactic acid (pH 5.0). Empty: empty plasmid. *ADY2*⁺: *ADY2^{C755G}* allele. *ADY2*⁺⁺: *ADY2^{C655G}* allele. *ATO2*⁺: *ATO2^{T653C}* allele. *ATO3*⁺: *ATO3^{T284C}* allele. Cells were grown on YNB-glucose, washed and incubated in YNB-lactate (0.5%, pH 5.0) for 4 hours at 30 °C. Statistical significance was estimated by one-way ANOVA followed by a post hoc Tukey's multiple comparisons test as follows: ** $p<0.01$, *** $p<0.001$, **** $p<0.0001$, acetate uptake significantly different from cells transformed with empty plasmid; ## $p<0.01$, ### $p<0.001$, #### $p<0.0001$, lactate uptake significantly different from cells transformed with empty plasmid.

Therefore, these transporter variants were not tested further (Figure S3.2). In accordance with previous research, strains overexpressing *ADY2*, *ADY2^{C755G}* and *ADY2^{C655G}* showed a maximum specific growth rate of 0.02 ± 0.01 h⁻¹, 0.08 ± 0.01 h⁻¹ and 0.10 ± 0.01 h⁻¹ when grown in medium containing 83 mM lactic acid as carbon source, respectively (de Kok *et al.*, 2012b). Surprisingly, strains expressing the evolved *ATO2^{T653C}* and *ATO3^{T284C}* alleles outperformed all the other tested strains, with maximum specific growth rates of 0.11 ± 0.01 h⁻¹ and 0.15 ± 0.01 h⁻¹, respectively (Figure 3.1, top right panel and Figure S3.5). These represent the highest growth rates reported for *S. cerevisiae* on this carbon source and indicate that, similar to the role of evolved Ato3 in IMS807-811, the mutations in Ato2 are responsible for the evolved phenotype observed in IMS1122 and IMS1123 (Table 3.3). The transport of radiolabelled lactic acid in strains expressing native *ATO3* and evolved *ADY2*, *ATO2* and *ATO3* is in accordance with the observed growth phenotypes (Figure 3.2). An increased uptake rate was observed for all strains overexpressing evolved transporters compared to the empty vector control strain, whereas expression of wildtype *ATO3* did not lead to a significant alteration in lactic acid uptake (Figure 3.2).

Mutations in *ATO2* and *ATO3* alter the uptake capacity for acetate and pyruvate

After demonstrating that the point mutations increased the catalytic activity of Ato2, Ato3 and Ady2 for lactic acid transport, we also investigated their ability to transport acetic and pyruvic acid (Figure 3.1, bottom panels and Figures S3.6 and S3.7). In liquid medium at pH 5.0 with 125 mM acetic acid (pK_a of 4.75), no growth was observed for any of the strains with the 25-deletion background, likely caused by acetic acid toxicity due to the absence of essential acetic acid exporters (Figure S3.3). However, at pH 6.0 different growth characteristics were observed. The empty vector control strain exhibited slow non-exponential growth, which was also observed for the strains expressing native *ADY2* and the evolved *ATO3* variant. On the other hand, expression of native *ATO3* and the evolved *ADY2* and *ATO2* variants improved growth performance on medium with acetic acid as sole carbon source. With the exception of native *ATO3*, these results are in accordance with improved uptake rates observed in these strains, determined with labelled acetate (Figure 3.2). In medium containing 83 mM pyruvic

acid, no exponential growth was observed for any of the strains expressing Ato2, Ato3 or Ady2 variants. However, slow, non-exponential growth was observed for strains expressing $ATO2^{T653C}$ or any variant of $ADY2$ which could indicate a minor change in affinity for this substrate caused by the point mutations.

Protein modelling reveals mutations in the central hydrophobic constriction site as important factor in determining substrate specificity

In order to establish a link between the observed phenotypes and the structural alterations of transporters carrying the mutated amino acid residues, the 3D protein structures of Ady2, Ato2 and Ato3 were predicted based on the crystal structure of the *Citrobacter koseri* acetate anion channel SatP (PDB 5YS3), a bacterial member of the AceTr family (Qui *et al.*, 2018). When combined with a sequence alignment of Ady2, Ato2 and Ato3, the 3D structures showed that the Leu219Val mutation in Ady2, the Leu218Ser mutation in Ato2 and the Phe95Ser mutation in Ato3 are amongst three amino acid residues that were previously identified to be essential for the formation of the central narrowest hydrophobic constriction of the anion pathway in *C. koseri* SatP (Qui *et al.*, 2018) (Figure 3.3 and Figure 3.4). Specifically, these changes result in the substitution of the amino acid side group with a smaller (and in the case of Ato2 and Ato3 a more hydrophilic) alternative (Ato3 is shown in Figure 3.4 and the models for Ady2 and Ato2 can be found in Figures S3.9 and S3.10). Based on these models, we estimated the distance between these three hydrophobic residues. Since these distances are based on model predictions and are, for instance, dependent on the rotation of the amino acid side chains, they should not be interpreted as exact values. However, when comparing the relative distances, we found an increased value for $ADY2^{C655G}$, $ATO3^{T284C}$ and $ATO2^{T653C}$ compared to their corresponding wildtype protein, leading to a larger aperture in the center of the channel

```
                                                       1stTMS
tr|A8ALU5|A8ALU5_CITK8  ---------------------------------MGNTKLANPAPLGLMGFGMTTILLN 25
sp|P25613|ADY2_YEAST    GDNNEYIYIGRQKFLKSDLYQAFGG--TLNPGLAPAPVHKFANPAPLGLSAFALTTFVLS 106
sp|P32907|ATO2_YEAST    GKNNEYIYIGRQKFLRDDLFEAFGG--TLNPGLAPAPVHKFANPAPLGLSGFALTTFVLS 105
sp|Q12359|ATO3_YEAST    YSDRDFITLGSSTYRRRDLLNALDRGDGEEGNCAKYTPHQFANPVPLGLASFSLSCLVLS 103   F95S
                                                      ::***.**** .*.:: ::*.

                            2ndTMS                  3rdTMS
tr|A8ALU5|A8ALU5_CITK8  LHNAGF--FALDGIILAMGIFYGGIAQIFAGLLEYKKGNTFGLTAFTSYGSFWLTLVAIL 83
sp|P25613|ADY2_YEAST    MFNARAQGITVPNVVVGCAMFYGGLVQLIAGIWEIALENTFGGTALCSYGGFWLSFAAIY 166
sp|P32907|ATO2_YEAST    MFNARAQGITIPNVVVGCAMFYGGLVQLIAGIWEIALENTFGGTALCSSFGGFWLSFGAIY 165
sp|Q12359|ATO3_YEAST    LINANVRGVTDGKWALSLFMFFGGAIELFAGLLCFVIGDTYAMTVFSSFGGFWICYGYGL 163
                        : **     .:      :.  :*:** :::**:     :*:. *.: *T*.**:

                              4thTMS                  5thTMS
tr|A8ALU5|A8ALU5_CITK8  LMPKMGLTE------APNAQFLGAYLGLWGVFTLFMFFGTLKAARALQFVFLSLTVLFAL 137
sp|P25613|ADY2_YEAST    -IPWFGILEAYEDNESDLNNALGFYLLGWAIFTFGLTVCTMKSTVMFFLLFFLLALTFLL 225   L219V
sp|P32907|ATO2_YEAST    -IPWFGILDAYKDKESDLGNALGFYLLGWALFTFGLSVCTMKSTIMFFALFFLLAVTFLL 224   L218S
sp|Q12359|ATO3_YEAST    -TDTDNLVSGYTD-PTMLNNVIGFFLAGWTVFTFLMLMCTLKSTWGLFLLLTFLDLTFLL 221
                            .:.     :     : :* :*    * :**: : .  *:*::  :   ::    * : * *

                              6thTMS
tr|A8ALU5|A8ALU5_CITK8  LAFGNIAGNEAVIHVAGWIGLVCGASAIYLAMGEVLNEQFGRTI-----LPIGEAH-- 188
sp|P25613|ADY2_YEAST    LSIGHFANRLGVTRAGGVLGVVVAFIAWYNAYAGVATKQNSYVLARPFPLPSTERVIF 283   A252G
sp|P32907|ATO2_YEAST    LSIANFTGEVGVTRAGGVLGVIVAFIAWYNAYAGIATRQNSYIMVHPFALPSNDKVFF 282
sp|Q12359|ATO3_YEAST    LCIGTFIDNNNLKMAGGYFGILSSCCGWYSLYCSVVSPSNSYLAFRAHTMPNAP---- 275
                        *.:. : ..  : ..* :*::. .  *      :  . .          :*
```

Figure 3.3: Multiple sequence alignment of *Citrobacter koseri* SatP and *Saccharomyces cerevisiae* Ady2, Ato2 and Ato3. The multiple sequence alignment was built with ClustalOmega (https://www.ebi.ac.uk/Tools/msa/clustalo/). Localization of transmembrane segments (TMSs) was predicted with PSI/TM-Coffee (http://tcoffee.crg.cat/apps/tcoffee/do:tmcoffee). Blue rectangles indicate residues of the narrowest constriction site F98-Y155-L219 (amino acid numbers refer to Ady2) (Qui *et al.*, 2018). Bold, underlined letters indicate the mutated residue.

(Table 3.4). We hypothesize that this increased size of the hydrophobic constriction may allow larger substrates to pass through, possibly altering substrate specificity and transport capacity.

To investigate if the mutations affected the presence and affinity of binding sites for acetate, lactate and pyruvate, docking of ligands in the protein structures was simulated using AutoDock Vina (Figure S3.10, Table S3.2). In all proteins, both wildtype and mutated, four binding sites were identified for acetate, which is in accordance with what has previously been reported for the homolog CkSatP (Qui *et al.*, 2018). Of these four binding sites, two, which are located closest to the hydrophobic constriction, also consistently bind lactate and pyruvate. Strikingly, mutations in Ady2, Ato2 and Ato3 led to an increased lactate affinity of at least one of these two sites closest to the hydrophobic constriction, which might have contributed to the increased lactate transport capacity. No clear correlation was found between the physiology observed for strains overexpressing the different protein variants when grown on acetate and pyruvate and the corresponding binding affinities of these two ligands (Table S3.2).
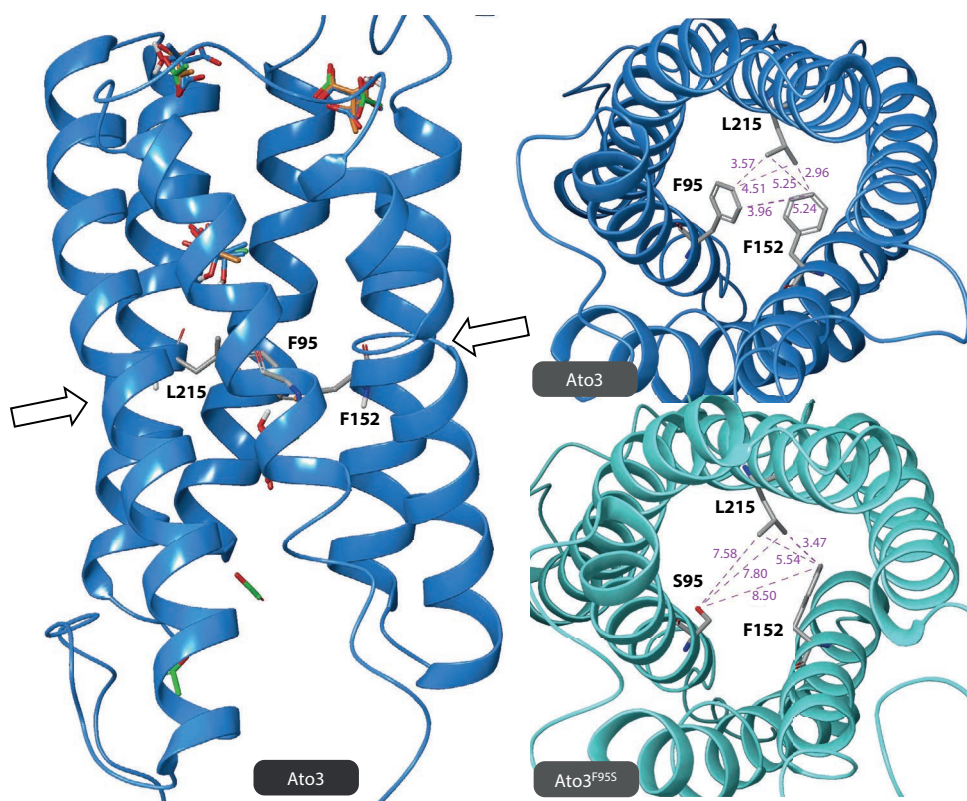
Figure 3.4: 3D models of the transporters Ato3 (dark blue) and Ato3[F95S] (light blue). Left: side view of Ato3. Arrows indicate the hydrophobic constriction site, consisting of F95, L215 and F152. Binding sites for acetate (green ligand), lactate (blue ligand) and pyruvate (orange ligand) are presented. Right, top view of Ato3 (top) and Ato3[F95S] (bottom). The amino acid residues involved in the constriction site are shown. Purple lines and values indicate estimated distances (in Å) between different anchor points of amino acid residues, calculated from the modelled protein structure.

Table 3.4: Estimated average distances (in Å) between different amino acids (AA) in the constriction pore of Ady2, Ato2, Ato3 and mutated alleles, calculated using the corresponding protein model. Bold values in the table indicate distances which are at least 1 Å larger than calculated in the reference structure.

Protein	Estimated distance between AA residues			Protein	Estimated distance between AA residues			Protein	Estimated distance between AA residues		
	219 & 98	98 & 155	155 & 219		218 & 97	97 & 154	154 & 218		215 & 95	95 & 152	152 & 215
Ady2	4.6	6.9	4.0	Ato2	4.2	5.7	4.4	Ato3	4.0	4.6	4.1
Ady2 L219V	4.4	6.9	**5.3**	Ato2 L218S	**5.9**	5.6	**5.6**	Ato3 F95S	**7.7**	**8.5**	4.5
Ady2 A252G	4.5	6.7	3.9								

3.4 Discussion

In this study, we report the identification and characterization of a family of transporter genes which, upon mutation, are able to efficiently catalyze the import of lactic acid in *S. cerevisiae*. As rational engineering to identify lactic acid transporters remains elusive (Borodina, 2019; Mans *et al.*, 2017), we used adaptive laboratory evolution to select for mutants capable of consuming lactic acid, which led to the identification of mutations in *ATO3* (*ATO3^{T284C}*) and *ATO2* (*ATO2^{T653C}*). Together with *ADY2*, *ATO2* and *ATO3* were previously described to code for ammonium transporters (Ammonium Transport Outwards) based on two observations: the high expression levels of these genes when *S. cerevisiae* exports ammonium, and the presence of a motif associated with ammonium transport in the encoded proteins (Palková *et al.*, 2002). However, the function of *ADY2* has previously been assessed by Rabitsch *et al.* (2001), who identified it as a gene required for correct spore formation, and thus named it as *ADY2* (Accumulation of DYads). In view of the observations in our study, where *ADY2*, *ATO2* and *ATO3* and their evolved variants catalyzed uptake of lactic and in some cases acetic acid, and the absence of mechanistic studies aimed at illustrating the phenomenon of ammonium export, we support the recent proposition by Alves *et al.* (2020) to rename these genes, present in *S. cerevisiae* and other yeasts, as "Acetate Transporter Ortholog".

For physiological studies focused on organic acid substrate uptake, a platform strain devoid of organic acid importers is a useful tool as it enables characterization based on growth rate. No growth was observed for IMC164 (25 deletions and empty vector) on medium containing either lactate or pyruvate as sole carbon source (Figure 3.1), demonstrating that this is a suitable strain background to test pyruvate and lactate transport capacity of transporter variants. Strain IMK982 (*jen1Δ ady2Δ ato3Δ ato2Δ)* was also unable to grow on lactic acid, nor could it evolve this trait, which suggests that this strain could also be employed as a platform strain to investigate both endogenous and heterologous lactic acid transporters, without requiring the additional 21 deletions. In contrast, when grown on acetic acid at pH 6.0, IMC164 exhibited non-exponential linear growth (Figure S3.6), suggesting simple diffusion of acetic acid, or the presence of at least one gene involved in acetate transport in this strain background. The observed increase in the uptake rate of acetic acid for the evolved Ady2 and Ato2 variants (Figure 3.2) corroborates with the increased growth rate on this carbon source. For the strain expressing native *ATO3* an improved growth rate was observed, but no increase in acetic acid uptake could be detected. This result led us to postulate the role of Ato3 as an

exporter of acetic acid, thereby limiting the negative effects caused by the passive diffusion of this monocarboxylic acid. The fact that the expression of native *ATO3*, besides *ADY2*, results in an increased growth rate on acetate is in accordance with previous data reporting that both genes are induced in cells shifted from glucose to acetic acid as sole carbon source (Paiva *et al.*, 2004).

It was reported by de Kok *et al.* (2012) that the overexpression of *ADY2*, under the control of the strong glycolytic promoter *TEF1*, was sufficient to enable slow growth (μ_{max} ~0.02 h^{-1}) in medium containing lactic acid as sole carbon source. While the native alleles of *ATO3* and likely *ATO2* were not able to sustain growth on lactic acid medium, their mutated versions (*ATO2*^{T653C} and *ATO3*^{T284C}) enabled high growth rates, with the highest growth rate determined at 0.15 ± 0.01 h^{-1} for the strain harboring *ATO3*^{T284C}. To the best of our knowledge this growth rate represents the highest reported growth rate of *S. cerevisiae* expressing a single transport protein on lactic acid and is close to the growth rate observed by de Kok *et al.* (2012) of 0.14 h^{-1} by a strain expressing *ADY2*^{C655G}. This 3-fold increase in growth rate of the engineered strain compared to the reference strain CEN.PK113-7D indicates that, in non-engineered *S. cerevisiae* strains, growth on lactic acid is likely limited by its transport into the cell, and not the capacity to be further metabolized. Therefore, for future work that requires fast consumption of lactic acid, overexpression of *ATO3*^{T284C} can be considered.

Based on the 3D structures of Ady2 (Ato1), Ato2 and Ato3 and the simulation of ligand docking in the predicted protein structures, we hypothesize that an increased binding affinity upon mutation may contribute to increased transport capacity by facilitating passage of the ligand through the hydrophobic constriction, although the increased size of the hydrophobic constriction is probably the main contributor to the evolved phenotype. Other mechanisms may also contribute to an improved transport capacity, as observed for the A252G mutation in Ady2, an amino acid residue located outside the constriction pore. These may include an improved transition between the closed to open state of the transporter or increased stability in the plasma membrane.

In this study, we show that laboratory evolution is a powerful tool for the identification of genes involved in substrate transport and resulted in the identification of Ato3^{F95S}, which enables the highest growth rate on lactic acid by *S. cerevisiae* reported in strains expressing a single transport protein thus far. In addition, the presented data on transport protein structure and function led to the identification of important amino acid residues that dictate substrate specificity of *S. cerevisiae* carboxylic acid transporters, which could potentially aid in future rational engineering and annotation of additional proteins involved in organic acid transport.

3.5 Funding

2020), under the PORTUGAL 2020 Partnership Agreement, through the European Regional Development Fund (ERDF); and UMINHO/BD/25/2016 PhD grant by the Norte2020 [grant number NORTE-08–5369-FSE-000060] and a FEBS Short-Term Fellowship to MSS.

3.6 Supplementary information

Table S3.1: Primers used in this study

Number	Name	Sequence (5'-> 3')	Purpose
8664	JEN1_targetRNA FW SspI	TGCGCATGTTTCGGCGTTCGAAACTTCTCCGCAGT-GAAAGATAAATGATCGTCACTCAATATTAATTTAC-GTTTTAGAGCTAGAAATAGCAAGTTAAAATAAG-GCTAGTCCGTTATCAAC	Construction of pUDR405
6262	CrRNA insert ADY2 fw	TGCGCATGTTTCGGCGTTCGAAACTTCTCCGCAGT-GAAAGATAAATGATCCCCACCGTAAGAACATAAT-GGTTTTAGAGCTAGAAATAGCAAGTTAAAATAAG-GCTAGTCCGTTATCAAC	Construction of pUDR405
6005	p426 CRISP rv	GATCATTTATCTTTCACTGCGGAGAAG	Construction of pUDR405 – pUDR420
8691	ATO3_targetRNA FW SspI	TGCGCATGTTTCGGCGTTCGAAACTTCTCCG-CAGTGAAAGATAAATGATCGAGTATATCTCTT-GAATATTGTTTTAGAGCTAGAAATAGCAAGTTA-AAATAAG	Construction of pUDR420
13552	ATO3_targetRNA_RV_SspI	CTTATTTTAACTTGCTATTTCTAGCTCTAAAACAATAT-TCAAGAGATATACTCGATCATTTATCTTTCACTGCG-GAGAAGTTTCGAACGCCGAAACATGCGCA	Construction of pUDR420
8688	ATO2_targetRNA FW Eco52I	TGCGCATGTTTCGGCGTTCGAAACTTCTCCGCAGT-GAAAGATAAATGATCCGGCCGTCAAAAATTTTTA-AGTTTTAGAGCTAGAAATAGCAAGTTAAAATAAG	Construction of pUDR767
6006	p426 CRISP fw	GTTTTAGAGCTAGAAATAGCAAGTTAAAATAAG-GCTAGTC	Construction of pUDR420 and pUDR767
5921	Primer_pTEF1_rv	AAAACTTAGATTAGATTGCTATGCTTTCTTTCTAAT-GAGC	Linear p426-TEF backbone amplification
10547	p426-GPD backbone rv	TCATGTAATTAGTTATGTCACGC	Linear p426-TEF backbone amplification
13513	pTEF1_ATO3	TACAACTTTTTTTACTTCTTGCTCATTAGAAAGAAAG-CATAGCAATCTAATCTAAGTTTTATGACATCGTCT-GCTTCTTC	Construction of pUDE813 and pUDE814
13514	tCYC1_ATO3	CGGTTAGAGCGGATGTGGGGGGAGGGCGTGAAT-GTAAGCGTGACATAACTAATTACATGATTAAGGAG-CATTTGGCATTG	Construction of pUDE813 and pUDE814
17168	pTEF1_ADY2_fw	TACAACTTTTTTTACTTCTTGCTCATTAGAAAGAAAG-CATAGCAATCTAATCTAAGTTTTATGTCTGACAAG-GAACAAACG	Construction of pUDE1002, pUDE1003 and pUDE1004
17169	tCYC1_ADY2_rv	CGGTTAGAGCGGATGTGGGGGGAGGGCGTGAAT-GTAAGCGTGACATAACTAATTACATGATTAAAAGAT-TACCCTTTCAGTAG	Construction of pUDE1002, pUDE1003 and pUDE1004

17170	pTEF1_JEN1_fw	TACAACTTTTTTTACTTCTTGCTCATTAGAAAGAAAG-CATAGCAATCTAATCTAAGTTTTATGTCGTCGTCAAT-TACAGATG	Construction of pUDE1001
17171	tCYC1_JEN1_rv	CGGTTAGAGCGGATGTGGGGGGAGGGCGTGAATG-TAAGCGTGACATAACTAATTACATGATTAAACGGTCT-CAATATGCTCC	Construction of pUDE1001
17452	pTEF1_ATO2_fw	TACAACTTTTTTTACTTCTTGCTCATTAGAAAGAAAG-CATAGCAATCTAATCTAAGTTTTATGTCTGACA-GAGAACAAAGC	Construction of pUDE1021 and pUDE1022
17453	tCYC1_ATO2_rv	CGGTTAGAGCGGATGTGGGGGGAGGGCGTGAATG-TAAGCGTGACATAACTAATTACATGATTAGAAGAA-CACCTTATCATTGC	Construction of pUDE1021 and pUDE1022
17742	p426_CENARS_fw	TAGAAAAATAAACAAATAGGGGTTCCGCGCA-CATTTCCCCGAAAAGTGCCACCTGAACGAACGGATC-GCTTGCCTGTAAC	Amplification of CEN6 from pUDC156
17743	p426_CENARS_rv	GATAATATCACAGGAGGTACTAGAC-TACCTTTCATCCTACATAAATAGACGCATATAAGTTC-CCCGAAAAGTGCCACCTG	Amplification of CEN6 from pUDC156
2949	F Tag Episomal Rev	CGTTCAGGTGGCACTTTTCG	Construction of pUDC319-pUDC327
17741	p426_originremoval	ACTTATATGCGTCTATTTATGTAGGATG	Construction of pUDC319-pUDC327
1742	LEU2 check fw	GGTCGCCTGACGCATATACC	*LEU2* amplification
1743	LEU2 check rv	TAAGGCCGTTTCTGACAGAG	*LEU2* amplification
1738	HIS3 check fw	GCAGGCAAGATAAACGAAGG	*HIS3* amplification
3755	his3 outside rv (B)	CACTTGTTCGCTCAGTTCAG	*HIS3* amplification
8597	JEN1_repair oligo fw	AAGAAGAGTAACAGTTTCAAAAGTTTTTCCT-CAAAGAGATTAAATACTGCTACTGAAAAT-TCACTTTTCATTGCTCTCTAGGGCGTGTTCGCTTCTC-TATGTAACTGCATTTCACATATA	Deletion of *JEN1*
8598	JEN1_repair oligo rv	TATATGTGAAATGCAGTTACATAGAGAAGCGAACAC-GCCCTAGAGAGCAATGAAAAGTGAATTTTCAGTAG-CAGTATTTAATCTCTTTGAGGAAAAACTTTTGAAACT-GTTACTCTTCTT	Deletion of *JEN1*
8665	ADY2_repair oligo fw	CGACAGCTAACACAGATATAACTAAACAACCA-CAAAACAACTCATATACAAACAAATAATGAGCAC-GACCTACTAATAACGAGAACTATTGAAATAAAAAA-GAGTAGTTTTTTATTTTTC	Deletion of *ADY2*
8666	ADY2_repair oligo rv	GAAAAATAAAAAAC-TACTCTTTTTTATTTCAATAGTTCTCGTTATTAGTAG-GTCGTGCTCATTATTGTTTGTATATGAGTTGTTTTGT-GGTTGTTTAGTTATATCTGTGTTAGCTGTCG	Deletion of *ADY2*
14120	ATO3_repair_syn_fw	ATTGAGACGCTCCCCCAGCAGGGTTCGATTGCAGG-CGTTTCGCAGGGCAGTAGAATTTCACCTAGACGTGG-CCTTCTTGATGTTGATGTGTACATTGAAGAGCACGTG-GGGTTTGTTCT	Deletion of *ATO3*

3

| 14121	ATO3_repair_syn_fw	AGAACAAACCCCACGTGCTCTTCAATGTACACAT-CAACATCAAGAAGGCCACGTCTAGGTGAAATTC-TACTGCCCTGCGAAACGCCTGCAATCGAACCCTGCT-GGGGGAGCGTCTCAAT	Deletion of *ATO3*
8689	ATO2_repair oligo fw	TATGTAACATTCTACAGATCAATCAAAAA-CAATCTTCAATCACAGAAAAAAATAAAAGGCAAA-CACAAAAGTGCAGGCTAAAATAACTTTTACCCCTAT-TATATATTCTTATGATCCATT	Deletion of *ATO2*
8690	ATO2_repair oligo rv	AATGGATCATAAGAATATATAATAGGGGTA-AAAGTTATTTTAGCCTGCACTTTTGTGTTTG-CCTTTTATTTTTTTCTGTGATTGAAGATTGTTTTT-GATTGATCTGTAGAATGTTACATA	Deletion of *ATO2*
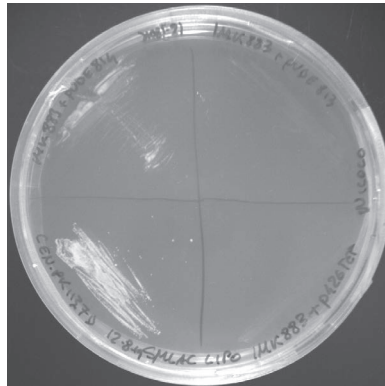
Figure S3.1: Growth of different strains on SM media with lactic acid as the sole carbon source. Bottom left quadrant: prototrophic strain CEN.PK113-7D. Bottom right quadrant: IMK883 (*ura3-52, jen1Δ, ady2Δ, ato3Δ*) carrying an empty p426-pTEF plasmid. Top right quadrant: IMK883 carrying pUDE813 (p426-*pTEF-ATO3*). Top left quadrant: IMK883 carrying pUDE814 (p426-*pTEF-ATO3*^{T284C}). Cells were streaked from a single colony and the plate was incubated at 30 °C for 5 days.
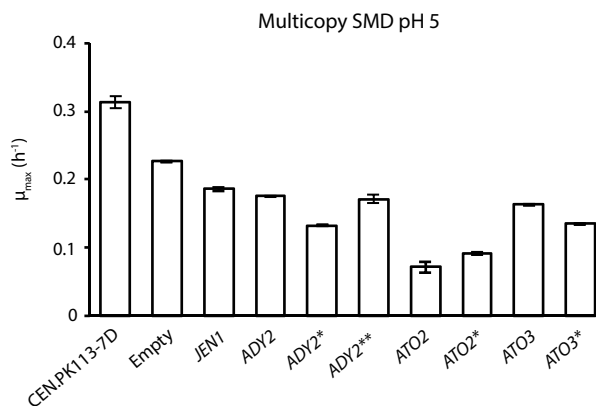
Figure S3.2: Growth rates on SMD of *S. cerevisiae* reference strain CEN.PK113-7D and the 25-transporter deletion strain IMX2488 expressing an empty multicopy vector or a multicopy vector containing the indicated organic acid transporter gene. Bars and error bars represent the average and standard deviation of three independent experiments. Empty: empty plasmid. *ADY2**: *ADY2*^{C755G} allele. *ADY2***: *ADY2*^{C655G} allele. *ATO2**: *ATO2*^{T653C} allele. *ATO3**: *ATO3*^{T284C} allele.
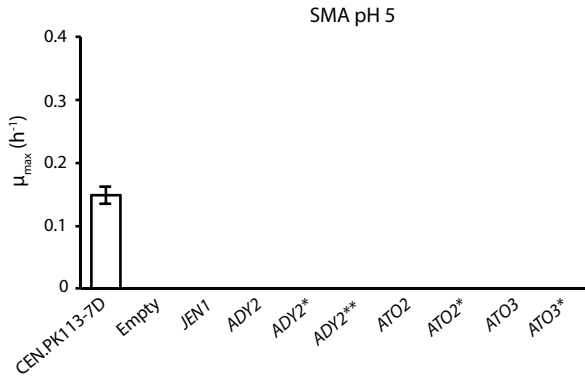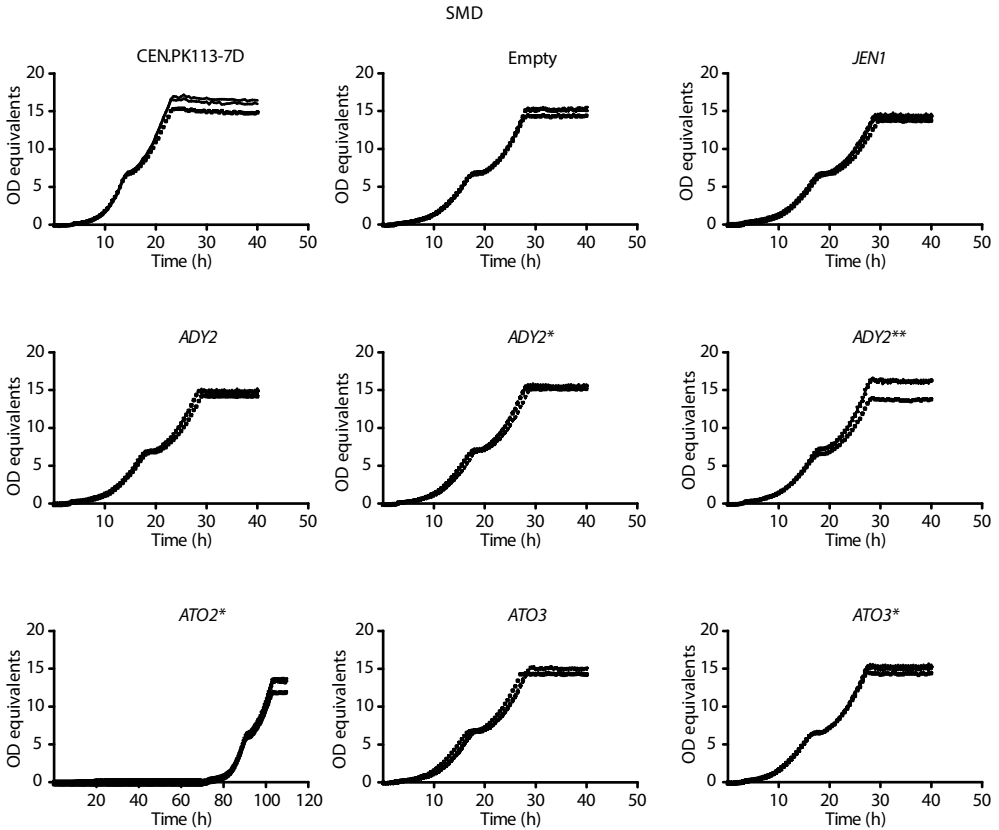
Figure S3.3: Growth rates of *S. cerevisiae* reference strain CEN.PK113-7D and the 25-transporter deletion strain IMX2488 expressing an empty centromeric vector or a centromeric vectors containing the indicated organic acid transporter gene. Growth on SMA medium set at pH 5.0. Bars and error bars represent the average and standard deviation of three independent experiments. Empty: empty plasmid. *ADY2**: *ADY2^{C755G}* allele. *ADY2***: *ADY2^{C655G}* allele. *ATO2**: *ATO2^{T653C}* allele. *ATO3**: *ATO3^{T284C}* allele.

Figure S3.4: Growth profiles in synthetic medium (pH 5.0) with glucose as the sole carbon source of CEN.PK113-7D and the 25-transporter deletion strain IMX2488 expressing an empty centromeric vector or a centromeric vector containing the indicated organic acid transporter gene. Empty: empty plasmid. *ADY2**: *ADY2^{C755G}* allele. *ADY2***: *ADY2^{C655G}* allele. *ATO2**: *ATO2^{T653C}* allele. *ATO3**: *ATO3^{T284C}* allele.

SML
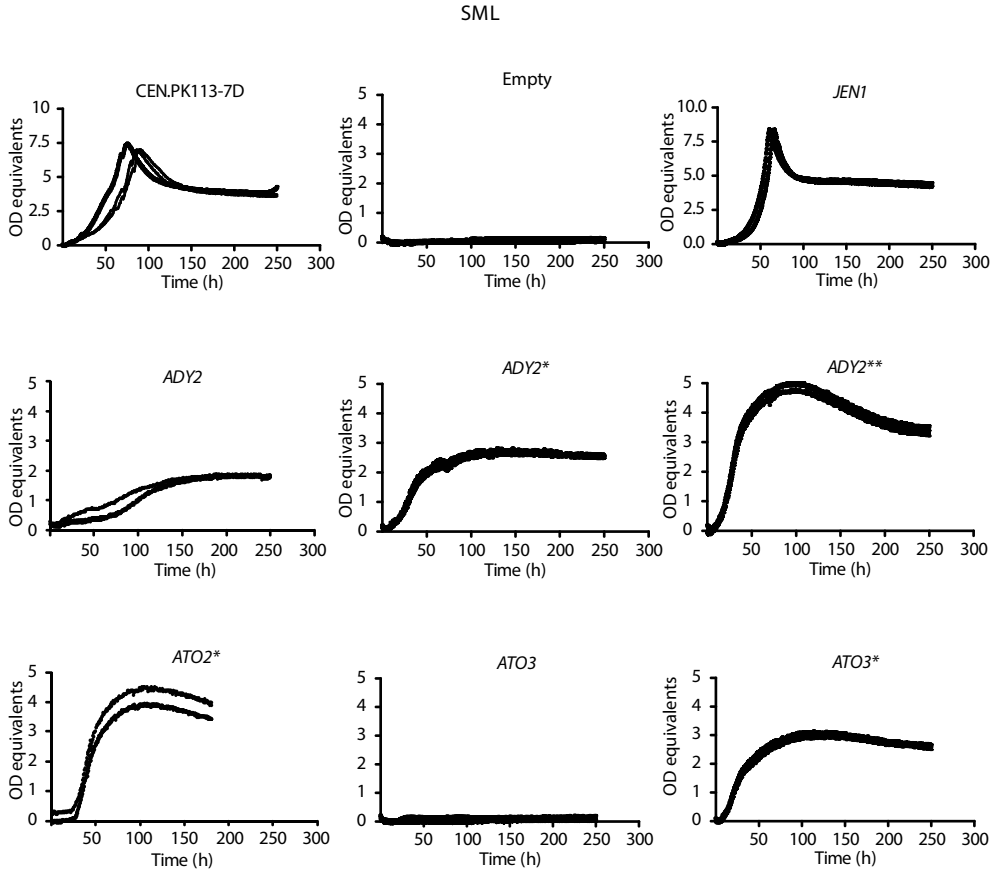
Figure S3.5: Growth profiles in synthetic medium (pH 5.0) with lactate as the sole carbon source of CEN.PK113-7D and the 25-transporter deletion strain IMX2488 expressing an empty centromeric vector or a centromeric vector containing the indicated organic acid transporter gene. Empty: empty plasmid. *ADY2**: *ADY2^{C755G}* allele. *ADY2***: *ADY2^{C655G}* allele. *ATO2**: *ATO2^{T653C}* allele. *ATO3**: *ATO3^{T284C}* allele.
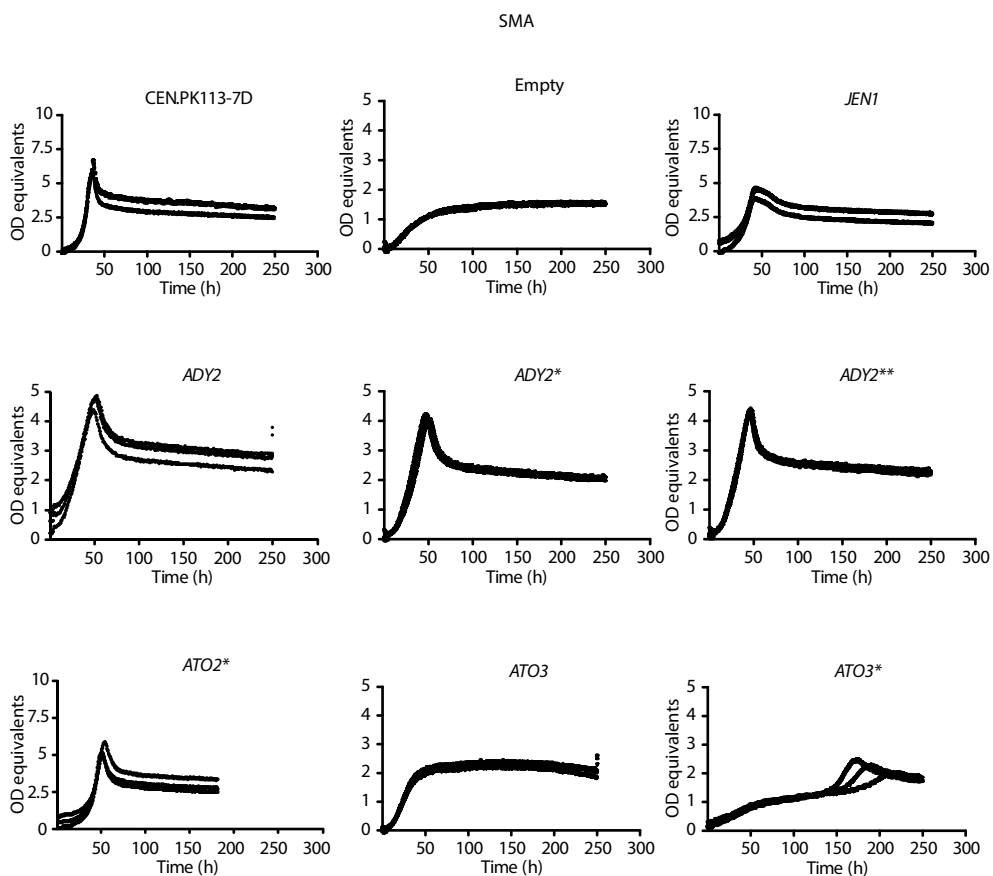
Figure S3.6: Growth profiles in synthetic medium (pH 6.0) with acetate as the sole carbon source of CEN.PK113-7D and the 25-transporter deletion strain IMX2488 expressing an empty centromeric vector or a centromeric vector containing the indicated organic acid transporter gene. Empty: empty plasmid. *ADY2**: *ADY2^{C755G}* allele. *ADY2***: *ADY2^{C655G}* allele. *ATO2**: *ATO2^{T653C}* allele. *ATO3**: *ATO3^{T284C}* allele.
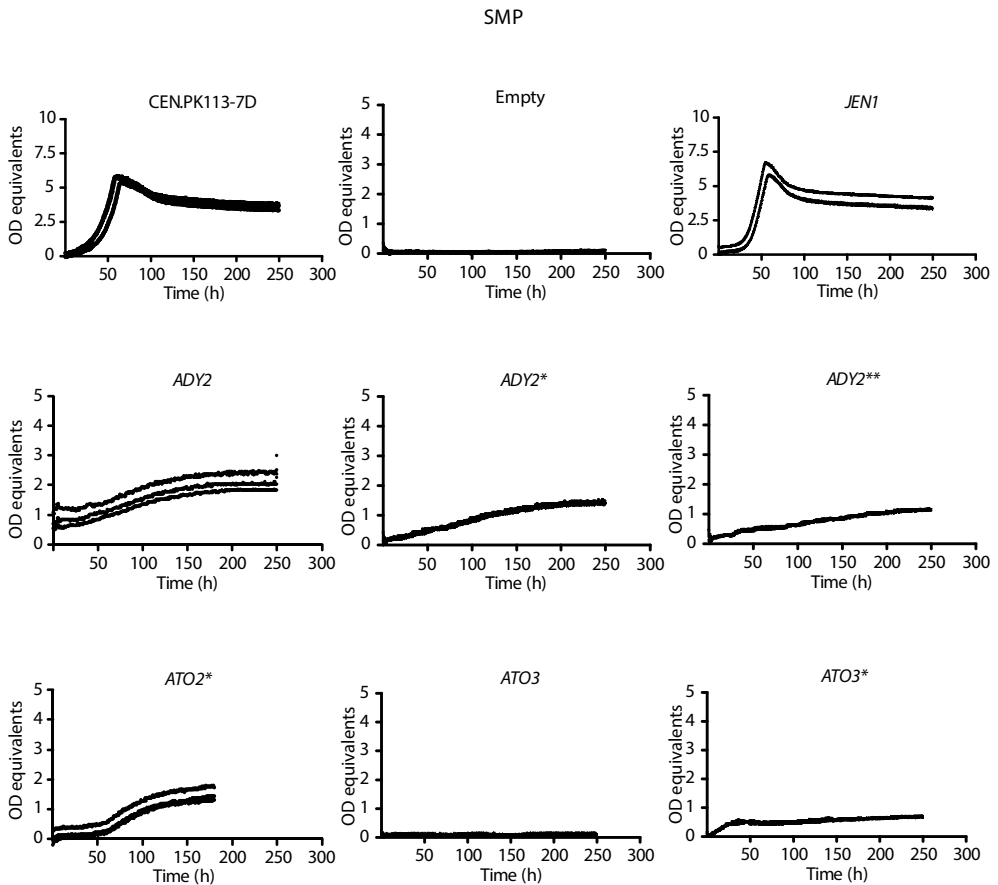
Figure S3.7: Growth profiles in synthetic medium (pH 5) with pyruvate as the sole carbon source of CEN.PK113-7D and the 25-transporter deletion strain IMX2488 expressing an empty centromeric vector or a centromeric vector containing the indicated organic acid transporter gene. Empty: empty plasmid. *ADY2**: *ADY2*^{C755G} allele. *ADY2***: *ADY2*^{C655G} allele. *ATO2**: *ATO2*^{T653C} allele. *ATO3**: *ATO3*^{T284C} allele.
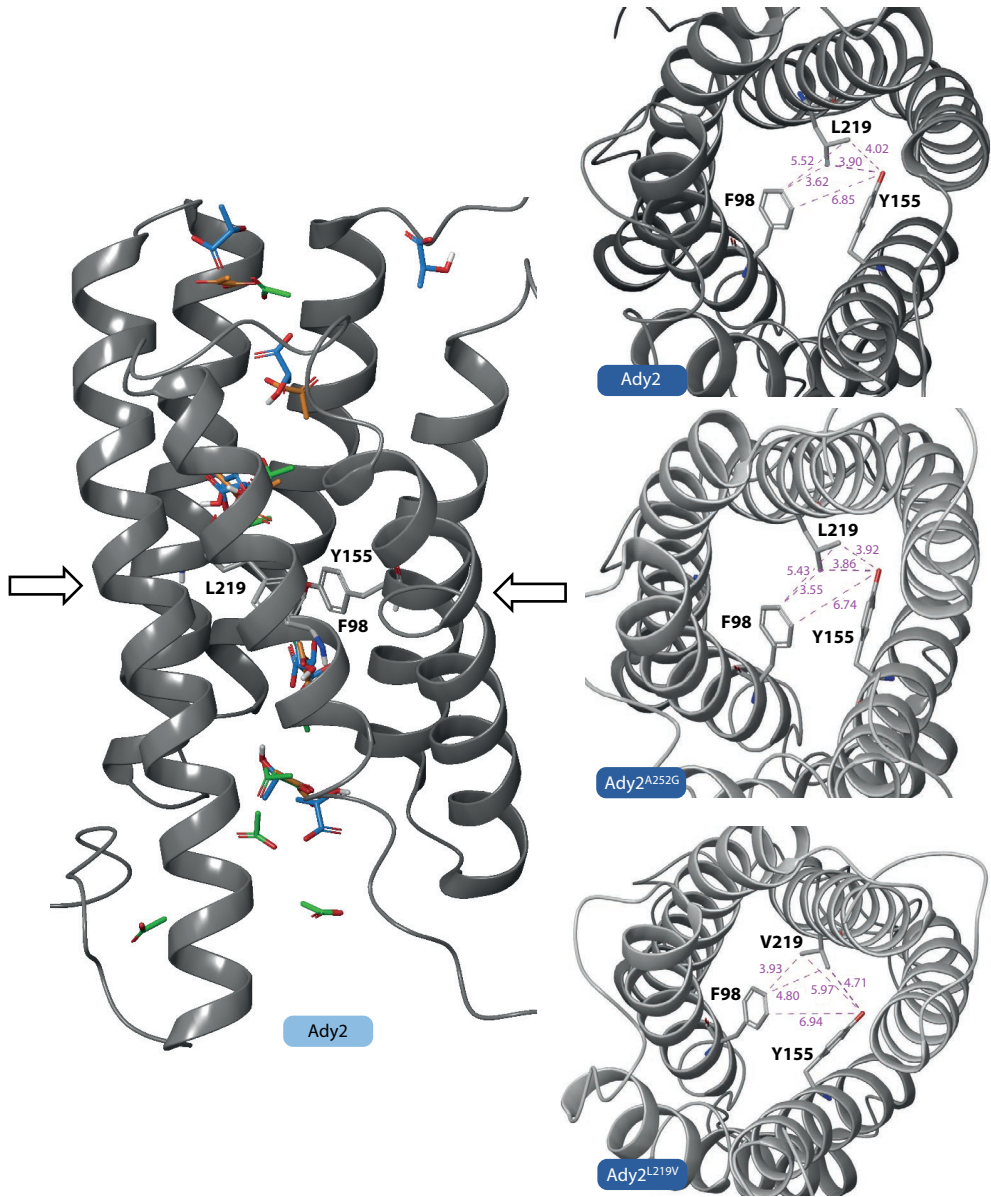
Figure S3.8: 3D model of Ady2, Ady2[L219V] and Ady2[A252G] proteins. Left: side view of Ady2. Arrows indicate the hydrophobic constriction site. Binding sites for acetate (green ligand), lactate (blue ligand) and pyruvate (orange ligand) are presented. Right: top view of Ady2, Ady2[L219V] and Ady2[A252G] alleles. The amino acid residues involved in the hydrophobic constriction site are shown. Purple lines and values indicate distances (in Å) between different anchor points of amino acid residues.
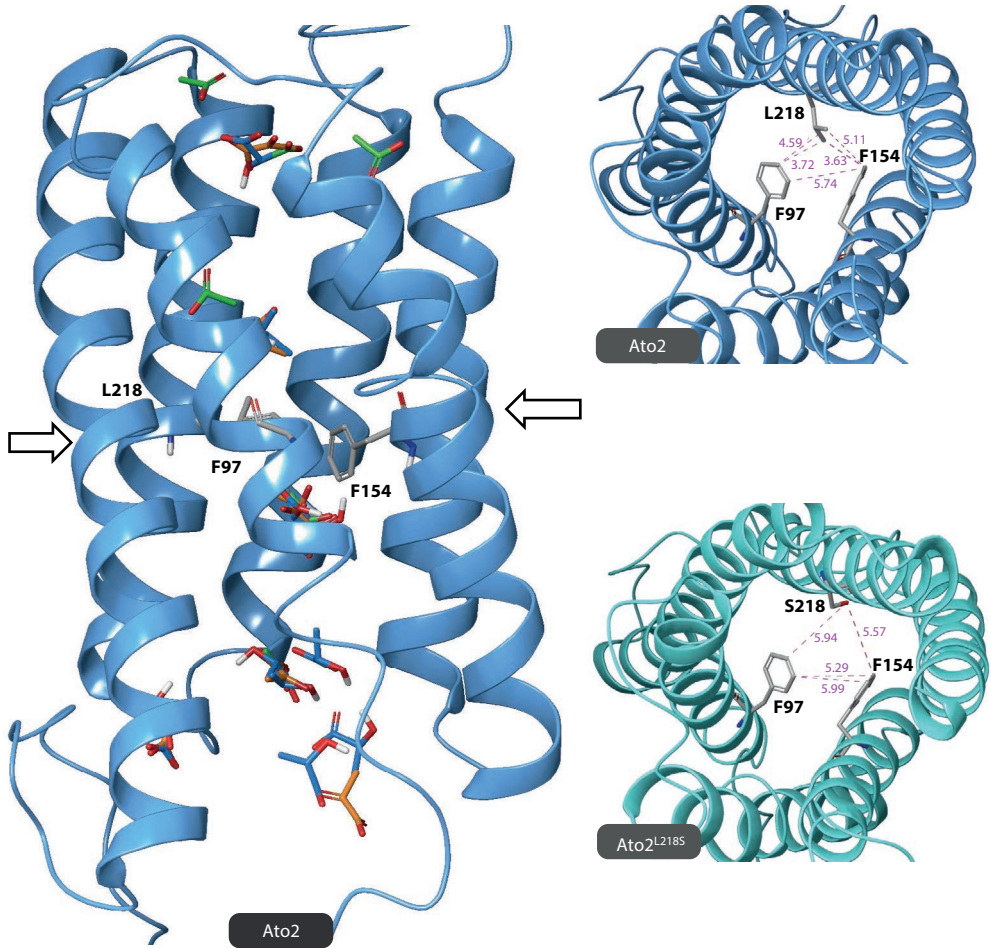
Figure S3.9: 3D model of Ato2 and Ato2[L218S]. Left, side view of Ato2. Arrows indicate the constriction site. Binding sites for acetate (green ligand), lactate (blue ligand) and pyruvate (orange ligand) are presented. Right: top view of either Ato2 or Ato2[L218S]. The amino acid residues involved in the constriction site are shown. Purple lines and values indicate distances (in Å) between different anchor points of amino acid residues.
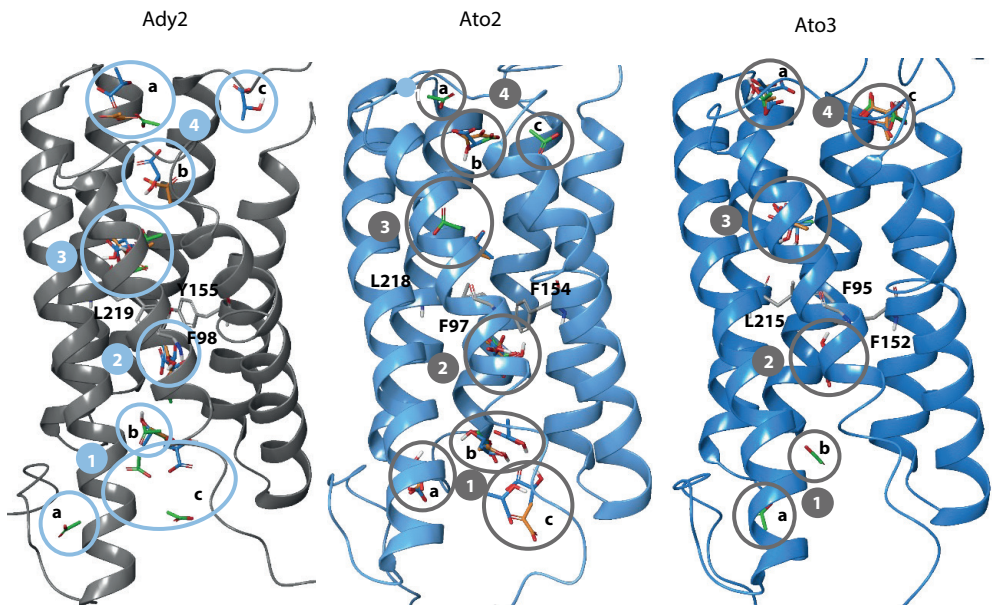
Figure S3.10: Molecular docking sites of acetate (green ligand), lactate (blue ligand) and pyruvate (orange ligand) in the predicted structure of Ady2, Ato2 and Ato3, identified using Autodock Vina.

Table S3.2: Average of the binding affinity values (kcal mol^{-1}) calculated with PyRx software for the docking of ligand in the predicted structures of wildtype and mutated Ady2, Ato2 and Ato3.

3D-Protein templates	Average of binding affinities (kcal mol^{-1}) at different binding sites								
	Acetate								
	1			**2**	**3**	**4**			
	a	b	c			a	b	c	
Ady2	-2,1	-2,4	-2,3	-2,7	-3,1	-2,7	-	-	
Ady2 A252G	-2,3	-2,2	-2,1	-3,1	-3,1	-2,6	-2,7	-	
Ady2 L219V	-2,4	-	-	-3,0	-3,0	-2,5	-2,7	-	
Ato2	-2,5	-2,6	-	-3,1	-2,9	-2,8	-2,9	-3	
Ato2 L218S	-2,7	-	-	-2,7	-3,1	-3,3	-2,6	-2,5	
Ato3	-2,3	-2,2	-	-2,9	-3,0	-2,2	-	-2,4	
Ato3 F95S	-2,6	-2,4	-	-3,0	-2,9	-2,4	-2,4	-2,4	
	Lactate								
	1			**2**	**3**	**4**			
	a	b	c			a	b	c	d
Ady2	-	-3,1	-3,0	-3,6	-4,3	-3,5	-3,1	-3,1	-
Ady2 A252G	-2,9	-2,8	-2,7	-3,7	-4,4	-3,3	-3,4	-	-2,1
Ady2 L219V	-3,4	-	-	-3,9	-4,4	-	-3,8	-	-
Ato2	-3,2	-3,1	-3,2	-3,9	-3,8	-	-2,9	-	-
Ato2 L218S	-3,5	-	-	-3,8	-4,2	-3,6	-	-3,4	-
Ato3	-	-	-	-3,4	-3,8	-3,1	-	-3,2	-
Ato3 F95S	-3,3	-	-	-4,2	-4,0	-3,2	-3,2	-3,2	-
	Pyruvate								
	1			**2**	**3**	**4**			
	a	b	c			a	b	c	
Ady2	-	-3,1	-	-3,7	-4,2	-3,2	-3,3	-	
Ady2 A252G	-3,0	-	-2,7	-3,9	-4,3	-3,3	-3,3	-	
Ady2 L219V	-3,2	-	-	-4,0	-4,2	-	-3,5	-	
Ato2	-3,3	-3,3	-3,1	-3,9	-4,1	-	-3,6	-	
Ato2 L218S	-3,5	-	-	-3,9	-4,3	-	-	-3,3	
Ato3	-	-	-	-3,6	-4,0	-3,0	-	-3,2	
Ato3 F95S	-3,4	-	-	-4,2	-3,9	-	-3,4	-	

3
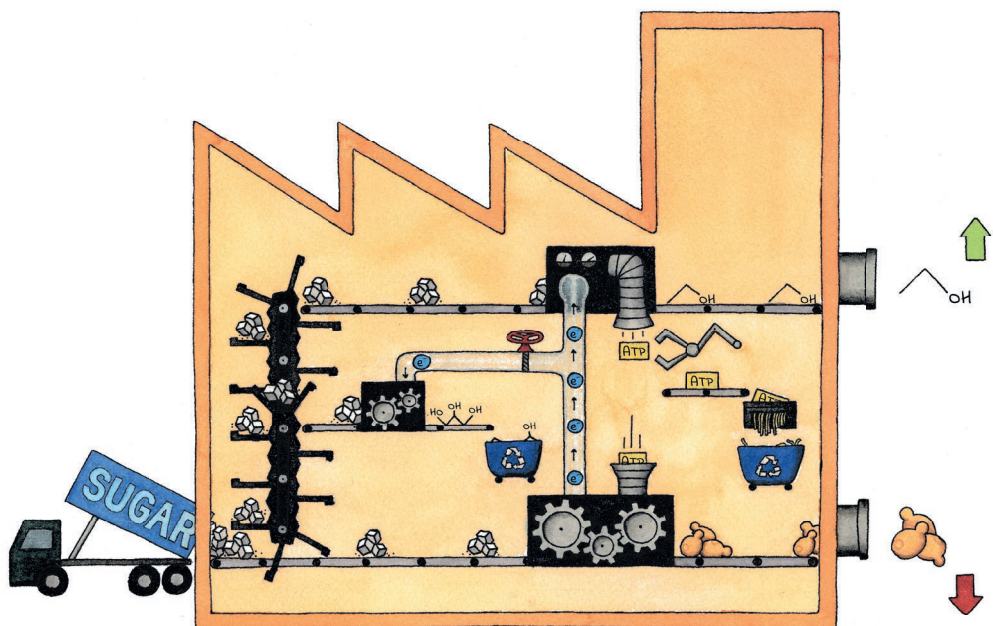
Chapter 4

Pathway engineering strategies for improved product yield in yeast-based industrial ethanol production

Aafke C. A. van Aalst[*], Sophie C. de Valk[*], Walter M. van Gulik, Mickel L. A. Jansen, Jack T. Pronk and Robert Mans

[*]These authors contributed equally to this work.

Abstract

Product yield on carbohydrate feedstocks is a key performance indicator for industrial ethanol production with the yeast *Saccharomyces cerevisiae*. This paper reviews pathway engineering strategies for improving ethanol yield on glucose and/or sucrose in anaerobic cultures of this yeast by altering the ratio of ethanol production, yeast growth and glycerol formation. Particular attention is paid to strategies aimed at altering energy coupling of alcoholic fermentation and to strategies for altering redox-cofactor coupling in carbon and nitrogen metabolism that aim to reduce or eliminate the role of glycerol formation in anaerobic redox metabolism. In addition to providing an overview of scientific advances, we discuss context dependency, theoretical impact and potential for industrial application of different proposed and developed strategies.

4

4.1 Introduction

In 2020, 99 billion liters of ethanol were produced by yeast-based fermentation of agriculture-derived carbohydrates (Renewable Fuels Association, 2020). Of this volume, approximately 30% was produced from Brazilian cane sugar (mainly consisting of sucrose) and approximately 54% from corn starch-derived glucose, mainly in the United States of America (Renewable Fuels Association, 2020). Ethanol is predominantly used as a renewable 'drop-in' transport fuel and ethanol-based value chains towards other compounds, including jet fuel and polyethylene, are under development (Capaz *et al.*, 2018; Mohsenzadeh *et al.*, 2017).

Despite a plethora of academic and industrial studies on alternative microbial platforms (Ruchala *et al.*, 2020), *Saccharomyces cerevisiae* remains the organism of choice for industrial ethanol production from carbohydrates. Factors that contribute to its popularity include rapid fermentation of glucose and sucrose to ethanol, insensitivity to phages, a long history of safe use in food applications and a high tolerance to ethanol. Ethanol concentrations in corn-starch-based, very-high-gravity fermentation processes can reach up to 21% (v/v) (Devantier *et al.*, 2005; Thomas and Ingledew, 1992). In bulk fermentation processes such as ethanol production, where costs of the carbohydrate feedstock can account for up to 70% of the total production costs (Pfromm *et al.*, 2010), every detectable improvement of the ethanol yield on sugar is economically relevant. The extensive toolbox for genetic modification of *S. cerevisiae* (Lian *et al.*, 2018) is therefore intensively used to explore options for maximizing ethanol yields by engineering its metabolic network.

In *S. cerevisiae*, anaerobic metabolism of glucose or sucrose starts with their conversion to pyruvate via the ATP-generating Embden-Meyerhof glycolytic pathway. NADH generated by this oxidative pathway is re-oxidized by the combined action of pyruvate decarboxylase (Pdc1, Pdc5, Pdc6, EC 4.1.1.1: pyruvate –> acetaldehyde + CO_2) and NAD^+-dependent alcohol dehydrogenases (predominantly Adh1, EC 1.1.1.1: acetaldehyde + NADH –> ethanol + NAD^+ (de Smidt *et al.*, 2008)) (Figure 4.1). This native yeast pathway for alcoholic fermentation perfectly conserves the degree of reduction of sugars (Roels, 1980) and almost completely captures their heat of combustion in ethanol (-2840 kJ per mol of glucose versus -2734 kJ per two mol of ethanol). Clearly, if alcoholic fermentation was the only relevant metabolic process in industrial ethanol production, attempts to improve ethanol yields on sugars as sole carbon and electron sources would be futile. Metabolic engineering strategies for improving ethanol yields are therefore directly or indirectly related to another cellular process that occurs during industrial ethanol production: anaerobic growth.

In the absence of growth, survival of yeast cells requires cellular maintenance metabolism, which encompasses use of ATP for growth-independent processes that maintain structural integrity and viability (Russell and Cook, 1995). In anaerobic yeast cultures, this ATP is exclusively generated via alcoholic fermentation (Figure 4.1). In contrast, growth of yeast cells not only requires ATP but also organic precursors for biomass components, whose biosynthetic pathways compete for carbon with ethanol production (Figure 4.1). Anaerobic growth occurs in all current industrial processes for ethanol production and the resulting surplus yeast biomass is valorized by its inclusion in a by-product stream sold as an animal feed supplement (Conroy *et al.*, 2016).

Growth is coupled to formation of glycerol, a second important byproduct of anaerobic yeast

4
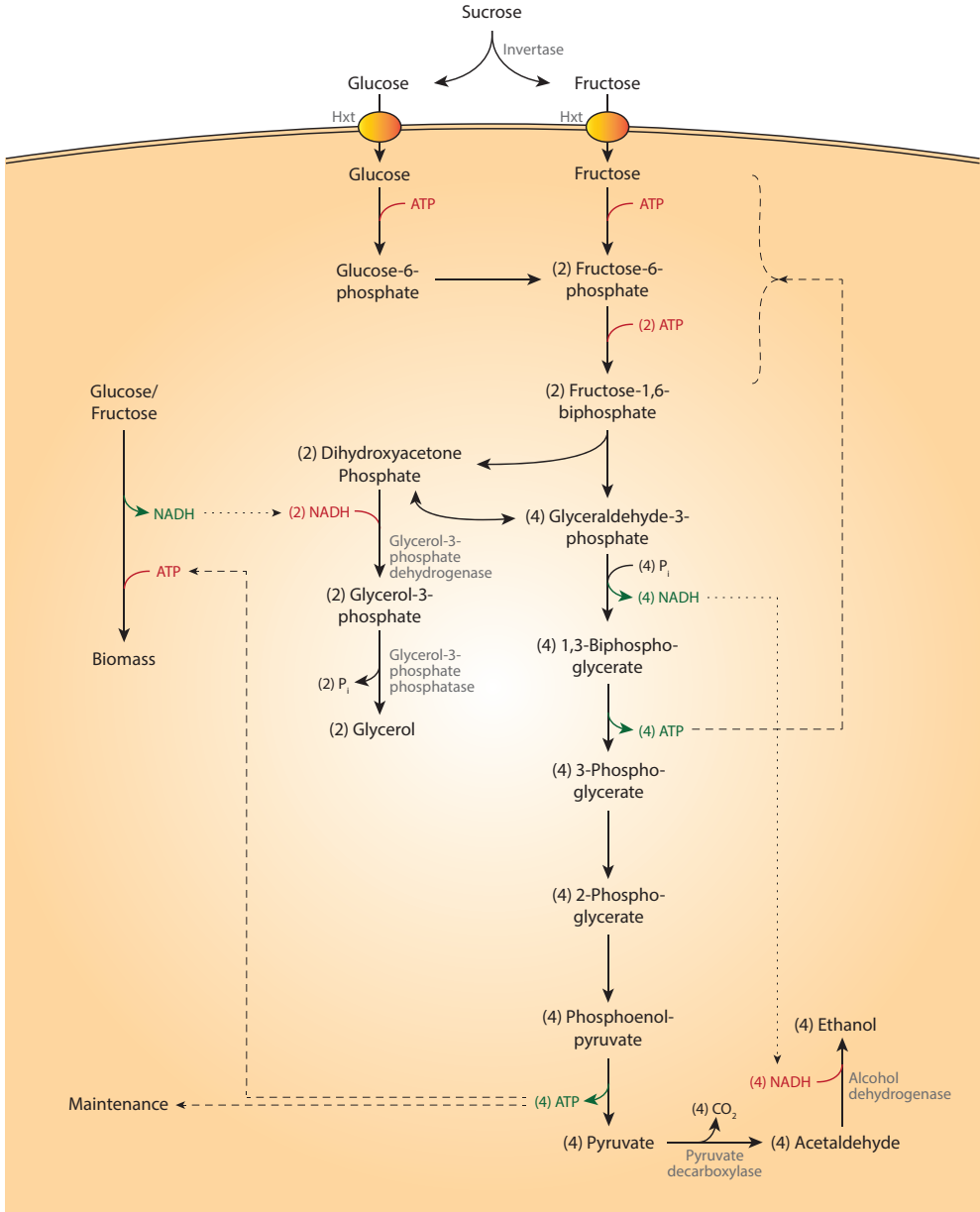
Figure 4.1: Schematic representation of the distribution of substrate over biomass, glycerol, ethanol and CO_2 in anaerobically growing *S. cerevisiae*. NADH/NAD+ redox-cofactor coupling and use of ATP for sugar phosphorylation, biomass formation and maintenance are indicated by dotted and dashed arrows, respectively. Glucose, fructose and (after hydrolysis) sucrose are converted into pyruvate via the Emden-Meyerhoff glycolysis, yielding 2 NADH and 2 ATP per glucose equivalent. ATP is used for cellular maintenance and synthesis of biomass (growth). NADH is primarily re-oxidized via alcoholic fermentation, but a surplus of NADH formed during biomass synthesis is re-oxidized via the production of glycerol.

metabolism, by redox-cofactor metabolism. Formation of *S. cerevisiae* biomass from sugar, ammonium or urea and other nutrients is coupled to a net reduction of NAD^+ to NADH (Bakker *et al.*, 2001; Verduyn *et al.*, 1990b) (Figure 4.1). Anaerobic *S. cerevisiae* cultures cannot re-oxidize this NADH by mitochondrial respiration and instead rely on NADH-dependent reduction of the glycolytic intermediate dihydroxyacetone phosphate to glycerol-3-phosphate, in a reaction catalyzed by NAD^+-dependent glycerol-3-phosphate dehydrogenase (Gpd1, Gpd2, EC 1.1.1.8 (Albertyn *et al.*, 1994; Eriksson *et al.*, 1995)). Glycerol-3-phosphate is then hydrolyzed by glycerol-3-phosphate-phosphatase (Gpp1, Gpp2, EC 3.1.3.21 (Norbeck *et al.*, 1996)) to yield phosphate and glycerol (Figure 4.1). In processes based on wild-type *S. cerevisiae* strains, approximately 4% of the potential ethanol yield on carbohydrate feedstocks was estimated to be lost to glycerol (Nissen *et al.*, 2000a). Based on current ethanol production volumes, this loss would correspond to approximately 4 billion liters of ethanol per year.

The aim of this paper is to review the current body of knowledge on pathway engineering strategies that focus on maximizing ethanol yields on glucose or sucrose by altering the ratio of ethanol, biomass and glycerol formation in *S. cerevisiae*. This scope excludes a large body of metabolic engineering research aimed at expanding the sugar- and polysaccharide substrate range of *S. cerevisiae* to enable its nascent application for industrial-scale fermentation of lignocellulosic hydrolysates generated from agricultural residues or energy crops (reviewed in (den Haan *et al.*, 2013; Jansen *et al.*, 2017a; Laluce *et al.*, 2012; Ruchala *et al.*, 2020)). However, the discussed strategies can, in principle, be applied in such 'second-generation' bioethanol processes as well as in 'first-generation' processes based on corn starch or cane sugar, once other metabolic engineering strategies have been successfully addressed.

4.2 Process conditions

Growth of anaerobic laboratory cultures of wild-type *S. cerevisiae* strains under different conditions provided insight in how distribution of sugar over biomass, glycerol and ethanol can be influenced and have therefore been a key source of inspiration for the design of metabolic engineering strategies.

In anaerobic, sugar-limited cultures of *S. cerevisiae*, maintenance-energy requirements are essentially growth-rate independent (Boender *et al.*, 2009; Tännler *et al.*, 2008; Vos *et al.*, 2015). The fraction of the consumed sugar that is fermented to ethanol therefore increases with decreasing specific growth rate (Russell and Cook, 1995) (Figure 4.2A). This correlation is clearly demonstrated in anaerobic retentostat cultures of *S. cerevisiae*, in which all biomass is retained in the culture and only cell-free effluent leaves the reactor. In such systems, near-theoretical ethanol yields on glucose were demonstrated during prolonged growth at near-zero specific growth rates (Boender *et al.*, 2009).

As an alternative to reducing the specific growth rate, the fraction of the sugar substrate that is fermented to ethanol by actively growing anaerobic cultures to meet maintenance-energy requirements can be increased by changing cultivation conditions. In particular, addition of weak organic acids such as lactate, acetate, propionate or benzoate to anaerobic batch and chemostat cultures grown at low pH was shown to lead to lower biomass yields and higher ethanol yields (Abbott *et al.*, 2008; Taherzadeh *et al.*, 1997; Verduyn *et al.*, 1990a; Verduyn *et al.*, 1990b; Verduyn *et al.*, 1992; Viegas and Sá-Correia, 1991). These results reflect an increased

4
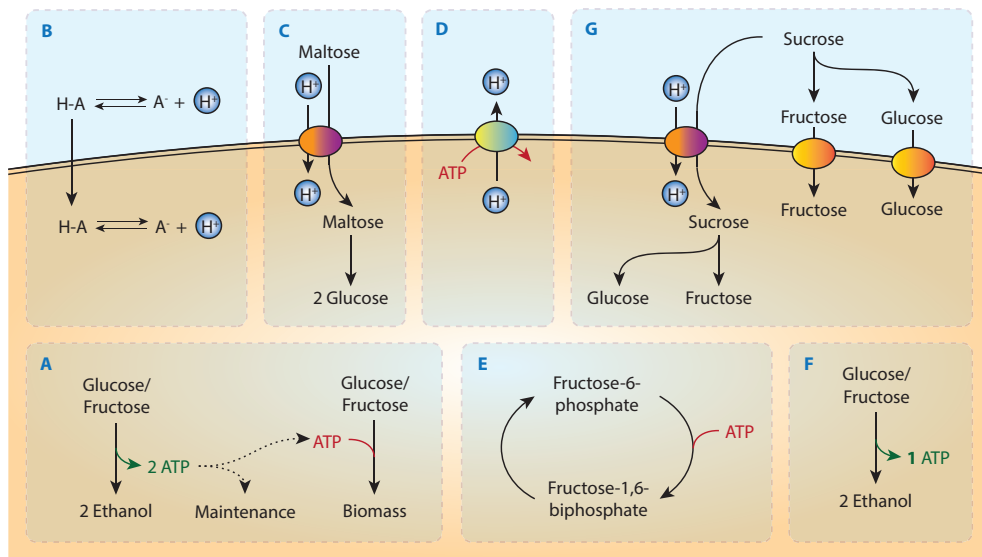
Figure 4.2: Schematic representation of energy metabolism in *S. cerevisiae* and strategies to improve ethanol yield on sugar. A: Alcoholic fermentation of glucose or fructose. B: Maintenance energy requirements can be increased by presence of weak organic acids in culture medium. C: The net ATP yield (mol ATP/mol glucose equivalent) of maltose utilization is lower than that of glucose, since maltose transport is proton coupled, whereas glucose is transported via facilitated diffusion. D: Plasma membrane ATPase exports protons at the cost of ATP. E: Example of a futile cycle, e.g. a set of reactions that leads to net hydrolysis of ATP, that can be introduced in order to enforce 'ATP wasting'. F: The Entner-Doudoroff glycolytic pathway yields only 1 ATP per glucose equivalent, instead of 2 ATP. G: Intracellular targeting of invertase (iSuc2) combined with uptake of sucrose by proton symport (left) lowers the ATP yield compared to wildtype *S. cerevisiae*, where sucrose is hydrolyzed extracellularly, after which the resulting monosaccharides are taken up via facilitated diffusion (right).

maintenance energy requirement for intracellular pH homeostasis, caused by an influx of protons into the yeast cytosol as a result of weak acid diffusion (Figure 4.2B) (Narendranath *et al.*, 2001). In anaerobic yeast cultures, countering this 'weak acid uncoupling' and maintenance of intracellular pH homeostasis critically depends on ATP-dependent proton export by the plasma membrane ATPase (Pma1, EC 7.1.2.1) (Figure 4.2D) (Serrano, 1977; Weusthuis *et al.*, 1993). These observations clearly indicate the potential of modifying maintenance-energy requirements as a means to improve ethanol yields. Practical issues such as costs of adding organic acids and their subsequent removal from process effluents, as well as potential synergies of weak organic acid and ethanol toxicity (Cardoso and Leão, 1992; Santos *et al.*, 2008), preclude direct application of weak organic acid uncoupling in industrial bioethanol production. Feedstocks for second-generation bioethanol production already contain inhibitors such as acetic acid, furfural and hydroxymethyl-2-furaldehyde (Dunlop, 1948; Jansen *et al.*, 2017a; Russell, 2003; Ulbricht *et al.*, 1984), which cause increased ATP requirements for cellular maintenance. In addition, high concentrations of ethanol also in themselves affect maintenance energy requirements by increasing permeability of the yeast plasma membrane to protons and thereby activating Pma1 (Monteiro *et al.*, 1994; Rosa and Sá-Correia, 1991).

Experiments on disaccharide metabolism by anaerobic *S. cerevisiae* cultures provided a first demonstration that ethanol yields can be modified by changing the mechanism of sugar import. In contrast to transport of glucose, which occurs via facilitated diffusion by Hxt transporters

(Boles and Hollenberg, 1997; Lagunas, 1993), uptake of its dimer maltose by *S. cerevisiae* is mediated by Malx1 transporters and involves symport with a single proton (Serrano, 1977; Van Leeuwen *et al.*, 1992). After intracellular hydrolysis of maltose by a Malx2 maltase (EC 3.2.1.20, maltose + H_2O –> 2 glucose), alcoholic fermentation of the resulting two glucose molecules yields 4 molecules of ATP. However, since one of these ATP molecules has to be used to enable expulsion of the symported proton by Pma1, which has a stoichiometry of 1 H^+/ATP (Serrano, 1977; Van Leeuwen *et al.*, 1992), the net ATP yield from maltose fermentation is only 1.5 ATP per glucose equivalent (Figure 4.2C). Indeed, based on hexose units, ethanol and biomass yields of *S. cerevisiae* in anaerobic maltose-limited chemostat cultures were shown to be 16% higher and 25% lower, respectively, than in corresponding glucose-limited cultures (Weusthuis *et al.*, 1993). These observations inspired metabolic engineering studies that were focused on sucrose-containing feedstock for bioethanol production.

During growth on ammonium or urea (Nissen *et al.*, 2000b; Nissen *et al.*, 1997), a significant part of the 'surplus' NADH generated in biosynthesis is derived from the synthesis of amino acids from these nitrogen sources and sugar. Several studies reported lower glycerol yields and higher ethanol yields on sugar in anaerobic cultures grown with amino acids or yeast extract as the nitrogen source (Albers *et al.*, 1996; Jørgensen, 2009; Radler and Schütz, 1982). Although use of amino acids as industrial nitrogen source is not an economically viable proposition, these observations highlighted the potential for engineering redox-cofactor metabolism to improve ethanol yields.

4.3 Engineering of energy coupling

Introduction of futile cycles

Several metabolic engineering strategies have been explored to increase the use of sugar for cellular maintenance energy requirements by introducing metabolic 'futile cycles', whose net effect is the hydrolysis of ATP to ADP and inorganic phosphate with a concomitant release of heat (Figure 4.2E). Such 'ATP wasting' cycles can either be introduced by constitutive expression of ATPases or by creating more complicated futile cycles that cause a net hydrolysis of ATP. Overexpression of the soluble F1 unit of the *Escherichia coli* H^+-ATPase in *S. cerevisiae* (Jensen *et al.*, 2007; Zahoor *et al.*, 2020) led to a 10% increase of the anaerobic ethanol yield on glucose relative to a reference strain, but also caused a 26% decrease of the specific growth rate (Zahoor *et al.*, 2020). Overexpression of *PHO5* or *PHO8*, which encode aspecific phosphatases (EC 3.1.3.1/2) (Rogers and Szostak, 1993; Semkiv *et al.*, 2014) was similarly reported to cause increased ATP turn-over. *PHO8* overexpression was reported to cause a 17% higher ethanol yield on glucose, without affecting growth rate (Semkiv *et al.*, 2014). Simultaneous activity of ATP-generating glycolytic and ATP-consuming gluconeogenic enzymes leads to textbook examples of futile metabolic cycles. Though not tested with the specific aim to improve ethanol yields, overexpression of the gluconeogenic enzyme fructose-1,6-bisphosphatase (Fbp1, EC 3.1.3.11: fructose-1,6-bisphosphate + H_2O –> fructose-6-phosphate + P_i) increased glucose consumption (19%) and CO_2 (10%) and ethanol (14%) production rates of aerobic suspensions of non-growing cells (Navas *et al.*, 1993). An even more pronounced effect on the ethanol production rate (22%) was found when the gluconeogenic enzyme phosphoenolpyruvate carboxykinase (PEPCK, EC 4.1.1.49: oxaloacetate + ATP –> phosphoenolpyruvate + ADP + CO_2) was simultaneously overexpressed (Navas *et al.*, 1993; Navas and Gancedo, 1996). More recently, *E. coli* PEPCK (*pckA*) was overexpressed together with the yeast anaplerotic enzyme pyruvate

carboxylase (Pyc2, EC 6.4.1.1: pyruvate + ATP + CO_2 –> oxaloacetate + ADP + P_i) (Semkiv *et al.*, 2016). Simultaneous activity of these enzymes results in hydrolysis of two ATP molecules for the formation of phosphoenolpyruvate (PEP) from pyruvate. Since, in glucose-grown cultures, the glycolytic enzyme pyruvate kinase (Pyk2, Cdc19, EC 2.7.1.40) converts PEP back to pyruvate with the formation of only a single ATP, the net result of this futile cycle is the hydrolysis of one ATP. The potential of this strategy was demonstrated by more ethanol production, related to yeast biomass, by the overexpression strain than by the control strain (Semkiv *et al.*, 2016).

An inherent risk of the constitutive expression of futile cycles is that, in industrial processes, situations may occur in which a too large drain of the cellular ATP content can no longer be compensated for by faster alcoholic fermentation. In extreme situations, net ATP synthesis might even decrease below maintenance energy-requirements and cause cell death. Careful 'tuning' of the *in vivo* activity of engineered futile cycles can, in principle, address this problem in cultures grown under constant conditions in the laboratory. However, such tuning would be much more difficult to achieve in large-scale industrial processes, which are highly dynamic, for example as a consequence of changing sugar and ethanol concentrations. Application-oriented pathway-engineering studies therefore mostly focus on strategies that, instead, aim at a fixed, stoichiometric reduction of the ATP yield from ethanol fermentation.

Decreasing the ATP stoichiometry of yeast glycolysis

The bacterium *Zymomonas mobilis* employs the Entner-Doudoroff (ED) pathway for alcoholic fermentation. Instead of the 2 mol ATP/mol glucose generated in yeast glycolysis, this pathway has a net ATP yield of only 1 mol ATP/mol glucose (Lee *et al.*, 1980; Rogers *et al.*, 1979). As a consequence, high ethanol yields can be achieved in growing *Z. mobilis* cultures (Lee *et al.*, 1980; Rogers *et al.*, 1979). A now expired patent proposed functional expression of the ED pathway in *S. cerevisiae* (Figure 4.2F) (Lancashire *et al.*, 1994). However, experimental studies failed to achieve the high *in vivo* activities of 6-phosphogluconate dehydratase (PGDH, EC 4.2.1.12: 6-phosphogluconate –> 2-dehydro-3-deoxy-gluconate-6-phosphate) in *S. cerevisiae* that would be required to demonstrate an impact on ethanol yield (Benisch and Boles, 2014; Morita *et al.*, 2017). A limiting activity of PGDH, which contains an [4Fe-4S] iron-sulfur cluster (Gardner and Fridovich, 1991), was attributed to the well-documented difficulties in expressing heterologous iron-sulfur-cluster enzymes in the yeast cytosol (Biz and Mahadevan, 2021).

An alternative approach to reduce the ATP yield of glycolysis in *S. cerevisiae* was based on functional expression of a heterologous, non-phosphorylating, $NADP^+$-dependent glyceraldehyde-3-phosphate dehydrogenase (GAPN, EC 1.2.1.9: glyceraldehyde-3-phosphate + $NADP^+$ –> 3-phosphoglycerate + NADPH), which bypasses the ATP-generating phosphoglycerate kinase reaction (Pgk1, EC 2.7.2.3: 1,3-biphosphoglycerate + ADP –> 3-phosphoglycerate + ATP) (Bro *et al.*, 2006; Guo *et al.*, 2011; Zhang *et al.*, 2011). Strains engineered with this strategy increased the ethanol yield in anaerobic cultures by 3% (Bro *et al.*, 2006) and 7.6% (Guo *et al.*, 2011). This increase was partly attributed to a lower ATP yield of glycolysis and partly to changes in redox-cofactor metabolism (see section 4.4).

Altering topology and energy coupling of disaccharide metabolism and transport

In contrast to maltose which, as described above, is taken up by proton symport prior to hydrolysis (Serrano, 1977; Van Leeuwen *et al.*, 1992; Weusthuis *et al.*, 1993), sucrose metabolism in wild-type *S. cerevisiae* strains is predominantly initiated by its extracellular hydrolysis

to glucose and fructose, catalysed by invertase (Suc2, EC 3.2.1.26) (Figure 4.1) (Carlson and Botstein, 1982; Gascón and Lampen, 1968). After uptake via facilitated diffusion, mediated by Hxt transporters (Kruckeberg, 1996), these hexoses are oxidized to pyruvate by yeast glycolysis.

Due to the presence of a second start codon in the *SUC2* transcript, a small fraction of the expressed invertase is retained in the cytosol (Carlson and Botstein, 1982) while, moreover, the Mal11 (Agt1) maltose-proton symporter is also able to import sucrose (Santos *et al.*, 1982; Stambuk *et al.*, 2000). Replacement of the native *SUC2* gene by a constitutively expressed, truncated *SUC2* gene that no longer encoded the N-terminal excretion sequence of Suc2 led to a near-complete targeting of invertase to the yeast cytosol (Figure 4.2G) (Basso *et al.*, 2011b). Adaptive laboratory evolution of an engineered *S. cerevisiae* strain expressing this internal invertase ('iSuc2') in anaerobic, sucrose-limited chemostat cultures yielded an evolved strain with increased expression of *MAL11*. When compared under identical conditions in anaerobic chemostat cultures, the evolved strain showed an 11% higher ethanol yield and a 30% lower biomass yield on sucrose than the reference strain (Basso *et al.*, 2011b). These results were in good agreement with predictions based on stoichiometric models of yeast metabolism and mirrored earlier comparisons of biomass and product yields of wild-type *S. cerevisiae* grown anaerobically on maltose and glucose (Weusthuis *et al.*, 1993). Using a similar strategy, it should also be possible to decrease the ATP yield of monosaccharide dissimilation by replacing the endogenous facilitated diffusion transporters by proton symporters (de Kok *et al.*, 2012a; Tiukova *et al.*, 2019).

4.4 Engineering of redox metabolism

Multiple pathway engineering strategies for improving ethanol yield on sugars aim to minimize production of glycerol. In aerobic *S. cerevisiae* cultures, generation of glycerol-3-phosphate by the Gpd1 and Gpd2 glycerol-3-phosphate dehydrogenases is non-essential due to the presence of an alternative route for glycerolipid synthesis that involves 1-acyldihydroxyacetone-phosphate as intermediate (Athenstaedt *et al.*, 1999). In contrast, due to the essential role of glycerol formation in NADH redox-cofactor balancing in non-respiratory cultures, double deletion of *GPD1* and *GPD2* prevents anaerobic growth (Ansell *et al.*, 1997; Björkqvist *et al.*, 1997). Anaerobic growth of *gpd1Δ gpd2Δ* strains can be rescued by supplementation of compounds such as acetaldehyde or acetoin, which can be reduced by intracellular NADH-dependent dehydrogenases (Ansell *et al.*, 1997; Björkqvist *et al.*, 1997). Glycerol-negative mutants are highly sensitive to osmotic stress due to the key role of glycerol in osmotolerance of *S. cerevisiae* (Ansell *et al.*, 1997; Blomberg and Adler, 1992).

In anaerobic, glucose-limited cultures of *S. cerevisiae* grown on synthetic media with ammonium as nitrogen source, approximately 12 mmol of glycerol is formed per gram of biomass dry weight (Ansell *et al.*, 1997; Papapetridis *et al.*, 2018), which closely matches calculated requirements for NADH re-oxidation (van Dijken and Scheffers, 1986). Strain-dependent diversity in glycerol production may reflect different biomass composition, formation of metabolites whose formation is coupled to a net generation of NADH (e.g. acetate (Björkqvist *et al.*, 1997)) and/or activity of the γ-butyric acid (GABA) shunt (Henriques *et al.*, 2021). 'Tuning' of *in vivo* activities of glycerol-3-phosphate dehydrogenase, by deletion of either *GPD1* or *GPD2* or by promoter engineering, has in different wild-type *S. cerevisiae* strain backgrounds and under different (semi-) anaerobic cultivation conditions, been shown to affect specific growth rates, glycerol and ethanol yields (Figure 4.3B) (Ansell *et al.*, 1997; Björkqvist *et al.*, 1997; Hubmann *et al.*, 2011;

4

Nissen *et al.*, 2000a).

While biomass synthesis in *S. cerevisiae* results in a net reduction of NAD^+ to NADH, it requires a net oxidation of NADPH to $NADP^+$ (Bruinenberg *et al.*, 1985; Bruinenberg *et al.*, 1983). Based on this observation, Anderlund *et al.* (1999) and Nissen *et al.* (2001) explored whether expression of heterologous soluble transhydrogenases (EC 1.6.1.1: $NADPH + NAD^+ -> NADP^+ + NADH$) from *E. coli* or *Azotobacter vinelandii*, respectively, could convert the 'surplus' NADH generated by anaerobic *S. cerevisiae* cultures into NADPH and thereby lower glycerol production. Physiological analysis of the resulting strains revealed that, instead, intracellular concentrations of reduced and oxidized forms of these cofactors favored the reverse reaction, thus resulting in higher glycerol yields and a lower ethanol yields than in the corresponding reference strains (Anderlund *et al.*, 1999; Nissen *et al.*, 2001).

Engineering redox-cofactor coupling of nitrogen assimilation

Based on observations that amino acid synthesis from ammonium or urea is a key contributor to the 'excess' NADH formed in yeast biosynthesis, an early redox engineering study (Nissen *et al.*, 2000a) focused on Gdh1, the $NADP^+$-dependent glutamate dehydrogenase (EC 1.4.1.4) that catalyses the key reaction in ammonium assimilation by nitrogen-sufficient *S. cerevisiae* cultures: (2-oxoglutarate $+ NH_4^+ + NADPH ->$ glutamate $+ NADP^+$, Figure 4.3A). Theoretical analysis predicted that making ammonium assimilation NADH-dependent could reduce glycerol production in anaerobic cultures by half. In one strategy, deletion of *GDH1* was combined with constitutive overexpression of *GLN1* and *GLT1*, which encode ATP-dependent glutamine synthetase (GS, EC 6.3.1.2: glutamate $+ NH_4^+ + ATP ->$ glutamine $+ ADP + P_i$) and NADH-dependent glutamate-2-oxoglutarate aminotransferase (EC 1.4.1.14: glutamine $+$ 2-oxoglutarate $+ NADH + H^+ ->$ 2 glutamate $+ NAD^+$ (GOGAT), respectively. In anaerobic bioreactor batch cultures, the resulting engineered strain grew at 90% of the specific growth rate of the reference strain, while its glycerol yield on glucose was 38% lower and its ethanol yield was 10% higher (Nissen *et al.*, 2000b). The increased ethanol yield was attributed to a combination of reduced NADH formation and increased ATP consumption in ammonium assimilation. In a second strategy, deletion of *GDH1* was combined with overexpression of the NADH-dependent glutamate dehydrogenase *GDH2* (EC 1.4.1.2: 2-oxoglutarate $+ NH_4^+ + NADH ->$ glutamate $+ NAD^+$). This approach led to a 30% lower glycerol yield. However, the ethanol yield was hardly affected and the biomass yield was 12% higher than that of the reference strain. This observation was attributed to a reduced loss of carbon via CO_2 formation in the oxidative pentose-phosphate pathway (Nissen *et al.*, 2000a), which is the main source of NADPH in *S. cerevisiae* (Nogae and Johnston, 1990; Vanrolleghem *et al.*, 1996). Since NADH re-oxidation in the first step of ammonium assimilation cannot completely replace glycerol formation, the GS-GOGAT strategy, as successfully implemented by Nissen *et al.* (2000b), left room for further reduction of glycerol yields.

Expression of $NADP^+$-dependent, non-phosphorylating glyceraldehyde 3-phosphate dehydrogenase (gapN)

In *S. cerevisiae*, the oxidative step in glycolysis is catalysed by the strictly NAD^+-dependent oxidation of glyceraldehyde-3-phosphate to 1,3-biphosphoglycerate by isoenzymes of glyceraldehyde-3-phosphate dehydrogenase (Tdh1, 2 or 3, EC 1.2.1.12). Based on stoichiometric modelling of yeast metabolism, Bro *et al.* (2006) identified expression of a heterologous non-phosphorylating, $NADP^+$-dependent glyceraldehyde-3-phosphate dehydrogenase (GAPN),
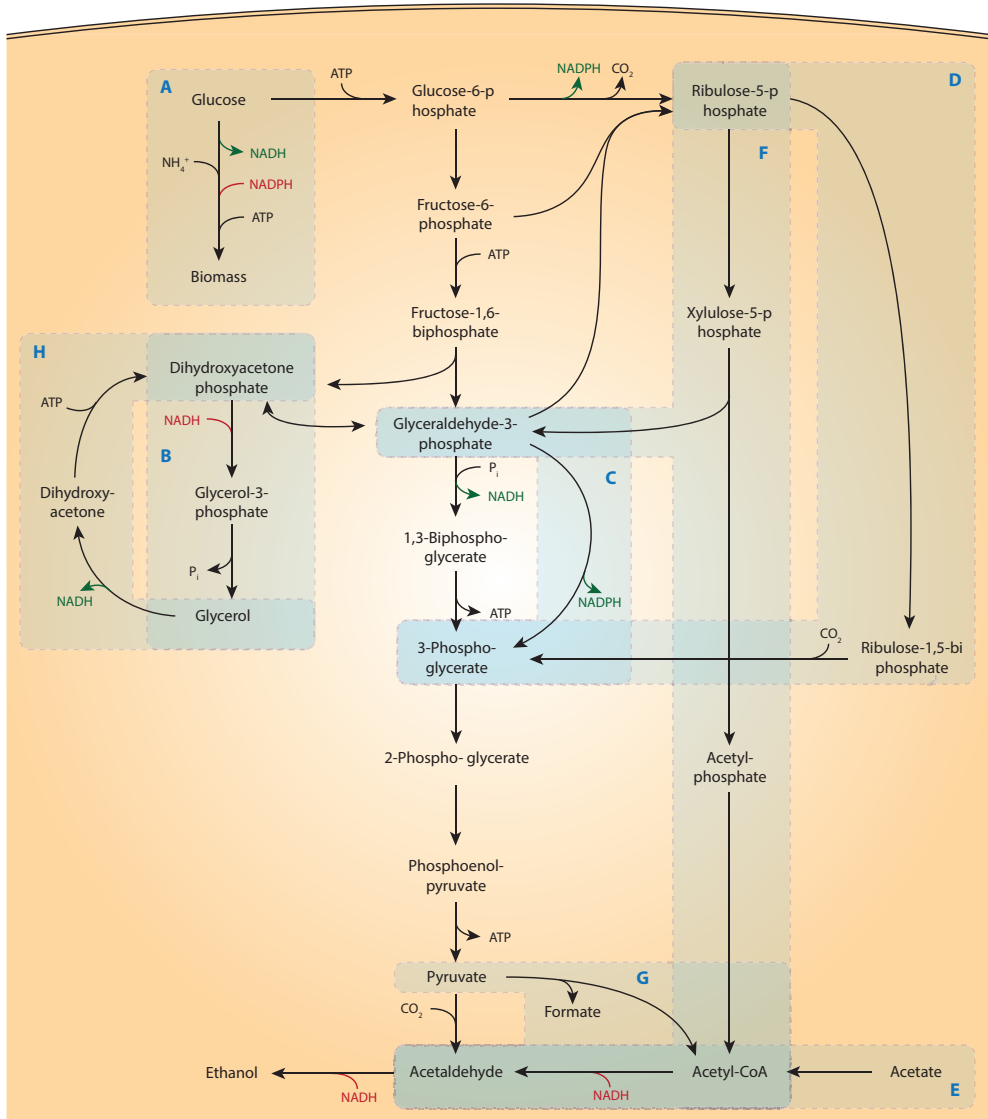
Figure 4.3: Schematic representation of pathway engineering strategies for minimizing formation of glycerol as 'redox' sink for re-oxidation of NADH generated in biosynthetic reactions during anaerobic growth of *S. cerevisiae*. A: Biosynthetic reactions require a net input of ATP and NADPH, while yielding NADH. Ammonium assimilation is the key contributor to NADH production, and replacing the NADP+-dependent step by an NADH-dependent step can reduce the NADH production in biosynthetic reactions. B: Native glycerol pathway. C: Bypass of NAD+-dependent glyceraldehyde-3-phosphate dehydrogenase by heterologous non-phosphorylating, NADP+-dependent glyceraldehyde-3-phosphate dehydrogenase (GAPN). D: Non-oxidative bypass of NAD+-dependent glyceraldehyde-3-phosphate dehydrogenase by heterologously expressed phosphoribulokinase and ribulose-1,5-bisphosphate carboxylase/oxygenase (Rubisco). E: Re-oxidation of NADH by heterologously expressed NADH-dependent acetylating acetaldehyde dehydrogenase (A-ALD), using exogenous acetate as electron acceptor. F: Re-oxidation of NADH enabled by combined expression of heterologously expressed A-ALD, phosphoketolase and phosphotransacetylase. G: Re-oxidation of NADH enabled by combined expression of heterologously expressed A-ALD and pyruvate-formate lyase. H: Combined expression of a heterologous NADH-dependent glycerol dehydrogenase and the native dihydroxyacetone kinase enables ethanol formation from glycerol when combined with strategies D, E, F and/or G.

which generates 3-phosphoglycerate instead of 1,3-biphosphoglycerate, as a promising option to increase ethanol yields (Figure 4.3C). Initial experimental verification of this model prediction by expression of *Streptococcus mutans gapN* showed a 44% lower glycerol yield in anaerobic, glucose-grown batch cultures than in a reference strain. No negative impact on specific growth rate or biomass yield was observed, but also the ethanol yield on glucose was not significantly altered (Bro *et al.*, 2006). Subsequent studies in which expression of *Bacillus cereus gapN* was tested, reported a 3.5% higher final ethanol concentration and a 23% reduction of the glycerol yield on sugar relative to a reference strain (Zhang *et al.*, 2011). Expression of *Bacillus cereus gapN* in combination with deletion of *GPD1*, yielded a strain that exhibited a 49% lower glycerol yield and 8% higher ethanol yield than the wild-type reference strain. However, the engineered strain was found to be highly sensitive to osmotic stress, thereby precluding its use in high-gravity industrial ethanol fermentation. When osmotolerance was restored by overexpression of *TPS1* and *TPS2*, which encode trehalose-6-phosphate synthase (EC 2.4.1.15: glucose-6-phosphate + UDP-glucose –> UDP + trehalose-6-phosphate) and trehalose-6-phosphate phosphatase (EC 3.1.3.12: trehalose-6-phosphate + H_2O –> trehalose + P_i), near-wild-type anaerobic growth rates were reported along with an up to 8% higher ethanol yield and 73% lower glycerol yield, respectively (Guo *et al.*, 2011). In a further study (Navarrete *et al.*, 2014), expression of *gapN* from *Streptococcus mutans* was combined with deletion of *FPS1*, which encodes a membrane channel protein involved in glycerol export, in some strains combined with overexpression of *UTR1*, which encodes *S. cerevisiae* NADH kinase (EC 2.7.1.86: ATP + NADH –> ADP + P_i + NADPH) (Remize *et al.*, 2001). While lower glycerol yields and higher ethanol yields were observed in micro-aerobic cultures, the engineered strains were unable to grow under fully anaerobic conditions.

NADH-dependent reduction of acetate to ethanol

In many fermentative bacteria, acetylating acetaldehyde dehydrogenase (A-ALD, EC1.2.1.10: acetyl-CoA + NADH + H^+ –> acetaldehyde + CoA + NAD^+) catalyzes a key reaction in alcoholic fermentation, that is followed by NADH-dependent reduction of acetaldehyde to ethanol (Ciriacy, 1975). The potential of using the combination of A-ALD and yeast alcohol dehydrogenase to re-oxidize NADH in anaerobic *S. cerevisiae* cultures, and thereby replace glycerol as NADH redox sink for ethanol, was explored by expressing the A-ALD-encoding *E. coli* gene *mhpF* in a *gpd1Δ gpd2Δ* strain (Guadalupe Medina *et al.*, 2010). Like other *gpd1Δ gpd2Δ S. cerevisiae* strains, the resulting strain did not grow anaerobically on glucose as sole carbon source. However, anaerobic growth was restored by addition of acetate to growth media (Figure 4.3E). In anaerobic *S. cerevisiae* cultures, acetate is activated to acetyl-CoA by the acetyl-CoA synthethase isoenzyme Acs2 (EC 6.2.1.1: acetate + ATP + CoA –> acetyl-CoA + AMP + PP_i, (van den Berg *et al.*, 1996)). In anaerobic bioreactor batch cultures supplemented with 2 g/L acetate, the engineered strain did not produce glycerol and showed a 13% higher apparent ethanol yield on glucose (note that part of the produced ethanol was derived from acetate rather than from glucose). Under these conditions, the *mhpF*-expressing strain grew at 44% of the specific growth rate of the *GPD1 GPD2* reference strain (Guadalupe Medina *et al.*, 2010). Introduction, in the same *gpd1Δ gpd2Δ* genetic background, of a single copy of an expression cassette for *eutE*, an alternative *E. coli* A-ALD gene, increased specific growth rate to 84% of that of the reference strain (Papapetridis *et al.*, 2017).

When *E. coli eutE* was expressed in a *GPD1 GPD2 S. cerevisiae* strain, a mere 10% reduction of the amount of glycerol produced per gram biomass was observed in anaerobic, glucose-grown batch cultures supplemented with acetate. This observation indicated that the native glycerol

pathway effectively competed with *E. coli* EutE for NADH in this genetic context. Deletion of *GPD2*, which encodes the redox-regulated isoenzyme of glycerol-3-phosphate dehydrogenase in *S. cerevisiae*, led to a 80% reduction of glycerol production, with a corresponding increase in acetate consumption (Papapetridis *et al.*, 2017).

Acetate is a common constituent and inhibitor of yeast performance in the hydrolysates of lignocellulosic biomass that are explored as feedstocks for 'second-generation' yeast-based ethanol production (Almeida *et al.*, 2007). Since, in such processes, expression of A-ALD offers an option to convert an inhibitor into additional product, further pathway engineering strategies were explored to increase the amount of NADH available for acetate reduction and to improve robustness of engineered *gpd1Δ gpd2Δ*, A-ALD-expressing strains. To enable additional NADH generation, the native *S. cerevisiae* $NADP^+$-dependent 6-phosphogluconate dehydrogenases Gnd1 and Gnd2 (EC 1.1.1.44: 6-phosphogluconate + $NADP^+$ –> ribulose-5-phosphate + CO_2 + NADPH) were replaced by the NAD^+-dependent enzyme GndA from *Methylobacillus flagellates* (EC 1.1.1.343). To force flux through the resulting, now partially NADH-coupled oxidative pentose-phosphate pathway, *ALD6*, which encodes $NADP^+$-dependent acetaldehyde dehydrogenase (EC 1.2.1.5: acetaldehyde + $NADP^+$ –> acetate + NADPH), was deleted. This metabolic engineering strategy resulted in a 29% higher acetate consumption per gram biomass than in the parental *gpd1Δ gpd2Δ*, *eutE*-expressing strain (Papapetridis *et al.*, 2016). Relative to a congenic *GPD1 GPD2* reference strain, the engineered strain showed a 13% higher ethanol yield and a 29% lower specific growth rate.

An alternative strategy to boost the acetate-reducing capacity of *eutE*-expressing strains focused on changing the cofactor preference of alcohol dehydrogenase, which in *S. cerevisiae* is strictly NADH-dependent (Henningsen *et al.*, 2015). Relative to an industrial *S. cerevisiae* strain expressing *Bifidobacterium adolescentis eutE* in a *gpd1Δ gpd2Δ* background, a further engineered strain that expressed an NADPH-dependent alcohol dehydrogenase from *Entamoeba histolytica*, combined with overexpression of *S. cerevisiae* NADP-dependent glucose-6-P dehydrogenase (Zwf1, EC 1.1.1.49: glucose-6-phosphate + $NADP^+$ –> 6-phospho-glucono-1,5-lactone + NADPH) and acetyl-CoA synthetase (Acs2) showed an almost 3-fold higher acetate consumption (Henningsen *et al.*, 2015).

A different strategy to increase the potential for acetate reduction by A-ALD expressing strains is to enable anaerobic co-conversion of glycerol, which is left in the final phases of fermentation or obtained from post-distillation stills (Kim *et al.*, 2008), to ethanol. In the patent literature, an NADH-specific glycerol dehydrogenase from *E. coli* (*gldA*, EC 1.1.1.6: glycerol + NAD^+ –> dihydroxyacetone + NADH + H^+) was expressed together with an additional copy of *DAK1*, encoding dihydroxyacetone kinase (EC 2.7.1.29: dihydroxyacetone + ATP –> dihydroxyacetone phosphate + ADP) (de Bont *et al.*, 2018; Klaassen and Hartman, 2019). Combined with enzymes from the lower half of glycolysis, pyruvate decarboxylase and alcohol dehydrogenase, GldA and Dak1 enable conversion of glycerol to ethanol with the formation of one mole of NADH (Figure 4.3H). When, besides sugars, glycerol and acetate are present as additional substrates in A-ALD expressing cultures, glycerol conversion to ethanol acts as source of NADH enabling more acetate reduction. Indeed, high apparent ethanol yields of 0.48-0.50 gram ethanol per gram of glucose were reported for *S. cerevisiae* strains in which *gldA* and *DAK1* overexpression was combined with expression of *E. coli mhpF* or *eutE* (de Bont *et al.*, 2018; Klaassen and Hartman, 2019).

4

Integration of acetyl-CoA reduction by A-ALD in yeast sugar metabolism

Organic acid concentrations in 'first generation' feedstocks for yeast-based ethanol production are generally around 1.3 g L^{-1}, (Rasmussen *et al.*, 2015; Russell, 2003), which limits the potential impact of the replacement of glycerol production by reduction of exogenous acetate via an engineered A-ALD pathway. In such settings, NADH re-oxidation by A-ALD could still replace glycerol production if acetyl-CoA is formed from glucose by pathways that yield fewer than two mol of NADH per mol of acetyl-CoA. The patent literature describes two strategies to achieve this goal, of which the first is based on heterologous expression of a bacterial pyruvate formate-lyase (PFL; EC 2.3.1.54: pyruvate –> acetyl-CoA + formate) in A-ALD-expressing *S. cerevisiae* (Argyros *et al.*, 2015; de Bont and Teunissen, 2012) (Figure 4.3G). PFL, which is an oxygen-sensitive enzyme, was shown to be able to functionally replace the native pathway for acetyl-CoA synthesis in anaerobic *S. cerevisiae* cultures (Kozak *et al.*, 2014; van Rossum *et al.*, 2016). Synthesis of acetyl-CoA via glycolysis and PFL yields only one NADH per acetyl-CoA and thus enables a net oxidation of one NADH when combined with ethanol production via A-ALD and yeast alcohol dehydrogenase. To prevent NADH formation by the yeast formate dehydrogenases Fdh1 and Fdh2 (EC 1.17.1.9: formate + NAD$^+$ –> CO_2 + NADH; (Overkamp *et al.*, 2002)), it was proposed to delete *FDH1* and *FDH2* from PFL/A-ALD expressing strains (Argyros *et al.*, 2015; de Bont and Teunissen, 2012).

A second strategy for coupling A-ALD to sugar metabolism proposed in the patent literature (Andrei and Munos, 2017) is based generation of acetyl-CoA through phosphoketolase (EC 4.1.2.9) and phosphotransacetylase (EC 2.3.1.8) (Figure 4.3F). In this strategy, xylulose-5-phosphate is first formed from glucose in a redox-cofactor neutral manner via the enzymes of the non-oxidative pentose-phosphate pathway. This sugar phosphate is then converted into glyceraldehyde-3-phosphate and acetyl-phosphate by a heterologously expressed phosphoketolase (PK, EC 4.1.2.9: xylulose-5-phosphate + P$_i$ –> acetyl-phosphate + glyceraldehyde-3-phosphate + H$_2$O). Subsequently, a heterologously expressed phosphotransacetylase (PTA, EC 2.3.1.8: acetyl-phosphate + CoA –> acetyl-CoA + P$_i$) converts acetyl phosphate to acetyl-CoA. This pathway has been successfully used for the ATP-efficient generation of acetyl-CoA as a precursor for aerobic product formation by engineered *S. cerevisiae* strains (Bergman *et al.*, 2016; Meadows *et al.*, 2016). While the exact impact on ethanol yields will depend on strain and process characteristics, both pathways have the theoretical potential to completely replace the role of glycerol formation in NADH re-oxidation.

Expression of Calvin-cycle enzymes

Phosphoribulokinase (PRK, EC 2.7.1.19: ribulose-5-phosphate + ATP –> ribulose-1,5-biphosphate + ADP) and ribulose-1,5-bisphosphate carboxylase/oxygenase (Rubisco, EC 4.1.1.39: ribulose-1,5-biphosphate + CO_2 + H$_2$O –> 2 glyceraldehyde-3-phosphate + 2H$^+$) are the two key enzymes of the Calvin cycle for autotrophic CO_2 fixation. By capturing CO_2, these enzymes together have the potential to generate a redox-cofactor-neutral bypass of the oxidative glyceraldehyde-3-phosphate dehydrogenase reaction in glycolysis when ribulose-5-phosphate, the substrate of phosphoribulokinase, is generated from glucose via the reactions of the non-oxidative pentose-phosphate pathway (Figure 4.3D). In theory, this bypass should enable the use of ethanol formation as a redox sink for NADH generated in biosynthetic reactions. This hypothesis was tested by Guadalupe-Medina *et al.* (2013), who demonstrated the presence of a functionally active Rubisco in cell extracts of an engineered *S. cerevisiae* strain that co-expressed the gene *Thiobacillus denitrificans* type-II Rubisco CbbM with the *E.*

coli genes encoding chaperonins GroEL and GroES. Co-expression of CbbM, GroEL, GroES with spinach phosphoribulokinase was shown to result in a 90% lower glycerol yield and a 10% higher ethanol yield in anaerobic, sugar-limited chemostat cultures grown at a dilution rate of 0.05 h^{-1} and sparged with CO_2-enriched nitrogen (Guadalupe-Medina *et al.*, 2013). In line with the low affinity of CbbM for CO_2 (Hernandez *et al.*, 1996), a less pronounced effect on glycerol and ethanol yields was observed when cultures were sparged with pure nitrogen gas.

Papapetridis *et al.* (2018) observed that an *S. cerevisiae* strain that combined constitutive expression of PRK, Rubisco, GroEL and GroES showed only a modest reduction of glycerol in fast-growing anaerobic batch cultures on glucose than the slow-growing chemostat cultures studied by Guadalupe-Medina *et al.* (2013). To improve competition of the Rubisco pathway for NADH with the native glycerol pathway, *GPD2* was deleted and the four key enzymes of the non-oxidative pentose phosphate pathway were overexpressed. In addition, PRK was expressed from a weaker, anaerobically inducible promoter to avoid reported toxic effects of PRK overexpression in microorganisms (Brandes *et al.*, 1996; Hudson *et al.*, 1992) during aerobic pre-cultivation. The resulting strain retained a wild-type growth rate in anaerobic, glucose-grown batch cultures, while showing an 86% lower glycerol yield and 15% higher ethanol yield on glucose than a congenic reference strain (Papapetridis *et al.*, 2018).

Table 4.1: Reported impacts on glycerol production, maximum specific growth rate and ethanol production in anaerobic batch cultures of *S. cerevisiae* strains subjected to different pathway engineering strategies aimed at reducing glycerol production and improving ethanol yield. Depending on the studies, changes in product yields were either expressed per amount of substrate or per amount of biomass. Subscript x denotes dry biomass, ↑ indicates overexpression of native *S. cerevisiae* genes, glc = glucose.

Strategy	Genotype	Glycerol yield	Growth rate	Ethanol yield	Reference
Altered cofactor specificity of ammonium assimilation	*gdh1Δ GLN1↑GLT1↑*	-38% (g/g glc)	-10%	+10% (g/g glc)	(Nissen *et al.*, 2000a)
	gdh1Δ GDH2↑	-30% (g/g glc)	-5%	+3% (g/g glc)	(Nissen *et al.*, 2000a)
NADH-dependent reduction of acetate to ethanol (Ec = *E. coli*)	*gpd1Δ gpd2Δ* Ec-*mphF*	-100% (g/g$_x$)	-56%	+13% (g/g glc)	(Guadalupe Medina *et al.*, 2010)
	gpd1Δ gpd2Δ Ec-*eutE*	-100% (g/g$_x$)	-7%	+9% (g/g glc)	(Papapetridis *et al.*, 2016)
NADH-dependent reduction of acetate to ethanol with increased NADH generation via pentose-phosphate pathway	*gnd2Δ gnd1Δ gndAΔ ald6Δ gpd1Δ gpd2Δ* Ec-*eutE*	-100% (g/g$_x$)	-29%	+11% (g/g glc)	(Papapetridis *et al.*, 2016)
NADH re-oxidation via expression of Calvin-cycle enzymes, optimized for anaerobic growth rate (So = *Spinacia oleracea*, Td = *Thiobacillus denitrificans*)	*gpd2Δ RPE1↑TKL1↑ TAL1↑ NQM1↑ RKI1↑ TKL2↑* So-*prk* Td-*cbbm* (9 copies) Ec-*groES,* Ec-*groEL*	-86% (g/g$_x$)	0%	+15% (g/g glc)	(Papapetridis *et al.*, 2018)
Reduced NADH and ATP formation in glycolysis by expression of *gapN* (Sm = *Streptococcus mutans*)	Sm-*gapN*	-40% (g/g glc)	0%	+2% (g/g glc)	(Bro *et al.*, 2006)
	gpd1Δ Sm-*gapN TPS1↑ TPS2↑*	-73 % (g/g glc)	0%	+8% (g/g glc)	(Guo *et al.*, 2011)

4

The strategies discussed above were first designed to reduce or eliminate the need for glycerol formation in alcoholic fermentation of disaccharides or hexoses. However, they can similarly be employed in conversion of other sugars into ethanol. Xylose-utilizing *S. cerevisiae* strains have been engineered either based on the functional expression of the fungal xylose reductase (XR, EC 1.1.1.307: xylose + NAD(P)H –> xylitol + NAD(P)$^+$) and xylitol dehydrogenase (XDH, EC 1.1.1.9: xylitol + NAD$^+$ –> xylulose + NADH), or the expression of a bacterial xylose isomerase (EC 5.3.1.5: xylose –> xylulose). A key challenge in the strategy based on XR and XDH is that XR typically prefers NADPH as cofactor, while XDH exclusively uses NAD$^+$ (Kötter and Ciriacy, 1993). As a consequence of this cofactor imbalance, xylitol is formed as a byproduct. Changing the cofactor preference of ammonium assimilation as demonstrated by Nissen *et al.* (2000) (Nissen *et al.*, 2000b) facilitated re-oxidation of NADH generated in the XDH reaction and improved ethanol yield in an XR/XDH-based *S. cerevisiae* strain (Roca *et al.*, 2003). Combined functional expression, of PRK and Rubisco (Li *et al.*, 2017; Xia *et al.*, 2017); phosphoketolase and phosphotransacetylase (Sonderegger *et al.*, 2004); or GAPN (Bro *et al.*, 2006) were similarly applied to improve redox co-factor balancing in XR/XDH-based strains and, thereby, ethanol yields on xylose.

4.5 Model-based comparison of maximum theoretical impact of individual engineering strategies.

Experimentally determined ethanol yields achieved with the pathway engineering strategies discussed in paragraphs 4.3 and 4.4 (Table 4.1) can be influenced by experimental conditions as well as by the *S. cerevisiae* genetic background into which genetic modifications were introduced, for example due to different biomass compositions. To eliminate these factors, different pathway strategies were implemented in a stoichiometric model of the core metabolic network of *S. cerevisiae* (Daran-Lapujade *et al.*, 2004) and used to calculate growth stoichiometries of anaerobic, sugar-grown cultures (Table 4.2). Although the resulting estimates cannot be used to predict performance of strategies in specific strain backgrounds or processes, they do enable comparison of the maximum impact of the different strategies and identification of trade-offs.

To evaluate pathway engineering strategies aimed at reducing the ATP yield from sugar fermentation, two scenarios were simulated. In the first, glucose import required a net input of 0.5 ATP, which corresponds to the ATP yield per hexose unit in strains that combine sucrose-proton symport with intracellular sucrose hydrolysis (Basso *et al.*, 2011b). The second scenario, in which glucose import required 1 ATP, corresponds to a situation in which hexose transport occurs via symport with a proton or, alternatively, glucose is fermented via an alternative glycolytic pathway with a net ATP yield of 1 mol/mol glucose (e.g. the Entner-Doudoroff pathway) in combination with a glucose facilitator. At a specific growth rate of 0.30 h^{-1}, simulation of these scenarios gave predicted increases of ethanol yield on hexose equivalents of 8.1% and 16.2%, respectively (Table 4.2). Due to a larger impact of a constant maintenance-energy requirement at low growth rate (Boender *et al.*, 2009; Pirt, 1965), predicted benefits of these engineering strategies declined as the specific growth rate approached zero (Table 4.2). An important consequence of these two strategies was that, at each specific growth rate, specific rates of sugar conversion were 33% and 100% higher, respectively, than in the reference situation (Table S4.1). Especially at high specific growth rates, which are important for supporting high volumetric productivities in industrial batch processes, achieving such high conversion rates may be challenging due to the requirement for a large resource allocation

to glycolytic proteins (Regueira *et al.*, 2021; Sánchez *et al.*, 2017) or for membrane space to accommodate the required number of sugar transporters (Hennaut *et al.*, 1970). In addition, concomitant reductions of the biomass yield on sugar by 25% and 50%, respectively (Table S4.2) may cause economic trade-offs when surplus yeast biomass is sold as a co-product for application in animal feed products (Conroy *et al.*, 2016).

To assess the maximum theoretical impact on ethanol yield of the strategies focused on redox-cofactor balancing, glycerol production was set to zero, so that re-oxidation of NADH generated in biosynthesis occurred exclusively via the engineered pathways. At a specific growth rate of 0.3 h^{-1}, the PFL/A-ALD, PK/PTA/A-ALD and PRK/Rubisco strategies yielded predicted improvements of the ethanol yield on glucose of 8.7%, 9.7% and 11.9%, respectively. The predicted differences between the impacts of the three strategies can be predominantly attributed to the different net ATP and ethanol yields for NADH re-oxidation via these pathways. Due to different ATP and carbon efficiencies of these heterologous pathways, implementation of these redox engineering strategies in the stoichiometric model also led to higher predicted biomass yields on glucose and correspondingly lower specific rates of glucose consumption (Tables S4.1 and S4.2). Thus, in contrast to strategies aimed at reducing the ATP stoichiometry of sugar fermentation, their industrial implementation should not be affected by a potentially limited capacity of sugar fermentation and/or transport or by a trade-off with revenues from surplus yeast biomass. As observed for the strategies aimed at engineering ATP coupling of sugar dissimilation, the impact of the redox-engineering strategies on ethanol yield declined with decreasing specific growth rate and, at the lowest simulated growth rate (0.001 h^{-1}), the predicted increase of ethanol yield on glucose was only approximately 1%.

Table 4.2: Maximum impact of different pathway engineering strategies for improving ethanol yield on sugar, estimated with a stoichiometric model of the core metabolic network of *S. cerevisiae* (Daran-Lapujade *et al.*, 2004). Assumptions on biomass composition, maintenance-energy requirements, as well as modifications to the model that were implemented to simulate each of the metabolic engineering strategies, are described in Supplementary Materials. For the strategies focused on NADH re-oxidation, glycerol production was set at zero and oxidation of surplus NADH from biosynthetic reactions was entirely routed through the engineered pathways.

| Specific growth rate (h^{-1}) | $Y_{ethanol/hexose}$ (mol/mol) | | | | | |
| | Reference | Altered ATP coupling of sugar dissimilation | | Alternative pathways for re-oxidation of NADH | | |
	Wild type	H^+ symport/ intracellular hydrolysis of sucrose (yields 1.5 ATP/ hexose)	H^+ symport of glucose (yields 1 ATP/ glucose)	PFL/A-ALD	PK/PTA/ A-ALD	PRK/ Rubisco
0.3	1.51	1.63 (+8.1%)	1.76 (+16.2%)	1.64 (+8.7%)	1.66 (+9.7%)	1.69 (+11.9%)
0.1	1.54	1.66 (+7.5%)	1.77 (+14.9%)	1.67 (+8.4%)	1.69 (+9.5%)	1.71 (+11.3%)
0.03	1.62	1.72 (+5.8%)	1.81 (+11.6%)	1.74 (+7.4%)	1.76 (+8.5%)	1.78 (+9.5%)
0.01	1.75	1.81 (+3.6%)	1.87 (+7.2%)	1.84 (+5.2%)	1.86 (+6.1%)	1.86 (+6.4%)
0.001	1.95	1.97 (+0.6%)	1.98 (+1.2%)	1.97 (+1.0%)	1.98 (+1.2%)	1.98 (+1.2%)

4

For several of the strategies, experimental studies (Table 4.1) yielded larger improvements of the ethanol yield than the maximum theoretical improvements shown in Table 4.2. In addition to differences in biomass composition and ethanol yields of reference *S. cerevisiae* strains, these differences may reflect unintended impacts of genetic modifications on cellular energy requirements. For example, high-level expression of heterologous proteins has been associated with increased cellular energy requirements (Glick, 1995; Gopal *et al.*, 1989) which, in anaerobic cultures can contribute to higher ethanol yields. In addition, alteration of the expression of membrane proteins may potentially lead to increased ATP dissipation, for exampling by futile cycling of glucose through overexpressed Mal11 and Hxt transporters.

4.6 Discussion and outlook

As outlined in this review, multiple pathway engineering strategies have been demonstrated to improve ethanol yields on sugars in anaerobic laboratory cultures of *S. cerevisiae* by altering the ratio of the formation of ethanol, biomass and glycerol. However, observations made under controlled conditions in laboratory-scale media are not necessarily representative for industrial processes. Even in anaerobic glucose-limited cultures of wild-type *S. cerevisiae*, ethanol yields on glucose approach the theoretical maximum of 2 mol ethanol/mol glucose at near-zero growth rates (Boender *et al.*, 2009). Consequently, predicted benefits of all investigated pathway engineering strategies strongly depend on the specific growth rate (Table 4.2). In industrial batch processes, the impact of the described engineering strategies on ethanol yield is likely to be highest during the initial phase in which vigorous growth occurs. Conversely, during the final phases of a batch fermentation process, where growth has essentially ceased and high ethanol concentrations lead to an increased maintenance energy requirement, their impact may well be negligible.

In addition to the inherent dynamics of industrial processes, development of industrial strains should take into account trade-offs between ethanol yield and other performance indicators. In particular, an improved product yield should not go at the expense of productivity. With few exceptions, academic studies reported that *S. cerevisiae* strains which were successfully engineered for improved ethanol yield grew slower than their non-engineered parental strains (Table 4.1). The extensive synthetic biology toolbox for genetic modification of *S. cerevisiae*, including approaches such as multiplexed Cas9-mediated genome editing and *in vivo* assembly and chromosomal integration of synthetic DNA fragments (Kuijpers *et al.*, 2013; Mans *et al.*, 2015), is therefore intensively used to explore options for maximizing ethanol yields by engineering its metabolic network. In addition, pathway engineering in this yeast benefits from the availability of genome-scale metabolic models (for reviews see Sánchez and Nielsen, (2015) and Lopes and Rocha, (2017)), which allow for fast predictions of the impact of genetic interventions on distribution of fluxes in metabolic networks. A dedicated study on PRK/Rubisco based strains (Papapetridis *et al.*, 2018) illustrates that restoring the specific growth rate of engineered strains to wild-type levels may require substantial additional engineering. Alternatively, adaptive laboratory evolution and/or reverse engineering of evolved strains (Mans *et al.*, 2018; Sandberg *et al.*, 2019) can be used for this purpose. Another important trade-off concerns cellular robustness. Until engineering strategies are available that fully restore osmotolerance in glycerol-negative strains, strategies aimed at reducing glycerol production should not completely eliminate glycerol production (Blomberg and Adler, 1992). In addition to targeted engineering strategies, robustness may be increased by using natural and industrial *S. cerevisiae* strains with a high innate tolerance to industrially relevant stress factors in strain

improvement programmes (Della-Bianca and Gombert, 2013; Radecka *et al.*, 2015).

Temperature, pH, pCO_2, ethanol concentration and their dynamics in large-scale industrial processes may affect the impact of engineering strategies, thus requiring process-specific strain optimization. The economic significance of small differences in ethanol yield, combined with the use of non-defined industrial media and dynamic industrial processes, raises non-trivial challenges in setting up high-throughput cultivation and analysis systems that faithfully predict strain performance in real-life applications. Although companies tend not to disclose the genetic make-up of industrial strains, the introduction of multiple 'high-ethanol-yield' *S. cerevisiae* strains into USA-based ethanol plants (Bryan, 2020; Lane, 2015; Lane, 2018) indicates that at least some of the strategies discussed in this review already contribute to profitability and sustainability of industrial ethanol production. Introduction into Brazil, the second-largest ethanol-producing economy, may involve additional challenges related to the use of non-aseptically operated, extended production campaigns. This mode of operation not only poses high demands on the genetic stability of engineered strains, for example to prevent recovery of glycerol production by strains with down-regulated *GPD1* and/or *GPD2* expression, but also on their ability to compete with 'wild' strains entering the process (Basso *et al.*, 2011a).

Improving ethanol yield on fermentable sugars is by no means the only target of metabolic engineering studies related to yeast-based ethanol production. Other targets of intensive research include the reduction of processing costs by expression of polysaccharide hydrolases (den Haan *et al.*, 2021), extending substrate range to convert more fermentable substrates in crude industrial media (Hahn-Hägerdal *et al.*, 2007; Parisutham *et al.*, 2017), improving performance at high temperature to improve heat economy and cope with process temperature profiles (Ingledew, 2017), increasing yeast tolerance to process inhibitors and ethanol (Gomes *et al.*, 2021; Ingledew, 2017), improving osmotolerance of engineered strains with reduced glycerol formation (Albertyn *et al.*, 1994; Guadalupe-Medina *et al.*, 2014) and simplification of nutritional requirements of industrial strains (Perli *et al.*, 2021; Perli *et al.*, 2020; Wiersma *et al.*, 2020; Wronska *et al.*, 2021). In addition, integration of corn-fiber from 1.5G processes (Jansen *et al.*, 2017a) and reducing the need for antibiotics (Ingledew, 2017; Lewis, 2016) are actively explored. Combination of these and other relevant traits with strategies for improving product yield in *S. cerevisiae* and potentially also in other yeast species (Dekker *et al.*, 2021; Kurylenko *et al.*, 2014; Radecka *et al.*, 2015) will, in the coming years, continue to generate interesting challenges for academic and industrial research.

4

4.7 Supplementary information

Table S4.1: Estimated impacts on the biomass-specific rate of hexose consumption for different pathway-engineering strategies to improve ethanol yields (see Table 4.1 for estimated maximum impacts on ethanol yield), calculated with a stoichiometric model of the core metabolic network of *S. cerevisiae* (Daran-Lapujade *et al.*, 2004). For the three strategies focused on NADH reoxidation, glycerol production was set at zero and oxidation of surplus NADH from biosynthetic reactions was entirely routed through the engineered pathways. Subscript x denotes yeast biomass.

Specific growth rate (h^{-1})	$-q_{hexose}$ (mmol/Cmol$_x$/h)					
	Reference	Altered ATP coupling of sugar dissimilation		Alternative pathways for reoxidation of NADH		
	Wild type	H$^+$ symport/ intracellular hydrolysis of sucrose (yields 1.5 ATP/ hexose)	H$^+$ symport of glucose (yields 1 ATP/ glucose)	PFL/A-ALD	PK/PTA/ A-ALD	PRK/Rubisco
0.3	402	536 (+33.3%)	803 (+100%)	307 (-23.6%)	278 (-30.8%)	308 (-23.4%)
0.1	143	190 (+33.3%)	285 (+100%)	111 (-22.1%)	102 (-28.9%)	111 (-22.0%)
0.03	52.1	69.4 (+33.3%)	104 (+100%)	42.6 (-18.2%)	39.7 (-23.8%)	42.7 (-18.1%)
0.01	26.2	34.9 (+33.3%)	52.3 (+100%)	23.0 (-12.1%)	22.0 (-15.8%)	23.0 (-12.0%)
0.001	14.5	19.3 (+33.3%)	29.0 (+100%)	14.2 (-2.2%)	14.1 (-2.8%)	14.2 (-2.2%)

Table S4.2: Estimated impacts on the biomass yield on hexose units for different pathway-engineering strategies to improve ethanol yields (see Table 4.1 for estimated maximum impacts on ethanol yield), calculated with a stoichiometric model of the core metabolic network of *S. cerevisiae* (Daran-Lapujade *et al.*, 2004). For the three strategies focused on NADH reoxidation, glycerol production was set at zero and oxidation of surplus NADH from biosynthetic reactions was entirely routed through the engineered pathways.

Specific growth rate (h^{-1})	$Y_{x/hexose}$ (g$_x$/g)					
	Reference	Altered ATP coupling of sugar dissimilation		Alternative pathways for reoxidation of NADH		
	Wild type	H$^+$ symport/ intracellular hydrolysis of sucrose (yields 1.5 ATP/ hexose)	H$^+$ symport of glucose (yields 1 ATP/ glucose)	PFL/A-ALD	PK/PTA/ A-ALD	PRK/ Rubisco
0.3	0.109	0.082 (-25%)	0.055 (-50%)	0.143 (+30.9%)	0.158 (+44.5%)	0.143 (+30.6%)
0.1	0.103	0.077 (-25%)	0.051 (-50%)	0.132 (+28.4%)	0.145 (+40.7%)	0.132 (+28.2%)
0.03	0.085	0.063 (-25%)	0.042 (-50%)	0.103 (+22.3%)	0.111 (+31.2%)	0.103 (+22.1%)
0.01	0.056	0.042 (-25%)	0.028 (-50%)	0.064 (+13.7%)	0.067 (+18.7%)	0.064 (+13.6%)
0.001	0.010	0.008 (-25%)	0.005 (-50%)	0.010 (+2.2%)	0.010 (+2.9%)	0.010 (+2.2%)

4

Model-based estimation of the impact of pathway engineering strategies on growth stoichiometry

Quantitative estimates of the impact of different pathway engineering strategies on ethanol yield, biomass-specific rate of glucose consumption and biomass yield in anaerobic, glucose-grown cultures were generated with a compartmented stoichiometric network model for growth of *Saccharomyces cerevisiae* (Daran-Lapujade *et al.*, 2004), with the following modifications:

Calculations were based on a growth-rate independent rate of ATP turnover for cellular maintenance (m_{ATP}) of 1 mmol (g biomass)$^{-1}$ h^{-1} (Boender *et al.*, 2009) and a growth-coupled ATP cost of 0.5 mol (Cmol biomass)$^{-1}$.

Molecular and elemental composition of *S. cerevisiae* biomass was assumed to correspond to the statistically reconciled composition calculated by Lange and Heijnen (2001) for glucose-limited cultures grown at a dilution rate of 0.10 h^{-1} (1 Cmol biomass = 26.4 g).

Pathway engineering strategies were simulated by introducing the following modifications:

H$^+$ symport and subsequent intracellular hydrolysis of sucrose

This scenario was simulated by coupling import of glucose, which in the reference model occurs via facilitated diffusion (no coupling with proton translocation), to the inward translocation of 0.5 H$^+$

H$^+$ symport of glucose

This scenario was simulated by coupling import of glucose, which in the reference model occurs via facilitated diffusion (no coupling with proton translocation), to the inward translocation of 1.0 H$^+$

Expression of pyruvate-formate lyase (PFL) and acetylating acetaldehyde dehydrogenase (A-ALD)

To simulate this scenario, the following changes were introduced in the model:

- the rate of glycerol production ($q_{glycerol}$) was set at 0

- NAD$^+$-dependent acetaldehyde dehydrogenase was removed from the model

- PFL was added to the model: pyruvate –> formate + acetyl-CoA

- A-ALD was added to the model: acetyl-CoA + NADH –> acetaldehyde + NAD$^+$

- formate export was assumed to occur by uniport of the formate anion

Expression of phosphoketolase (PK), phosphotransacetylase (PTA) and acetylating acetaldehyde dehydrogenase (A-ALD):

To simulate this scenario, the following changes were introduced in the model:

- the rate of glycerol production ($q_{glycerol}$) was set at 0

- NAD$^+$-dependent acetaldehyde dehydrogenase (cACTAL deh(NAD)) was removed from the model

- PK was added to the model: xylulose-5P + P$_i$ –> glyceraldehyde-3P + acetyl-P

- Phosphotransacetylase was added to the model: acetyl-P + CoA –> acetyl-CoA + P$_i$

- A-ALD was added to the model: acetyl-CoA + NADH –> acetaldehyde + NAD$^+$

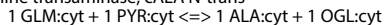*Expression of phosphoribulokinase (PRK) and ribulose-1,5-bisphosphate carboxylase/oxygenase (Rubisco):*

To simulate this scenario, the following changes were introduced in the model:

- the rate of glycerol production ($q_{glycerol}$) was set at 0

- PRK was added to the model: ribulose-5P + ATP –> ribulose-1,5P + ADP

- Rubisco was added to the model: ribulose-1,5P + CO_2 –> 2 3P-glycerate

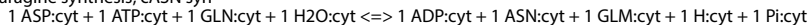The reaction list for stoichiometric model is given below.
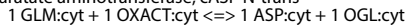
amino acid synthesis
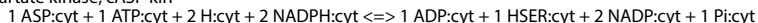   alanine transaminase; cALA N-trans
        1 GLM:cyt + 1 PYR:cyt <=> 1 ALA:cyt + 1 OGL:cyt
    arginine synthesis; cARG syn
        1 ASP:cyt + 1 ATP:cyt + 1 CARP:cyt + 1 ORN:cyt <=> 1 AMP:cyt + 1 ARG:cyt + 1 FUM:cyt + 3 H:cyt + 1 Pi:cyt + 1 PPi:cyt
    asparagine synthesis; cASN syn
        1 ASP:cyt + 1 ATP:cyt + 1 GLN:cyt + 1 H2O:cyt <=> 1 ADP:cyt + 1 ASN:cyt + 1 GLM:cyt + 1 H:cyt + 1 Pi:cyt
    asparatate aminotransferase; cASP N-trans
        1 GLM:cyt + 1 OXACT:cyt <=> 1 ASP:cyt + 1 OGL:cyt
    aspartate kinase; cASP kin
        1 ASP:cyt + 1 ATP:cyt + 2 H:cyt + 2 NADPH:cyt <=> 1 ADP:cyt + 1 HSER:cyt + 2 NADP:cyt + 1 Pi:cyt
    branched chain amino acid transferase (isoleucine); mILE N-trans
        1 GLM:mit + 1 H:mit + 1 NADPH:mit + 1 OBU:mit + 1 PYR:mit <=> 1 CO2:mit + 1 H2O:mit + 1 ILE:mit + 1 NADP:mit + 1 OGL:mit
    branched chain amino acid transferase (leucine); cLEU N-trans
        1 GLM:cyt + 1 IPM:cyt + 1 NAD:cyt <=> 1 CO2:cyt + 1 LEU:cyt + 1 NADH:cyt + 1 OGL:cyt
    branched chain amino acid transferase (valine) cyt; cVAL N-trans
        1 GLM:cyt + 1 OIV:cyt => 1 OGL:cyt + 1 VAL:cyt
    branched chain amino acid transferase (valine) mit; mVAL N-trans
        1 GLM:mit + 1 OIV:mit <=> 1 OGL:mit + 1 VAL:mit
    carbamoyl phoshate synthase; cCARP syn
        2 ATP:cyt + 1 CO2:cyt + 1 GLN:cyt + 2 H2O:cyt <=> 2 ADP:cyt + 1 CARP:cyt + 1 GLM:cyt + 3 H:cyt + 1 Pi:cyt
    cysteine synthese; cCYS syn
        2 H:cyt + 1 HCYS:cyt + 1 SER:cyt <=> 1 CYS:cyt + 1 NH4:cyt + 1 OBU:cyt
    glutamate ammonia ligase; cGLM N-lig
        1 ATP:cyt + 1 GLM:cyt + 1 NH4:cyt <=> 1 ADP:cyt + 1 GLN:cyt + 1 H:cyt + 1 Pi:cyt
    glutamate dehydrogenase; cGLM deh
        1 H:cyt + 1 NADPH:cyt + 1 NH4:cyt + 1 OGL:cyt <=> 1 GLM:cyt + 1 H2O:cyt + 1 NADP:cyt
    glycine hydroxymethyl transferase; cGLY transf
        1 SER:cyt + 1 THF:cyt <=> 1 GLY:cyt + 1 H2O:cyt + 1 METHF:cyt
    histidine synthesis; cHIS syn
        1 ATP:cyt + 1 GLN:cyt + 3 H2O:cyt + 2 NAD:cyt + 1 PRPP:cyt <=> 1 AICAR:cyt + 6 H:cyt + 1 HIS:cyt + 2 NADH:cyt + 1 OGL:cyt + 1 Pi:cyt + 2 PPi:cyt
    homocitrate synthesis; cHCIT syn
        1 ACCoA:cyt + 1 H2O:cyt + 1 OGL:cyt <=> 1 CoA:cyt + 1 H:cyt + 1 HCIT:cyt
    homocysteine synthesis; cHCYS syn
        1 ACCoA:cyt + 1 H2S:cyt + 1 HSER:cyt <=> 1 ACT:cyt + 1 CoA:cyt + 2 H:cyt + 1 HCYS:cyt
    isopropylmalate synthase cyt; cIPM syn
        1 ACCoA:cyt + 1 H2O:cyt + 1 OIV:cyt => 1 CoA:cyt + 1 H:cyt + 1 IPM:cyt
    methionine synthase; cMET syn
        1 H:cyt + 1 HCYS:cyt + 1 MYTHF:cyt <=> 1 MET:cyt + 1 THF:cyt
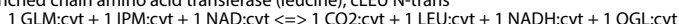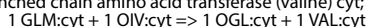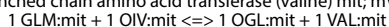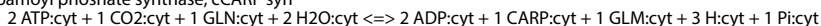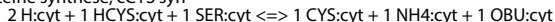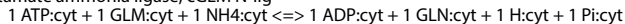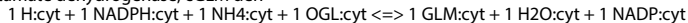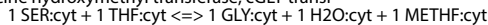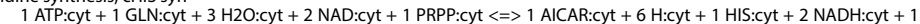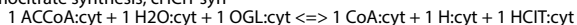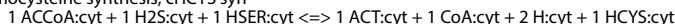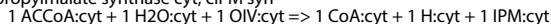
4
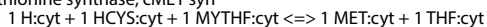
ornithine synthesis; mORN syn
    1 ATP:mit + 2 GLM:mit + 1 H:mit + 1 NADPH:mit => 1 ADP:mit + 1 NADP:mit + 1 OGL:mit + 1 ORN:mit + 1 Pi:mit
oxoadipate synthesis; mOAD syn
    1 HCIT:mit + 1 NAD:mit <=> 1 CO2:mit + 1 NADH:mit + 1 OAD:mit
oxoisovalerate synthesis mit; mOIV syn
    2 H:mit + 1 NADPH:mit + 2 PYR:mit <=> 1 CO2:mit + 1 H2O:mit + 1 NADP:mit + 1 OIV:mit
phenylalanine synthesis; cPHE syn
    1 CHO:cyt + 1 GLM:cyt + 1 H:cyt <=> 1 CO2:cyt + 1 H2O:cyt + 1 OGL:cyt + 1 PHE:cyt
proline dehydrogenase; cPRO deh
    1 ATP:cyt + 1 GLM:cyt + 2 H:cyt + 2 NADPH:cyt <=> 1 ADP:cyt + 1 H2O:cyt + 2 NADP:cyt + 1 Pi:cyt + 1 PRO:cyt
serine synthesis; cSER syn
    1 3PG:cyt + 1 GLM:cyt + 1 H2O:cyt + 1 NAD:cyt <=> 1 H:cyt + 1 NADH:cyt + 1 OGL:cyt + 1 Pi:cyt + 1 SER:cyt
shikimate pathway; cSHI path
    1 ATP:cyt + 1 E4P:cyt + 1 NADPH:cyt + 2 PEP:cyt <=> 1 ADP:cyt + 1 CHO:cyt + 1 NADP:cyt + 4 Pi:cyt
threonine aldolase; cTHR ald
    1 THR:cyt => 1 ACTAL:cyt + 1 GLY:cyt
threonine dehydratase mit; mTHR deh
    1 H:mit + 1 THR:mit => 1 NH4:mit + 1 OBU:mit
threonine synthesis; cTHR syn
    1 ATP:cyt + 1 H2O:cyt + 1 HSER:cyt <=> 1 ADP:cyt + 1 H:cyt + 1 Pi:cyt + 1 THR:cyt
tryptophan synthesis; cTRP syn
    1 CHO:cyt + 1 GLN:cyt + 1 PRPP:cyt + 1 SER:cyt <=> 1 CO2:cyt + 1 GAP:cyt + 1 GLM:cyt + 1 H:cyt + 1 H2O:cyt + 2 Pi:cyt + 1 PYR:cyt + 1 TRP:cyt
tyrosine synthesis; cTYR syn
    1 CHO:cyt + 1 GLM:cyt + 1 NADP:cyt <=> 1 CO2:cyt + 1 NADPH:cyt + 1 OGL:cyt + 1 TYR:cyt

biomass formation
    biomass formation G4; biom-G4
        0.398 CARBHYD:cyt + 0.0037 DNA:cyt + 0.0561 H2O:cyt + 0.101 LIPID:cyt + 0.018 metal:cyt + 0.00245 Pi:cyt + 0.451 PROT:cyt + 0.047 RNA:cyt + 0.00094 SO4:cyt + 0.5 ATP:cyt => 1 biom-G4:ext + 0.5 ADP:cyt + 1 H:cyt + 1 Pi:cyt

C-1 metabolism
    dihydrofolate reductase; cDHF red
        1 DHF:cyt + 1 H:cyt + 1 NADPH:cyt => 1 NADP:cyt + 1 THF:cyt
    methylenetetrahydrofolate dehydrogenase; cMETHF deh
        1 FTHF:cyt + 1 H:cyt + 1 NADPH:cyt => 1 H2O:cyt + 1 METHF:cyt + 1 NADP:cyt
    methylenetetrahydrofolate reductase; cMETHF red
        1 H:cyt + 1 METHF:cyt + 1 NADPH:cyt => 1 MYTHF:cyt + 1 NADP:cyt
    phosphoribulokinase; PRK
        1 ATP:cyt + 3 H:cyt + 1 RIBU5P:cyt => 1 ADP:cyt + 1 RIBU15P:cyt
    ribulose-15-bisphosphate carboxylase oxygenase; Rubisco
        1 CO2:cyt + 1 H2O:cyt + 1 RIBU15P:cyt => 2 3PG:cyt + 6 H:cyt

catabolism
    acetylating acetaldehyde dehydrogenase; cACACTAL deh(NAD)
        1 ACTAL:cyt + 1 CoA:cyt + 1 NAD:cyt <=> 1 ACCoA:cyt + 1 H:cyt + 1 NADH:cyt
    sulfate assimilation; cSO4 ass
        2 ATP:cyt + 3 H:cyt + 4 NADPH:cyt + 1 SO4:cyt => 1 ADP:cyt + 1 AMP:cyt + 2 H2O:cyt + 1 H2S:cyt + 4 NADP:cyt + 1 Pi:cyt + 1 PPi:cyt

diffusion
    CO2 diffusion; eCO2<-cCO2
        1 CO2:cyt <=> 1 CO2:ext
    intracellular carbon dioxide diffusion; cCO2<-mCO2
        1 CO2:mit => 1 CO2:cyt
    intracellular water diffusion; cH2O<-mH2O
        1 H2O:mit => 1 H2O:cyt
    water diffusion; eH2O<-cH2O
        1 H2O:cyt <=> 1 H2O:ext

glycerol metabolism
    glycerol 3-phosphatase; cGOH3P pho
        1 GOH3P:cyt + 1 H2O:cyt => 1 GOH:cyt + 1 Pi:cyt

glycolysis, lower
    enolase; cEnol
        1 2PG:cyt <=> 1 H2O:cyt + 1 PEP:cyt
    glyceraldehyde phosphate dehydrogenase; cGAP deh
        1 GAP:cyt + 1 NAD:cyt + 1 Pi:cyt <=> 1 13PG:cyt + 1 H:cyt + 1 NADH:cyt
    phosphoglycerate kinase; c13PG kin
        1 13PG:cyt + 1 ADP:cyt <=> 1 3PG:cyt + 1 ATP:cyt
    phosphoglycerate mutase; c3PG mut
        1 3PG:cyt <=> 1 2PG:cyt
    pyruvate kinase; cPYR kin
        1 ADP:cyt + 1 H:cyt + 1 PEP:cyt => 1 ATP:cyt + 1 PYR:cyt

glycolysis, upper
    fructosebisphosphate aldolase; cF16P ald
        1 F16P:cyt <=> 1 DHAP:cyt + 1 GAP:cyt

4

glucose 6-phosphate isomerase; cG6P iso
    1 G6P:cyt <=> 1 F6P:cyt
hexokinase; cHX kin
    1 ATP:cyt + 1 GLUC:cyt => 1 ADP:cyt + 1 G6P:cyt + 1 H:cyt
phosphofructokinase; cPF kin
    1 ATP:cyt + 1 F6P:cyt => 1 ADP:cyt + 1 F16P:cyt + 1 H:cyt
triose phophate isomerase; cTP iso
    1 DHAP:cyt <=> 1 GAP:cyt

intracellular transport
    ADP-ATP antiport cyt/mit; ADPc<->ATPm
        1 ADP:cyt + 1 ATP:mit => 1 ADP:mit + 1 ATP:cyt
    mit. ammonium carrier protein; NH4m car
        1 H:cyt + 1 NH4:mit => 1 H:mit + 1 NH4:cyt
    mit. homocitrate carrier; HCITm car
        4 H:cyt + 1 HCIT:cyt => 4 H:mit + 1 HCIT:mit
    mit. isoleucine carrier; ILEm car
        1 H:cyt + 1 ILE:mit => 1 H:mit + 1 ILE:cyt
    mit. ornithine carrier; ORNm car
        1 H:cyt + 1 ORN:mit => 1 H:mit + 1 ORN:cyt
    mit. oxaloacetate exporter; OXACTm ex
        1 H:mit + 1 OXACT:mit => 1 H:cyt + 1 OXACT:cyt
    mit. oxobutyrate carrier; OBUm car
        1 H:cyt + 1 OBU:cyt => 1 H:mit + 1 OBU:mit
    mit. oxogluterate/malate carrier; ODC1m car
        1 MAL:cyt + 1 OGL:mit => 1 MAL:mit + 1 OGL:cyt
    mit. oxogluterate/oxoadipate carrier; ODC2m car
        1 OAD:mit + 1 OGL:cyt => 1 OAD:cyt + 1 OGL:mit
    mit. oxoisovalerate carrier; OIVm car
        1 OIV:mit => 1 OIV:cyt
    mit. phosphate carrier mit; Pi_m car
        2 H:cyt + 1 Pi:cyt => 2 H:mit + 1 Pi:mit
    mit. pyruvate proton symport; PYRm car
        2 H:cyt + 1 PYR:cyt => 2 H:mit + 1 PYR:mit
    mit. threonine carrier; THRm car
        1 H:cyt + 1 THR:cyt => 1 H:mit + 1 THR:mit
    mit. valine importer; VALm imp
        1 H:cyt + 1 VAL:cyt => 1 H:mit + 1 VAL:mit
    NADH shuttle; NADH shuttle
        1 NAD:cyt + 1 NADH:mit => 1 NAD:mit + 1 NADH:cyt
    succinate malate carrier; mSUC MAL car
        1 MAL:cyt + 1 SUC:mit <=> 1 MAL:mit + 1 SUC:cyt

lipid synthesis
    acetyl-CoA carboxylase; cACCoA carb
        1 ACCoA:cyt + 1 ATP:cyt + 1 CO2:cyt + 1 H2O:cyt => 1 ADP:cyt + 2 H:cyt + 1 MACoA:cyt + 1 Pi:cyt
    adenosly homocysteinase; cSAH hyd
        1 H2O:cyt + 1 SAH:cyt => 1 A:cyt + 1 H:cyt + 1 HCYS:cyt
    average fatty acid formation; cAvFA form
        1.7 OLE-CoA:cyt + 4.4 PLLM-CoA:cyt + 1.4 PLM-CoA:cyt + 1 STE-CoA:cyt => 8.5 avFA-CoA:cyt
    average phospholipid formation; cAvPL form
        11 PHD-CHO:cyt + 4 PHD-ETA:cyt + 3 PHD-SER:cyt => 18 avPL:cyt
    FAT formation; cFAT form
        1 avFA-CoA:cyt + 1 H2O:cyt + 1 PHD:cyt => 1 CoA:cyt + 1 FAT:cyt + 1 Pi:cyt
    glycerol 3-phosphate acyltransferase; cGOH3P trans
        2 avFA-CoA:cyt + 1 GOH3P:cyt => 2 CoA:cyt + 1 PHD:cyt
    glycerol 3-phosphate dehydrogenase; cGOH3P deh
        1 DHAP:cyt + 1 H:cyt + 1 NADH:cyt => 1 GOH3P:cyt + 1 NAD:cyt
    methionine adenosyl transferase; cMET Atrans
        1 ATP:cyt + 2 H2O:cyt + 1 MET:cyt => 1 H:cyt + 3 Pi:cyt + 1 SAM:cyt
    oleate CoA ligase; OLE CoA lig
        1 ATP:cyt + 1 CoA:cyt + 1 H2O:cyt + 1 OLE:cyt => 1 AMP:cyt + 1 H:cyt + 1 OLE-CoA:cyt + 2 Pi:cyt
    palmitate CoA ligase; cPLM lig
        1 ATP:cyt + 1 CoA:cyt + 1 H2O:cyt + 1 PLM:cyt => 1 AMP:cyt + 1 H:cyt + 2 Pi:cyt + 1 PLM-CoA:cyt
    palmitic acid synthesis; cPLM syn
        1 ACCoA:cyt + 20 H:cyt + 7 MACoA:cyt + 14 NADPH:cyt => 7 CO2:cyt + 8 CoA:cyt + 6 H2O:cyt + 14 NADP:cyt + 1 PLM:cyt
    palmitoleate CoA ligase; PLLM CoA lig
        1 ATP:cyt + 1 CoA:cyt + 1 H2O:cyt + 1 PLLM:cyt => 1 AMP:cyt + 1 H:cyt + 2 Pi:cyt + 1 PLLM-CoA:cyt
    phosphatidate cytidyl transferase; cPHD-C trans
        1 CTP:cyt + 1 H2O:cyt + 1 PHD:cyt => 1 CMP-DGOH:cyt + 2 Pi:cyt
    phosphatidyl-ethanolamine methyltransferase; cPHD-EA mtrans
        1 PHD-ETA:cyt + 3 SAM:cyt => 3 H:cyt + 1 PHD-CHO:cyt + 3 SAH:cyt
    phosphatidyl-serine decarboxylase; cPHD-SER dcarb
        1 PHD-SER:cyt => 1 CO2:cyt + 1 PHD-ETA:cyt
    phosphatidyl-serine synthase; cPHD-SER syn
        1 CMP-DGOH:cyt + 1 SER:cyt => 1 CMP:cyt + 1 PHD-SER:cyt
    stearate CoA ligase; cSTE ligase
        1 ATP:cyt + 1 CoA:cyt + 1 H2O:cyt + 1 STE:cyt => 1 AMP:cyt + 1 H:cyt + 2 Pi:cyt + 1 STE-CoA:cyt
    stearic acid synthesis; cSTE syn

1 ACCoA:cyt + 23 H:cyt + 8 MACoA:cyt + 16 NADPH:cyt => 8 CO2:cyt + 9 CoA:cyt + 7 H2O:cyt + 16 NADP:cyt + 1 STE:cyt

macromolecule synthesis
average amino acid formation; cAvAA form
0.977 ALA:cyt + 0.386 ARG:cyt + 0.408 ASN:cyt + 0.52 ASP:cyt + 0.0139 CYS:cyt + 1.02 GLM:cyt + 0.526 GLN:cyt + 0.889 GLY:cyt + 0.193 HIS:cyt + 0.589 ILE:cyt + 0.801 LEU:cyt + 0.657 LYS:cyt + 0.114 MET:cyt + 0.0238 ORN:cyt + 0.376 PHE:cyt + 0.422 PRO:cyt + 0.533 SER:cyt + 0.557 THR:cyt + 0.0649 TRP:cyt + 0.196 TYR:cyt + 0.733 VAL:cyt <=> 10 avAA:cyt
carbohydrate synthesis; cCARBHYD syn
1 ATP:cyt + 1 G6P:cyt + 1 H2O:cyt => 1 ADP:cyt + 6 CARBHYD:cyt + 1 H:cyt + 2 Pi:cyt
DNA polymerisation; cDNA poly
0.3 ATP:cyt + 0.2 CTP:cyt + 0.2 GTP:cyt + 1 H:cyt + 0.3 METHF:cyt + 1 NADPH:cyt + 0.3 UTP:cyt => 0.3 DHF:cyt + 9.8 DNA:cyt + 1 H2O:cyt + 1 NADP:cyt + 1 PPi:cyt
lipid formation; cLipid form
0.45 avPL:cyt + 0.55 FAT:cyt => 47.2 LIPID:cyt
lysine synthesis; cLYS syn
1 ATP:cyt + 2 GLM:cyt + 1 NAD:cyt + 2 NADPH:cyt + 1 OAD:cyt <=> 1 AMP:cyt + 1 LYS:cyt + 1 NADH:cyt + 2 NADP:cyt + 2 OGL:cyt + 1 PPi:cyt
protein polymerisation; cPROT poly
3 ATP:cyt + 1 avAA:cyt + 2 H2O:cyt <=> 2 ADP:cyt + 1 AMP:cyt + 4 H:cyt + 2 Pi:cyt + 1 PPi:cyt + 4.81 PROT:cyt
RNA polymerisation; cRNA syn
0.3 ATP:cyt + 0.2 CTP:cyt + 0.2 GTP:cyt + 0.3 UTP:cyt => 1 PPi:cyt + 9.5 RNA:cyt

maintenance
maintenance; cMaintenance
1 ATP:cyt + 1 H2O:cyt => 1 ADP:cyt + 1 H:cyt + 1 Pi:cyt

nucleotide synthesis
adenosine kinase; cA kin
1 A:cyt + 1 ATP:cyt <=> 1 ADP:cyt + 1 AMP:cyt + 1 H:cyt
adenylate kinase; cAMP kin
1 AMP:cyt + 1 ATP:cyt <=> 2 ADP:cyt
AMP synthesis; cAMP syn
1 ASP:cyt + 1 ATP:cyt + 1 IMP:cyt <=> 1 ADP:cyt + 1 AMP:cyt + 1 FUM:cyt + 2 H:cyt + 1 Pi:cyt
CTP synthetase; cCTP syn
1 ATP:cyt + 1 GLN:cyt + 1 H2O:cyt + 1 UTP:cyt <=> 1 ADP:cyt + 1 CTP:cyt + 1 GLM:cyt + 2 H:cyt + 1 Pi:cyt
cytidylate kinase; cCMP kin
1 ATP:cyt + 1 CMP:cyt <=> 1 ADP:cyt + 1 CDP:cyt
GMP synthesis; cGMP syn
1 ATP:cyt + 1 GLN:cyt + 2 H2O:cyt + 1 IMP:cyt + 1 NAD:cyt <=> 1 AMP:cyt + 1 GLM:cyt + 1 GMP:cyt + 4 H:cyt + 1 NADH:cyt + 1 PPi:cyt
guanylate kinase; cGMP kin
1 ATP:cyt + 1 GMP:cyt => 1 ADP:cyt + 1 GDP:cyt
IMP synthesis; cIMP syn
1 AICAR:cyt + 1 FTHF:cyt => 1 H2O:cyt + 1 IMP:cyt + 1 THF:cyt
nucleoside diphosphate kinase 1; cGDP kin
1 ATP:cyt + 1 GDP:cyt <=> 1 ADP:cyt + 1 GTP:cyt
nucleoside diphosphate kinase 2; cUDP kin
1 ATP:cyt + 1 UDP:cyt => 1 ADP:cyt + 1 UTP:cyt
nucleoside diphosphate kinase 3; cCDP kin
1 ATP:cyt + 1 CDP:cyt => 1 ADP:cyt + 1 CTP:cyt
phosphoribosyl pyrophosphate synthesis; cPRPP syn
1 ATP:cyt + 1 RIBU5P:cyt <=> 1 AMP:cyt + 1 H:cyt + 1 PRPP:cyt
phosphoribosyl-5-amino 4-imidazole carboxamide; cAICAR syn
1 ASP:cyt + 4 ATP:cyt + 1 CO2:cyt + 1 FTHF:cyt + 2 GLN:cyt + 1 GLY:cyt + 2 H2O:cyt + 1 PRPP:cyt <=> 4 ADP:cyt + 1 AICAR:cyt + 1 FUM:cyt + 2 GLM:cyt + 8 H:cyt + 4 Pi:cyt + 1 PPi:cyt + 1 THF:cyt
pyrophosphatase; cPPi ase
1 H2O:cyt + 1 PPi:cyt => 2 Pi:cyt
UMP synthesis anaerobic; cUMP syn an
1 ASP:cyt + 1 CARP:cyt + 1 NAD:cyt + 1 PRPP:cyt <=> 1 CO2:cyt + 1 H:cyt + 1 H2O:cyt + 1 NADH:cyt + 1 Pi:cyt + 1 PPi:cyt + 1 UMP:cyt
uridylate kinase; cUMP kin
1 ATP:cyt + 1 UMP:cyt <=> 1 ADP:cyt + 1 UDP:cyt

Mitochondrial ATPase
F1-F0 ATPase; mATPase
3 ADP:mit + 10 H:cyt + 3 Pi:mit <=> 3 ATP:mit + 7 H:mit + 3 H2O:mit

pentose phosphate pathway
glucose-6-phosphate dehydrogenase (NADP); cG6P deh
1 G6P:cyt + 1 H2O:cyt + 2 NADP:cyt => 1 CO2:cyt + 2 H:cyt + 2 NADPH:cyt + 1 RIBU5P:cyt
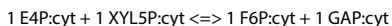ribosephosphate isomerase; cRIBU iso
1 RIBU5P:cyt <=> 1 RIB5P:cyt
ribulosephosphate 3-epimerase; cRIBUP epi
1 RIBU5P:cyt <=> 1 XYL5P:cyt
transaldolase; cTA1
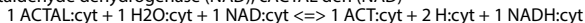1 GAP:cyt + 1 SED7P:cyt <=> 1 E4P:cyt + 1 F6P:cyt
transketolase 1; cTK1
1 RIB5P:cyt + 1 XYL5P:cyt <=> 1 GAP:cyt + 1 SED7P:cyt
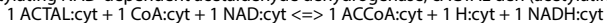transketolase 2; cTK2

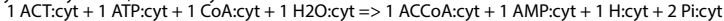1 E4P:cyt + 1 XYL5P:cyt <=> 1 F6P:cyt + 1 GAP:cyt

pyruvate branchpoint
    acetaldehyde dehydrogenase (NAD); cACTAL deh (NAD)
        1 ACTAL:cyt + 1 H2O:cyt + 1 NAD:cyt <=> 1 ACT:cyt + 2 H:cyt + 1 NADH:cyt
    acetylating NAD-dependent acetaldehyde dehydrogenase; cACTAL deh (acetylating)
        1 ACTAL:cyt + 1 CoA:cyt + 1 NAD:cyt <=> 1 ACCoA:cyt + 1 H:cyt + 1 NADH:cyt
    acetyl-CoA synthase; cACCoA syn
        1 ACT:cyt + 1 ATP:cyt + 1 CoA:cyt + 1 H2O:cyt => 1 ACCoA:cyt + 1 AMP:cyt + 1 H:cyt + 2 Pi:cyt
    alcohol dehydrogenase; cETOH deh
        1 ACTAL:cyt + 1 H:cyt + 1 NADH:cyt <=> 1 ETOH:cyt + 1 NAD:cyt
    lactate dehydrogenase; cLAC deh
        1 LAC:cyt + 1 NAD:cyt => 1 H:cyt + 1 NADH:cyt + 1 PYR:cyt
    pyruvate carboxylase; cPYR carb
        1 ATP:cyt + 1 CO2:cyt + 1 H2O:cyt + 1 PYR:cyt => 1 ADP:cyt + 2 H:cyt + 1 OXACT:cyt + 1 Pi:cyt
    pyruvate decarboxylase; cPYR dec
        1 H:cyt + 1 PYR:cyt => 1 ACTAL:cyt + 1 CO2:cyt
    pyruvate dehydrogenase mit; mPYR deh
        1 CoA:mit + 1 NAD:mit + 1 PYR:mit => 1 ACCoA:mit + 1 CO2:mit + 1 NADH:mit
    Pyruvate formate lyase; PFL
        1 CoA:cyt + 1 PYR:cyt => 1 ACCoA:cyt + 1 FOR:cyt
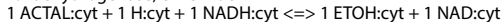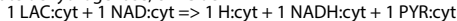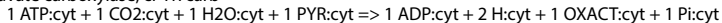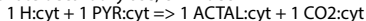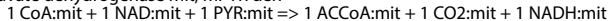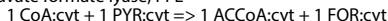
TCA cycle
    aconitase 1 mit; mACON 1
        1 CIT:mit => 1 ACO:mit + 1 H2O:mit
    aconitase 2 mit; mACON 2
        1 ACO:mit + 1 H2O:mit => 1 ICIT:mit
    citrate synthase mit; mCIT syn
        1 ACCoA:mit + 1 H2O:mit + 1 OXACT:mit => 1 CIT:mit + 1 CoA:mit + 1 H:mit
    fumarate hydrase; cFUM hy
        1 FUM:cyt + 1 H2O:cyt <=> 1 MAL:cyt
    fumarate hydrase mit; mFUM hy
        1 FUM:mit + 1 H2O:mit <=> 1 MAL:mit
    fumarate reductase mit; mFUM red
        1 FUM:mit + 1 H:mit + 1 NADH:mit <=> 1 NAD:mit + 1 SUC:mit
    isocitrate dehydrogenase (NAD) mit; mICIT deh_NAD
        1 ICIT:mit + 1 NAD:mit => 1 CO2:mit + 1 NADH:mit + 1 OGL:mit
    isocitrate dehydrogenase (NADP) mit; mICIT deh_NADP
        1 ICIT:mit + 1 NADP:mit => 1 CO2:mit + 1 NADPH:mit + 1 OGL:mit
    malate dehydrogenase; cMAL deh
        1 MAL:cyt + 1 NAD:cyt <=> 1 H:cyt + 1 NADH:cyt + 1 OXACT:cyt
    malate dehydrogenase mit; mMAL deh
        1 MAL:mit + 1 NAD:mit <=> 1 H:mit + 1 NADH:mit + 1 OXACT:mit
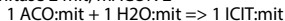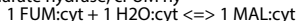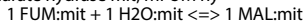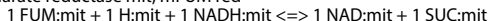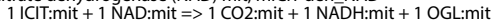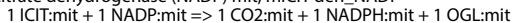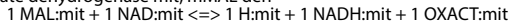
transport
    acetate transport; eACT trans
        1 ACT:ext + 1 H:ext => 1 ACT:cyt + 1 H:cyt
    ATPase plasmamembrane; eATPase
        1 ATP:cyt + 1 H2O:cyt => 1 ADP:cyt + 1 H:ext + 1 Pi:cyt
    ethanol transport; eETOH trans
        1 ETOH:cyt => 1 ETOH:ext
    glucose uptake; eGLUC fdiff
        1 GLUC:ext => 1 GLUC:cyt
    glycerol transport; eGOH trans
        1 GOH:cyt + 1 H:ext <=> 1 GOH:ext + 1 H:cyt
    lactate excretion; cLAC trans
        1 H:cyt + 1 LAC:cyt => 1 H:ext + 1 LAC:ext
    malate export; Mal exp
        1 H:ext + 1 MAL:cyt => 1 H:cyt + 1 MAL:ext
    metal import; eMET imp
        1 metal:ext => 1 metal:cyt
    NH4 transport; eNH4 trans
        1 NH4:ext => 1 NH4:cyt
    oleate transport; OLE trans
        1 OLE:ext => 1 OLE:cyt
    palmitoleate transport; PLLM trans
        1 PLLM:ext => 1 PLLM:cyt
    phosphate transport; ePi trans
        2 H:ext + 1 Pi:ext => 2 H:cyt + 1 Pi:cyt
    SO4 transport; eSO4 trans
        3 H:ext + 1 SO4:ext => 3 H:cyt + 1 SO4:cyt
    succinate transport; suc trans
        1 H:ext + 1 SUC:cyt => 1 H:cyt + 1 SUC:ext
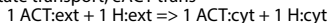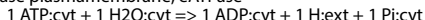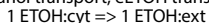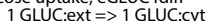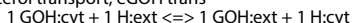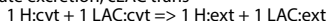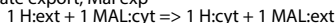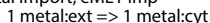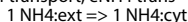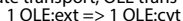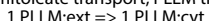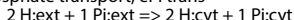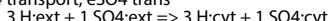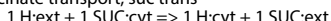
Component List

Name	ShortName	Composition
1,3-phosphoglycerate	13PG	C3H4O10P2-4
2-phosphoglycerate	2PG	C3H4O7P-3

3-phosphoglycerate	3PG	C3H4O7P-3
acetaldehyde	ACTAL	C2H4O
acetate	ACT	C2H3O2-1
acetyl-CoA	ACCoA	C23H34N7O17P3S-4
adenosine	A	C10H13N5O4
ADP	ADP	C10H12N5O10P2-3
alanine	ALA	C3H7NO2
AMP	AMP	C10H12N5O7P-2
arginine	ARG	C6H15N4O2+1
asparagine	ASN	C4H8N2O3
aspartate	ASP	C4H6NO4-1
ATP	ATP	C10H12N5O13P3-4
average amino acid	avAA	C4.81H9.61N1.32O2.53S0.0128-0.0282
AVERAGE FATTY ACID-CoA	avFA-CoA	C37.6H61.8N7O17P3S-4
average phospholipid	avPL	C40.3H77.3NO8.33P
biomass G4	biom-G4	CH1.74N0.145O0.595P0.00873S0.0018X0.018
carbamoyl phoshate	CARP	CH2NO5P-2
CARBOHYDRATES	CARBHYD	CH1.67O0.833
Carbon dioxide	CO2	CO2
CDP	CDP	C9H12N3O11P2-3
chorismate	CHO	C10H8O6-2
cis-aconitate	ACO	C6H3O6-3
citrate	CIT	C6H5O7-3
citydine diphosphate-diacylglycerol	CMP-DGOH	C45.3H78.7N3O15P2-2
CMP	CMP	C9H12N3O8P-2
CoA	CoA	C21H32N7O16P3S-4
CTP	CTP	C9H12N3O14P3-4
cystein	CYS	C3H7NO2S
dihydrofolate	DHF	C19H19N7O6-2
dihydroxyacetone-phosphate	DHAP	C3H5O6P-2
DNA	DNA	CH1.26N0.378O0.612P0.102
E4P	E4P	C4H7O7P-2
ETOH	ETOH	C2H6O
FAT	FAT	C52.9H97.5O6
Formate	FOR	CHO2-1
formyl-THF	FTHF	C20H21N7O7-2
fructose 1,6-bisphosphate	F16P	C6H10O12P2-4
fructose 6-phosphate	F6P	C6H11O9P-2
fumarate	FUM	C4H2O4-2
GDP	GDP	C10H12N5O11P2-3
glucose	GLUC	C6H12O6
glucose 6-phosphate	G6P	C6H11O9P-2
glutamate	GLM	C5H8NO4-1
glutamine	GLN	C5H10N2O3
glyceraldehyde 3-phosphate	GAP	C3H5O6P-2
glycerol	GOH	C3H8O3
glycerol 3-phosphate	GOH3P	C3H7O6P-2
glycine	GLY	C2H5NO2
GMP	GMP	C10H12N5O8P-2
GTP	GTP	C10H12N5O14P3-4
histidine	HIS	C6H10N3O2+1
homocitrate	HCIT	C7H7O7-3
homocysteine	HCYS	C4H8NO2S-1
homoserine	HSER	C4H9NO3
hydrogen	H	H+1
IMP	IMP	C10H11N4O8P-2
isocitrate	ICIT	C6H5O7-3
isoleucine	ILE	C6H13NO2
isopropylmalate	IPM	C7H10O5-2
lactate	LAC	C3H5O3-1
leucine	LEU	C6H13NO2
LIPID	LIPID	CH1.87N0.00953O0.149P0.00953
lysine	LYS	C6H15N2O2+1
malate	MAL	C4H4O5-2
malonyl-CoA	MACoA	C24H33N7O19P3S-5
metal	metal	X
metheonine	MET	C5H11NO2S
methylene-THF	METHF	C20H21N7O6-2
methyl-THF	MYTHF	C20H23N7O6-2
NAD	NAD	+1
NADH	NADH	H
NADP	NADP	+1
NADPH	NADPH	H
NH4	NH4	H4N+1
oleic acid	OLE	C18H33O2-1
oleoyl-CoA	OLE-CoA	C39H64N7O17P3S-4
ornithine	ORN	C5H13N2O2+1
oxaloacetate	OXACT	C4H2O5-2
oxoadipate	OAD	C6H6O5-2

oxobutyrate	OBU	C4H6O3
oxoglutarate	OGL	C5H4O5-2
oxoisovalerate	OIV	C5H7O3-1
palmitic acid	PLM	C16H31O2-1
palmitoleic acid	PLLM	C16H29O2-1
palmitoleoyl-CoA	PLLM-CoA	C37H60N7O17P3S-4
palmityl-CoA	PLM-CoA	C37H62N7O17P3S-4
phenylalanine	PHE	C9H11NO2
phosphate	Pi	HO4P-2
phosphatidate	PHD	C36.3H66.7O8P-2
phosphatidyl-choline	PHD-CHO	C41.3H79.7NO8P
phosphatidyl-ethanolamine	PHD-ETA	C38.3H73.7NO8P
phosphatidyl-serine	PHD-SER	C39.3H73.7NO10P
phosphoenol-pyruvate	PEP	C3H2O6P-3
phosphoribosyl-formamido-imidazole-carboamide	AICAR	C9H13N4O8P-2
proline	PRO	C5H9NO2
PROTEIN	PROT	CH1.58N0.275O0.318S0.00265-0.00587
PRPP	PRPP	C5H8O14P3-5
pyrophosphate	PPi	O7P2-4
pyruvate	PYR	C3H3O3-1
RIB5P	RIB5P	C5H9O8P-2
RIBU5P	RIBU5P	C5H9O8P-2
ribulose-15-bisphosphate	RIBU15P	C5H12O11P2
RNA	RNA	CH1.23N0.389O0.737P0.105
s-adenosyl-homocysteine	SAH	C14H20N6O5S
s-adenosylmetheonine	SAM	C15H23N6O5S+1
SED7P	SED7P	C7H13O10P-2
serine	SER	C3H7NO3
stearate	STE	C18H35O2-1
stearoyl-CoA	STE-CoA	C39H66N7O17P3S-4
succinate	SUC	C4H4O4-2
sulfide	H2S	H2S
sulphate	SO4	O4S-2
tetrahydrofolate	THF	C19H21N7O6-2
threonine	THR	C4H9NO3
tryptophane	TRP	C11H12N2O2
tyrosine	TYR	C9H11NO3
UDP	UDP	C9H11N2O12P2-3
UMP	UMP	C9H11N2O9P-2
UTP	UTP	C9H11N2O15P3-4
valine	VAL	C5H11NO2
water	H2O	H2O
XYL5P	XYL5P	C5H9O8P-2

4
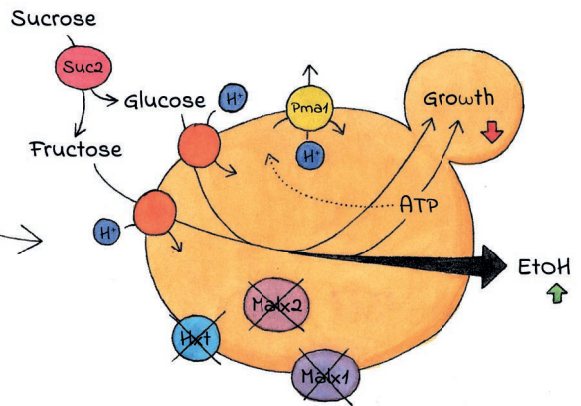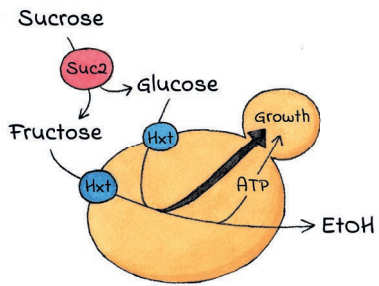
Chapter 5

Engineering proton-coupled hexose uptake in *Saccharomyces cerevisiae* for improved ethanol yield

Sophie C. de Valk, Susan E. Bouwmeester, Erik de Hulster, Robert Mans

Abstract

In the yeast *Saccharomyces cerevisiae*, which is widely applied for industrial bioethanol production, uptake of hexoses is mediated by transporters with a facilitated diffusion mechanism. In anaerobic cultures, a higher ethanol yield can be achieved when transport of hexoses is proton-coupled, because it results in a lower net ATP yield of sugar dissimilation. In this study, the facilitated diffusion transport system for hexose sugars of *S. cerevisiae* was replaced by hexose-proton symport. Introduction of heterologous glucose- or fructose-proton symporter genes in a hxt^0 yeast background strain (derived from CEN.PK2-1C) restored growth on the corresponding sugar under aerobic conditions. After applying an evolutionary engineering strategy to enable anaerobic growth, the hexose-proton symporter-containing strains were grown in anaerobic, hexose-limited chemostats on synthetic defined medium, which showed that their biomass yield was decreased by 44.0-47.6%, whereas the ethanol yield had increased by up to 17.2% (from 1.51 to 1.77 mol mol hexose^{-1}) compared to an isogenic strain expressing the hexose uniporter *HXT5*. To apply this strategy to increase the ethanol yield on sucrose, we constructed a platform strain in which all genes encoding hexose transporters, disaccharide transporters and disaccharide hydrolases were deleted, after which a combination of genes encoding a glucose proton symporter, fructose proton symporter and extracellular invertase (*SUC2*) were introduced. After evolution, the resulting strain exhibited a 16.6% increased anaerobic ethanol yield (from 1.51 to 1.76 mol mol hexose equivalent^{-1}) and 46.6% decreased biomass yield on sucrose. To conclude, this study provides a proof-of-concept for the replacement of the endogenous hexose transporters of *S. cerevisiae* by hexose proton symport, and the concomitant decrease in ATP yield, to greatly improve the anaerobic yield of ethanol on sugar. Moreover, the sugar-negative platform strain constructed in this study acts as a valuable starting point for future studies on sugar transport or development of cell factories requiring specific sugar transport mechanisms.

5

5.1 Introduction

The yeast *Saccharomyces cerevisiae* is well known as an excellent producer of ethanol, and has therefore been widely applied to produce alcoholic beverages, as well as for the industrial scale production of bioethanol (Jacobus *et al.*, 2021; Russel, 2003). Even under aerobic conditions, this yeast preferentially dissimilates glucose via alcoholic fermentation when glucose is present in sufficiently high concentrations (>1 g L^{-1}, Crabtree effect), which is remarkable since respiration yields substantially more ATP per molecule of dissimilated glucose (De Deken, 1966; Swanson and Clifton, 1948). Different hypotheses have been proposed to explain the occurrence of such 'inefficient' modes of substrate dissimilation, but to date this topic is still subject to discussion (de Groot *et al.*, 2020; Goel *et al.*, 2015; Niebel *et al.*, 2019; Regueira *et al.*, 2021). The emergence of Crabtree positive yeasts 100-150 million years ago probably coincided with the emergence of fruit-bearing plants, providing a sugar-rich niche in which these yeasts evolved (Conant and Wolfe, 2007; Piškur and Langkjær, 2004). In such environments, the high extracellular glucose concentration can drive the uptake of glucose by yeast cells via diffusion, which is exemplified by the occurrence of many hexose transporters with a facilitated diffusion mechanism in *S. cerevisiae*. In total, a set of 20 hexose transporter genes has been described in this yeast, each encoding proteins with various kinetic properties. Their condition-dependent expression allows for fast uptake of glucose at high (> 20 g L^{-1}) to near-zero glucose concentrations (André, 1995; Lagunas, 1993; Nevado *et al.*, 1994; Wieczorke *et al.*, 1999). To facilitate uptake and conversion of glucose at low extracellular concentrations, activity of high-affinity transporters (K_M ~1 mM) is required, in combination with hexokinase activity to 'trap' the sugar inside the cell in its phosphorylated form. This way, a glucose concentration gradient is maintained across the plasma membrane (Smits *et al.*, 1996). There are other yeast species that, on the contrary, rely on hexose-proton symporters that make use of the proton motive force to drive transport of sugar into the cells, which can give a selective advantage when environmental hexose concentrations are very low (K_M 20 – 200 µM) (Boles and Hollenberg, 1997; Deak, 1978; Loureiro-Dias, 1988; van Urk *et al.*, 1989). The proton motive force is maintained by export of protons by a plasma membrane H$^+$-ATPase, and therefore this sugar transport system requires net investment of ATP for its activity (Serrano, 1977). Thus, the transport mechanism of sugar uptake can have a substantial effect on the overall efficiency of sugar dissimilation in terms of ATP yield, especially when the substrate is dissimilated via fermentation, which results in a low amount of ATP produced per mol of substrate.

This concept and its effect on yeast physiology and bioethanol production was previously demonstrated for dissimilation of the disaccharide sucrose in *S. cerevisiae* (Basso *et al.*, 2011b). In wildtype *S. cerevisiae*, sucrose is mainly hydrolyzed outside of the cell by the invertase Suc2, after which the resulting monosaccharides are taken up by facilitated diffusion (Hawthorne, 1958; Lagunas, 1993; Winge and Roberts, 1952). However, when the extracellular invertase activity is diminished via gene editing, sucrose is taken up by disaccharide transporters, which employ a proton symport mechanism (Santos *et al.*, 1982) and is subsequently hydrolyzed intracellularly. In *S. cerevisiae*, export of a proton via the plasma membrane ATPase Pma1 comes at the cost of 1 ATP (Malpartida and Serrano, 1981; Nelson and Taiz, 1989; Serrano, 1977; Van Leeuwen *et al.*, 1992; Weusthuis *et al.*, 1993). As a result of the decreased overall ATP yield of sucrose dissimilation, less ATP is available for the energy-requiring production of biomass and glycerol, and therefore a larger fraction of the substrate is fermented to ethanol. Basso *et al.* (2011) constructed such a strain with predominantly intracellular sucrose hydrolysis, resulting in a decrease of the overall ATP yield from 4 moles of ATP to 3 moles of ATP per mol of sucrose.

5

The decreased efficiency of sucrose dissimilation was reflected in a 33% decrease in biomass yield and an 11% increase in ethanol yield (Basso *et al.*, 2011b). This increased ethanol yield on sucrose could be of relevance for the industrial production of bioethanol from sucrose-rich sources, such as sugarcane and sugar beet, especially since the sucrose-containing feedstock can make up to 70% of the total process cost (Pfromm *et al.*, 2010).

In theory, the ethanol yield in anaerobic *S. cerevisiae* cultures can be further improved by lowering the ATP yield of sucrose dissimilation in this yeast even more. Extracellular hydrolysis and subsequent uptake of the resulting monosaccharides via proton symport, instead of facilitated diffusion, would lower the yield from 4 to 2 moles of ATP per mole of sucrose. In this study, we investigated whether the facilitated diffusion mechanism for hexose uptake could be replaced by hexose-proton symport in *S. cerevisiae*. To this end, two glucose- and two fructose-proton symporter-encoding genes were introduced in a strain background that is devoid of all native hexose transporter genes, and the physiology of the resulting strains when growing on the corresponding hexose was studied. Subsequently, we investigated whether these hexose-proton symporters could also be applied in a strain background in which sucrose is exclusively hydrolyzed extracellularly and uptake of the resulting monosaccharides is mediated via a proton symport mechanism.

5.2 Materials and Methods

Strains and maintenance

All *Saccharomyces cerevisiae* strains used in this study are derived from the CEN.PK lineage (Entian and Kötter, 2007). For long term storage, glycerol was added to cells that were grown in synthetic medium (see section 'Media and cultivation) until late exponential phase, to obtain a final concentration of 30 % (v/v) glycerol, after which 1 mL aliquots were stored at -80 °C. Plasmids were propagated in *Escherichia coli* XL1-Blue cells (Agilent, Santa Clara, CA, USA), which were also stored at -80 °C after addition of glycerol to a final concentration of 25% (v/v) to overnight cultures.

Molecular biology techniques

Plasmids were isolated from *E. coli* cells using GeneJET Plasmid Miniprep Kit (Thermo Fisher Scientific). *S. cerevisiae* genomic DNA was isolated as previously described, using 0.2 M LiAc and 1% SDS to lyse the cells (Lõoke *et al.*, 2011). Genomic DNA from yeast species other than *S. cerevisiae* was isolated using the Yeastar Genomic DNA Isolation Kit (Baseclear, Leiden, The Netherlands). Amplification of DNA fragments for the purpose of cloning was performed using Phusion High Fidelity DNA polymerase (Thermo Fisher Scientific, Waltham, MA, USA), and for diagnostic PCRs, DreamTaq PCR Mastermix (Thermo Fisher Scientific) was used, both according to the manufacturer's protocol. Oligonucleotide primers were purchased from Sigma Aldrich (Saint Louis, MO, USA) either PAGE purified (for cloning purposes), or desalted (for diagnostic purposes). Sequences of all primers used in this study are listed in Table S5.1. DNA fragments were separated and visualized on 1% agarose TAE gel by 30 min electrophoresis at 100 V. DNA fragments excised from this gel were isolated using the Zymoclean Gel DNA recovery Kit (Baseclear), whereas the GeneJET PCR Purification Kit (Thermo Fisher Scientific) was used for isolation of DNA fragments directly from the PCR reaction mixture. Gibson assembly of plasmids was performed using the NEBuilder HiFi DNA Assembly Master Mix (New England

5

Biolabs, Ipswich, MA, USA) according to the manufacturer's instructions, after which 1 µL of this mixture was introduced into XL1-Blue chemically competent *E. coli* cells (Agilent) for plasmid propagation, according to the manufacturer's protocol. Transformation of *S. cerevisiae* strains was performed using LiAC/ssDNA/PEG, as previously described (Gietz and Woods, 2002). After transformation, single colonies were re-streaked three consecutive times to ensure an isogenic single cell line. Genomic deletions and integrations were confirmed by performing diagnostic PCR using genomic DNA of transformants as template. gRNA plasmids were removed from strains as described previously (Mans *et al.*, 2015). Plasmids were isolated from yeast strains using the Zymoprep Yeast Plasmid Miniprep II kit (Baseclear).

Plasmid construction

All plasmids used in this study are listed in Table 5.1.

Table 5.1: Plasmids used in this study. The prefixes 'Se', 'Kl' and 'Km' indicate genes originating from *Saccharomyces eubayanus*, *Kluyveromyves lactis* and *Kluyveromyces marxianus*, respectively.

Plasmid name	Relevant genotype	Source
p426TEF	2µm ampR *URA3 pTEF1-tCYC1*	(Mumberg *et al.*, 1995)
pUDE432	2µm ampR *URA3 pTEF1-MAL11-tCYC1*	(Marques *et al.*, 2018a)
pUDE897	2µm ampR *URA3 pTEF1-KlFRT1-tCYC1*	This study
pUDE898	2µm ampR *URA3 pTEF1-SeFSY1-tCYC1*	This study
pUDE914	2µm ampR *URA3 pTEF1-HXT5-tCYC1*	This study
pUDE920	2µm ampR *URA3 pTEF1-KmHGT1-tCYC1*	This study
pUDE206	2µm ampR *natNT1 pTPI1-I-SceI-tTEF1*	(González-Ramos *et al.*, 2016)
pUDE1024	2µm ampR *URA3 pTPI1-SeFSY1-tTEF1*	This study
pUDE1028	2µm ampR *URA3 pTEF1-KmHGT1-tCYC1 pTPI1-SeFSY1-tTEF1*	This study
p414-TEF1p-Cas9-CYC1t	*CEN6/ARS4* ampR *TRP1 pTEF1-cas9-tCYC1*	(DiCarlo *et al.*, 2013)
pUG-natNT2	ampR *loxP-natNT2-loxP*	(de Kok *et al.*, 2012b)
pROS12	2µm ampR *hphNT1* gRNA-*CAN1*.Y gRNA-*ADE2*.Y	(Mans *et al.*, 2015)
pUDR313	2µm ampR *hphN* gRNA-*HIS3* gRNA-*mTurquoise2*	This study
pROS10	2µm ampR *URA3* gRNA-*CAN1*.Y gRNA-*ADE2*.Y	(Mans *et al.*, 2015)
pUDR766	2µm ampR *URA3* gRNA-*kanMX* gRNA-*kanMX*	This study
pUDR211	2µm ampR *KlLEU2* gRNA-*HXT8* gRNA-*HXT14*	(Wijsman *et al.*, 2018)
pUDR295	2µm ampR *HIS3* gRNA-*GAL2* gRNA-*HXT4-1-5;HXT3-6-7*	(Wijsman *et al.*, 2018)
pRS416	*CEN6/ARS4* ampR *URA3*	(Sikorski and Hieter, 1989)
pUDR214	2µm ampR *URA3* gRNA-*HXT13-15-16* gRNA-*HXT2*	(Wijsman *et al.*, 2018)
pUDR220	2µm ampR *KlLEU2* gRNA-*HXT10* gRNA-*HXT9-11-12*	(Wijsman *et al.*, 2018)
pUDR418	2µm ampR *URA3* gRNA-*STL1* gRNA-*STL1*	(Wijsman *et al.*, 2018)
pUDE262	2µm ampR *URA3 pTDH3-LmSPase-tADH1*	(Marques *et al.*, 2018a)
pUDE1103	2µm ampR *URA3 pTDH3-SUC2-tADH1*	This study
pUDR119	2µm ampR *amdS* gRNA-*SGA1*	(Papapetridis *et al.*, 2018)
pUDE1089	2µm ampR *URA3 pTEF1-KlFRT1^{T767C} -tCYC1*	This study
pUDE1221	2µm ampR *URA3 pTEF1-KmHGT1^{T1058C}-tCYC1 pTPI1-SeFSY1-tTEF1*	This study

For construction of plasmids pUDE897, pUDE898, pUDE914 and pUDE920 via Gibson assembly, the backbone of pUDE432 was amplified using primers 7812 and 7999. *KlFRT1* (GenBank

AJ315952.1) was amplified from *Kluyveromyces lactis* CBS 2359 genomic DNA using primers 15985 and 15986, and subsequently assembled with the pUDE432 backbone, resulting in plasmid pUDE897. *SeFSY1* (GenBank HE858449.1) was amplified from *Saccharomyces eubayanus* CBS 12357 genomic DNA using primers 15987 and 15988, and subsequently assembled with the pUDE432 backbone, resulting in plasmid pUDE898. *HXT5* was amplified from CEN. PK113-7D genomic DNA using primers 16387 and 16388, and subsequently assembled with the pUDE432 backbone, resulting in plasmid pUDE914. *KmHGT1* (*KMXK_A02960* in Varela *et al.* 2019) was amplified from *Kluyveromyces marxianus* CBS 6556 genomic DNA using primers 16508 and 16509, and subsequently assembled with the pUDE432 backbone, resulting in plasmid pUDE920.

Plasmids pUDE1024 and pUDE1025 were constructed by Gibson assembly of the pUDE206 backbone, amplified using primers 6486 and 9719, with *SeFSY1*, amplified from pUDE898 using primers 17347 and 17348, or with *KlFRT1*, amplified from pUDE897 using primers 17349 and 17350, respectively. For construction of plasmids pUDE1026 and pUDE1027, pUDE432 was linearized by PCR using primers 10307 and 10308, and assembled with the *SeFSY1* expression cassette, amplified from pUDE1024 using primers 10305 and 10306, or with the *KlFRT1* expression cassette, amplified from pUDE1025 using primers 10305 and 10306, respectively. Similarly, for construction of plasmids pUDE1028 and pUDE1029, pUDE920 was linearized using primers 10307 and 10308, and assembled with the *SeFSY1* expression cassette, amplified from pUDE1024 using primers 10305 and 10306, or with the *KlFRT1* expression cassette, amplified from pUDE1025 using primers 10305 and 10306, respectively.

pUDR313 and pUDR766 were constructed as described previously (Mans *et al.*, 2015). The backbone of pROS12 was amplified using primer 6005 and the 2µm fragment was amplified from pROS12 using primers 10519 and 11826. Gibson assembly of the two resulting DNA fragments resulted in pUDR313. The backbone of pROS10 was amplified using primer 6005 and the 2µm fragment was amplified from pROS10 using primer 12743, which contains the gRNA sequence for targeting *KanMX*. Gibson assembly of the two resulting DNA fragments resulted in pUDR766.

For construction of plasmid pUDE1103, the backbone of pUDE262 was amplified using primers 17586 and 17587, and *SUC2* was amplified from CEN.PK113-7D genomic DNA using primers 17584 and 17585. Gibson assembly of the pUDE262 backbone and *SUC2* insert resulted in pUDE1103.

Strain construction

All strains used in this study are listed in **Table 5.2**.

Table 5.2: Strains used in this study. Unless specified otherwise, these concern *S. cerevisiae* strains.

Strain name	Relevant genotype	Source
CEN.PK113-7D	*MATa URA3 HIS3 LEU2 TRP1 MAL2-8c SUC2*	(Entian and Kötter, 2007)
Kluyveromyces lactis CBS 2359	Wildtype	CBS-KNAW
Saccharomyces eubayanus CBS 12357	Wildtype	CBS-KNAW
Kluyveromyces marxianus CBS 6556	Wildtype	CBS-KNAW

IMX1812	*MATa ura3-52 trp1-1 leu2-3,112 his3Δ can1::Spcas9-natNT2 gal2Δ hxt4-1-5Δ hxt3-6-7::ars4 hxt8Δ hxt14Δ hxt2Δ hxt9Δ hxt10Δ hxt11Δ hxt12Δ hxt13Δ hxt15Δ hxt16Δ mph2Δ mph3Δ mal11Δ stl1Δ*	(Wijsman *et al.*, 2018)
IMX2115	*MATa ura3-52 trp1-1 leu2-3,112 **HIS3** can1::Spcas9-natNT2 gal2Δ hxt4-1-5Δ hxt3-6-7::ars4 hxt8Δ hxt14Δ hxt2Δ hxt9Δ hxt10Δ hxt11Δ hxt12Δ hxt13Δ hxt15Δ hxt16Δ mph2Δ mph3Δ mal11Δ stl1Δ*	This study
IMX2125	*MATa ura3-52 trp1-1 **LEU2** HIS3 can1::Spcas9-natNT2 gal2Δ hxt4-1-5Δ hxt3-6-7::ars4 hxt8Δ hxt14Δ hxt2Δ hxt9Δ hxt10Δ hxt11Δ hxt12Δ hxt13Δ hxt15Δ hxt16Δ mph2Δ mph3Δ mal11Δ stl1Δ*	This study
IMX2144	*MATa ura3-52 **TRP1** LEU2 HIS3 can1::Spcas9-natNT2 gal2Δ hxt4-1-5Δ hxt3-6-7::ars4 hxt8Δ hxt14Δ hxt2Δ hxt9Δ hxt10Δ hxt11Δ hxt12Δ hxt13Δ hxt15Δ hxt16Δ mph2Δ mph3Δ mal11Δ stl1Δ*	This study
IMZ756	IMX2144 + pUDE432 (*URA3 MAL11*)	This study
IMZ757	IMX2144 + pUDE897 (*URA3 KlFRT1*)	This study
IMZ759	IMX2144 + pUDE898 (*URA3 SeFSY1*)	This study
IMZ763	IMX2144 + pUDE914 (*URA3 HXT5*)	This study
IMZ767	IMX2144 + pUDE920 (*URA3 KmHGT1*)	This study
IMZ796	IMX2144 + p426GPD (*URA3*)	This study
IMS1058	Single colony isolate of anaerobically evolved IMZ756	This study
IMS1059	Single colony isolate of anaerobically evolved IMZ757	This study
IMS1060	Single colony isolate of anaerobically evolved IMZ759	This study
IMS1061	Single colony isolate of anaerobically evolved IMZ767	This study
IMK698	*MATa ura3-52 leu2-112 MAL2-8C mal11-mal12::loxP mal21-mal22::loxP mal31-mal32::loxP mph2/3::loxP mph2/3::loxP-hphNT1-loxP suc2::loxP-kanMX-loxP ima1Δ ima2Δ ima3Δ ima4Δ ima5Δ*	(Marques *et al.*, 2018a)
IMX2572	*MATa ura3-52 leu2-112 MAL2-8C mal11-mal12::loxP mal21-mal22::loxP mal31-mal32::loxP mph2/3::loxP mph2/3::loxP-hphNT1-loxP suc2::loxP-kanMX-loxP ima1Δ ima2Δ ima3Δ ima4Δ ima5Δ **can1::cas9-natNT2***	This study
IMK980	*MATa ura3-52 leu2-112 MAL2-8C mal11-mal12::loxP mal21-mal22::loxP mal31-mal32::loxP mph2/3::loxP mph2/3::loxP-hphNT1-loxP **suc2::loxP** ima1Δ ima2Δ ima3Δ ima4Δ ima5Δ can1::cas9-natNT2*	This study
IMK983	*MATa ura3-52 leu2-112 **his3Δ** MAL2-8C mal11-mal12::loxP mal21-mal22::loxP mal31-mal32::loxP mph2/3::loxP mph2/3::loxP-hphNT1-loxP suc2::loxP ima1Δ ima2Δ ima3Δ ima4Δ ima5Δ can1::cas9-natNT2*	This study
IMK985	*MATa ura3-52 leu2-112 his3Δ MAL2-8C mal11-mal12::loxP mal21-mal22::loxP mal31-mal32::loxP mph2/3::loxP mph2/3::loxP-hphNT1-loxP suc2::loxP ima1Δ ima2Δ ima3Δ ima4Δ ima5Δ can1::cas9-natNT2 **hxt8Δ hxt14Δ gal2Δ hxt4Δ hxt1Δ hxt5Δ hxt3Δ hxt6Δ hxt7Δ***	This study
IMK990	*MATa ura3-52 leu2-112 his3Δ MAL2-8C mal11-mal12::loxP mal21-mal22::loxP mal31-mal32::loxP mph2/3::loxP mph2/3::loxP-hphNT1-loxP suc2::loxP ima1Δ ima2Δ ima3Δ ima4Δ ima5Δ can1::cas9-natNT2 hxt8Δ hxt14Δ gal2Δ hxt4Δ hxt1Δ hxt5Δ hxt3Δ hxt6Δ hxt7Δ **hxt13Δ hxt15Δ hxt16Δ hxt2Δ***	This study

5

IMK992	*MATa ura3-52 leu2-112 his3Δ MAL2-8C mal11-mal12::loxP mal21-mal22::loxP mal31-mal32::loxP mph2/3::loxP mph2/3::loxP-hphNT1-loxP suc2::loxP ima1Δ ima2Δ ima3Δ ima4Δ ima5Δ can1::cas9-natNT2 hxt8Δ hxt14Δ gal2Δ hxt4Δ hxt1Δ hxt5Δ hxt3Δ hxt6Δ hxt7Δ hxt13Δ hxt15Δ hxt16Δ hxt2Δ **hxt10Δ hxt9Δ hxt11Δ hxt12Δ***	This study
IMK1003	*MATa ura3-52 leu2-112 his3Δ MAL2-8C mal11-mal12::loxP mal21-mal22::loxP mal31-mal32::loxP mph2/3::loxP mph2/3::loxP-hphNT1-loxP suc2::loxP ima1Δ ima2Δ ima3Δ ima4Δ ima5Δ can1::cas9-natNT2 hxt8Δ hxt14Δ gal2Δ hxt4Δ hxt1Δ hxt5Δ hxt3Δ hxt6Δ hxt7Δ hxt13Δ hxt15Δ hxt16Δ hxt2Δ hxt10Δ hxt9Δ hxt11Δ hxt12Δ **stl1Δ***	This study
IMK1008	*MATa ura3-52 **LEU2** his3Δ MAL2-8C mal11-mal12::loxP mal21-mal22::loxP mal31-mal32::loxP mph2/3::loxP mph2/3::loxP-hphNT1-loxP suc2::loxP ima1Δ ima2Δ ima3Δ ima4Δ ima5Δ can1::cas9-natNT2 hxt8Δ hxt14Δ gal2Δ hxt4Δ hxt1Δ hxt5Δ hxt3Δ hxt6Δ hxt7Δ hxt13Δ hxt15Δ hxt16Δ hxt2Δ hxt10Δ hxt9Δ hxt11Δ hxt12Δ stl1Δ*	This study
IMK1010	*MATa ura3-52 LEU2 **HIS3** MAL2-8C mal11-mal12::loxP mal21-mal22::loxP mal31-mal32::loxP mph2/3::loxP mph2/3::loxP-hphNT1-loxP suc2::loxP ima1Δ ima2Δ ima3Δ ima4Δ ima5Δ can1::cas9-natNT2 hxt8Δ hxt14Δ gal2Δ hxt4Δ hxt1Δ hxt5Δ hxt3Δ hxt6Δ hxt7Δ hxt13Δ hxt15Δ hxt16Δ hxt2Δ hxt10Δ hxt9Δ hxt11Δ hxt12Δ stl1Δ*	This study
IMX2719	*MATa ura3-52 LEU2 HIS3 MAL2-8C mal11-mal12::loxP mal21-mal22::loxP mal31-mal32::loxP mph2/3::loxP mph2/3::loxP-hphNT1-loxP suc2::loxP ima1Δ ima2Δ ima3Δ ima4Δ ima5Δ can1::cas9-natNT2 hxt8Δ hxt14Δ gal2Δ hxt4Δ hxt1Δ hxt5Δ hxt3Δ hxt6Δ hxt7Δ hxt13Δ hxt15Δ hxt16Δ hxt2Δ hxt10Δ hxt9Δ hxt11Δ hxt12Δ stl1Δ **sga1::SUC2***	This study
IMZ783	IMX2719 + pUDE1028 (*URA3 KmHGT1 SeFSY1*)	This study
IMZ785	IMX2719 + pUDE914 (*URA3 HXT5*)	This study
IMS1214	Single colony isolate of anaerobically evolved IMZ783	This study
IMS1215	Single colony isolate of anaerobically evolved IMZ783	This study
IME666	IMX2144 + pUDE1089 (*URA3 KlFRT1*[T767C])	This study
IME752	IMX2719 + pUDE1221 (*URA3 KmHGT1*[T1058C] *SeFSY1*)	This study

Saccharomyces eubayanus strain CBS 12357 (CRUB 1568; PYCC 6148), *Kluyveromyces lactis* strain CBS 2359 (ATCC 8585; CCRC 21716; DBVPG 6725; DBVPG 6731; DBVPG 6833; DSM 70799; IFO 1267; NRRL Y-1140; VKPM Y 1174) and *Kluyveromyces marxianus* strain CBS 6556 (ATCC 26548; NCYC 2597; 359 NRRL Y-7571) were obtained from the Westerdijk Fungal Biodiversity 360 Institute (Utrecht, The Netherlands).

To restore histidine prototrophy in IMX1812, *HIS3* was amplified from CEN.PK113-7D genomic DNA using primers 1738 and 3755 and introduced into IMX1812, resulting in IMX2115. To restore leucine prototrophy in IMX2115, *LEU2* was amplified from CEN.PK113-7D genomic DNA using primers 1742 and 1743 and introduced into IMX2115, resulting in IMX2125. The tryptophan auxotrophy in this strain (*trp1-1*) is the result of a single point mutation in the *TRP1* gene (Botstein *et al.*, 1979). By plating on medium without tryptophan, colonies were obtained that spontaneously reverted this mutation, resulting in strain IMX2144. Introduction

of plasmids pUDE432, pUDE897, pUDE898, pUDE914, pUDE920 and p426TEF into IMX2144 resulted in strains IMZ756, IMZ757, IMZ759, IMZ763, IMZ767 and IMZ796, respectively.

IMZ756, IMZ757, IMZ759 and IMZ767 were each evolved in bioreactors to select for growth under anaerobic conditions (see below). From each individual bioreactor, single colonies were isolated by plating on SM with glucose (IMZ756 and IMZ767) or SM with fructose (IMZ757 and IMZ759) and re-streaking three consecutive times on the same medium, resulting in IMS1058, IMS1059, IMS1060 and IMS1061, respectively.

To facilitate genetic engineering of IMK698, *Spcas9* was integrated into its genome. To this end, *cas9* was amplified from p414-*TEF1*p-*cas9*-*CYC1*t using primers 2873 and 4653, and the *natNT2* marker was amplified from pUG-natNT2 using primers 3093 and 5542. Both DNA fragments were introduced into IMK698, resulting in IMX2572. Prior deletions in this strain were performed using the Cre-*loxP* system (Güldener *et al.*, 1996), but for the last deletion (*suc2*), the marker (*kanMX*) had not been recycled. To stimulate loop out of the *loxP*-flanked *kanMX* expression cassette, IMX2572 was transformed with pUDR766, resulting in IMK980. Further Cas9-assisted gene deletions were performed as previously described (Mans *et al.*, 2015). In IMK980, *HIS3* was deleted by introducing pUDR313, along with a double stranded DNA repair fragment obtained by annealing primers 10521 and 10522, resulting in strain IMK983. For deletion of all hexose transporters, the previously designed Cas9-assisted toolkit was used (Wijsman *et al.*, 2018). pUDR211 and pUDR295 were introduced into IMK983 along with five double stranded DNA repair fragments, obtained by annealing primers 9532 and 9533, 9551 and 9552, 9563 and 9564, 9522 and 9523 and by amplification from plasmid pRS416 with primers 9525 and 9526. The resulting strain was named IMK985. pUDR214 was introduced into IMK985, along with double stranded DNA repair fragments, obtained by annealing primers 9547 with 9548, 9555 with 9556, and 9528 with 9529, resulting in strain IMK990. pUDR220 was introduced into IMK990, along with double stranded DNA repair fragments, obtained by annealing primers 9538 with 9539, 9535 with 9536 and 9542 with 9543, resulting in strain IMK992. Finally, pUDR418 was introduced into IMK992, along with a double stranded DNA repair fragment, obtained by annealing primers 13617 and 13618, resulting in strain IMK1003. To regain leucine prototrophy, *LEU2* was amplified from CEN.PK113-7D genomic DNA using primers 1742 and 1743 and introduced into IMK1003, resulting in strain IMK1008. To regain histidine prototrophy, *HIS3* was amplified from CEN.PK113-7D genomic DNA using primers 1738 and 3755 and introduced into IMK1008, resulting in strain IMK1010.

A *SUC2* integration cassette was amplified from pUDE1103 using primers 9355 and 9356 and introduced into IMK1010, along with plasmid pUDR119, resulting in IMX2719. Introduction of plasmids pUDE1028 and pUDE914 into IMX2719 resulted in strains IMZ783 and IMZ785, respectively.

Plasmid pUDE1089 was isolated from IMS1059 and introduced into IMX2144, resulting in IME666. Similarly, plasmid pUDE1221 was isolated from IMS1215 and introduced into IMX2719, resulting in IME752.

Media and cultivation

E. coli cultures were grown at 37 °C in LB medium, supplemented with 100 µg mL^{-1} ampicillin for selection and maintenance of plasmids. Yeast strains were grown on synthetic medium (SM), which was heat sterilized for 20 min at 121 °C, after which a filter-sterilized vitamin solution

was added (Verduyn *et al.*, 1992). Depending on the transporters expressed, the medium was supplemented with either 20 g L^{-1} glucose or 20 g L^{-1} fructose (both added from 500 g L^{-1} stock solutions that were heat sterilized for 20 min at 110 °C), 20 g L^{-1} sucrose (added from a filter-sterilized 500 g L^{-1} solution) or 2% (v/v) ethanol in combination with 2% (v/v) glycerol (added from a 99% (v/v) solution that was heat sterilized for 20 min at 121 °C). For complementation of auxotrophic requirements, either 150 mg L^{-1} uracil, 100 mg L^{-1} histidine, 500 mg L^{-1} leucine and/or 75 mg L^{-1} tryptophan was added (Pronk, 2002). Medium for anaerobic cultivations was additionally supplemented with 10 mg L^{-1} ergosterol and 420 mg L^{-1} Tween 80, which were added from a concentrated solution (800x) in absolute ethanol (Verduyn *et al.*, 1990b). For preparation of solid medium plates, 2% (w/v) agar was added to the media prior to heat sterilization. Medium used in bioreactor cultivations was additionally supplemented with 0.2 g L^{-1} Antifoam C (Sigma Aldrich). Aerobic shake flask cultures were grown in 500 mL round bottom flasks with 100 mL medium, which were incubated in a New Brunswick Scientific Innova 44 Incubator Shaker (Eppendorf, Nijmegen, the Nederlands) at 200 rpm at 30 °C. Anaerobic shake flask cultures were grown at 30 °C in a Bactron anaerobic chamber with an atmosphere of 5% (v/v) H_2, 6% (v/v) CO_2 and 89% (v/v) N_2, on a IKA KS 260 basic shaker (IKA-Werke GmbH & Co, Staufen, Germany) at 200 rpm, using 50 mL Erlenmeyer flasks containing 30 mL medium. For preparation of spot plates, strains were pre-grown on YP with 2% (v/v)ethanol and 2% (v/v) glycerol. Exponentially growing cells were collected by centrifugation (3000 g, 5 min at 4 °C), washed with sterile water and resuspended to a concentration of 10^7 cells mL^{-1}, determined using a Z2 Coulter Counter (Beckman Coulter, Woerden, the Netherlands) using a 50 μm aperture. Subsequently, dilutions were made of 10^6, 10^5, 10^4 and 10^2 cells mL^{-1}, of which 10 μL was spotted on solid medium plates. Glucose-, fructose-, sucrose- and maltose-containing plates were incubated for two days, galactose-containing plates for three days and ethanol and glycerol-containing plates for eight days, all at 30 °C.

Laboratory evolution of IMZ756, IMZ757, IMZ759 and IMZ767 was conducted in Minifors 2 bioreactors (INFORS HT, Velp, the Netherlands) with a working volume of 100 mL in a sequential batch reactor (SBR) setup. IMZ756 and IMZ767 were evolved in SM with 20 g L^{-1} glucose, whereas IMZ757 and IMZ759 were evolved in SM with 20 g L^{-1} fructose. The cultures were stirred at 800 rpm and the temperature was kept constant at 30 °C. The pH was maintained at 5.0 by automated addition of a 2.0 M KOH solution. Cultures were sparged with 50 mL min^{-1} of a gas mixture of air and nitrogen. Starting with 100% air, the air content of the gas mixture was stepwise decreased over the course of the evolution, until the cultures were sparged with 100% nitrogen (<5 ppm O_2). The CO_2 concentration in the off-gas was continuously measured to monitor sugar consumption and growth. A sharp decrease in off-gas CO_2 concentration was interpreted as an indication that exponential growth had ceased. When the concentration of CO_2 in the off-gas dropped by at least 0.3% below the highest CO_2 concentration observed ('the peak') in that batch, an empty-refill cycle was automatically triggered. To prevent automatic triggering of empty-refill cycles due to noise in CO_2 measurements in the early phase of the batch, the empty-refill cycle was only triggered after the off-gas CO_2 concentration of that batch cycle had reached a value of at least 0.5%.

All other bioreactor cultivations were conducted in 2 L laboratory bioreactors (Applikon, Delft, The Netherlands) with a 1 L working volume. Cultures were stirred at 800 rpm, the temperature was controlled at 30 °C and the pH was kept constant at 5.0 through automated addition of 2.0 M KOH. Anaerobic cultures were sparged with 500 mL N_2 min^{-1} (<5 ppm O_2), and medium vessels were sparged with nitrogen as well. IMZ783 and IMZ784 were evolved in SM with 20

g L^{-1} sucrose in an SBR setup. During the evolution, the CO_2 concentration in the-off gas was continuously measured using a MultiExact 4100 analyser (Servomex, Egham, Surrey, United Kingdom) to monitor growth. The end of the batch phase automatically triggered an empty-refill cycle when, after at least 8 hours, the CO_2 concentration in the off-gas had decreased to 50% of the maximum CO_2 concentration of that batch. Cultures were sparged with 0.5 L min^{-1} of a gas mixture of air and nitrogen. To be able to control the gas composition, compressed air at 3 bar overpressure was led through a mass flow controller, before connection to tubing with nitrogen at 2 bar. A second mass flow controller after this connection allowed for the control of the flowrate of the gas mixture. Starting with 100% air, the air content of the gas mixture was stepwise decreased over the course of the evolution, until the cultures were sparged with 100% nitrogen and anaerobic conditions were attained. For chemostat cultivations, medium pumps were switched on after sugar depletion in a preceding batch phase, to obtain a constant flowrate. The volume was kept constant at 1 L using an effluent pump that was controlled by an electric level sensor, resulting in a stable dilution rate. Chemostat cultures were assumed to be in steady state when, after five volume changes, the culture dry weight, extracellular concentrations of sugar, ethanol and glycerol and CO_2 production rate varied by less than 2% over at least 2 more volume changes.

Analytical methods

Optical density (OD) of yeast cultures was measured at 660 nm using a Libra S11 spectrophotometer (Biochrom, Cambridge, United Kingdom). For dry weight measurements, 10 or 20 mL culture samples (depending on culture density) were filtered on a pre-weighed nitrocellulose filter with pore size 0.45 μm. Subsequently, the filters were washed with demineralized water and dried for 20 min in a microwave oven at 360 W, after which they were weighed again. Concentrations of sugars, ethanol, glycerol and organic acids were measured via HPLC analysis on an Agilent 1260 HPLC, equipped with a Bio-Rad HPX 87H column. Detection was performed by means of an Agilent refractive index detector and an Agilent 1260 VWD detector.

The carbon recovery was calculated as the percentage of the carbon per liter of medium that could be traced back per liter of culture in CO_2, biomass and products that were measured via HPLC analysis of the culture supernatant. The 'ingoing' carbon, in the medium, was calculated from the concentrations of carbon source (glucose, fructose or sucrose) and ethanol (present due to supplementation of Tween 80 and ergosterol) in the medium, which were also determined via HPLC analysis. For the recovered carbon, concentrations of glucose, fructose, glycerol, ethanol, succinate, pyruvate, lactate, acetate and formate were determined in the culture supernatant via HPLC analysis. The amount ethanol that evaporated per liter of culture was estimated using a previously determined volume-dependent ethanol evaporation constant (Guadalupe Medina *et al.*, 2010). The amount of CO_2 produced per liter of culture was calculated by multiplying of the fraction of CO_2 in the reactor off-gas with the flowrate of the reactor off-gas and the dilution rate, and subsequently dividing by the reactor volume. The flowrate of outgoing, spent media was assumed to be identical to the determined inflow rate. Finally, to calculate the amount of carbon in biomass from dry weight measurements, the composition of 1 Cmol of biomass was assumed to be $CH_{1.8}O_{0.5}N_{0.2}$, and thus a molar weight of 24.6 g Cmol biomass^{-1} was assumed.

5

Structural modeling of KlFrt1 and KmHgt1 proteins

Homology modeling of both KlFrt1 and KmHgt1 was performed using the SWISS-MODEL server (Biasini *et al.*, 2014). For KlFrt1, the structure of *Escherichia coli* XylE (PDB 4GBY.1.A) was used as template to predict the structure, whereas for modelling of KmHgt1, the structure of *Arabidopsis thaliana* STP10 (PDB 7AAQ.1.A) was used.

5.3 Results

Expression of single hexose-proton symporters is sufficient to enable aerobic growth on glucose or fructose

The first step towards the construction of *S. cerevisiae* strains that are dependent on proton-coupled hexose transport was the selection of suitable transporter candidates. *S. cerevisiae* possesses a native proton-coupled transporter with affinity for glucose (Mal11), however, this transporter also has affinity for maltose and sucrose (Han *et al.*, 1995; Stambuk and de Araujo, 2001; Wieczorke *et al.*, 1999). Therefore, *FSY1* from *Saccharomyces eubayanus (SeFSY1)*, *FRT1* from *Kluyveromyces lactis (KlFRT1)* and KMXK_A02960 from *Kluyveromyces marxianus (KmHGT1)*, which have been described in previous literature as glucose- or fructose-proton symporters (Anjos *et al.*, 2013; Diezemann and Boles, 2003; Galeote *et al.*, 2010; Gonçalves *et al.*, 2000; Varela *et al.*, 2019), were selected for heterologous expression in *S. cerevisiae*, in addition to *MAL11*. To be able to investigate strains in which the sole transport mechanism for hexose uptake is proton symport, without interference of transporters with a facilitated diffusion mechanism, the selected proton symporters were individually overexpressed in strain IMX2144, a derivative of IMX1812 (Wijsman *et al.*, 2018), which is devoid of all native hexose transporters (*hxt⁰*). The resulting strains were grown aerobically in shake flasks with SM with 20 g L^{-1} glucose (SMD) or 20 g L^{-1} fructose (SMF) as the sole carbon source. No growth was observed for the empty vector-carrying strain IMZ796 after ten days, which reflects the absence of any glucose or fructose transporters in *hxt⁰*-strain IMX2144. Overexpression of either *MAL11* or *KmHGT1* restored growth on glucose, and the corresponding strains had a specific growth rate (μ) of 0.19 ± 0.00 h^{-1} (*MAL11*) and 0.09 ± 0.00 h^{-1} (*KmHGT1*) on this carbon source, whereas no growth was observed for these strains in SMF after ten days. On the other hand, overexpression of *SeFSY1* and *KlFRT1* restored growth on fructose (μ= 0.18 ± 0.00 h^{-1} and

5
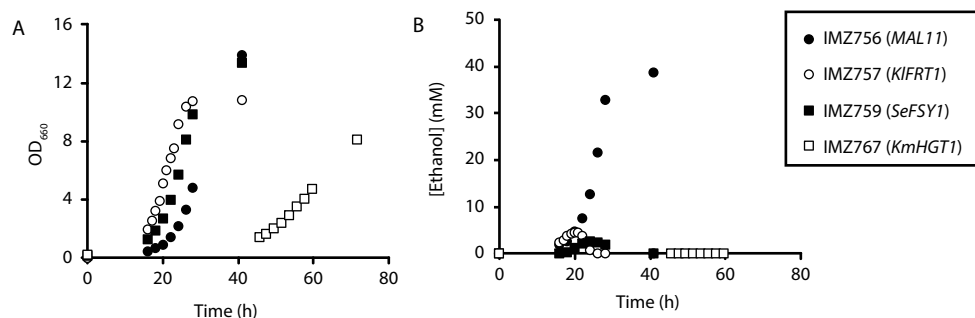
Figure 5.1: Growth (A) and ethanol production (B) of IMZ756 (*MAL11*), IMZ757 (*KlFRT1*), IMZ759 (*SeFSY1*) and IMZ767 (*KmHGT1*) in shake flasks with either SMD (IMZ756 and IMZ767) or SMF (IMZ757 and IMZ759) under aerobic conditions. Data shown represents one of two independent replicates.

0.23 ± 0.00 h^{-1}, respectively), but not on glucose. Interestingly, only for strain IMZ756 (*MAL11*) aerobic fermentation was clearly observed, as apparent from the production of ethanol (up to 39 mM) in these cultures (Figure 5.1). For IMZ757 (*KlFRT1*) and IMZ759 (*SeFSY1*), some ethanol was produced (up to 4.5 mM and 2.5 mM, respectively) in the early exponential phase, which was subsequently co-consumed with fructose.

Laboratory evolution enables anaerobic growth on hexoses

The replacement of facilitated diffusion by proton symport of hexose uptake is expected to decrease the ATP yield of dissimilation by 1 ATP per glucose or fructose molecule due to the ATP requirement of proton extrusion. In this scenario, the resulting impact on the cellular energy metabolism and thereby strain physiology is more pronounced when the hexoses are fermented and only 2 ATP is produced per hexose, compared to the estimated 16 ATP per hexose for aerobic respiration (Pronk *et al.*, 1994; Verduyn *et al.*, 1991). However, when investigated in anaerobic shake flasks (with SMD for *MAL11* and *KmHGT1*, SMF for *KlFRT1* and *SeFSY1*), only the *MAL11*-overexpressing strain IMZ756 grew on SMD, whereas no growth was observed for IMZ757 (*KlFRT1*), IMZ759 (*SeFSY1*) and IMZ767 (*KmHGT1*) after incubation for ten days. Therefore, an evolutionary engineering strategy was applied to select for anaerobically growing mutants. To this end, all four strains were grown in sequential batch reactor (SBR) setups that were sparged with a mixture of air and nitrogen. Over the course of the evolution, the supply of air (and thus oxygen) was decreased stepwise until the strains exhibited growth under anaerobic conditions (Online Supplementary Information). IMZ756 (*MAL11*) was also included in these evolution experiments to potentially improve its fermentation kinetics. Since this strain was already able to grow under anaerobic conditions, the switch from aerobic to anaerobic conditions was made without intermediate steps. After approximately 85 (*MAL11*), 106 (*KmHGT1*), 230 (*SeFSY1*) and 200 (*KlFRT1*) generations, the cultures were switched to fully anaerobic conditions, and after approximately 132 (*MAL11*), 30 (*KmHGT1*), 51 (*SeFSY1*) and 35 (*KlFRT1*) additional generations, single colonies were isolated from each reactor, resulting in IMS1058 (*MAL11*), IMS1059 (*KlFRT1*), IMS1060 (*SeFSY1*) and IMS1061 (*KmHGT1*).

Replacement of hexose diffusion by proton-coupled hexose transport decreases the ATP yield of glucose and fructose fermentation

Subsequently, the four evolved strains were characterized in anaerobic chemostats, which were glucose-limited for IMS1058 (*MAL11*) and IMS1061 (*KmHGT1*) and fructose-limited for IMS1059 (*KlFRT1*) and IMS1060 (*SeFSY1*). As a reference, *HXT5*, encoding a hexose uniporter, was overexpressed in IMX2144 (*hxt⁰*) and the resulting strain was characterized in both glucose- and fructose-limited chemostats. From measurements of the CO_2 concentration in the reactor off-gas during the preceding batch phase, the anaerobic maximum specific growth rates (μ_{max}) were estimated (Table 5.3). Based on these growth rates, the flowrate of the ingoing medium was adjusted to obtain a dilution rate of 0.07 h^{-1} after the batch phase, so that all strains could be compared at the same growth rate. Compared to the *HXT5*-expressing reference strain, the biomass yield of the strains expressing hexose-proton symporters was reduced by 44.0–47.6% (Table 5.3), which is close to the reduction of 50% that is expected when the energetic efficiency of dissimilation is also decreased by 50% (from 2 to 1 mol of ATP per mol of hexose) (Weusthuis *et al.*, 1993). Consequently, since these strains were grown at identical growth rates, a two-fold increase in the biomass specific glucose consumption, ethanol production and CO_2 production rates of the proton symporter-expressing strains were expected. Indeed, a fold increase between 1.8 and 2.2 of these biomass specific rates

5

was observed for all proton-coupled strains (Table 5.3). Based on the ethanol yields that were measured for the *HXT5*-expressing reference strain, the ethanol yields of the proton symporter-expressing strains were predicted to be increased by 16.2% on glucose and 13.3% on fructose when hexose transport is completely proton coupled (Supplementary Information). In line with this prediction, compared to the reference strain, the ethanol yields of the strains carrying the glucose-proton symporters *MAL11* and *HGT1* were increased by 17.2% and 14.6% respectively, while the ethanol yields of the strains carrying the fructose-proton symporters *FRT1* and *FSY1* were increased by 13.3% and 10.8%, respectively (Table 5.3). Differences in kinetic properties of the transporters were reflected in the varying residual sugar concentrations amongst the different strains, suggesting that *KmHGT1* exhibits the highest affinity for glucose (0.11 ± 0.00 g L⁻¹) and *SeFSY1* the highest affinity for fructose (0.12 ± 0.02 g L⁻¹, Table 5.3).

Table 5.3: Growth characteristics of anaerobically evolved hxt^0-strains expressing proton symporters and a hxt^0 strain expressing *HXT5* in either glucose- or fructose-limited anaerobic steady state chemostat cultures at a dilution rate of 0.07 h⁻¹. The maximum specific growth rate (μ_{max}) was determined based on measurements of the CO_2 concentration in the reactor off-gas during the preceding batch phase. Biomass-specific production and consumption rates are depicted as $q_{metabolite}$. The carbon recovery represents the percentage of the carbon entering the reactor system via the medium that could be traced back in biomass, products and residual substrate. The data represent average values and mean deviations obtained from duplicate experiments.

Strain	IMZ763	IMS1058	IMS1061	IMZ763	IMS1059	IMS1060
Hexose transporter	*HXT5*	*MAL11*	*KmHGT1*	*HXT5*	*KlFRT1*	*SeFSY1*
Carbon source	Glucose	Glucose	Glucose	Fructose	Fructose	Fructose
μ_{max} (h⁻¹)	0.22 ± 0.00	0.21 ± 0.01	0.13 ± 0.00	0.23 ± 0.00	0.16 ± 0.00	0.11 ± 0.00
Biomass yield (g_x g_s^{-1})	0.084 ± 0.001	0.044 ± 0.000	0.047 ± 0.000	0.088 ± 0.003	0.047 ± 0.000	0.048 ± 0.001
Ethanol yield (mol mol$_s^{-1}$)	1.51 ± 0.01	1.77 ± 0.01	1.73 ± 0.00	1.58 ± 0.02	1.79 ± 0.01	1.75 ± 0.02
q_s (mmol g_x^{-1} h⁻¹)	-4.69 ± 0.06	-8.87 ± 0.15	-8.38 ± 0.16	-4.46 ± 0.13	-8.38 ± 0.02	-8.11 ± 0.36
$q_{ethanol}$ (mmol g_x^{-1} h⁻¹)	7.08 ± 0.05	15.70 ± 0.13	14.53 ± 0.28	7.03 ± 0.10	14.98 ± 0.12	14.16 ± 0.50
$q_{glycerol}$ (mmol g_x^{-1} h⁻¹)	0.59 ± 0.01	0.68 ± 0.00	0.59 ± 0.00	0.53 ± 0.00	0.58 ± 0.02	0.55 ± 0.03
q_{CO2} (mmol g_x^{-1} h⁻¹)	7.85 ± 0.06	15.91 ± 0.09	15.36 ± 0.33	7.32 ± 0.12	15.36 ± 0.05	14.88 ± 0.39
Residual sugar (g L⁻¹)	0.16 ± 0.03	2.87 + 0.16	0.11 ± 0.00	0.93 ± 0.05	1.02 ± 0.02	0.12 ± 0.02
Carbon recovery (%)	96.4 ± 0.1	99.0 ± 1.1	98.4 ± 0.1	98.3 ± 1.4	99.8 ± 0.0	98.7 ± 1.2
Actual dilution rate (h⁻¹)	0.071 ± 0.002	0.071 ± 0.001	0.071 ± 0.001	0.071 ± 0.004	0.071 ± 0.000	0.070 ± 0.001

Development of a 'sugar-negative' *S. cerevisiae* strain devoid of all hexose transport and disaccharide transport and hydrolysis

The increased ethanol yields of strains expressing hexose-proton symporters (Table 5.3) could be of relevance to industrial ethanol production processes. In addition to (corn-derived) glucose, the disaccharide sucrose is widely used as sugar substrate for bioethanol production, especially in Brazilian sugar-cane based ethanol production plants (Renewable Fuels Association, 2021). Therefore, we aimed to investigate whether the combined expression

of a glucose-proton symporter with a fructose-proton symporter also allowed for an increased ethanol yield on sucrose, similar to what was achieved on glucose and fructose (Table 5.3). For this strategy, sucrose should exclusively be hydrolyzed extracellularly, after which the resulting monosaccharides are taken up by proton coupled transporters. To prevent the uptake and intracellular hydrolysis of sucrose, a platform strain was required that is devoid of all genes involved in sucrose transport and hydrolysis, on top of the absence of all native hexose transporter genes. Therefore, all hexose transporter genes were deleted in the previously constructed 'sucrose-negative' strain IMK698 (*suc⁰*) (Marques *et al.*, 2018a) using a CRISPR-Cas9 based toolkit developed for the construction of a hexose transporter-deficient strain (Wijsman *et al.*, 2018). In IMK698, consumption of maltose and sucrose is completely abolished by deletion of all disaccharide transport and hydrolysis genes, whereas the strategy used by Wijsman *et al.* (2018) results in a strain that is unable to consume glucose, fructose and galactose (*hxt⁰*). A combination of these two strategies resulted in the 'sugar-negative' strain IMK1010 (*sugar⁰*), which contained deletions in 23 transporter genes and 9 hydrolysis genes. Growth of IMK1010 was compared to that of the previously constructed strains IMX1812 (*hxt⁰*) and IMK698 (*suc⁰*) and their parental strains CEN.PK2-1C and CEN.PK102-3A to test its ability to grow on any of the relevant sugar substrates (Figure 5.2). Indeed, growth of IMK1010 was only observed on SM with ethanol and glycerol, whose transport and conversion are not dependent on any of the deleted genes, whereas growth on glucose, fructose, galactose, sucrose and maltose was absent.
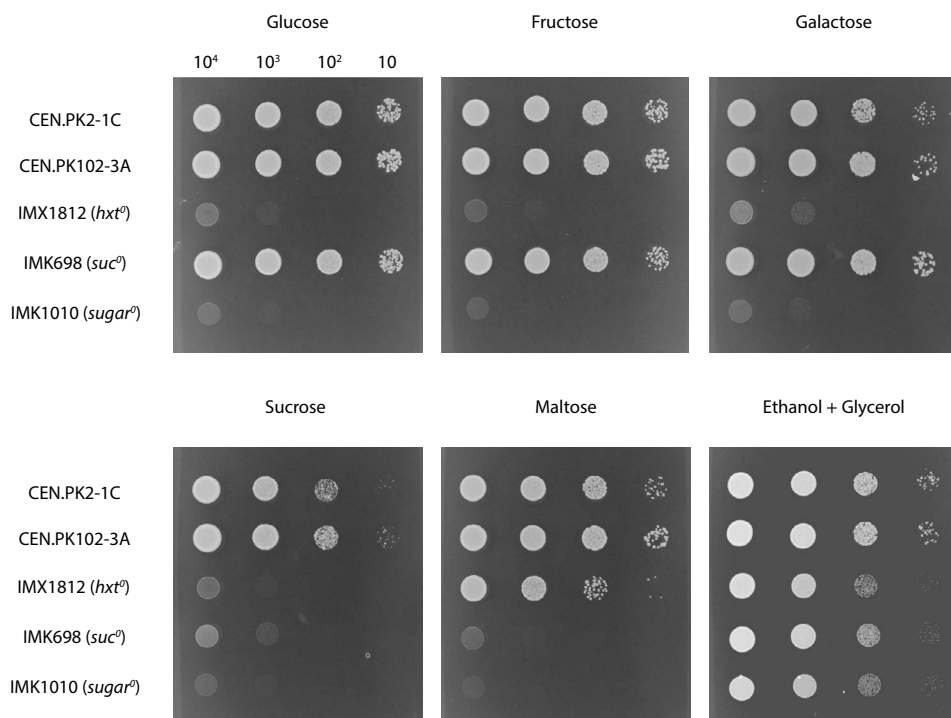
Figure 5.2: Growth of hexose transport-negative strain IMX1812, sucrose-negative strain IMK698 and sugar-negative strain IMK1010 and their ancestors (CEN.PK2-1C and CEN.PK102-3A) on SM with 20 g L⁻¹ glucose, fructose, galactose, sucrose or maltose, or 2% (v/v) ethanol and 2% (v/v) glycerol. Pictures were taken after two days of incubation for the plates with glucose, fructose, maltose and sucrose, after three days of incubation for the plate with galactose and after eight days of incubation for the plate with ethanol and glycerol, all at 30 °C.

Table 5.4: Growth characteristics of IMZ785 and IMS1215 in sucrose-limited anaerobic steady state chemostat cultures at a dilution rate of 0.1 h^{-1}. The maximum specific growth rate (μ_{max}) was determined based on measurements of the CO_2 concentration in the reactor off-gas during the preceding batch phase. Biomass-specific production and consumption rates are depicted as q$_{metabolite}$. The carbon recovery represents the percentage of the carbon entering the reactor system via the medium that could be traced back in biomass, products and residual substrate. The data represent average values and mean deviations obtained from duplicate experiments.

Strain	IMZ785	IMS1215
Relevant genotype	*HXT5*	*HGT1 + FSY1*
Carbon source	Sucrose	Sucrose
μ_{max} (h^{-1})	0.28 ± 0.00	0.15 ± 0.00
Biomass yield (g$_x$ g$_{hexose\ eq}^{-1}$)	0.088 ± 0.005	0.047 ± 0.000
Ethanol yield (mol mol$_{hexose\ eq}^{-1}$)	1.51 ± 0.00	1.76 ± 0.02
q_s (mmol g$_x^{-1}$ h^{-1})	6.41 ± 0.43	11.9 ± 0.23
$q_{ethanol}$ (mmol g$_x^{-1}$ h^{-1})	9.71 ± 0.63	20.9 ± 0.19
$q_{glycerol}$ (mmol g$_x^{-1}$ h^{-1})	0.86 ± 0.08	0.85 ± 0.02
q_{CO2} (mmol g$_x^{-1}$ h^{-1})	10.1 ± 0.76	20.2 ± 0.40
Residual sugar (g L^{-1})	0.40 ± 0.01 (glucose) 0.56 ± 0.07 (fructose)	0.70 ± 0.00 (glucose) 4.86 ± 0.10 (fructose)
Carbon recovery (%)	95.8 ± 0.10	97.7 ± 0.45
Actual dilution rate (h^{-1})	0.102 ± 0.001	0.102 ± 0.002

Functional replacement of native sucrose metabolism with exclusively extracellular hydrolysis and proton-coupled hexose uptake

Next, the (predominantly) extracellular invertase gene *SUC2* was integrated under control of the strong, constitutive *TDH3* promoter, after which a plasmid carrying both *KmHGT1* and *SeFSY1* was introduced. *KmHGT1* and *SeFSY1* were selected since they appeared to exhibit the highest affinity for their respective sugar (Table 5.3) and, in contrast to *MAL11*, were not expected to have any affinity for sucrose. The resulting strain, IMZ783, was able to grow in SM with sucrose as the sole carbon source under aerobic conditions, but not under anaerobic conditions. Similar to the previous evolution with the single hexose-proton symporter-expressing strains, IMZ783 was evolved in duplicate SBRs on SM with 20 g L^{-1} sucrose, with a stepwise decreasing oxygen supply until growth under anaerobic conditions was achieved (Online Supplementary Information). From both reactors, single colonies were isolated, resulting in IMS1214 and IMS1215. To investigate whether the engineering strategy indeed led to an increased ethanol yield, IMS1215 (which was isolated first), was grown in anaerobic, sucrose-limited chemostats and compared to IMZ785, an isogenic *SUC2*-expressing strain that overexpressed *HXT5* instead of *KmHGT1* and *SeFSY1*. In the preceding batch phase, the maximum specific growth rates were estimated from the CO_2 concentration measurements in the off-gas. Since these estimated growth rates were 0.15 ± 0.00 h^{-1} for IMS1215 (*KmHGT1* and *SeFSY1*) and 0.28 ± 0.00 h^{-1} for IMZ785 (*HXT5*), the subsequent chemostats were operated at an identical dilution rate of 0.10 h^{-1}. For both strains, no residual sucrose was detected in the culture supernatant, and it appeared to be completely hydrolyzed to glucose and fructose. As expected for a strain in which hexose diffusion has been replaced with proton-coupled transport, the biomass yield of IMS1215 (*KmHGT1* and *SeFSY1*) was decreased by 46.6% compared to the *HXT5*-expressing reference strain (Table 5.4), which is close to the theoretical 50% decrease (Weusthuis *et al.*, 1993). This observation is in accordance with the biomass-specific rates of sucrose consumption, ethanol

production and CO_2 production, for which a fold-increase between 1.9 and 2.2 was observed. Consequently, the ethanol yield, which was predicted to increase by 16.2% (Supplementary Information), was increased from 1.51 to 1.76 mol ethanol mol hexose equivalent^{-1}, which is a 16.6% increase.

Mutations in overexpressed transporter genes enabled growth under anaerobic conditions

The strains expressing heterologous transporters that were constructed in this study were only able to grow under anaerobic conditions after applying evolutionary engineering. To investigate which mutations enabled anaerobic growth of the evolved strains, the genomes of single colony isolates IMS1058 (*MAL11*), IMS1059 (*KlFRT1*), IMS1060 (*SeFSY1*), IMS1061 (*KmHGT1*), IMS1214 (*KmHGT1* and *SeFSY1*, first reactor) and IMS1215 (*KmHGT1* and *SeFSY1*, second reactor) were sequenced, along with their parental strains (IMX2144 and IMZ783) to identify single

A

Strain	Transporter	Approximate no. of generations	Mutations in transporter
IMS1058	Mal11	217	-
IMS1059	KlFrt1	235	Frt1^{L256S}
IMS1060	SeFsy1	281	-
IMS1061	KmHgt1	136	-
IMS1214	SeFsy1 + KmHgt1	213	Hgt1^{F353S}
IMS1215	SeFsy1 + KmHgt1	255	Hgt1^{F353S}
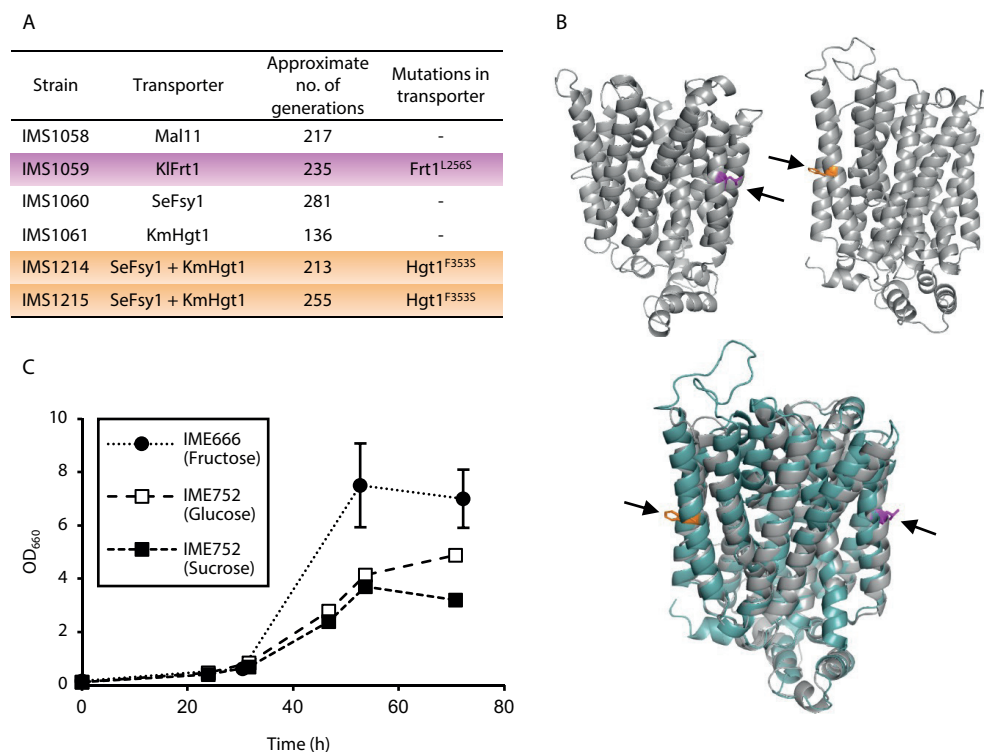
Figure 5.3: Evolution of strains expressing hexose-proton for growth under anaerobic conditions. A: Mutations that arose in transporters during evolution of hexose-proton symporter-expressing strains under anaerobic conditions. B: Structural models of KlFrt1 (top left) and KmHgt1 (top right) and both structures superimposed (bottom), highlighting the locations of amino acid residues that mutated during evolution in magenta and orange. C: Growth of reverse engineered strains IME666 (*KlFRT1^{T767C}*) in SM with 20 g L^{-1} fructose and IME752 (*KmHGT1^{T1058C}* and *SeFSY1*) in SM with 20 g L^{-1} sucrose or in SM with 20 g L^{-1} glucose in anaerobic shake flasks. Data represent average and mean deviation of two replicate experiments.

nucleotide polymorphisms (SNPs), insertions or deletions (indels) in coding sequences and copy number variations that occurred during the evolutions (Table S5.2). Strikingly, whereas only few genomic mutations were identified in open reading frames, a SNP was found in (one of) the introduced transporter gene(s) in three of the strains: a thymine to cytosine substitution in position 767 of *KlFRT1* in IMS1059 (*KlFRT1*^{T767C}), resulting in a leucine-to-serine substitution in amino acid position 256, and a thymine to cytosine substitution in position 1058 of *KmHGT1* in both IMS1214 and IMS1215 (*KmHGT1*^{T1058C}), resulting in a phenylalanine-to-serine substitution in amino acid position 353 (Figure 5.3A). The locations of these mutations were investigated through homology modelling of the corresponding protein structures, which predicted that both mutations occurred in the center of one of the membrane-facing transmembrane helices, at approximately the same height (Figure 5.3B). To exclude that other genomic mutations were essential for anaerobic growth of the evolved strains, the plasmids containing the mutated transporter genes were isolated and reintroduced into an unevolved strain background, which was IMX2144 (*hxt*^{0}) in case of the plasmid containing *KlFRT1*^{T767C} and IMX2719 (*sugar*^{0} *SUC2*) in case of the plasmid containing *FSY1* and *KmHGT1*^{T1058C}. Subsequently, the resulting *KlFRT1*^{T767C}-expressing strain IME666 was grown in anaerobic shake flasks on SM with fructose as the sole carbon source, whereas anaerobic growth of the *FSY1*- and *KmHGT1*^{T1058C}-expressing strain IME752 was tested in both SM with sucrose, in which the corresponding strain IMS1215 was evolved, and SM with glucose, which is the substrate of the mutated KmHgt1 transporter. After a relatively short lag phase, both strains exhibited anaerobic growth, and cultures were fully grown within 54 h (Figure 5.3), suggesting that the mutations in *KlFRT1* and in *KmHGT1* are largely responsible for the evolved phenotype of the corresponding strains.

5.4 Discussion

In this study, we successfully replaced facilitated transport of hexoses by proton-coupled transport. In the resulting strains, the energetic difference between these two modes of transport was apparent by the yield of biomass and ethanol on sugar, which were up to 46.6% decreased and up to 17.2% increased, respectively, and close to the theoretical predicted values. Ethanol yield on carbohydrates is one of the main performance indicators for industrial bioethanol production. With an annual production volume of ~99 billion liters of ethanol in 2020 (Renewable Fuels Association, 2021), even small improvements of the ethanol yield would have large economic benefits. Most of the annually produced bioethanol (~53%) originates from fermentation of corn starch-derived glucose in the USA (Renewable Fuels Association, 2021), for which the strategy tested in this work, with strains that depend on a single glucose-proton symporter for their hexose uptake could be relevant. Another ~30% is produced from sugarcane-derived sucrose in Brazil (Renewable Fuels Association, 2021), which prompted us to combine hexose-proton symport and extracellular hydrolysis in the sugar-negative strain. An additional advantage of this strategy is that the decrease in biomass yield also results in a lower yield of the by-product glycerol, which is formed to re-oxidize the 'surplus' of NADH that arises through biomass synthesis. It should be noted that the aforementioned beneficial effects of decreasing the ATP yield of dissimilation are growth rate dependent, since a larger fraction of sugar is dissimilated to meet growth-rate-independent maintenance requirements at the lower growth rates (Pirt, 1965). Consequently, in industrial batch processes, lowering the ATP yield would be most beneficial in fermentation phases where high growth rates are observed, whereas the effect decreases towards the end of the fermentation, when growth ceases due to high concentrations of ethanol (Thomas and Ingledew, 1992). Additionally, for industrial implementation, engineered yeast cells should be able to cope with high maintenance

5

energy requirements that arise due to such high ethanol concentrations and the presence of other inhibitors in the culture (Jansen *et al.*, 2017a; Monteiro *et al.*, 1994; Rosa and Sá-Correia, 1991; Thomas and Ingledew, 1992). Therefore, in addition to other practical considerations of efficient use of such engineered strains in industrial fermentations (van Aalst *et al.*, 2022), the expressed sugar transporters should allow for very high dissimilation rate for maintenance energy provision.

The strains in which heterologous transporters were introduced were unable to directly grow under anaerobic conditions. We hypothesize that an insufficient rate of ATP production might be underlying this absence of anaerobic growth in strains expressing *KmHGT1*, *KlFRT1* and *SeFSY1* for their sugar uptake. Although these strains exhibited reasonable growth rates (up to 0.23 h^{-1}) under aerobic conditions, the transition from respiration to fermentation, which in these strains corresponds to a transition from an estimated 15 ATP to 1 ATP per hexose equivalent, might have decreased the ATP production rate to below maintenance energy requirements. Unlike these strains, the *MAL11*-expressing strain IMZ756, exhibited aerobic fermentation without evolution (Figure 5.1B), which suggests that 1) there is a smaller transition of the ATP yield between aerobic and anaerobic conditions for this strain, since under aerobic conditions, already part of the overall sugar dissimilation yields 1 ATP; and therefore 2) this strain should have exhibited a substantially higher sugar uptake rate than the other strains to achieve its similar aerobic growth rate. The latter could be confirmed in future experiments by quantifying the biomass-specific sugar consumption rates of these strains in aerobic batch bioreactor cultures. Such a high sugar uptake rate might have enabled IMZ756 (*MAL11*) to grow directly under anaerobic conditions, without evolution. Moreover, since *MAL11* is the only endogenous transport gene tested, these observations might point out a difficulty in the functional expression of heterologous transporters in the anaerobic membrane of *S. cerevisiae*, which has a lower unsaturated fatty acid and ergosterol content than the membrane of aerobically grown *S. cerevisiae* (Jollow *et al.*, 1968; Snoek and Steensma, 2007; Steels *et al.*, 1994). Especially for transporters such as *KmHGT1* and *KlFRT1,* which originate from obligate aerobic yeasts (Merico *et al.*, 2007; Snoek and Steensma, 2006), their functional expression under anaerobic conditions could have been impacted by differences in membrane composition. Possibly, the evolution of the *KmHGT1*-, *KlFRT1*- and *SeFSY1*-expressing strains allowed for selection of mutant cells with an increased sugar uptake rate, thereby enabling a sufficient supply of free energy under anaerobic conditions. In case of IMS1059 (*KlFRT1*), IMS1214 and IMS1215 (both expressing *KmHGT1* and *SeFSY1*), mutations in transporter sequences probably underlie such an increased sugar uptake rate, since their reintroduction in an unevolved strain background allowed for immediate anaerobic growth. Both mutations led to the substitution of a hydrophobic residue (leucine or phenylalanine) in the center of one of the transmembrane helices to a (polar) serine residue (Figure 5.3B). Further investigation of the molecular mechanism of these mutations could provide valuable information to facilitate the introduction of heterologous transporters. From whole genome sequencing data of IMS1060 (*SeFSY1*) and IMS1061 (*KmHGT1*) no clear leads could be found in SNPs and indels in coding regions or copy number variations that could be related to the evolved phenotype, and thus, the mutations underlying their evolved phenotype was not investigated via reverse engineering. The absence of mutations in *KmHGT1* in IMS1061 was especially striking since this gene was mutated in both IMS1214 and IMS1215 (*KmHGT1* and *SeFSY1* combined). Potentially, mutations outside of open reading frames, which were not analyzed in this research, led to changes in gene expression that allowed for anaerobic growth, which could be further elucidated in future work by transcriptome analysis.

5

Since transport by proton symporters is not only driven by the concentration gradient of the solute, but also by the proton motive force, these transporters allow for the intracellular accumulation of sugars, and therefore theoretically allow for growth at lower extracellular sugar concentrations. This property can be advantageous in industrial fermentations (not necessarily bioethanol), as it decreases the likelihood of culture contamination by competing microorganisms that require higher extracellular sugar concentrations (Beckner *et al.*, 2011; Tiukova *et al.*, 2014; Tiukova *et al.*, 2019). Another advantage for sucrose-grown cultures is that expression of proton coupled hexose transporters could prevent the accumulation of fructose at the end of cultivation processes, which often occurs due to preferred uptake of glucose over fructose by wild type *S. cerevisiae* (Beato *et al.*, 2016; Berthels *et al.*, 2004; Wu *et al.*, 2010). The residual glucose and fructose concentrations that were measured in this study for strains expressing proton symporters were not (substantially) lower than previously measured for reference strain CEN.PK113-7D (Diderich *et al.*, 1999), indicating that the kinetics of glucose and fructose transport were not improved by expression of the transporters that were investigated in this study. High-throughput screening of heterologous proton symporters may lead to the identification of transporters with better kinetics when expressed in *S. cerevisiae*. Alternatively, another evolutionary engineering approach could be applied, in which prolonged cultivation of the strains constructed in this study in continuous cultures under substrate limitation may lead to selection of mutants with improved performance. This approach has been successfully applied to improve the uptake of the disaccharides sucrose (Basso *et al.*, 2011b) and maltose (Jansen *et al.*, 2004).

To the best of our knowledge, the platform strain IMK1010 (*sugar^0*) constructed in this study is the first reported *S. cerevisiae* strain that is completely devoid of all sugar transporters and disaccharide hydrolases. This strain can form a valuable basis for thorough investigation of the function of individual sugar transporters, especially for those with a broad substrate range. The absence of any other sugar transport activity allows for complementation studies and for the conductance of transport assays without 'background signal'. In addition, this strain can be used in engineering strategies aimed at substrate liberation and uptake and associated (directed) evolution strategies. For instance, IMK1010 could be used to combine extracellular maltose hydrolysis and glucose-proton symport to alter the efficiency of maltose dissimilation, which could be of relevance in the baking and beer brewing industry (Dequin, 2001).

Concluding, we showed that the replacement of the hexose transporters with a facilitated diffusion mechanism in *S. cerevisiae* by glucose-proton symporters (*MAL11* or *KmHGT1*) or fructose-proton symporters (*KlFRT1* or *SeFSY1*) results in a substantial (~17%) increase in the ethanol yield on glucose and fructose, respectively, at the cost of biomass synthesis. Although the expression of heterologous transporters could initially only restore aerobic growth on the corresponding hexose in an *hxt^0* strain background, anaerobically-growing mutants for each of the tested transporters were obtained via evolutionary engineering. By combining the expression of an extracellular sucrose hydrolase, the glucose-proton symporter *KmHGT1* and fructose-proton symporter *SeFSY1* in a novel platform strain, devoid of all native hexose transporters and disaccharide transporters and hydrolases, a similar increase in ethanol yield and decrease in biomass yield was obtained in anaerobic cultures grown on sucrose. These results show the potential of engineering the energy coupling mechanism of sugar transport in strains used for industrial bioethanol production. Moreover, the novel 'sugar-negative' platform strain constructed in this study could be valuable for the development of yeast cell factories for other bioproducts or investigation of endogenous and heterologous sugar

5

transporters in future studies, especially those focusing on transport proteins that mediate the uptake of multiple different types of sugars.

5.5 Acknowledgements

5.6 Supplementary information

Theoretical analysis of impact of decreased ATP yield on ethanol yield

When the ethanol yield on sugar of a reference strain is known, a prediction can be made of the ethanol yield of a strain that, compared to that reference strain, conserves less ATP per mol of dissimilated substrate, as previously described by Basso *et al*. (2011). In this study, strains were engineered in which the net ATP yield of dissimilation was decreased, either from 2 to 1 ATP per hexose, or from 4 to 2 ATP per sucrose (which comes down to 2 to 1 ATP per hexose equivalent), by replacing the facilitated diffusion mechanism of hexoses by proton symport. Consequently, for every hexose entering the cell, an additional hexose equivalent should be completely fermented to ethanol to supply the energy required for transport, which results in a 50% decreased biomass yield compared to a strain with a facilitated diffusion mechanism. The ethanol yield of a strain with proton symport mechanism can be predicted according to Equation 5.1:

$$Y_{EtOH,1ATP} = 0.5*Y_{EtOH,2ATP} + 0.5*Y_{EtOH,max} \qquad (5.1)$$

In Equation 1, $Y_{EtOH,1ATP}$ is the predicted ethanol yield for strains that exclusively take up hexoses by proton symport, $Y_{EtOH,2ATP}$ the measured ethanol yield for a reference strain that takes up hexoses via facilitated diffusion (both in mol ethanol mol hexose equivalent^{-1}) and $Y_{EtOH,max}$ the ethanol yield that is obtained upon complete dissimilation via alcoholic fermentation, in this case 2 mol ethanol mol hexose equivalent^{-1}

Table S5.1: Primers used in this study

Primer name	Sequence (5'-3')
1738	GCAGGCAAGATAAACGAAGG
1742	GGTCGCCTGACGCATATACC
1743	TAAGGCCGTTTCTGACAGAG
2873	TCAGACTTCTTAACTCCTGTAAAAACAAAAAAAAAAAAAAGGCATAGCAATAAGCTGGAGCTCATAGCTTC
3093	ACTATATGTGAAGGCATGGCTATGGCACGGCAGACATTCCGCCAGATCATCAATAGGCACCTTCGTACGCTGCAG-GTCGAC
3755	CACTTGTTCGCTCAGTTCAG
4653	GTGCCTATTGATGATCTGGCGGAATGTCTGCCGTGCCATAGCCATGCCTTCACATATAGTCCGCAAATTAAAG-CCTTCGAG
5542	CTATGCTACAACATTCCAAAATTTGTCCCAAAAAGTCTTTGGTTCATGATCTTCCCATACGCATAGGCCACTAGTG-GATCTG
6005	GATCATTTATCTTTCACTGCGGAGAAG

6486	TTTTAGTTTATGTATGTGTTTTTTGTAGTTATAGATTTAAGCAAG
7812	TCATGTAATTAGTTATGTCACGCTTACATTC
7999	GGATCCACTAGTTCTAGAAAACTTAGATTAG
9355	TGTAAATATCTAGGAAATACACTTGTGTATACTTCTCGCTTTTCTTTTATTTTTTTTTGTAGTTTATCATTAT-CAATACTCGCCATTTC
9356	TTTACAATATAGTGATAATCGTGGACTAGAGCAAGATTTCAAATAAGTAACAGCAGCAAAGTGTGGAAGAAC-GATTACAACAG
9522	CCTACTTTTTTCCGAACATCTTCTTGTAAAATGGTTGATCATCATGCATTAGATCATCAGTCTTTCTTTACCTCTA-ATATATTCTTTTTTCTAGAAAAATAATATTTTTTGCTGGTTTTA
9523	TAAAACCAGCAAAAAATATTATTTTTCTAGAAAAAAGAATATATTAGAGGTAAAGAAAGACTGATGATCTAATG-CATGATGATCAACCATTTTACAAGAAGATGTTCGGAAAAAAGTAGG
9525	AGCGGGATACAGAAAAAGAAGATATTTCCCATTTCAAAAAGGCTCTACTATATCCTTACCAAGACTCTAGGGG-GATCGCC
9526	GGTCATTATACTGACCGCCATTATAATGACTGTACAACGACCTTCTGGAGAAAGAAACAAGCGCCTCG-TATCTTTAATG
9528	TTACTATCAAGATACCGTAGAAAAGAAAAAGAACCGGGGATGAATAATAACAAAACGGGCGAGATTATACTTA-AACTAGCACTGATTTTTTTAAGGCTAATGGCTACTAATACTTTAATA
9529	TATTAAAGTATTAGTAGCCATTAGCCTTAAAAAAATCAGTGCTAGTTTAAGTATAATCTCGCCCGTTTTGTTATTAT-TCATCCCCGGTTCTTTTTCTTTTCTACGGTATCTTGATAGTAA
9532	TATTTTAGATTGCATTTTTTATAAGTCACTTTTAGTTAGCTCAGAACGCCAGCAAAAACCCCCGTCAGGACTAC-CAAAATATAACAAAGTATTGATTATCGTCAACGCTTTATAGATCAC
9533	GTGATCTATAAAGCGTTGACGATAATCAATACTTTGTTATATTTTGGTAGTCCTGACGGGGGTTTTTGCTGGC-GTTCTGAGCTAACTAAAAGTGACTTATAAAAAATGCAATCTAAAATA
9535	TTGGAAAAAATAATCATTGCACAATTGAGTACTAAAAGCTTTCGTATCTTACCCAATATCTCTTCCGGTTTTTAGTA-ACTGGAAAAAAATACATGAACTTAATTATTTATTATATACAAT
9536	ATTGTATATAATAAATAATTAAGTTCATGTATTTTTTTCCAGTTACTAAAAACCGGAAGAGATATTGGGTAAGATAC-GAAAGCTTTTAGTACTCAATTGTGCAATGATTATTTTTTCCAA
9538	TCATCAATTTCGGCTGTCTGGATGGCGACAACGAGAGGAAGCTTGCTTGCCATGATAGGAATCAGGCAATGTA-AGGTCAAACTTGTACCATCGACATATATAATGCTTTGAGATATAAGT
9539	ACTTATATCTCAAAGCATTATATATGTCGATGGTACAAGTTTGACCTTACATTGCCTGATTCCTATCATGGCAAG-CAAGCTTCCTCTCGTTGTCGCCATCCAGCACAGCCGAAATTGATGA
9542	TTACATAATCATTTCTCCGTGCGAGTTATAAGTGCTTTTCTCGTGCATCCCTTGGCACTTTCTTCTAGTTTTCGGTA-AATTGGTAAAAAAGCAAAAAAAAAAATTGACGAAACTAATTCT
9543	AGAATTAGTTTCGTCAATTTTTTTTTTTGCTTTTTTACCAATTTACCGAAAACTAGAAGAAAGTGCCAAGGGATG-CACGAGAAAAGCACTTATAACTCGCACGGAGAAATGATTATGTAA
9547	CCTTTTACCAATTTAATAATGTCTAGGATTTATCGCTGTACTGCCAAATGCTTCACAACGGAGTGCATAT-GTTTGTCTTGATAGGCAACATTGTATATTATAGTTTACATAATAATGTGT
9548	ACACATTATTATGTAAACTATAATATACAATGTTGCCTATCAAGACAAACATATGCACTCCGTTGTGAAGCATTTGG-CAGTACAGCGATAAATCCTAGACATTATTAAATTGGTAAAAGG
9551	ACTAACAAAGAATTTGTTAACGTATTCTTAGGAAGTAAAGTACTTCAATTATTGCTAGAACAGTAACTAAGTGGC-CGTGAGGACTGACCACATTTTCTTTACATACAGTAAAGTAAATAA
9552	TTATTTACTTTACTGTATGTAAAGAAAATGTGGTCAGTCCTCACGGCCACTTAGTTACTGTTCTAGCAATAATT-GAAGTACTTTACTTCCTAAGAATACGTTAACAAATTCTTTGTTAGT
9555	GATTCCACCTTAAAAGACGACAATAGTAACTTTGTCCTTGATCTGGGTTACTAAATCAGCACATAGGTCCACTT-GAGTGCTTATGGAAGATCCTTAAAAATGCATTTCCAGGAACGTAAC
9556	GTTACGTTCCTGGAAATGCATTTTTAAGGATCTTCCATAAGCACTCAAGTGGACCTATGTGCTGATTTAGTAAC-CCAGATCAAGGACAAAGTTACTATTGTCGTCTTTTAAGGTGGAATC
9563	GGATTGAAAATTTGGTGTTGTGAATTGCTCTTCATTATGCACCTTATTCAATTATCATCAGATAACATGCTCTGC-CATCCTTTGTTCACCGAGCAAAATTAAAAACGCAAATGAATTGT
9564	ACAATTCATTTTGCGTTTTTAATTTTGCTCGGTGAACAAAGGATGGCAGAGCATGTTATCTGATGATAATTGAATA-AGGTGCATAATGAAGAGCAATTCACAACACCAAATTTTCAATCC
9719	TCAAGAACTTGTCATTTGTATAG
10305	GGTTAATTGCGCGCTTGGCGTAATCATGGTCATAGCTGTTTAGTGTGAGCGGGATTTAAACTGTGAGG

10306	GTTGTGTGGAATTGTGAGCGGATAACAATTTCACACAGGACAGTATAGCGACCAGCATTC
10307	AACAGCTATGACCATGATTA
10308	TCCTGTGTGAAATTGTTATC
10519	TGCGCATGTTTCGGCGTTCGAAACTTCTCCGCAGTGAAAGATAAATGATCTTTTCTTGAAAGCTTTGCAG-GTTTTAGAGCTAGAAATAGCAAGTTAAAATAAGGCTAGTCCGTTATCAAC
10521	AATGTGATTTCTTCGAAGAATATACTAAAAAATGAGCAGGCAAGATAAACGAAGGCAAAGTGACACCGAT-TATTTAAAGCTGCAGCATACGATATATATACATGTGTATATATGTATACC
10522	GGTATACATATATACACATGTATATATATCGTATGCTGCAGCTTTAAATAATCGGTGTCACTTTGCCTTC-GTTTATCTTGCCTGCTCATTTTTTAGTATATTCTTCGAAGAAATCACATT
11826	TGCGCATGTTTCGGCGTTCGAAACTTCTCCGCAGTGAAAGATAAATGATCTATCAACAAAATACTCCAATGTTTTA-GAGCTAGAAATAGCAAGTTAAAATAAG
12743	TGCGCATGTTTCGGCGTTCGAAACTTCTCCGCAGTGAAAGATAAATGATCACCGGATTCAGTCGTCACT-CAGTTTTAGAGCTAGAAATAGCAAGTTAAAATAAG
13617	CTAGCATACAAGTTAGAATAAATAAAAAATAGAAAAATAGAACATAGAAAGTTTTAGACCTTCATACACAACTCA-CAAATCATATTTTGTAATTTACTTAAGAAAGCATTTTGCGGGGTT
13618	AACCCCGCAAAATGCTTTCTTAAGTAAATTACAAAATATGATTTGTGAGTTGTGTATGAAGGTCTAAAACTTTC-TATGTTCTATTTTTCTATTTTTTATTTATTCTAACTTGTATGCTAG
15985	CTTGCTCATTAGAAAGAAAGCATAGCAATCTAATCTAAGTTTTCTAGAACTAGTGGATCCATGTCTAGTAATCT-GTCTGAAA
15986	CGGTTAGAGCGGATGTGGGGGGAGGGCGTGAATGTAAGCGTGACATAACTAATTACATGATTAAATAGATTTAC-GGTTACCAG
15987	CTTGCTCATTAGAAAGAAAGCATAGCAATCTAATCTAAGTTTTCTAGAACTAGTGGATCCATGTCACATGTTAACG-CGTCGT
15988	CGGTTAGAGCGGATGTGGGGGGAGGGCGTGAATGTAAGCGTGACATAACTAATTACATGATTAATAACT-CAATTGGCCCTTCTTC
16387	CTTGCTCATTAGAAAGAAAGCATAGCAATCTAATCTAAGTTTTCTAGAACTAGTGGATCCATGTCGGAACTT-GAAAACGC
16388	CGGTTAGAGCGGATGTGGGGGGAGGGCGTGAATGTAAGCGTGACATAACTAATTACATGATTCTACAAGAGAT-TATTTTTCTTTAGTG
16508	CTTGCTCATTAGAAAGAAAGCATAGCAATCTAATCTAAGTTTTCTAGAACTAGTGGATCCATGTCATTGAAAGA-CAAGATTTTG
16509	CGGTTAGAGCGGATGTGGGGGGAGGGCGTGAATGTAAGCGTGACATAACTAATTACATGATTAGTTAGAGTTT-GAGTTTGAGTTG
17347	TTAAATCTATAACTACAAAAAACACATACATAAACTAAAAATGTCACATGTTAACGCGTCGT
17348	ACTACAATATAAAAAAACTATACAAATGACAAGTTCTTGATGATTAATAACTCAATTGGCCCTTCTTC
17349	TTAAATCTATAACTACAAAAAACACATACATAAACTAAAAATGTCTAGTAATCTGTCTGAAA
17350	ACTACAATATAAAAAAACTATACAAATGACAAGTTCTTGATTAAATAGATTTACGGTTACCAG
17584	ACACCGAACTTAGTTTCGACGGATTCTAGAACTAGTAATATGCTTTTGCAAGCTTTCCTTTTCCTTTTG
17585	CTTTAAGAATGCCTTAGTCATGCCAACCCTCGAGGTCGACCTATTTTACTTCCCTTACTTGGAACTTGTCAATG
17586	ATTACTAGTTCTAGAATCCGTCGAAACTAAGTTC
17587	GTCGACCTCGAGGGTTGG

Evolution of hexose proton symporter-expressing strains for anaerobic growth

A separate excel file is available with the online article.

5

Table S5.2: Mutations found in strains evolved for anaerobic growth via whole genome sequencing. Gene annotations were acquired from the *Saccharomyces* Genome Database.

Strain	Mutated gene or region	Nucleotide change	Amino acid change	Gene annotation
IMS1058 (*MAL11*)	*YPR202w*	G653A	S218N	Putative protein of unknown function; similar to telomere-encoded helicases
	SED4	A1457AAAG	F486FS (insertion)	Integral ER membrane protein that stimulates Sar1p GTPase activity
	SWR1	G1287T	R429S	Swi2/Snf2-related ATPase; catalytic subunit of SWR1 complex
	RGT2	G2191A	D731N	Plasma membrane glucose sensor that regulates glucose transport
	HRK1	G315GTGT	S105SS (insertion)	Protein kinase; implicated in activation of the plasma membrane H(+)-ATPase Pma1p in response to glucose metabolism
IMS1059 (*KlFRT1*)	*KlFRT1*	T767C	L256S	Fructose proton symporter
	ECM21	G972GT (frameshift)	N.A.	Alpha-arrestin, ubiquitin ligase adaptor for Rsp5p; regulates starvation- and substrate-induced Ub-dependent endocytosis of select plasma membrane localized amino acid transporters
	ATG1	C1130T	A377V	Protein serine/threonine kinase; required for vesicle formation in autophagy and the cytoplasm-to-vacuole targeting (Cvt) pathway
IMS1060 (*SeFSY1*)	Duplication of Chr. I			
	MAL23	C935T C936A C938G A939C	T312I T313S	Maltose-responsive transcription factor
	DTD1	C436T	L146F	D-Tyr-tRNA(Tyr) deacetylase
	NFT1	C1591G	L531V	Putative transporter of the MRP family
	WHI2	A861AG (frameshift)	N.A.	Negative regulator of TORC1 in response to limiting leucine
	Duplication of Chr. VIII	N.A.	N.A.	N.A.
IMS1061 (*KmHGT1*)	*DOS2*	G903 GGACGACGACGAC	K301KDDDD (insertion)	Protein of unknown function; (GFP)-fusion protein localizes to the cytoplasm
IMS1214 (*KmHGT1 + SeFSY1*)	*KmHGT1*	T1058C	F353S	Glucose proton symporter
	VAC8	C1190T	S397F	Vacuole-specific Myo2p receptor and Myo2p-Vac17p-Vac8p transport complex subunit required for vacuolar inheritance
	PSK2	G3019A	V1007I	PAS-domain containing serine/threonine protein kinase; regulates sugar flux and translation in response to an unknown metabolite.
IMS1215 (*KmHGT1 + SeFSY1*)	*KmHGT1*	T1058C	F353S	Glucose proton symporter
	SED4	T1331A	Q444L	Integral ER membrane protein that stimulates Sar1p GTPase activity

5
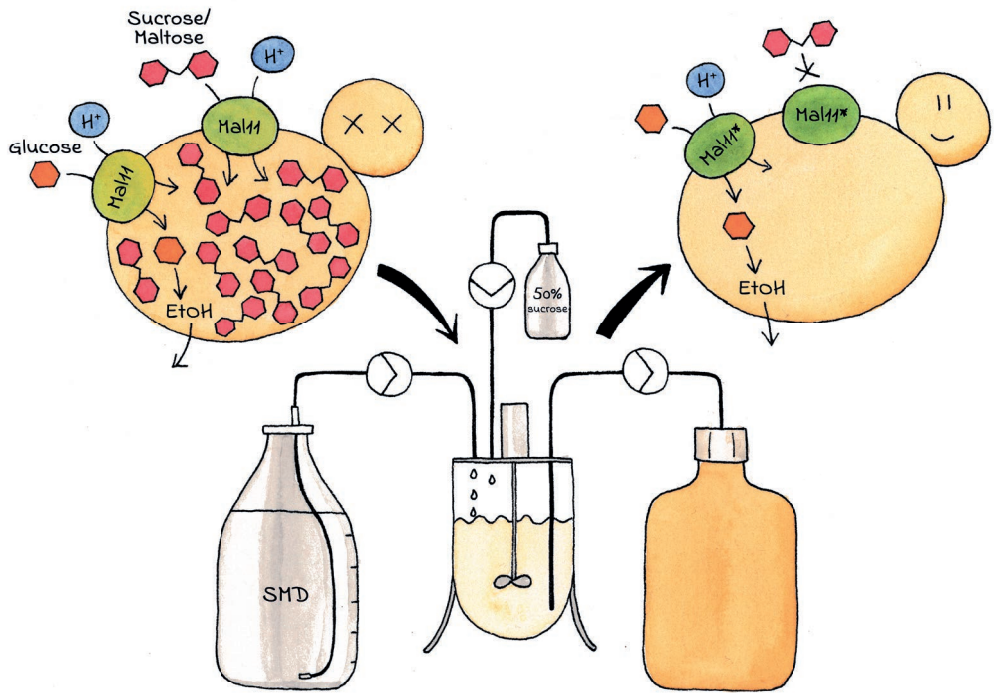
Chapter 6

Novel evolutionary engineering approach
to alter substrate specificity of disaccharide
transporter Mal11 in *Saccharomyces cerevisiae*

Sophie C. de Valk, Robert Mans

Abstract

A major challenge in the research of transport proteins is to understand how single amino acid residues contribute to their structure and biological function. Amino acid substitutions that provide a selective advantage in adaptive laboratory evolution experiments can provide valuable hints at their role in transport proteins. In this study, we applied an evolutionary engineering strategy to alter the substrate specificity of the proton-coupled disaccharide transporter Mal11 in *Saccharomyces cerevisiae*, which has affinity for sucrose, maltose and glucose. Introduction of *MAL11* in a strain devoid of all other sugar transporters and disaccharide hydrolases restored growth on glucose, but rendered the strain highly sensitive to the presence of sucrose or maltose. Evolution in glucose-limited continuous cultures with pulse-wise addition of a concentrated sucrose solution at increasing frequency resulted in the enrichment of spontaneous mutant cells that were less sensitive to the presence of sucrose and maltose. Sequence analysis showed that in each of two independent evolution lines, two overlapping and one unique non-synonymous single nucleotide mutation(s) occurred in *MAL11*, which were found responsible for the disaccharide-insensitive phenotype via reverse engineering. We hypothesize that the resulting amino acid changes lower the binding affinity of Mal11 for disaccharides without impacting its ability to transport glucose. Our work demonstrates how laboratory evolution with proton-motive force-driven uptake of a non-metabolizable substrate can be a powerful tool to study transport proteins by providing novel insights into the role of specific amino acid residues in the transport function of Mal11.

6

6.1 Introduction

Over the course of evolution, a myriad of sugar transporters have emerged with diverse mechanisms, kinetics, regulation and substrate specificities (Chen *et al.*, 2015; Saier, 2016). Whereas some transporters are highly specific towards one sugar substrate, such as the fructose-specific Ffz1 from *Zygosaccharomyces rouxii* (Leandro *et al.*, 2011), others are able to mediate the uptake of multiple sugars, such as Mal11 from *Saccharomyces cerevisiae* (Han *et al.*, 1995; Stambuk *et al.*, 1999; Wieczorke *et al.*, 1999). Knowledge on the three-dimensional organization of amino acid residues and how they interact to bind and translocate substrates is highly relevant to understand how transporters with broad substrate range evolved into specific transporters (or vice versa) in nature. Since sugars are important substrates of industrial biotechnology, their transporters are also relevant targets in engineering strategies for the improvement of microbial cell factories (Agrimi and Steiger, 2021; Nijland and Driessen, 2020; Nogueira *et al.*, 2020; Soares-Silva *et al.*, 2020). Ideally, transport proteins (and thus their encoding genes) can be designed at will, to obtain strains with unrestricted transport of the desired substrate without undesired inhibition or competition by other molecules. This scenario requires extensive knowledge on the structure and mechanism of transport proteins and the function of individual amino acid residues on their overall activity.

The steadily increasing number of resolved protein structures through methods such as X-ray crystallography has contributed to our understanding of the tertiary structure of membrane proteins (Moraes *et al.*, 2014; von Heijne, 2006). Still, compared to soluble proteins, membrane protein structures are rather underrepresented in the protein data bank, partially due to the difficulty of membrane protein crystallization (Grisshammer and Tate, 2009). In addition, computational methods for protein structure prediction, based on the crystal structure of a homologous protein, have provided valuable insights (Arinaminpathy *et al.*, 2009), and promising results are now obtained using the AI system AlphaFold (Jumper *et al.*, 2021). Knowledge on the role of individual amino acid residues can be acquired by studying mutant transporter variants acquired via (targeted) mutagenesis (Packer and Liu, 2015; Yuen and Liu, 2007) or adaptive laboratory evolution (ALE) (Dragosits and Mattanovich, 2018; Mans *et al.*, 2018; Sandberg *et al.*, 2019). For the latter approach, cultivation conditions are carefully designed to allow for the enrichment of mutants with a desired phenotype. By analyzing the genome of evolved strains, mutations can be identified that underlie the evolved phenotype, and (point) mutations in transport proteins hints at an important role of specific amino acid residues for transport function. This method is especially powerful when the investigated transport process is essential for growth (Packer and Liu, 2015; Sandberg *et al.*, 2019). For example, ALE has been applied to improve kinetics of proteins that mediate the uptake of an essential substrate by selecting for mutants with an improved growth rate through serial propagation in batch conditions (Apel *et al.*, 2016; Henderson *et al.*, 2021; Lim *et al.*, 2021; Marques *et al.*, 2018b). Alternatively, transporters with improved affinity can be obtained by prolonged cultivation in substrate-limited continuous cultures (Brickwedde *et al.*, 2017; Jansen *et al.*, 2004). Some evolutionary engineering approaches were aimed at specializing transporters with broad substrate affinity for one of its substrates. For example, Hxt transporters in *S. cerevisiae*, which transport glucose and xylose (albeit with moderate affinity and glucose inhibition), were specialized for xylose transport by evolving a hexokinase-deficient strain for growth on xylose in the presence of glucose (Farwick *et al.*, 2014; Li *et al.*, 2016; Nijland *et al.*, 2014). The resulting mutant transporter variants were found to contain amino acid substitutions that decreased or abolished the affinity of the transporter for glucose but not for xylose. However, complete

6

abolishment of glucose affinity was accompanied by a ~60% reduction of the V_{max} for xylose.

A more stringent selection for specialized transporters could be achieved if transport of the undesired substrate can be made toxic to the cells (counter-selection), while transport of the desired substrate provides an evolutionary benefit. Transport of a metabolizable sugar is usually not toxic, but exceptions can be found when sugar uptake is coupled to the uptake of a proton (proton symport). Uptake via such a proton symporter is not only driven by the concentration gradient of the sugar, but also by the chemical and electrical potential difference of the proton-motive force (pmf). At typical values of the pmf in *S. cerevisiae* (-150 to -200 mV (Cartwright *et al.*, 1986)), this driving force could enable a 1000-fold accumulation of sugar inside the cell. Such accumulation would lead to osmotic bursting of cells and therefore excessive substrate accumulation is prevented by regulation of transporters and enzymes that catalyze the intracellular degradation of the sugar. The importance of this regulation is demonstrated by the phenomenon referred to as 'substrate-accelerated cell death' which has for example been observed when a pulse of maltose was administered to prolonged, maltose-limited *S. cerevisiae* chemostat cultures (Jansen *et al.*, 2004; Postma *et al.*, 1990). The sudden switch from maltose-limited to maltose-excess conditions decreased culture viability by up to 70%, which was hypothesized to be due to uncontrolled, sudden and fast uptake of maltose and protons into the cells, leading to rapid acidification and an osmotic burst.

In this study, we investigated whether the proton-motive force could be employed to create a selective pressure against substrate uptake by proton coupled transporters. To this end, we introduced *MAL11*, which encodes a proton symporter with affinity for sucrose, maltose, and glucose (Han *et al.*, 1995; Stambuk *et al.*, 1999; Wieczorke *et al.*, 1999) as the sole sugar transporter gene in an *S. cerevisiae* strain that is not able to hydrolyze sucrose or maltose. Since these disaccharides are not metabolized, we expected that cells would suffer negative effects from their intracellular accumulation, which is 'forced' by the proton-motive force due to proton coupled uptake. By evolving this strain in glucose-limited chemostats with increasing addition of sucrose, we selected for mutants that were less sensitive to the presence of sucrose, while maintaining their ability to take up glucose. This evolution was followed by analysis of mutations and growth characterization of evolved and reverse engineered strains in medium with glucose, supplemented with various concentrations of sucrose or maltose.

6.2 Materials and methods

Strains and maintenance

All *Saccharomyces cerevisiae* strains used in this study are derived from the CEN.PK lineage (Entian and Kötter, 2007). For long term storage, glycerol was added to cells that were grown until late exponential phase, to obtain a final concentration of 30% (v/v) glycerol, after which 1 mL aliquots were stored at -80 °C. Plasmids were propagated in *Escherichia coli* XL1-Blue cells (Agilent, Santa Clara, CA, USA), which were also stored at -80 °C after addition of glycerol to a final concentration of 25% (v/v) to overnight cultures.

Molecular biology techniques

Plasmids were isolated from yeast strains using the Zymoprep Yeast Plasmid Miniprep II kit (Baseclear, Leiden, The Netherlands), after which 1 µL of this mixture was transformed,

according to the manufacturer's protocol, into XL1-Blue chemically competent *E. coli* cells (Agilent) for plasmid propagation. Plasmids were isolated from *E. coli* cells using the GeneJET Plasmid Miniprep Kit (Thermo Fisher Scientific, Waltham, MA, USA). Transformation of *S. cerevisiae* strains was performed using LiAc/ssDNA/PEG, as previously described (Gietz and Woods, 2002). After transformation, single colonies were re-streaked three consecutive times to ensure an isogenic single cell line. For whole genome sequencing, genomic DNA was isolated from stationary *S. cerevisiae* cultures using the QIAGEN Blood & Cell Culture DNA Kit with 100/G Genomics-tips (Qiagen, Hilden, Germany) according to the manufacturer's protocol. Sanger sequencing of genes was performed using the Macrogen EZ-seq sequencing service (Amsterdam, the Netherlands) according to the provided instructions.

Strain construction

All *S. cerevisiae* strains used in this study are listed in Table 6.1. Plasmid pUDE432 (Marques *et al.*, 2018a) was introduced into strain IMK1010, resulting in strain IMZ786, which was subsequently evolved in duplicate using independent bioreactor cultures. After evolution, the evolved population from each bioreactor was stocked, resulting in IMS1225 and IMS1226. Both strains were plated on SMD with 5 g L^{-1} sucrose and restreaked three consecutive times. The resulting single colony isolates were grown in liquid SMD with 5 g L^{-1} sucrose and stocked as IMS1230 and IMS1231, respectively. The plasmids pUDE1222 and pUDE1223 were isolated from IMS1230 and IMS1231, respectively, and reintroduced in IMK1010, resulting in strains IME753 and IME754, respectively.

Table 6.1: *S. cerevisiae* strains used in this study. The prefix 'pUDE' is used to represent episomal plasmids.

Strain	Description or relevant genotype	Source
CEN.PK113-7D	*MATa URA3 HIS3 LEU2 TRP1 MAL2-8c SUC2*	(Entian and Kötter, 2007)
IMK1010	*MATa ura3-52 LEU2 HIS3 MAL2-8C mal11-mal12::loxP mal21-mal22::loxP mal31-mal32::loxP mph2/3::loxP mph2/3::loxP-hphNT1-loxP suc2::loxP ima1Δ ima2Δ ima3Δ ima4Δ ima5Δ can1::cas9-natNT2 hxt8Δ hxt14Δ gal2Δ hxt4Δ hxt1Δ hxt5Δ hxt3Δ hxt6Δ hxt7Δ hxt13Δ hxt15Δ hxt16Δ hxt2Δ hxt10Δ hxt9Δ hxt11Δ hxt12Δ stl1Δ*	Chapter 5
IMZ786	*MATa ura3-52 LEU2 HIS3 MAL2-8C mal11-mal12::loxP mal21-mal22::loxP mal31-mal32::loxP mph2/3::loxP mph2/3::loxP-hphNT1-loxP suc2::loxP ima1Δ ima2Δ ima3Δ ima4Δ ima5Δ can1::cas9-natNT2 hxt8Δ hxt14Δ gal2Δ hxt4Δ hxt1Δ hxt5Δ hxt3Δ hxt6Δ hxt7Δ hxt13Δ hxt15Δ hxt16Δ hxt2Δ hxt10Δ hxt9Δ hxt11Δ hxt12Δ stl1Δ pUDE432 (URA3 MAL11)*	This study
IMS1225	IMZ786 evolved in chemostats on SMD with addition of sucrose, first reactor, evolved population	This study
IMS1226	IMZ786 evolved in chemostats on SMD with addition of sucrose, second reactor, evolved population	This study
IMS1230	IMZ786 evolved in chemostats on SMD with addition of sucrose, first reactor, single colony isolate	This study
IMS1231	IMZ786 evolved in chemostats on SMD with addition of sucrose, second reactor, single colony isolate	This study
IME753	*MATa ura3-52 LEU2 HIS3 MAL2-8C mal11-mal12::loxP mal21-mal22::loxP mal31-mal32::loxP mph2/3::loxP mph2/3::loxP-hphNT1-loxP suc2::loxP ima1Δ ima2Δ ima3Δ ima4Δ ima5Δ can1::cas9-natNT2 hxt8Δ hxt14Δ gal2Δ hxt4Δ hxt1Δ hxt5Δ hxt3Δ hxt6Δ hxt7Δ hxt13Δ hxt15Δ hxt16Δ hxt2Δ hxt10Δ hxt9Δ hxt11Δ hxt12Δ stl1Δ pUDE1222 (URA3 MAL11*$^{C490T/G682C/G1163C}$*)*	This study

6

| IME754 | *MATa ura3-52 LEU2 HIS3 MAL2-8C mal11-mal12::loxP mal21-mal22::loxP mal31-mal32::loxP mph2/3::loxP mph2/3::loxP-hphNT1-loxP suc2::loxP ima1Δ ima2Δ ima3Δ ima4Δ ima5Δ can1Δ::cas9-natNT2 hxt8Δ hxt14Δ gal2Δ hxt4Δ hxt1Δ hxt5Δ hxt3Δ hxt6Δ hxt7Δ hxt13Δ hxt15Δ hxt16Δ hxt2Δ hxt10Δ hxt9Δ hxt11Δ hxt12Δ stl1Δ pUDE1223 (URA3 MAL11[G682C/G1079C/G1163T])* | This study |

Media and cultivation

E. coli cultures were grown at 37 °C in LB medium, supplemented with 100 µg mL^{-1} ampicillin for selection and maintenance of plasmids. Yeast strains were grown on synthetic medium (SM), which was heat sterilized for 20 min at 121 °C, after which a filter-sterilized vitamin solution and 20 g L^{-1} glucose was added (SMD) (Verduyn *et al.*, 1992). Medium for anaerobic cultivations was additionally supplemented with 10 mg L^{-1} ergosterol and 420 mg L^{-1} Tween 80, which were added in from a concentrated solution (800x) in absolute ethanol (Verduyn *et al.*, 1990b). For preparation of solid medium plates, 2% (w/v) agar was added to the media prior to heat sterilization. Medium used in bioreactor cultivations was additionally supplemented with 0.2 g L^{-1} Antifoam C (Sigma Aldrich, Saint Louis, MO, USA). Aerobic shake flask cultures were grown in 500 mL round bottom flasks with 100 mL medium, which were incubated in an Innova orbital shaker (Eppendorf, Nijmegen, the Nederlands) at 200 rpm at 30 °C. Laboratory evolution of IMZ786 was conducted in 2 L laboratory bioreactors (Applikon, Delft, The Netherlands) with a 1 L working volume. Cultures were stirred at 800 rpm, the temperature was controlled at 30 °C and the pH was kept constant at 5.0 through automated addition of 2.0 M KOH. The cultures were sparged with 500 mL N$_2$ min^{-1} (<5 ppm O$_2$), and medium vessels were sparged with nitrogen as well. To enable evolution in continuous culture set-up, SMD medium pumps were switched on after glucose depletion in a preceding batch phase, to obtain a constant flowrate. The volume was kept constant at 1 L using an effluent pump that was controlled by an electric level sensor, resulting in a stable dilution rate. After a stable CO$_2$ concentration in the reactor off-gas was observed, a filter-sterilized, 500 g L^{-1} sucrose solution was added to the culture in one-second pulses via a separate pump. Based on observations on the online measurements of the CO$_2$ concentration in the reactor off-gas, the frequency of these pulses was manually increased and decreased to exert a selective pressure on the culture, but prevent culture washout. Maximum specific growth rates were determined in a Growth-Profiler system (EnzyScreen, Heemstede, The Netherlands) equipped with 96-well plates in a culture volume of 250 µL, set at 250 rpm and 30 °C. The measurement interval was set at 20 minutes. Raw green values were corrected for well-to-well variation using measurements of a 96-well plate containing a culture with an externally determined optical density, measured at 660 nm using a Libra S11 spectrophotometer (Biochrom, Cambridge, United Kingdom), of 4.19 in all wells. Optical densities were calculated by converting green values (corrected for well-to-well variation) using a calibration curve that was determined by fitting a third-degree polynomial through 71 measurements of cultures with known OD values between 0.75 and 24.5 (Online Supplementary Information). Growth rates were determined using the calculated optical densities of at least 10 points (corresponding to at least 200 minutes) in the exponential phase. Exponential growth was assumed when an exponential curve could be fitted with an R^2 of at least 0.985. To validate the experimental procedure and data analysis, the growth rates of laboratory strain CEN.PK113-7D was also determined in all conditions, which corresponded to within 5% of previously determined values for this strain grown aerobically in SMD (Nijkamp *et al.*, 2012).

6.3 Results

Evolution for decreased sucrose sensitivity

The previously constructed strain IMK1010 is devoid of all hexose transporters, disaccharide transporters and disaccharide hydrolases and is therefore unable to grow on any sugar substrate (Chapter 5). *MAL11*, encoding a proton-symporter with affinity for maltose, sucrose and glucose, was introduced in IMK1010 via the episomal expression vector pUDE432. Subsequently, growth of the resulting strain (IMZ786) was investigated on synthetic medium (SM) with only glucose, maltose or sucrose as carbon source, and on SM with mixtures of glucose with either sucrose or maltose. Although introduction of *MAL11* was expected to enable the uptake of glucose, sucrose and maltose, in IMZ786 it only complemented growth on medium with glucose (SMD, Figure 6.2). We hypothesized that the inability to grow on disaccharides was caused by the absence of disaccharide hydrolysis activity in IMZ786, which is essential for their further metabolism (Marques *et al.*, 2017) (Online Supplementary Information). Moreover, IMZ786 was found to be sensitive to the presence of either sucrose or maltose, as could be observed from its inability to grow on SMD with the addition of 20 g L^{-1} sucrose or maltose (Figure 6.2). We attributed this detrimental effect to the proton symport mechanism of the constitutively expressed Mal11, which enabled proton-motive force-driven intracellular accumulation of the disaccharides that, in this specific strain background, could not be relieved by their degradation or export. To investigate whether this inability to grow on SMD in the presence of sucrose or maltose was not only due to competitive inhibition of the transporter, cultures of IMK1010 (*sugar^0*) and IMZ786 (*sugar^0 MAL11*), which were pre-grown in SM with 2% (v/v) ethanol as carbon source, were transferred to SM with 2% (v/v) ethanol and 20 g L^{-1} sucrose. While the optical density of IMK1010 in the presence of sucrose increased from 0.11 to 17.9 in 45.5 hours, that of IMZ786 only increased from 0.07 to 0.12 within the same time span. These results indicate that growth on carbon sources not transported by Mal11 such as ethanol, which passively diffuses across the plasma membrane, is strongly impaired and likely caused by Mal11-mediated intracellular accumulation of sucrose.

The sensitivity of IMZ786 towards sucrose when grown on glucose inspired us to investigate whether this property could enable a laboratory evolution strategy to decrease the substrate specificity of Mal11 for sucrose, while retaining its glucose transport activity. To this end, IMZ786 was first grown in two independent anaerobic, glucose-limited continuous cultures at a dilution rate of 0.07 h^{-1}. In these cultures, online measurements of the CO_2 concentrations in the reactor off-gas were used as a means to monitor metabolic activity and growth (Figure 6.1). After a stable off-gas CO_2 concentration of ~0.83% was observed, we then investigated whether the presence of sucrose was also toxic to IMZ786 under glucose-limited conditions by separately adding a concentrated sucrose solution (500 g L^{-1}) to the culture in one-second pulses, which resulted an average flowrate of ~16 mL h^{-1}. Indeed, a near instant decrease of the CO_2 production towards 0.08% was observed (within 1 h), indicating that growth and metabolic activity had ceased due to the addition of sucrose (Figure 6.1A). To prevent culture washout, the addition of sucrose was stopped until a stable CO_2 concentration of ~0.85% was observed again. Then, the frequency at which the pulses of the sucrose solution was added was adjusted to obtain an average flowrate of ~0.09 mL h^{-1}, which again led to a gradual decrease in CO_2 production (Figure 6.1B), indicating significant sucrose toxicity in the culture. After approximately 480 hours, the off-gas CO_2 concentration first stabilized at 0.22%, and then increased to reach a new stable value at ~0.7% (Figure 6.1C). We hypothesized

6
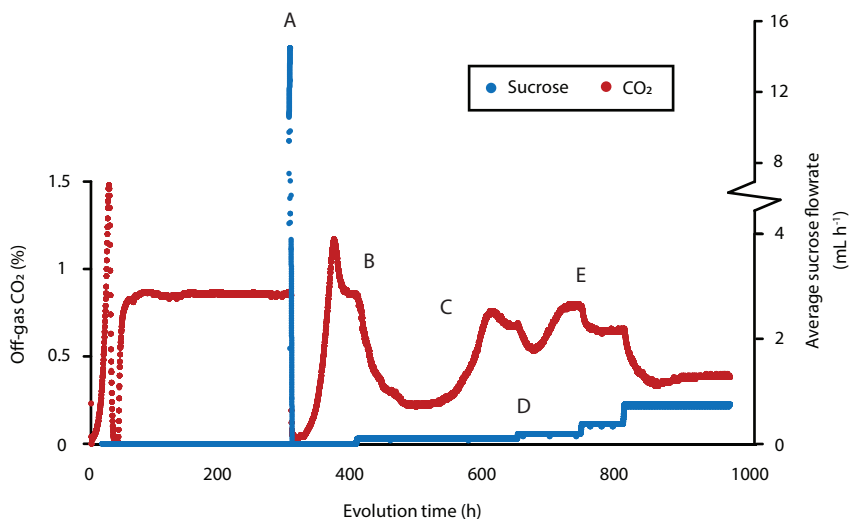
Figure 6.1: CO_2 concentrations in the reactor off-gas and average flowrate of a 500 g L^{-1} sucrose solution during adaptive laboratory evolution of IMZ786 (*sugar^0 MAL11*) in anaerobic glucose-limited chemostats at a dilution rate of 0.07 h^{-1} with pulse-wise addition of sucrose. The off-gas CO_2 concentrations were used as a read-out to monitor growth and metabolic activity. One representative of the two independent evolution experiments is shown. A: After a stable CO_2 concentration of ~0.83% in the reactor off-gas was observed, sucrose was administered separately to the cultures at an average flowrate of 16 mL h^{-1}. At this flowrate, the CO_2 concentration decreased to 0.08% in 1 h. To subsequently prevent washout of cells and allow for evolution, the addition of sucrose was temporarily stopped. B: After ~400 h, the average sucrose flowrate was set to 0.09 mL h^{-1}. This resulted in a decrease of the off-gas CO_2 concentration to a value of 0.22% C: The decrease in the off-gas CO_2 concentration was, at the ~480 h time point, followed by a strong increase, until it stabilized at ~0.64%. D: Subsequently, the average flowrate of sucrose was increased to 0.19 mL h^{-1} and the culture was again left to evolve until a stable CO_2 output was reached (E). An overview of the full experiment, which lasted ~3400 h, is presented in Figure S6.1.

that this decrease, followed by an increase in CO_2 production was the result of washout of the original strain IMZ786, followed by the emergence and enrichment of less sensitive mutants. To increase the selective pressure of sucrose insensitivity, the frequency of the sucrose pulses was then manually increased (Figure 6.1D), after which the CO_2 concentration was allowed to stabilize again (Figure 6.1E). This cycle was repeated until a stable CO_2 output (0.53% for the first replicate, 0.68% for the second) was observed at an average flowrate of 1.6 mL h^{-1} (Figure S6.1), which, under the assumptions of steady-state, ideal mixing and that sucrose is not consumed, corresponded to approximately 11.4 g L^{-1} sucrose in the reactor. After a total of approximately 350 generations, evolved populations were stocked from each reactor, resulting in IMS1225 and IMS1226, from which single cell lines were isolated (IMS1230 and IMS1231, respectively).

Evolved strains are less sensitive to sucrose and maltose

To investigate whether the bioreactor-derived strains were less sensitive to the presence of the disaccharides sucrose and maltose, the maximum specific growth rates of the evolved populations IMS1230 and IMS1231 were determined in SMD medium with various concentrations of either sucrose or maltose and compared to those of the unevolved parental strain IMZ786. Once again, the toxic effect that sucrose has on IMZ786 was apparent by the absence of growth on SMD in the presence of ≥2.5 g L^{-1} sucrose, and only at a concentration

6
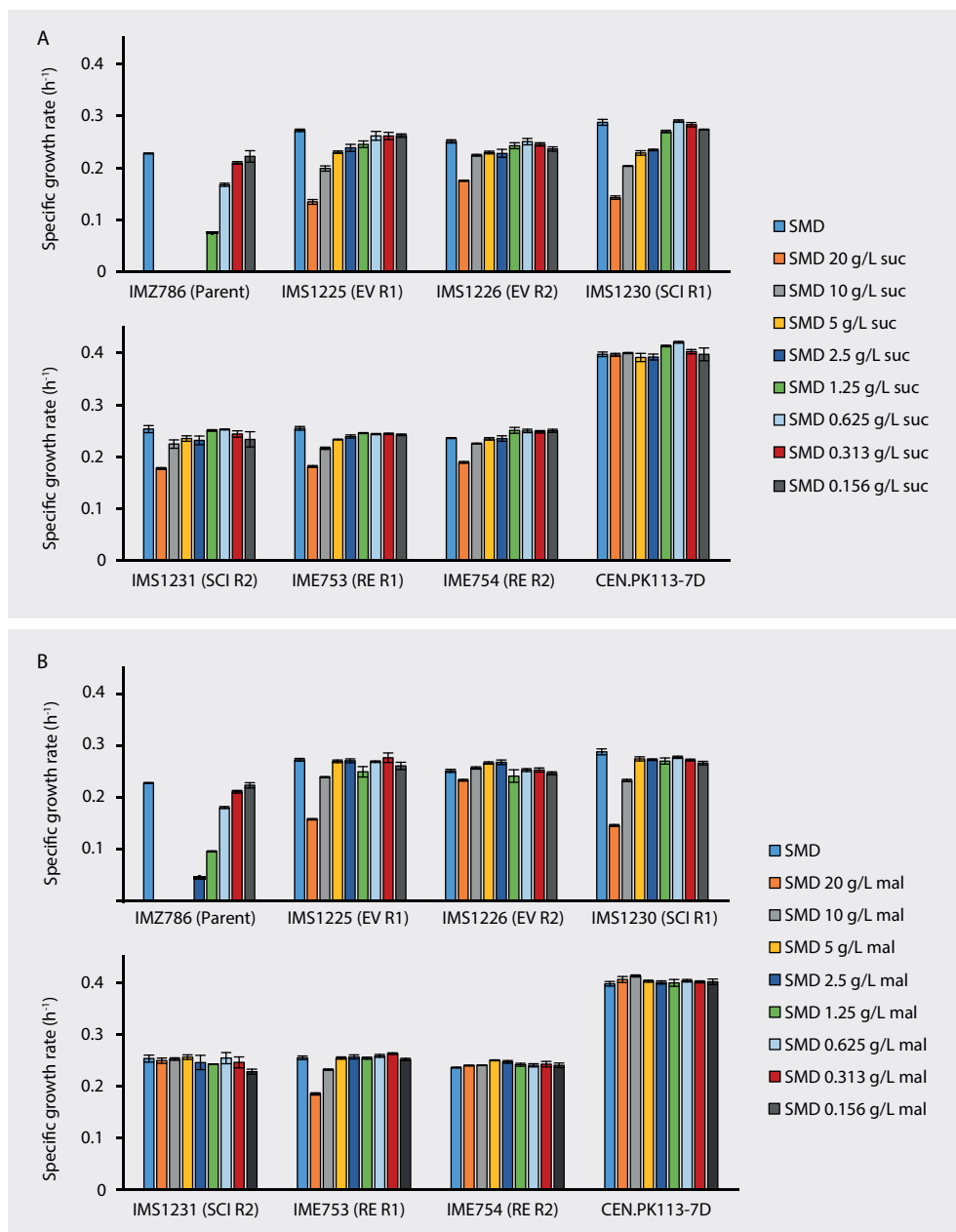
Figure 6.2: Maximum specific growth rates of IMZ786 (*sugar⁰ MAL11*) and strains that originate thereof, which were the evolved populations (EV) after laboratory evolution in glucose-limited continuous cultures with increasing addition of sucrose in two independent reactors (R1 and R2), the corresponding single colony isolates (SCI) and the corresponding reverse engineered strains (RE). A: Maximum specific growth rates on SMD in the presence of different concentrations of sucrose (suc). B: Maximum specific growth rates on SMD in the presence of different concentrations of maltose (mal). Data represent average and mean deviation of three replicate experiments. To validate the experimental procedure and data analysis, the growth rates of laboratory strain CEN.PK113-7D were also determined in all conditions.

of 0.16 g L^{-1} sucrose no effect on the growth rate could be observed compared to growth on SMD without sucrose (Figure 6.2A). On the contrary, the evolved strains IMS1225 and IMS1226 exhibited growth in all tested conditions, and in each condition, their growth rates were higher than that of the unevolved parental strain. For IMS1225, no effect on the growth rate could be observed between the SMD control and cultures with sucrose concentrations up to 0.625 g L^{-1}, and for IMS1226 up to 1.25 g L^{-1} (Figure 6.2A). The presence of maltose had a similar effect on the growth rates of the three strains, although the toxicity effect was slightly less apparent than for sucrose (Figure 6.2B). For instance, the parental strain IMZ786 also exhibited growth in the presence of up to 2.5 g L^{-1} maltose, and compared to the growth rates of IMS1225 and IMS1226 on SMD, no effects were observed upon addition of up to 5 g L^{-1} and 10 g L^{-1} of maltose, respectively. Strikingly, addition of 20 g L^{-1} of maltose only led to a 7% decrease of the growth rate of IMS1226. These results indicate that the evolution not only affected the sensitivity towards sucrose, but also its isomer maltose. Moreover, the growth rates of both strains on SMD without sucrose or maltose were 19.4% (IMS1225) and 10.1% (IMS1226) higher than that of the parental strain. In all conditions, growth rates of IMS1230 were highly similar to those of IMS1225, whereas the growth rates of IMS1231 where highly similar to those of IMS1226, indicating that the isolated single colonies are phenotypical representatives of the evolved population.

Mutations occurred in *MAL11* during evolution

To investigate whether mutations occurred in the transporter gene *MAL11* during the laboratory evolution experiment, the plasmids from single colony isolates IMS1230 and IMS1231 were isolated and the *MAL11* open reading frame was sequenced. Strikingly, three non-synonymous mutations had occurred in each independently evolved strain: C490T, G682C, G1163C in IMS1230 and G682C, G1079C and G1163T in IMS1231 (Figure 6.3A). Although G1163 was mutated to a different base in each strain, the resulting amino acid substitution in the protein was identical, indicating that there were two common amino acid changes (Ala-228-Pro and Gly-388-Ala) in Mal11 that evolved independently in the two cultures.

The locations of these mutations were investigated using a previously constructed homology model of Mal11 (Henderson and Poolman, 2017) (Figure 6.3B,C). The mutations that where shared in the two evolved strains were both found to be located in the central cavity of the protein, as well as the Leu-164-Phe mutation that was identified in IMS1230, albeit at different heights in the protein structure. To investigate the proximity of these mutations to the sugar binding sites, the Mal11 structure was compared to that of the homologous human GLUT3 sugar transporter, for which crystal structures have been determined for the glucose- and maltose-bound proteins (Deng *et al.*, 2015). These crystal structures showed that binding of one of the glucose units comprising maltose in GLUT3 completely overlaps with binding of a glucose molecule. Superimposition of the Mal11 homology model with the two GLUT3 structures suggested that the three mutations in the central cavity of Mal11 might be relatively close to the amino acids that form the sugar binding pocket (Figure 6.4). Strikingly, L164F and G388A appeared to be in near proximity to the glucose-monomer of maltose that does not overlap with glucose.

Mutations in *MAL11* are responsible for decreased sucrose and maltose sensitivity

To investigate whether the mutations that were identified in *MAL11* were responsible for the decreased sensitivity of the evolved strains towards sucrose and maltose, the plasmids

A

Strain	Mutations in *MAL11* gene	Amino acid substitution
	C490T	L164F
IMS1230	G682C	A228P
	G1163C	G388A
	G682C	A228P
IMS1231	G1079C	C360S
	G1163T	G388A

C

B
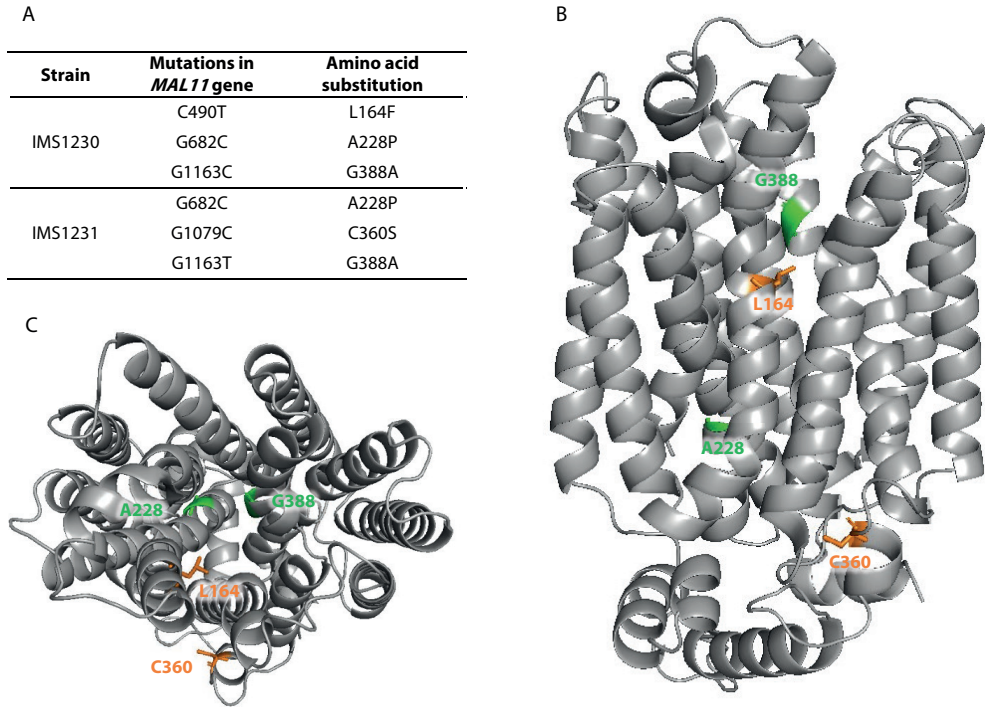
Figure 6.3: Mutations identified in *MAL11* after evolution of IMZ786 (*sugar⁰ MAL11*) in two independent, glucose-limited continuous cultures with increasing addition of sucrose. A: In single colony isolates from two independent reactors, three mutations were identified in *MAL11*. B (side view), C (top view): Structural model of Mal11, highlighting the location of the amino acid changes resulting from the mutations that occurred during evolution. Mutations that were identical in both strains are indicated in green, and mutation that were unique in each strain are indicated in orange. All structure figures were prepared with PyMol.

containing the mutated variants of *MAL11* were isolated from IMS1230 and IMS1231, and reintroduced in the unevolved IMK1010 (*sugar⁰*) strain background. When the resulting strains (IME753 and IME754) were grown on SMD in the presence of different concentrations of sucrose or maltose (Figure 2), they performed similarly to their corresponding evolved strain from which the respective *MAL11* allele originated. These observations indicate that the mutations in *MAL11* are solely responsible for the evolved phenotype and no other genomic mutations contributed to the decreased sensitivity of evolved strains towards sucrose and maltose.

6.4 Discussion

In this study, we successfully applied an evolutionary engineering strategy to decrease the sensitivity of a *MAL11*-expressing strain lacking maltose or sucrose hydrolases towards sucrose while maintaining its ability to consume glucose. Concurrently, the sensitivity towards maltose was also decreased, which suggests that the mechanism behind the decreased sensitivity towards both disaccharides is highly similar. Expression of the evolved *MAL11* alleles in an unevolved strain background and characterization of the resulting strains confirmed that the
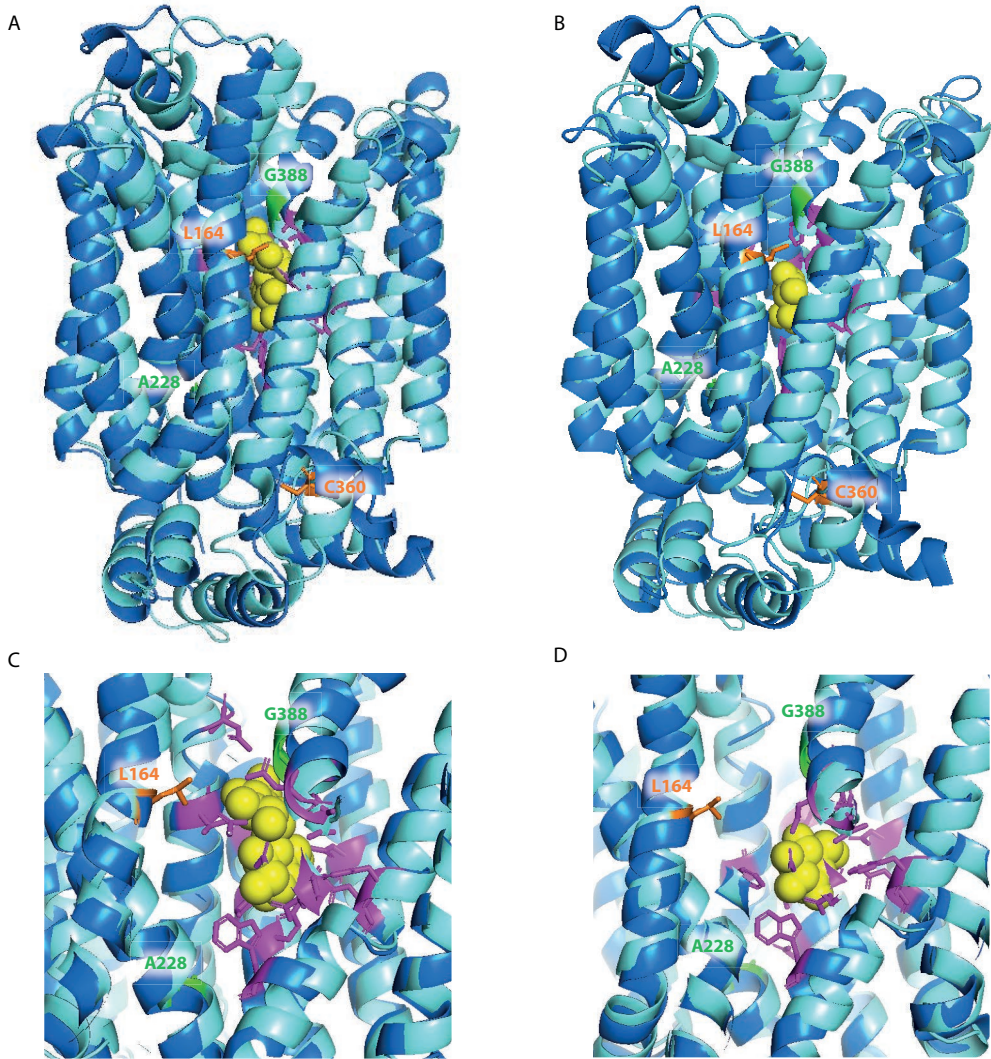
Figure 6.4: Superimposition of homology model of *S. cerevisiae* Mal11 (light blue) (Henderson and Poolman, 2017) and crystal structures of human GLUT3 (dark blue) (Deng *et al.*, 2015) bound to maltose (PDB: 4ZWB) (A and C) and bound to glucose (PDB: 4ZW9) (B and D). Glucose and maltose are represented by yellow spheres. Amino acid residues involved in sugar binding in GLUT3 are shown in purple, and amino acid residues in Mal11 that were substituted during evolution of IMZ786 are shown in orange and green.

mutations in *MAL11*, which result in amino acid changes in the Mal11 protein, underlie the evolved phenotype. We hypothesize that the improved growth performance in the presence of these sugars could be due to (one of) the following alterations: 1) a decreased binding affinity of Mal11 for disaccharides; 2) an overall lower disaccharide transport capacity of the protein, resulting in less toxic accumulation of disaccharides in growing cultures; 3) glucose-specialized uptake, due to glucose inhibition of disaccharide uptake, similar to what is observed for Hxt transporters in mixtures of glucose and pentose sugars in *S. cerevisiae* (Nijland and Driessen,

2020); 4) loss of proton coupling to sugar uptake, resulting in a facilitated diffusion mechanism. In the latter case, intracellular accumulation of disaccharides is limited to their extracellular concentrations. Future work to investigate which mechanism is responsible for the evolved phenotype could involve the determination of kinetic parameters of the Mal11 variants (K_M, K_i and V_{max}) via transport assays with radiolabeled sucrose, maltose and glucose (Henderson and Poolman, 2017; Postma *et al.*, 1988; Santos *et al.*, 1982). The accumulation ratio (ratio between intra- and extracellular sugar concentrations) combined with proton-uptake assays could also provide insight into the transport mechanisms of the evolved Mal11 proteins. Additionally, the effect of expressing these transporters on strain physiology, and more specifically, anaerobic biomass yield on sugar, can also be used to elucidate their transport mechanism (Henderson *et al.*, 2021; Marques *et al.*, 2018a; Weusthuis *et al.*, 1993).

Two identical amino acid substitutions (A228P and G388A) occurred in both independent evolution lines, which suggests that these two amino acid residues play an important role in determining the substrate specificity of Mal11 towards glucose and disaccharides and that their substitution resulted in the most substantial fitness benefit under the conditions of the evolution experiment. In previous work, it was found that in *Escherichia coli* XylE and the human GLUT transporters, which are homologous to Mal11, the position that corresponds to Gly-388 in Mal11 is occupied by a tyrosine residue (Henderson *et al.*, 2019a). In those transporters, this tyrosine residue is involved in closing off the sugar-binding site from the aqueous extracellular space (Wisedchaisri *et al.*, 2014; Yan, 2015). Since in Mal11, a tyrosine residue is located one helix-turn above this position, the location of this hydrophobic residue may sterically dictate the size of the sugar that can be transported by the protein (Henderson *et al.*, 2019a). We speculate that the substitution of Gly-388 by alanine, which has a larger hydrophobic side chain, results in a functional similarity to the tyrosine residues occupying this position in the homologous monosaccharide transporters. A similar mechanism could be envisioned as a result of the L164F mutation, which was also predicted to be in close proximity to the 'additional' glucose unit of Mal11-bound maltose and does not overlap with glucose binding (Figure 6.4). Here, substitution of the leucine side chain by the bulky aromatic side chain of phenylalanine could sterically hinder binding of disaccharides. The roles of the other amino acid residues in Mal11 that were mutated during evolution have not been predicted previously, which further demonstrates the power of evolutionary engineering to pinpoint amino acid residues with important roles in the transport mechanism. Testing the effects of the individual and different combinations of the mutations in Mal11 identified in this study on sucrose, maltose and glucose transport capacity could provide valuable insights into the importance of each mutation for the evolved phenotype and potential synergistic effects of mutation combinations.

To the best of our knowledge, this is the first demonstration of an evolutionary engineering strategy where proton-coupled substrate uptake is used as a counter-selective pressure to change the substrate specificity of a transporter. One of the mutations that we identified corresponded to an amino acid residue whose role could be predicted based on known crystal structures. This strategy could therefore also be valuable to identify important amino acid residues in other, less well studied transport proteins for which no crystal structure is available yet. When selecting targets for such an evolutionary strategy, we consider three criteria to be especially important.

First, the transporter of interest should remain essential for growth under the selective

6

conditions. Otherwise, cells are likely to 'escape' the selective pressure by evolving loss-of-function mutations in the targeted transporter. For example, when the aim of an evolution experiment is to evolve the amino acid permease Put4, which actively transports alanine, glycine and proline (Regenberg *et al.*, 1999), into a proline-specific transporter, Put4-mediated proline transport can be made essential for growth by using a strain background in which all other related transporter genes have been deleted, as wel as *PRO3*. The *PRO3* deletion results in a proline-auxotrophic strain that relies on uptake of proline from the medium (Brandriss, 1979), while transport of alanine and glycine, for which *S. cerevisiae* is prototrophic, can be lost.

Second, the counter-selectable 'substrate' should not be metabolized once taken up by cells, to allow for toxic accumulation. In this study, the absence of disaccharide hydrolases was sufficient to prevent intracellular conversion of sucrose or maltose. Another relatively straightforward application could be similar to the aforementioned transporters with affinity for both pentose and hexose sugars, where deletion of hexokinase-encoding genes is sufficient to prevent the conversion of glucose, while the introduction of a novel metabolic route allows for pentose conversion (Farwick *et al.*, 2014; Li *et al.*, 2016; Nijland *et al.*, 2014; Verhoeven *et al.*, 2018). Such a strain design could therefore also be used for evolution of proton-coupled hexose/pentose transporters, such as Gxs1 from *Candida intermedia* (Leandro *et al.*, 2006). However, this criterium might be less straightforward with other substrates, especially when considering that the ability to grow on the essential substrate should be maintained. For example, when aiming to decrease the glucose affinity of *MAL11*, a difficulty arises by the fact that utilization of sucrose and maltose is also dependent on the hexokinase reaction. In such cases, the deletion of hexokinase genes cannot be used to disable glucose conversion and instead the use of non-metabolizable glucose analogs (for instance, 2-deoxy-glucose (Heredia *et al.*, 1964)) in cultures could provide the desired counter-selective pressure on glucose transport by its intracellular accumulation.

Third, the driving force of the transport process mediated by the targeted transporter should be sufficient to achieve (toxic) levels of accumulation of the counter-selectable substrate. This can be especially challenging if the proton-coupled transport process does not result in net transfer of charge due to transport of an anion, as is for example the case for proton-coupled monocarboxylic acid transporters such as Jen1 (Casal *et al.*, 1999). Proton symport of the negatively charged lactate, acetate, pyruvate and propionate anions via this transporter is electroneutral, therefore only the chemical component of the proton-motive force contributes to its driving force. To promote toxic accumulation of lactate without the contribution of the electrical component of the proton-motive force, the evolution could be performed at a low extracellular pH to maximize the chemical potential difference of protons across the plasma membrane (Cássio *et al.*, 1987). An evolution experiment aimed at losing the ability of Jen1 to transport lactate could then be performed in a strain devoid of all other lactic acid importers (Baldi *et al.*, 2021; Mans *et al.*, 2017) and lactate dehydrogenase activity (Guiard, 1985).

6.5 Acknowledgements

6.6 Supplementary information

Raw data of evolution experiments and growth profiler experiments are available with the online article.
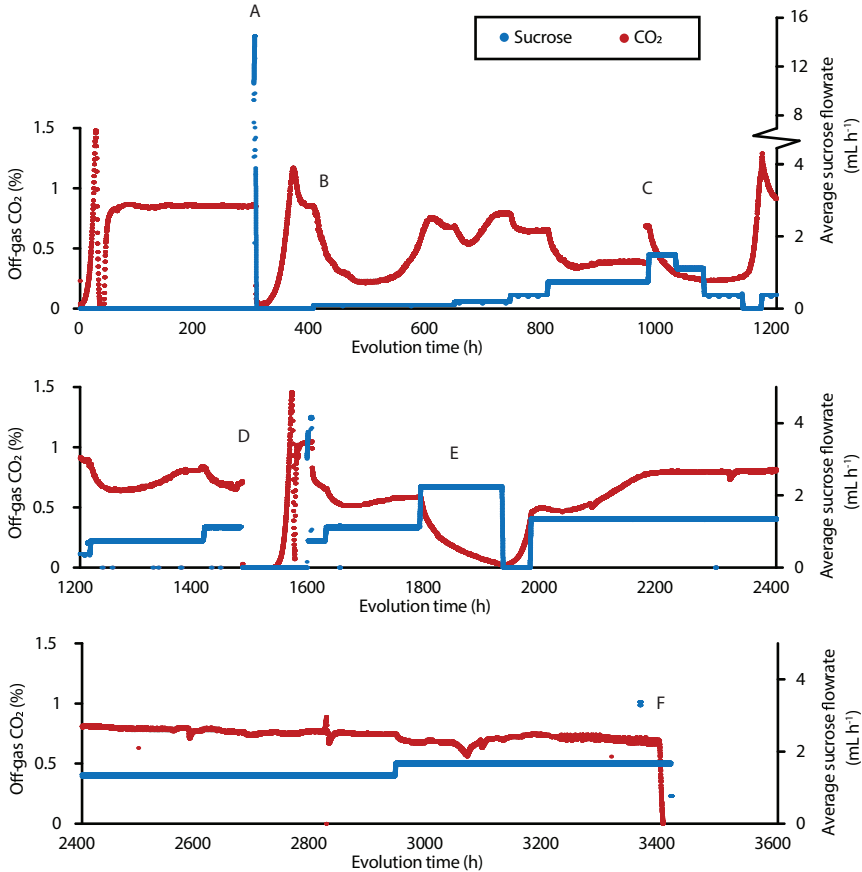
Figure S6.1: CO_2 concentrations in the reactor off gas and average flowrate of a 500 g L^{-1} sucrose solution during adaptive laboratory evolution of IMZ786 (*sugar0 MAL11*) in anaerobic glucose-limited chemostats with pulse-wise addition of sucrose. The off-gas CO_2 concentrations were used as a read-out to monitor growth. One representative of the two independent evolution experiments is shown. A: After a stable CO_2 concentration of ~0.83% in the reactor off-gas was observed, sucrose was administered separately to the culture at an average flowrate of 16 mL h^{-1}. At this average flowrate, the CO_2 concentration decreased to zero. To subsequently prevent washout of cells and allow for evolution, the addition of sucrose was temporarily stopped. B: After ~400 h, the average sucrose flowrate was set to 0.09 mL h^{-1}. This resulted in a decrease of the off-gas CO_2 concentration to a value of 0.22%. C: After 975 h, there was a temporal disturbance (increase) in the constant medium flowrate as a new medium vessel was connected, resulting in a sudden peak in off-gas CO_2 concentration (0.63%, whereas before connection of the medium vessel it was relatively stable at ~0.37%). After this peak, the ever-decreasing CO_2 concentration motivated the decision to decrease the average sucrose flowrate stepwise, until an increase of the CO_2 concentration was once again observed as no more sucrose was added. D: Due to laboratory maintenance, the cultures were temporarily stocked and terminated. After approximately one month, these stocks were used to proceed with the evolution. E: The average sucrose flowrate (2.2 mL h^{-1}) set after ~1785 h resulted in gradual wash-out of cells, as can be observed from the decreasing off-gas CO_2 concentration (from 0.58% to 0.02%). Addition of sucrose was therefore temporarily stopped to allow for accumulation of biomass, after which the average flowrate of the sucrose solution was adjusted to a lower setting that still permitted sufficient growth. F: After ~3400 h, aliquots of the cultures were stocked and the evolution experiment was terminated.

6

Outlook

Metabolite transport is a key process in living organisms, and its role in import of substrates and export of products should be taken into account in the design and construction of microbial cell factories. The research described in this thesis contributes fundamental knowledge on metabolite transport and engineering strategies for its modification in *Saccharomyces cerevisiae*, which can be applied in future strain designs. **Chapter 2** describes how a combination of rational protein engineering and evolutionary engineering was applied to change the transport mechanism of the disaccharide transporter Mal11 from proton symport to facilitated diffusion. Replacing the wild-type Mal11 transporter with such uncoupled variants was expected to increase the ATP yield from sucrose fermentation from 4 to 5 moles of ATP per mole of sucrose. However, this modification did not lead to the expected 25% increase of the biomass yield on sucrose in anaerobic cultures. It is therefore questionable whether this transporter can be applied to increase the yield of assimilatory products on sucrose. Since specific engineering targets for further strain optimization were not identified in this work, an evolutionary engineering approach could be applied in future research to select for mutants that exhibit an increased biomass yield, closer to the theoretical 25%. This future work could focus on selection of mutants with an increased biomass yield, which is possible via serial propagation in water-in-oil emulsions (Bachmann *et al.*, 2013). Although this strategy has already been applied for selection of *S. cerevisiae* mutants with higher biomass yields (van Tatenhove-Pel *et al.*, 2021), enrichment of mutants that show small (incremental) improvements of the biomass yield might require many cycles of serial propagation. An alternative evolution strategy could encompass the design and construction of an engineered strain in which the improved efficiency of sucrose uptake and phosphorylation is essential for growth. A suitable strain could, for instance, be based on a homo-fermentative, lactic acid-producing *S. cerevisiae* strain, in which conversion of glucose into (extracellular) lactic acid does not yield ATP (Abbott *et al.*, 2009a; van Maris *et al.*, 2004). In principle, mutants of such a strain that have a more efficient energy metabolism may be selected under anaerobic conditions, since their net positive ATP yield could support growth if the rate of ATP formation exceeds maintenance-energy requirements. This strategy should also prevent enrichment of mutants in which proton coupling of uncoupled variants of Mal11 is restored, as was observed for some evolution lines in **Chapter 2**.

Chapter 3 describes the discovery of two *S. cerevisiae* genes (*ATO2* and *ATO3*) that, after acquiring mutations, encode transporters that facilitate the uptake of lactate. Similar to the approach described by de Kok *et al*. (2012), these alleles were identified in strains that lacked previously identified lactate transporter genes (*JEN1* and *ADY2*) and which were evolved for growth on lactic acid as sole carbon source. Absence of growth on lactic acid, even after prolonged incubation, of a strain in which *JEN1*, *ADY2*, *ATO2* and *ATO3* were deleted suggests that Ato2 and Ato3 complete the set of transporters that, with only few amino acid substitutions, can mediate uptake of lactic acid. To further investigate the evolutionary plasticity of transporter proteins, it would be interesting to perform a similar selection experiment after exposure of a strain devoid of all known lactic acid transporters to random mutagenesis. Whereas the work described in **Chapter 3** focussed on lactic acid import, the identification of proteins that facilitate lactic acid export remains highly relevant for engineering of yeast strains for industrial production of lactic acid. A possible evolutionary engineering strategy to identify lactic acid exporters could be coupling of lactate production to growth, for instance by coupling presence of intracellular lactic acid to the expression of an essential gene via a synthetic regulatory circuit (Mans *et al.*, 2018). This regulatory circuit would require a biosensor for lactic acid, or a lactic acid-responsive promoter, which could be identified by analyzing the transcriptome response to the presence of lactic acid (Shi *et al.*, 2017). Evolution of strains with such a sensor in combination with overexpression of a lactate dehydrogenase-encoding gene (*ldh*) may yield novel insights into the elusive lactic acid export system of *S. cerevisiae*. Alternatively, transcriptome analysis of lactate-producing and non-producing strains could be used as a tool for the identification of potential candidate lactic acid exporter genes. In the yeast *Yarrowia lipolitica*, a citrate exporter was identified by analysis of differential gene expression amongst predicted Major Facilitator Superfamily genes, between strains with different citrate productivities (Erian *et al.*, 2020). A similar strategy could be employed with strains with and without *ldh*-overexpression to identify candidate lactic acid exporters in *S. cerevisiae*.

The results described in **Chapter 5** show how replacement of the transport mechanism of hexose uptake was used to decrease the ATP stoichiometry of sugar dissimilation and, thereby, led to a significantly higher ethanol yield on sugar. Evolutionary engineering improved the sugar consumption rate of the engineered strains so that it supported growth under anaerobic conditions. As discussed in **Chapter 4**, the ATP generation rate that results from sugar dissimilation in engineered strains should be sufficient to achieve high productivities, even under the harsh conditions that cells experience in industrial fermentations. To meet this requirement, the strains developed in **Chapter 5** should be further improved since their maximum specific growth rates (0.11 – 0.21 h^{-1}) in anaerobic cultures were still considerably lower than that of a wild-type strain (0.42 h^{-1} (Dekker *et al.*, 2019)). Prolonged evolution in a sequential batch reactor setup may be a suitable strategy to select for mutants with even faster sugar uptake rates and, consequently, higher ATP production rates. The relatively high residual sugar concentrations (0.1 - 5 g L^{-1}) in chemostat cultures of hexose-proton symporter-expressing strains could represent another challenge in the development of industrially applicable strains based on this engineering strategy. In future work, the affinity of the investigated sugar transporters (V_{max}/K_M) might be improved by adaptive laboratory evolution under sugar-limited conditions. Since both the rate of dissimilation and the affinity for sugars are important optimization targets, an adaptive laboratory evolution setup should ideally select for both characteristics simultaneously. One such system is the accelerostat: a continuous culture in which the dilution rate is feed-back controlled based on continuous online measurements (for example the CO_2 concentration in the reactor off gas) (Mans *et al.*, 2018; Paalme and Vilu, 1992).

The engineering strategy to improve ethanol yields described in **Chapter 5** may also be relevant for other applications, such as the alcoholic beverage industry and second-generation bioethanol industry. For instance, the glucose-proton symporters described in this study could be combined with extracellular hydrolases that have been described for maltose (Jansen *et al.*, 2006) and cellobiose (Fritscher *et al.*, 1990). In addition, the 'sugar-negative' strain constructed in this study provides a valuable starting point for future investigations of sugar transporters. For example, the genomes of several industrial filamentous fungi are predicted to contain a large number of genes involved in sugar transport, with a broad range of potential substrates (Nogueira *et al.*, 2020). This strain can directly be applied to investigate whether these transporters complement growth on hexose sugars that are metabolized via the Embden-Meyerhof-Parnas glycolytic pathway, but it can also be readily engineered for the degradation of other sugars. For instance, genes encoding sucrose or maltose hydrolase could be re-introduced to enable disaccharide utilization, as well as genes encoding pathways for the utilization of pentose sugars such as xylose and arabinose.

The sugar-negative *S. cerevisiae* strain can also be applied for directed evolution of specific transport proteins, especially for those that transport multiple sugar substrates. Such research can contribute to our understanding of the evolution of transporters in nature (Saier, 2003), as well as for engineering of strains for industrial application (Nijland and Driessen, 2020). A first proof-of-principle for such an adaptive laboratory evolution strategy was demonstrated in **Chapter 6**, in which this concept was successfully applied to change the substrate specificity of Mal11.

References

Abbott, D. A., Suir, E., van Maris, A. J. A., Pronk, J. T., (2008). Physiological and transcriptional responses to high concentrations of lactic acid in anaerobic chemostat cultures of *Saccharomyces cerevisiae*. *Applied and Environmental Microbiology* **74** (18)**,** 5759–5768.

Abbott, D. A., van den Brink, J., Minneboo, I. M. K., Pronk, J. T., van Maris, A. J. A., (2009a). Anaerobic homolactate fermentation with *Saccharomyces cerevisiae* results in depletion of ATPand impaired metabolic activity. *FEMS Yeast Research* **9,** 349-357.

Abbott, D. A., Zelle, R. M., Pronk, J. T., van Maris, A. J. A., (2009b). Metabolic engineering of *Saccharomyces cerevisiae* for production of carboxylic acids: current status and challenges. *FEMS Yeast Research* **9,** 1123-1136.

Agrimi, G., Steiger, M. G., (2021). Metabolite transport and its impact on metabolic engineering approaches. *FEMS Microbiology Letters* **368**.

Albers, E., Larsson, C., Lidén, G., Niklasson, C., Gustafsson, L., (1996). Influence of the nitrogen source on *Saccharomyces cerevisiae* anaerobic growth and product formation. *Applied and environmental microbiology* **62** (9)**,** 3187-3195.

Albertyn, J., Hohmann, S., Thevelein, J. M., Prior, B. A., (1994). *GPD1*, which encodes glycerol-3-phosphate dehydrogenase, is essential for growth under osmotic stress in *Saccharomyces cerevisiae*, and its expression is regulated by the high-osmolarity glycerol response pathway. *Molecular and cellular biology* **14** (6)**,** 4135-4144.

Alexander, J. K., (1968). Purification and specificity of cellobiose phosphorylase from *Clostridium thermocellum*. *Journal of Biological Chemistry* **243** (11)**,** 2899-2904.

Almeida, J. R. M., Modig, T., Petersson, A., Hähn-Hägerdal, B., Lidén, G., Gorwa-Grauslund, M., (2007). Increased tolerance and conversion of inhibitors in lignocellulosic hydrolysates by *Saccharomyces cerevisiae*. *Journal of Chemical Technology and Biotechnology* **82,** 340-349.

Alves, R., Sousa-Silva, M., Vieira, D., Soares, P., Chebaro, Y., Lorenz, M. C., Casal, M., Soares-Silva, I., Paiva, S., (2020). Carboxylic acid transporters in *Candida* pathogenesis. *mBio* **11** (3).

Anderlund, M., Nissen, T. L., Nielsen, J., Villadsen, J., Rydström, J., Hahn-Hägerdal, B., Kielland-Brandt, M. C., (1999). Expression of the *Escherichia coli pntA* and *pntB* genes, encoding nicotinamide nucleotide transhydrogenase, in *Saccharomyces cerevisiae* and its effect on product formation during anaerobic glucose fermentation. *Applied and environmental microbiology* **65** (6)**,** 2333-2340.

André, B., (1995). An overview of membrane transport proteins in *Saccharomyces cerevisiae*. *Yeast* **11,** 1575-1611.

Andrei, M., Munos, J. W., Altered host cell pathway for improved ethanol production. Vol. US2017088861A1. Danisco US Inc, 2017.

Anjos, J., de Sousa, H. R., Roca, C., Cásio, F., Luttik, M. A., Pronk, J. T., Salema-Oom, M., Gonç̧alves, P., (2013). Fsy1, the sole hexose-proton transporter characterized in *Saccharomyces yeasts*, exhibits a variable fructose:H+ stoichiometry. *Biochimica et Biophysica Acta* **1828,** 201-207.

Ansell, R., Granath, K., Hohmann, S., Thevelein, J. M., Adler, L., (1997). The two isoenzymes for yeast NAD+-dependent glycerol 3-phosphate dehydrogenase encoded by *GPD1* and *GPD2* have distinct roles in osmoadaptation and redox regulation. *The EMBO journal* **16** (9)**,** 2179-2187.

Apel, A. R., Ouellet, M., Szmidt-Middleton, H., Keasling, J. D., Mukhopadhyay, A., (2016). Evolved hexose transporter enhances xylose uptake and glucose/xylose co-utilization in *Saccharomyces cerevisiae*. *Scientific Reports* **6** (19512).

Arastu-Kapur, S., Arendt, C. S., Purnat, T., Carter, N. S., Ullman, B., (2005). Second-site suppression of a nonfunctional mutation within the *Leishmania donovani* inosine-guanosine transporter. *Journal of Biological Chemistry* **280** (3)**,** 2213-2219.

Argyros, A., Sillers, W. R., Barrett, T., Caiazza, N., Shaw, A. J. I., Methods for the improvement of product yield and production in a microorganism through the addition of alternate electron acceptors. Vol. US 008956851B2. Lallemand Hungary Liquidity Management, 2015.

Arinaminpathy, Y., Khurana, E., Engelman, D. M., Gerstein, M. B., (2009). Computational analysis of membrane proteins: the largest class of drug targets. *Drug Discovery Today* **14** (23/24)**,** 1130-1135.

Athenstaedt, K., Weys, S., Paltauf, F., Daum, G., (1999). Redundant systems of phosphatidic acid biosynthesis via acylation of glycerol-3-phosphate or dihydroxyacetone phosphate in the yeast *Saccharomyces cerevisiae*. *Journal of Bacteriology* **181** (5)**,** 1458–1463.

Bachmann, H., Fischlechner, M., Rabbers, I., Barfa, N., Branco dos Santos, F., Molenaar, D., Teusink, B., (2013). Availability of public goods shapes the evolution of competing metabolic strategies. *PNAS* **110** (35)**,** 14302–14307.

Bakker, B. M., Overkamp, K. M., van Maris, A. J. A., Kötter, P., Luttik, M. A. H., van Dijken, J. P., Pronk, J. T., (2001). Stoichiometry and compartmentation of NADH metabolism in *Saccharomyces cerevisiae*. *FEMS Microbiology Reviews* **25,** 15-37.

Baldi, N., de Valk, S. C., Sousa-Silva, M., Casal, M., Soares-Silva, I., Mans, R., (2021). Evolutionary engineering reveals amino acid substitutions in Ato2 and Ato3 that allow improved growth of *Saccharomyces cerevisiae* on lactic acid. *FEMS Yeast Research* **21** (4)**,** 1-12.

Basso, L. C., Basso, T. O., Rocha, S. N., 2011a. Ethanol production in Brazil: The industrial process and its impact on yeast fermentation. In: Dos Santor Bernades, M. A., (Ed.), Biofuel production-recent developments and prospects. Rijeka, Croatia, pp. 85-100.

Basso, T. O., de Kok, S., Dario, M., do Espirito-Santo, J. C. A., Müller, G., Schlölg, P. S., Silva, C. P., Tonso, A., Daran, J.-M. G., Gombert, A. K., Van Maris, A. J. A., Pronk, J. T., Stambuk, B. U., (2011b). Engineering topology and kinetics of sucrose metabolism in *Saccharomyces cerevisiae* for improved ethanol yield. *Metabolic Engineering* **13,** 694-703.

Batista, A. S., Miletti, L. C., Stambuk, B. U., (2004). Sucrose fermentation by *Saccharomyces cerevisiae* lacking hexose transport. *Journal of Molecular Microbiology and Biotechnology* **8,** 26-33.

Beato, F. B., Bergdahl, B., Rosa, C. A., Forster, J., Gombert, A. K., (2016). Physiology of *Saccharomyces cerevisiae* strains isolated from Brazilian biomes: new insights into biodiversity and industrial applications. *FEMS Yeast Research* **16** (7).

Beckner, M., Ivey, M. L., Phister, T. G., (2011). Microbial contamination of fuel ethanol fermentations. *Letters in Applied Microbiology* **53,** 387–394.

Belocopitow, E., Maréchal, L. R., (1970). Trehalose phosphorylase from *Euglena gracilis*. *Biochimica et Biophysica Acta* **198** (1)**,** 151-154.

Benisch, F., Boles, E., (2014). The bacterial Entner–Doudoroff pathway does not replace glycolysis in *Saccharomyces cerevisiae* due to the lack of activity of iron–sulfur cluster enzyme 6-phosphogluconate dehydratase. *Journal of Biotechnology* **171,** 45-55.

Bergman, A., Siewers, V., Nielsen, J., Chen, Y., (2016). Functional expression and evaluation of heterologous phosphoketolases in *Saccharomyces cerevisiae*. *Amb Express* **6** (1)**,** 1-13.

Berthels, N. J., Cordero Otero, R. R., Bauer, F. F., Thevelein, J. M., Pretorius, I. S., (2004). Discrepancy in glucose and fructose utilisation during fermentation by *Saccharomyces cerevisiae* wine yeast strains. *FEMS Yeast Research* **4** (7)**,** 683–689.

Bianchi, F., van't Klooster, J. S., Ruiz, S. J., Poolman, B., (2019). Regulation of amino acid transport in *Saccharomyces cerevisiae*. *Microbiology and Molecular Biology Reviews* **83** (4).

Biasini, M., Bienert, S., Waterhouse, A., Arnold, K., Studer, G., Schmidt, T., Kiefer, F., Cassarino, T. G., Bertoni, M., Bordoli, L., Schwede, T., (2014). SWISS-MODEL: modelling protein tertiary and quaternary structure using evolutionary information. *Nucleic Acids Research* **42,** W252–W258.

Biz, A., Mahadevan, R., (2021). Overcoming challenges in expressing iron–sulfur enzymes in yeast. *Trends in Biotechnology* **39** (7)**,** 665-677.

Björkqvist, S., Ansell, R., Adler, L., Liden, G., (1997). Physiological response to anaerobicity of glycerol-3-phosphate dehydrogenase mutants of *Saccharomyces cerevisiae*. *Applied and Environmental Microbiology* **63** (1)**,** 128-132.

Blomberg, A., Adler, L., (1992). Physiology of osmotolerance in fungi. *Advances in Microbial Physiology* **33,** 145-212.

Boender, L. G. M., de Hulster, E., van Maris, A. J. A., Daran-Lapujade, P., Pronk, J. T., (2009). Quantitative physiology of *Saccharomyces cerevisiae* at near-zero specific growth rates. *Applied and Environmental Microbiology* **75** (17)**,** 5607-5617.

Boles, E., Hollenberg, C. P., (1997). The molecular genetics of hexose transport in yeasts. *FEMS Microbiology Reviews* **21,** 85-111.

Borodina, I., (2019). Understanding metabolite transport gives an upper hand in strain development. *Microbial Biotechnology* **12** (1)**,** 69-70.

Borodina, I., Nielsen, J., (2014). Advances in metabolic engineering of yeast *Saccharomyces cerevisiae* for production of chemicals. *Biotechnology Journal* **9** (5)**,** 609-620.

Bos, H. L., Broeze, L., (2020). Circular bio-based production systems in the context of current biomass and fossil demand. *Biofuels Bioproducts & Biorefining* **14,** 187-198.

Botstein, D., Falco, S. C., Steward, S. E., Brennan, M., Scherer, S., Stinchcomb, D. T., Struhl, K., Davis, R. W., (1979). Sterile Host Yeasts (SHY): A eukaryotic system of biological containment for recombinant DNA techniques. *Gene* **8,** 17-24.

Bracher, J. M., Verhoeven, M. D., Wisselink, H. W., Crimi, B., Nijland, J. G., Driessen, A. J. M., Klaassen, P., van Maris, A. J. A., Daran, J. M. G., Pronk, J. T., (2018). The *Penicillium chrysogenum* transporter *Pc*AraT enables high-affinity, glucose-insensitive l-arabinose transport in *Saccharomyces cerevisiae*. *Biotechnology for Biofuels* **11** (63).

Brandes, H. K., Hartman, F. C., Lu, T.-Y. S., Larimer, F. W., (1996). Efficient expression of the gene for spinach phosphoribulokinase in *Pichia pastoris* and utilization of the recombinant enzyme to explore the role of regulatory cysteinyl residues by site-directed mutagenesis. *The Journal of Biological Chemistry* **271** (11)**,** 6490–6496.

Brandriss, M. C., (1979). Isolation and preliminary characterization of *Saccharomyces cerevisiae* proline auxotrophs. *Journal of Bacteriology* **138** (2)**,** 816-822.

Brickwedde, A., van den Broek, M., Geertman, J.-M., Magalhães, F., Kuijpers, N., Gibson, B., Pronk, J. T., Daran, J.-M. G., (2017). Evolutionary engineering in chemostat cultures for improved maltotriose fermentation kinetics in *Saccharomyces pastorianus* lager brewing yeast. *Frontiers in Microbiology* **8** (1690).

Bro, C., Regenberg, B., Förster, J., Nielsen, J., (2006). In silico aided metabolic engineering of *Saccharomyces cerevisiae* for improved bioethanol production. *Metabolic engineering* **8** (2)**,** 102-111.

Brouwers, N., Gorter de Vries, A. R., van den Broek, M., Weening, S. M., Schuurman, T. D. E., Kuijpers, N. G. A., Pronk, J. T., Daran, J. M. G., (2018). *In vivo* recombination of *Saccharomyces eubayanus* maltose-transporter genes yields a chimeric transporter that enables maltotriose fermentation. *PLoS Genetics* **15** (4).

Bruinenberg, P. M., Jonker, R., van Dijken, J. P., Scheffers, W. A., (1985). Utilization of formate as an additional energy source by glucose-limited chemostat cultures of *Candida utilis* CBS 621 and *Saccharomyces cerevisiae* CBS 8066. *Archives of microbiology* **142** (3)**,** 302-306.

Bruinenberg, P. M., van Dijken, J. P., Scheffers, W. A., (1983). A theoretical analysis of NADPH production and consumption in yeasts. *Journal of General Microbiology* **129,** 953-964.

Bryan, T., DuPont Nutrition & Biosciences - When 'best-of-both' traits shine. Ethanol Producer Magazine, 2020.

Bu, X., Lin, J. Y., Cheng, J., Yang, D., Duan, C. Q., Koffas, M., Yan, G. L., (2020). Engineering endogenous ABC transporter with improving ATP supply and membrane flexibility enhances the secretion of β-carotene in *Saccharomyces cerevisiae*. *Biotechnology for Biofuels* **13** (168).

Bueno, J. G. R., Borelli, G., Corrêa, T. L. R., Fiamenghi, M. B., José, J., de Carvalho, M., de Oliveira, L. C., Pereira, G. A. G., dos Santos, L. V., (2020). Novel xylose transporter Cs4130 expands the sugar uptake repertoire in recombinant *Saccharomyces cerevisiae* strains at high xylose concentrations. *Biotechnology for Biofuels* **13** (145).

Canelas, A. B., Harrison, N., Fazio, A., Zhang, J., Pitkänen, J.-P, Van den Brink, J., Bakker, B. M., Bogner, L., Bouwman, J., Castrillo, J., (2010). Integrated multilaboratory systems biology reveals differences in protein metabolism

between two reference yeast strains. *Nature communications* **1** (145).

Canelas, A. B., Ras, C., ten Pierick, A., van Gulik, W. M., Heijnen, J. J., (2011). An *in vivo* data-driven framework for classification and quantification of enzyme kinetics and determination of apparent thermodynamic data. *Metabolic Engineering* **13,** 294–306.

Capaz, R., Posada, J., Seabra, J., Osseweijer, P., Life cycle assessment of renewable jet fuel from ethanol: an analysis from consequential and attributional approaches. Proceedings of the 26th European Biomass Conference and Exhibition, Copenhagen, Denmark, 2018, pp. 14-18.

Cardoso, H., Leão, C., (1992). Mechanisms underlying the low and high enthalpy death induced by short-chain monocarboxylic acids and ethanol in *Saccharomyces cerevisiae*. *Applied Microbiology and Biotechnology* **38,** 388-392.

Carlson, M., Botstein, D., (1982). Two differentially regulated mRNAs with different 5' ends encode secreted and intracellular forms of yeast invertase. *Cell* **28,** 145-154.

Carmelo, V., Bogaerts, P., Sá-Correia, I., (1996). Activity of plasma membrane H^+-ATPase and expression of *PMA1* and *PMA2* genes in *Saccharomyces cerevisiae* cells grown at optimal and low pH. *Archives of microbiology* **166,** 315-320.

Cartwright, C. P., Juroszek, J., Beavan, M. J., Ruby, F. M. S., de Morais, S. M. F., Rose, A. H., (1986). Ethanol dissipates the proton-motive force across the plasma-membrane of *Saccharomyces cerevisiae*. *Journal of General Microbiology* **132,** 369-377.

Casal, M., Paiva, S., Andrade, R. P., Gancedo, C., Leão, C., (1999). The lactate-proton symport of *Saccharomyces cerevisiae* is encoded by *JEN1*. *Journal of Bacteriology* **181** (8)**,** 2620-2623.

Casal, M., Queirós, O., Talaia, G., Ribas, D., Paiva, S., 2016. Carboxylic acids plasma membrane transporters in *Saccharomyces cerevisiae*. In: Ramos, J., Sychrová, H., Kschischo, M., Eds.), Yeast Membrane Transport. Springer International Publishing, Cham, pp. 229-251.

Cássio, F., Leão, C., van Uden, N., (1987). Transport of Lactate and Other Short-Chain Monocarboxylates in the Yeast *Saccharomyces cerevisiae*. *Applied and Environmental Microbiology* **53** (3)**,** 509-513.

Chattopadhyay, A., Singh, R., Das, A. K., Maiti, M. K., (2020). Characterization of two sugar transporters responsible for efficient xylose uptake in an oleaginous yeast *Candida tropicalis* SY005. *Archives of Biochemistry and Biophysics* **695** (108645).

Chen, L.-Q., Cheung, L. S., Feng, L., Tanner, W., Frommer, W. B., (2015). Transport of sugars. *Annual Review of Biochemistry* **84** (1)**,** 865-894.

Cherry, J. M., Hong, E. L., Amundsen, C., Balakrishnan, R., Binkley, G., Chan, E. T., Christie, K. R., Costanzo, M. C., Dwight, S. S., Engel, S. R., Fisk, D. G., Hirschman, J. E., Hitz, B. C., Karra, K., Krieger, C. J., Miyasato, S. R., Nash, R. S., Park, J., Skrzypek, M. S., Simison, M., Weng, S., Wong, E. D., (2012). *Saccharomyces* Genome Database: the genomics resource of budding yeast. *Nucleic Acids Research* **40,** D700-D705.

Ciriacy, M., (1975). Genetics of alcohol dehydrogenase in *Saccharomyces cerevisiae*. I. Isolation and genetic analysis of *adh* mutants. *Mutation Research* **29,** 315-326.

Ciriacy, M., Reifenberger, E., 1997. Hexose transport. In: Zimmermann, F. K., Entian, K.-D., Eds.), Yeast sugar metabolism. Technomic Publishing AG, Lancaster, Pensylvania, USA.

Colabardini, A. C., Ries, L. N. A., Brown, N. A., dos Reis, T. F., Savoldi, M., Goldman, M. H. S., Menino, J. F., Rodrigues, F., Goldman, G. H., (2014). Functional characterization of a xylose transporter in *Aspergillus nidulans*. *Biotechnology for Biofuels* **7** (46).

Conant, G. C., Wolfe, K. H., (2007). Increased glycolytic flux as an outcome of whole-genome duplication in yeast. *Molecular Systems Biology* **3** (129).

Conroy, B. B., Bittner, C. J., Donald, J. C. M., Luebbe, M. K., Erickson, G. E., (2016). Effects of feeding isolated nutrient components in MDGS on growing cattle performance. *Nebraska Beef Cattle Reports* **871**.

Dai, Z., Liu, Y., Guo, J., Huang, L., Zhang, X., (2015). Yeast synthetic biology for high-value metabolites. *FEMS yeast Research* **15,** 1-11.

Daran-Lapujade, P., Jansen, M. L. A., Daran, J.-M., van Gulik, W. M., de Winde, J. H., Pronk, J. T., (2004). Role of transcriptional regulation in controlling fluxes in central carbon metabolism of *Saccharomyces cerevisiae*. *The Journal of Biological Chemistry* **279** (10)**,** 9125–9138.

Darbani, B., Stovicek, V., van der Hoek, S. A., Borodina, I., (2019). Engineering energetically efficient transport of dicarboxylic acids in yeast *Saccharomyces cerevisiae*. 201900287.

de Bont, J. A. M., Teunissen, A. W. R. H., Yeast strains engineered to produce ethanol from glycerol. Yeast Company B.V., 2012.

de Bont, J. A. M., Teunissen, A. W. R. H., Klaasen, P., Hartman, W. W. A., van Beusekom, S., Yeast strains engineered to produce ethanol from acetic acid and glycerol. Vol. US 009988649B2. DSM IP ASSETS B.V., 2018.

De Deken, R. H., (1966). The Crabtree effect: A regulatory system in yeast. *Journal of General Microbiology* **44** (2)**,** 149-156.

de Groeve, M. R. M., de Baere, M., Hoflack, L., Desmet, T., Vandamme, E. J., Soetaert, W., (2009). Creating lactose phosphorylase enzymes by directed evolution of cellobiose phosphorylase. *Protein Engineering, Design & Selection* **22** (7)**,** 393-399.

de Groot, D. H., Lischke, J., Muolo, R., Planqué, R., Bruggeman, F. J., Teusink, B., (2020). The common message of constraint-based optimization approaches: overflow metabolism is caused by two growth-limiting constraints. *Cellular and Molecular Life Sciences* **77,** 441–453.

de Kok, S., Kozak, B. U., Pronk, J. T., van Maris, A. J. A., (2012a). Energy coupling in *Saccharomyces cerevisiae*: selected opportunities for metabolic engineering. *FEMS Yeast Research* **12,** 387-397.

de Kok, S., Nijkamp, J. F., Oud, B., Roque, F. C., de Ridder, D., Daran, J.-M. G., Pronk, J. T., van Maris, A. J. A., (2012b). Laboratory evolution of new lactate transporter genes in a *jen1Δ* mutant of *Saccharomyces cerevisiae* and their identification as *ADY2* alleles by whole-genome resequencing and transcriptome analysis. *FEMS Yeast Research* **12,** 359-374.

de Kok, S., Yilmaz, D., Suir, E., Pronk, J. T., Daran, J.-M. G., Van Maris, A. J. A., (2011). Increasing free-energy (ATP) conservation in maltose-grown *Saccharomyces cerevisiae* by expression of a heterologous maltose phosphorylase. *Metabolic Engineering* **13,** 518-526.

de Smidt, O., du Preez, J. C., Albertyn, J., (2008). The alcohol dehydrogenases of *Saccharomyces cerevisiae*: a comprehensive review. *FEMS Yeast Research* **8,** 967–978.

Deak, T., (1978). On the existence of H⁺-symport in yeasts. *Archives of microbiology* **116,** 205-211.

Deamer, D. W., Bramhall, J., (1986). Permeability of lipid bilayers to water and ionic solutes. *Chemistry and Physics of Lipids* **40,** 167-188.

Dekker, W. J. C., Ortiz-Merino, R. A., Kaljouw, A., Battjes, J., Wiering, F. W., Mooiman, C., de la Torre Cortés, P., Pronk, J. T., (2021). Engineering the thermotolerant industrial yeast *Kluyveromyces marxianus* for anaerobic growth. *Metabolic Engineering* **67,** 347-364.

Dekker, W. J. C., Wiersma, S. J., Bouwknegt, J., Mooiman, C., Pronk, J. T., (2019). Anaerobic growth of *Saccharomyces cerevisiae* CEN.PK113-7D does not depend on synthesis or supplementation of unsaturated fatty acids. *FEMS Yeast Research* **19** (6).

Della-Bianca, B. E., Gombert, A. K., (2013). Stress tolerance and growth physiology of yeast strains from the Brazilian fuel ethanol industry. *Antonie van Leeuwenhoek* **104,** 1083-1095.

den Haan, R., Kroukamp, H., Mert, M., Bloom, M., Görgens, J. F., van Zyl, W. H., (2013). Engineering *Saccharomyces cerevisiae* for next generation ethanol production. *Chemical Technology and Biotechnology* **88,** 983–991.

den Haan, R., Rose, S. H., Cripwell, R. A., Trollope, K. M., Myburgh, M. W., Viljoen-Bloom, M., van Zyl, W. H., (2021). Heterologous production of cellulose- and starch-degrading hydrolases to expand *Saccharomyces cerevisiae* substrate utilization: Lessons learnt. *Biotechnology Advances* **53** (107859).

Deng, D., Sun, P., Yan, C., Ke, M., Jiang, X., Xiong, L., Ren, W., Hirata, K., Yamamoto, M., Fan, S., Yan, N., (2015). Molecular basis of ligand recognition and transport by glucose transporters. *Nature* **526,** 391–396.

Dequin, S., (2001). The potential of genetic engineering for improving brewing, wine-making and baking yeasts. *Applied Microbiology and Biotechnology* **56,** 577–588.

Devantier, R., Pedersen, S., Olsson, L., (2005). Characterization of very high gravity ethanol fermentation of corn mash. Effect of glucoamylase dosage, pre-saccharification and yeast strain. *Applied Microbiology and Biotechnology* **68,** 622-629.

DiCarlo, J. E., Norville, J. E., Mali, P., Rios, X., Aach, J., Church, G. M., (2013). Genome engineering in *Saccharomyces cerevisiae* using CRISPR-Cas systems. *Nucleic Acids Research* **41** (7)**,** 4336–4343.

Diderich, J. A., Schepper, M., van Hoek, P., Luttik, M. A., van Dijken, J. P., Pronk, J. T., Klaassen, P., Boelens, H. F. M., Teixeira de Mattos, M. J., van Dam, K., Kruckeberg, A. L., (1999). Glucose uptake kinetics and transcription of *HXT* genes in chemostat cultures of *Saccharomyces cerevisiae*. *The Journal of Biological Chemistry* **274** (22)**,** 15350–15359.

Diezemann, A., Boles, E., (2003). Functional characterization of the Frt1 sugar transporter and of fructose uptake in *Kluyveromyces lactis*. *Current Genetics* **43,** 281-288.

Dragosits, M., Mattanovich, D., (2018). Adaptive laboratory evolution – principles and applications for biotechnology. *Microbial Cell Factories* **12** (64).

Dreyer, I., Horeau, C., Lemaillet, G., Zimmermann, S., Bush, D. R., Rodríguez-Navarro, A., Schachtman, D. P., Spalding, E. P., Sentenac, H., Gaber, R. F., (1999). Identification and characterization of plant transporters using heterologous expression systems. *Journal of Experimental Botany* **50,** 1073-1087.

Duff, K. C., Ashley, R. H., (1992). The transmembrane domain of influenza A M2 protein forms amantadine-sensitive proton channels in planar lipid bilayers. *Virology* **190,** 485-489.

Dunlop, A. P., (1948). Furfural formation and behavior. *Industrial and Engineering Chemistry* **40** (2)**,** 204-209.

Eide, D. J., (1998). The molecular biology of metal ion transport in *Saccharomyces cerevisiae*. *Annual Review of Nutrition* **18,** 441–469.

Entian, K.-D., Kötter, P., (2007). Yeast genetic strain and plasmid collections. *Methods in Microbiology* **36,** 629-666.

Erian, A. M., Egermeier, M., Rassinger, A., Marx, H., Sauer, M., (2020). Identification of the citrate exporter Cex1 of *Yarrowia lipolytica*. *FEMS Yeast Research* **20** (7).

Eriksson, P., André, L., Ansell, R., Blomberg, A., Adler, L., (1995). Cloning and characterization of *GPD2*, a second gene encoding *sn*-glycerol 3-phosphate dehydrogenase (NAD+) in *Saccharomyces cerevisiae*, and its comparison with *GPD1*. *Molecular Microbiology* **17,** 95-107.

Farwick, A., Bruder, S., Schadeweg, V., Oreb, M., Boles, E., (2014). Engineering of yeast hexose transporters to transport D-xylose without inhibition by D-glucose. *PNAS* **111** (14)**,** 5159–5164.

Forrest, L. R., Krämer, R., Ziegler, C., (2011). The structural basis of secondary active transport mechanisms. *Biochimica et Biophysica Acta* **1807,** 167–188.

Fritscher, C., Messner, R., Kubicek, C. P., (1990). Cellobiose metabolism and cellobiohydrolase I Biosynthesis by *Trichoderma reesei*. *Experimental Mycology* **14** (4)**,** 405-415.

Gabba, M., Frallicciardi, J., van 't Klooster, J., Henderson, R., Syga, L., Mans, R., van Maris, A. J. A., Poolman, B., (2020). Weak Acid Permeation in Synthetic Lipid Vesicles and Across the Yeast Plasma Membrane. *Biophysical Journal* **118,** 422-434.

Gadsby, D. C., (2009). Ion channels versus ion pumps: the principal difference, in principle. *Nature Reviews Molecular Cell Biology volume* **10,** 344–352.

Galeote, V., Novo, M., Salema-Oom, M., Brion, C., Valério, E., Gonçalves, P., Dequin, S., (2010). *FSY1,* a horizontally transferred gene in the *Saccharomyces cerevisiae* EC1118 wine yeast strain, encodes a high-affinity fructose/H+ symporter. *Microbiology* **156,** 3754–3761.

Gao, M., Ploessl, D., Shao, Z., (2019). Enhancing the co-utilization of biomass-derived mixed sugars by yeasts. *Frontiers in Microbiology* **9** (3264).

Gardner, P. R., Fridovich, I., (1991). Superoxide sensitivity of *Escherichia coli* 6-phosphogluconate dehydratase. *The Journal of Biological Chemistry* **266** (3)**,** 1478-1283.

Gascón, S., Lampen, J. O., (1968). Purification of the internal invertase of yeast. *Journal of Biological Chemistry* **243** (7)**,** 1567-1572.

Gibson, D. G., Benders, G. A., Andrews-Pfannkoch, C., Denisova, E. A., Baden-Tillson, H., Zaveri, J., Stockwell, T. B., Brownley, A., Thomas, D. W., Algire, M. A., Merryman, C., Young, N., Noskov, V. N., Glass, J. I., Venter, J. C., Hutchison, C. A., Smith, H. O., (2008). Complete chemical synthesis, assembly, and cloning of a *Mycoplasma genitalium* genome. *Science* **319** (5867)**,** 1215-1220.

Gietz, R. D., Woods, R. A., (2002). Transformation of yeast by lithium acetate/single-stranded carrier DNA/polyethylene glycol method. *Methods in Enzymology* **350,** 87-96.

Glick, B. R., (1995). Metabolic load and heterologous gene expression. *Biotechnology Advances* **13** (2)**,** 247-261.

Goel, A., Eckhardt, T. H., Puri, P., de Jong, A., Branco dos Santos, F., Giera, M., Fusetti, F., de Vos, W. M., Kok, J., Poolman, B., Molenaar, D., Kuipers, O. P., Teusink, B., (2015). Protein costs do not explain evolution of metabolic strategies and regulation of ribosomal content: does protein investment explain an anaerobic bacterial Crabtree effect? *Molecular Microbiology* **97** (1)**,** 77–92.

Goffeau, A., Barrell, B. G., Bussey, H., Davis, R. W., Dujon, B., Feldmann, H., Galibert, F., Hoheisel, J. D., Jacp, C., Johnston, M., Louis, E. J., Mewes, H. W., Murakami, Y., Philippsen, P., Tettelin, H., Oliver, S. G., (1996). Life with 6000 genes. *Science* **274** (546)**,** 563-567.

Gomes, D., Cruz, M., de Resende, M., Ribeiro, E., Teixeira, J., Domingues, L., (2021). Very high gravity bioethanol revisited: Main challenges and advances. *Fermentation* **7** (38).

Gonçalves, D. L., Matsushika, A., de Sales, B. B., Goshima, T., Bon, E. P. S., Stambuk, B. U., (2014). Xylose and xylose/glucose co-fermentation by recombinant *Saccharomyces cerevisiae* strains expressing individual hexose transporters. *Enzyme and Microbial Technology* **63,** 13-20.

Gonçalves, P., Rodrigues de Sousa, H., Spencer-Martins, I., (2000). *FSY1*, a Novel Gene Encoding a Specific Fructose/H^{+} Symporter in the Type Strain of *Saccharomyces carlsbergensis*. *Journal of Bacteriology* **182** (19)**,** 5628–5630.

González-Ramos, D., Gorter de Vries, A. R., Grijseels, S. S., van Berkum, M. C., Swinnen, S., van den Broek, M., Nevoigt, E., Daran, J. M., Pronk, J. T., van Maris, A. J. A., (2016). A new laboratory evolution approach to select for constitutive acetic acid tolerance in *Saccharomyces cerevisiae* and identification of causal mutations. *Biotechnology for Biofuels* **9** (173).

Gopal, C. V., Broad, D., Lloyd, D., (1989). Bioenergetic consequences of protein overexpression in *Saccharomyces cerevisiae*. *Applied Microbiology and Biotechnology* **30,** 160-165.

Grisshammer, R., Tate, C. G., (2009). Overexpression of integral membrane proteins for structural studies. *Quartely Reviews of Biophysics* **28** (3)**,** 315-422.

Guadalupe-Medina, V., Wisselink, H. W., Luttik, M. A. H., de Hulster, E., Daran, J.-M., Pronk, J. T., van Maris, A. J. A., (2013). Carbon dioxide fixation by Calvin-Cycle enzymes improves ethanol yield in yeast. *Biotechnology for Biofuels* **6** (125).

Guadalupe-Medina, V., Metz, B., Oud, B., van Der Graaf, C. M., Mans, R., Pronk, J. T., van Maris, A. J., (2014). Evolutionary engineering of a glycerol-3-phosphate dehydrogenase-negative, acetate-reducing *Saccharomyces cerevisiae* strain enables anaerobic growth at high glucose concentrations. *Microbial biotechnology* **7** (1)**,** 44-53.

Guadalupe Medina, V., Almering, M. J., van Maris, A. J., Pronk, J. T., (2010). Elimination of glycerol production in anaerobic cultures of a *Saccharomyces cerevisiae* strain engineered to use acetic acid as an electron acceptor. *Appl. Environ. Microbiol.* **76** (1)**,** 190-195.

Guiard, B., (1985). Structure, expression and regulation of a nuclear gene encoding a mitochondrial protein: the yeast L(+)-lactate cytochrome *c* oxidoreductase (cytochrome b_2). *The EMBO Journal* **4** (12), 3265-3272.

Guimarães, P. M. R., Londesborough, J., (2008). The adenylate energy charge and specific fermentation rate of brewer's yeasts fermenting high- and very high-gravity worts. *Yeast* **25** (1)**,** 47-58.

Güldener, U., Heck, S., Fiedler, T., Beinhauer, J., Hegemann, J. H., (1996). A new efficient gene disruption cassette for repeated use in budding yeast. *Nucleic Acids Research* **24** (13)**,** 2519–2524.

Guo, Z.-p., Zhang, L., Ding, Z.-y., Shi, G.-y., (2011). Minimization of glycerol synthesis in industrial ethanol yeast without influencing its fermentation performance. *Metabolic Engineering* **13,** 49–59.

Haferkamp, I., Linka, N., (2012). Functional expression and characterisation of membrane transport proteins. *Plant Biology* **14,** 675–690.

Hahn-Hägerdal, B., Karhumaa, K., Jeppsson, M., Gorwa-Grauslund, M. F., (2007). Metabolic engineering for pentose utilization in *Saccharomyces cerevisiae*. *Advances in Biochemical Engineering and Biotechnology* **108,** 147-177.

Han, E.-K., Cotty, F., Sottas, C., Jiang, H., Michels, C. A., (1995). Characterization of *AGT1* encoding a general α-glucoside transporter from *Saccharomyces*. *Molecular Microbiology* **17** (6)**,** 1093-1107.

Hatti-Kaul, R., 2010. Downstream processing in industrial biotechnology. In: Soetaert, W., Vandamme, E. J., Eds.), Industrial biotechnology: Sustainable growth and economic success. Wiley-VCH.

Hawthorne, D. C., (1958). The genetics of alpha-methyl-glucoside fermentation in *Saccharomyces*. *Heredity* **12** (3)**,** 273-284.

Henderson, R. K., Ayudya, L. N., Poolman, B., (2019a). Characterization of maltose-binding residues in the central cavity of Mal11. *In: On the mechanism of proton-coupled transport by the maltose permease of Saccharomyces cerevisiae (PhD Thesis)*.

Henderson, R. K., de Valk, S. C., Poolman, B., Mans, R., (2021). Energy coupling of membrane transport and efficiency of sucrose dissimilation in yeast. *Metabolic Engineering* **65,** 243–254.

Henderson, R. K., Fendler, K., Poolman, B., (2019b). Coupling efficiency of secondary active transporters. *Current Opinion in Biotechnology* **58,** 62-71.

Henderson, R. K., Poolman, B., (2017). Proton-solute coupling mechanism of the maltose transporter from *Saccharomyces cerevisiae*. *Scientific Reports* **7** (14375).

Hennaut, C., Hilger, F., Grenson, M., (1970). Space limitation for permease insertion in the cytoplasmic membrane of *Saccharomyces cerevisiae*. *Biochemical and Biophysical Research Communications* **39** (4).

Henningsen, B. M., Hon, S., Covalla, S. F., Sonu, C., Argyros, D. A., Barrett, T. F., Wiswall, E., Froehlich, A. C., Zelle, R. M., (2015). Increasing anaerobic acetate consumption and ethanol yields in *Saccharomyces cerevisiae* with NADPH-specific alcohol dehydrogenase. *Applied and environmental microbiology* **81** (23), 8108-8117.

Henriques, D., Minebois, R., Mendoza, S. N., Macías, L. G., Pérez-Torrado, R., Barrio, E., Teusink, B., Querol, A., Balsa-Canto, E., (2021). A multiphase multiobjective dynamic genome-scale model shows different redox balancing among yeast species of the *Saccharomyces* genus in fermentation. *mSystems* **6** (4).

Heredia, C. F., de la Fuenta, G., Sols, A., (1964). Metabolic studies with 2-deoxyhexoses. I. Mechanisms of inhibition of growth and fermentation in baker's yeast. *Biochimica et Biophysica Acta* **86** (2), 216-223.

Hernandez, J. M., Baker, S. H., Lorbach, S. C., Shively, S. M., Tabita, F. R., (1996). Deduced amino acid sequence, functional expression, and unique enzymatic properties of the form I and form II ribulose bisphosphate carboxylase/oxygenase from the chemoautotrophic bacterium *Thiobacillus denitrificans*. *Journal of Bacteriology* **178** (2), 347–356.

Higgins, C. F., (1992). ABC transporters: From microorganism to man. *Annual Reviews of Cell Biology* **8,** 67-113.

Hong, K.-K., Hou, J., Shoaie, S., Nielsen, J., Bordel, S., (2012). Dynamic 13C-labeling experiments prove important differences in protein turnover rate between two *Saccharomyces cerevisiae* strains. *FEMS Yeast Research* **12** (7), 741-747.

Horák, J., (2013). Regulations of sugar transporters: insights from yeast. *Current Genetics* **59** (1), 1-31.

Hu, Y., Zhu, Z., Nielsen, J., Siewers, V., (2018). Heterologous transporter expression for improved fatty alcohol secretion in yeast. *Metabolic Engineering* **45,** 51–58.

Huang, W., Hu, B., Liu, J., Zhou, Y., Liu, S., (2020). Identification and characterization of tonoplast sugar transporter (TST) gene family in cucumber. *Horticultural Plant Journal* **6** (3), 145–157.

Hubmann, G., Guillouet, S., Nevoigt, E., (2011). Gpd1 and Gpd2 fine-tuning for sustainable reduction of glycerol formation in *Saccharomyces cerevisiae*. *Applied and environmental microbiology* **77** (17), 5857-5867.

Hudson, G., Morell, M., Arvidsson, Y., Andrews, T., (1992). Synthesis of spinach phosphoribulokinase and ribulose-1,5-bisphosphate in *Escherichia coli*. *Functional Plant Biology* **19,** 213-221.

Ikeda, M., Arai, M., Lao, D. M., Shimizu, T., (2002). Transmembrane topology prediction methods: A re-assessment and improvement by a consensus method using a dataset of experimentally-characterized transmembrane topologies. *In Silico Biology* **2,** 19-33.

Ingledew, W. M., 2017. Yeast stress and fermentation. In: Walker, G. M., Abbas, C. A., Ingledew, W. M., Pilgrim, C., Eds.), The Alcohol Textbook. Duluth, pp. 273-285.

Jacobus, A. P., Gross, J., Evans, J. H., Ceccato-Antonini, S. R., Gombert, A. K., (2021). *Saccharomyces cerevisiae* strains used industrially for bioethanol production. *Essays in Biochemistry* **65,** 147–161.

Jansen, M. L. A., Bracher, J. M., Papapetridis, I., Verhoeven, M. D., de Bruin, H., de Waal, P. P., van Maris, A. J. A., Klaassen, P., Pronk, J. T., (2017a). *Saccharomyces cerevisiae* strains for second-generation ethanol production: from academic exploration to industrial implementation. *FEMS Yeast Research* **17** (5).

Jansen, M. L. A., Daran-Lapujade, P., de Winde, J. H., Piper, M. D. W., Pronk, J. T., (2004). Prolonged maltose-limited cultivation of *Saccharomyces cerevisiae* selects for cells with improved maltose affinity and hypersensitivity. *Applied and Environmental Microbiology* **70** (4), 1956–1963.

Jansen, M. L. A., Heijnen, J. J., Verwaal, R., Process for preparing dicarboxylic acids employing fungal cells. DSM IP Assets B.V., 2017b.

Jansen, M. L. A., Krook, D. J. J., De Graaf, K., van Dijken, J. P., Pronk, J. T., de Winde, J. H., (2006). Physiological characterizationand fed-batch production of an extracellular maltase of *Schizosaccharomyces pombe* CBS356. *FEMS Yeast Research* **6,** 888-901.

Jarvis, S. M., 2000. Assay of membrane transport in cells and membrane vesicles. In: Baldwin, S. A., (Ed.), Membrane transport: A practical approach. Oxford University Press, Oxford.

Jensen, P. R., Snoep, J. L., Westerhoff, H. V., Method for improving the production of biomass or a desired product from a cell. Vol. US 7250280B2. Peter Ruhdal Jensen, 2007.

Jessen-Marshall, A. E., Parker, N. J., Brooker, R. J., (1997). Suppressor analysis of mutations in the loop 2-3 motif of lactose permease: evidence that glycine-64 is an important residue for conformational changes. *Journal of Bacteriology* **179** (8)**,** 2616-2622.

Jollow, D., Kellerman, G. M., Linnane, A. W., (1968). The biogenesis of mitochondria III. The lipid composition of aerobically and anaerobically grown *Saccharomyces cerevisiae* as related to the membrane systems of the cells. *The Journal of Cell Biology* **37** (2)**,** 221-230.

Jordan, P., Choe, J.-y., Boles, E., Oreb, M., (2016). Hxt13, Hxt15, Hxt16 and Hxt17 from *Saccharomyces cerevisiae* represent a novel type of polyol transporters. *Scientific Reports* **6** (23502).

Jørgensen, H., (2009). Effect of nutrients on fermentation of pretreated wheat straw at very high dry matter content by *Saccharomyces cerevisiae*. *Applied Biochemistry and Biotechnology* **153,** 44–57.

Jumper, J., Evans, R., Pritzel, A., Green, T., Figurnov, M., Ronneberger, O., Tunyasuvunakool, K., Bates, R., Žídek, A., Potapenko, A., Bridgland, A., Meyer, C., Kohl, S. A. A., Ballard, A. J., Cowie, A., Romera-Paredes, B., Nikolov, S., Jain, R., Adler, J., Back, T., Petersen, S., Reiman, D., Clancy, E., Zielinski, M., Steinegger, M., Pacholska, M., Berghammer, T., Bodenstein, S., Silver, D., Vinyals, O., Senior, A. W., Kavukcuoglu, K., Kohli, P., Hassabis, D., (2021). Highly accurate protein structure prediction with AlphaFold. *Nature* **596,** 583-589.

Karathia, H., Vilaprinyo, E., Sorribas, A., Alves, R., (2011). *Saccharomyces cerevisiae* as a model organism: A comparative study. *PLoS ONE* **6** (2).

Kim, H., Lee, W.-H., Galazka, J. M., Cate, J. H. D., Jin, Y.-S., (2014). Analysis of cellodextrin transporters from *Neurospora crassa* in *Saccharomyces cerevisiae* for cellobiose fermentation. *Applied Microbiology and Biotechnology* **98,** 1087-1094.

Kim, Y., Mosier, N. S., Hendrickson, R., Ezeji, T., Blaschek, H., Dien, B., Cotta, M., Dale, B., Ladisch, M. R., (2008). Composition of corn dry-grind ethanol by-products: DDGS, wet cake, and thin stillage. *Bioresource Technology* **99,** 5165–5176.

Klaassen, P., Hartman, W. W. A., Glycerol and acetic acid converting yeast cells with improved acetic acid conversion. In: B.V., D. I. A., (Ed.), Vol. US 010450588B2. DSM IP ASSETS B.V., 2019.

Klein, M., Swinnen, S., Thevelein, J. M., Nevoigt, E., (2017). Glycerol metabolism and transport in yeast and fungi: established knowledge and ambiguities. *Environmental Microbiology* **19** (3)**,** 878–893.

Kötter, P., Ciriacy, M., (1993). Xylose fermentation by *Saccharomyces cerevisiae*. *Applied Microbiology and Biotechnology* **38,** 776-783.

Kozak, B. U., van Rossum, H. M., Benjamin, K. R., Wu, L., Daran, J.-M. G., Pronk, J. T., van Maris, A. J., (2014). Replacement of the *Saccharomyces cerevisiae* acetyl-CoA synthetases by alternative pathways for cytosolic acetyl-CoA synthesis. *Metabolic engineering* **21,** 46-59.

Kruckeberg, A. L., (1996). The hexose transporter family of *Saccharomyces cerevisiae*. *Archives of microbiology* **166,** 283–292.

Kruckeberg, A. L., Dickinson, J. R., 2004. Carbon Metabolism. In: Dickinson, J. R., Schweizer, M., Eds.), The metabolism and molecular physiology of *Saccharomyces cerevisiae*. Taylor & Francis Ltd, London, pp. 42-103.

Kschischo, M., Ramos, J., Sychrová, H., 2016. Membrane transport in yeast, an introduction. In: Ramos, J., Sychrová, H., Kschischo, M., Eds.), Yeast Membrane Transport. Springer International Publishing, Cham, pp. 1-10.

Kuijpers, N. G., Solis-Escalante, D., Bosman, L., van den Broek, M., Pronk, J. T., Daran, J.-M., Daran-Lapujade, P., (2013). A versatile, efficient strategy for assembly of multi-fragment expression vectors in *Saccharomyces cerevisiae*

using 60 bp synthetic recombination sequences. *Microbial cell factories* **12,** 47.

Kurylenko, O. O., Ruchala, J., Hryniv, O. B., Abbas, C. A., Dmytruk, K. V., Sibirny, A. A., (2014). Metabolic engineering and classical selection of the methylotrophic thermotolerant yeast *Hansenula polymorpha* for improvement of high-temperature xylose alcoholic fermentation. *Microbial Cell Factories* **13** (122).

Lagunas, R., (1993). Sugar transport in *Saccharomyces cerevisiae*. *FEMS Microbiology Reviews* **104,** 229-242.

Laizé, A., Tacnet, F., Ripoche, P., Hohmann, S., (2000). Polymorphism of *Saccharomyces cerevisiae* aquaporins. *Yeast* **16,** 897-903.

Laluce, C., Schenberg, A. C. G., Gallardo, J. C. M., Coradello, L. F. C., Pombeiro-Sponchiado, S. R., (2012). Advances and developments in strategies to improve strains of *Saccharomyces cerevisiae* and processes to obtain the lignocellulosic ethanol—A review. *Applied Biochemistry and Biotechnology* **166,** 1908–1926.

Lam, V. H., Lee, J.-H., Silverio, A., Chan, H., Gomolplitinant, K. M., Povolotsky, T. L., Orlova, E., Sun, E. I., Welliver, C. H., Saier, M. H. J., (2011). Pathways of transport protein evolution: Recent advances. *Journal of Biological Chemistry* **392,** 5-12.

Lancashire, W. E., Dickinson, J. R., Malloch, R. A., DNA encoding enzymes of the glycolytic pathway of for use in alcohol producing yeast. Vol. US 005786186A. Cardiff University College Consultants Ltd Whitbread PLC, USA, 1994.

Lane, I., Lallemand acquires patent for pathways which reduce glycerol production. Biofuels Digest, 2015.

Lane, J., The battle for yeast supremacy: DSM, DuPont, Novozymes and more. Biofuels Digest, 2018.

Lange, H. C., Heijnen, J. J., (2001). Statistical reconciliation of the elemental and molecular biomass composition of *Saccharomyces cerevisiae*. *Biotechnology and Bioengineering* **75** (3)**,** 334-344.

Lazar, Z., Neuvéglise, C., Rossignol, T., Devillers, H., Morin, N., Robak, M., Nicaud, J., Crutz-Le Coq, A.-M., (2017). Characterization of hexose transporters in *Yarrowia lipolytica* reveals new groups of Sugar Porters involved in yeast growth. *Fungal Genetics and Biology* **100,** 1–12.

Leandro, M. J., Gonçalves, P., Spencer-Martins, I., (2006). Two glucose/xylose transporter genes from the yeast *Candida intermedia*: first molecular characterization of a yeast xylose–H$^+$ symporter. *Biochemical Journal* **395,** 543–549.

Leandro, M. J., Sychrová, H., Prista, C., Loureiro-Dias, M. C., (2011). The osmotolerant fructophilic yeast *Zygosaccharomyces rouxii* employs two plasmamembrane fructose uptake systems belonging to a new family of yeast sugar transporters. *Microbiology* **157,** 601–608.

Lear, J. D., Wasserman, Z. R., Degrado, W. F., (1988). Synthetic amphiphilic peptide models for protein ion channels. *Science* **240** (4856)**,** 1177-1181.

Lee, K. J., Skotnicki, M. L., Tribe, D. E., Rogers, P. L., (1980). Kinetic studies on a highly productive strain of *Zymomonas mobilis*. *Biotechnology Letters* **2** (8)**,** 339-344.

Lewis, S., Options expand for effective bacterial control in ethanol production. Ethanol Producer Magazine, 2016.

Li, H., Durbin, R., (2010). Fast and accurate long-read alignment with Burrows–Wheeler transform. *Bioinformatics* **26** (5)**,** 589-595.

Li, H., Handsaker, B., Wysoker, A., Fennell, T., Ruan, J., Homer, N., Marth, G., Abecasis, G., Durbin, R., Subgroup, G. P. D. P., (2009). The Sequence Alignment/Map format and SAMtools. *Bioinformatics* **25** (16)**,** 2078-2079.

Li, H., Schmitz, O., Alper, H. S., (2016). Enabling glucose/xylose co-transport in yeast through the directed evolution of a sugar transporter. *Applied Microbiology and Biotechnology* **100,** 10215–10223.

Li, J., Xu, J., Cai, P., Wang, B., Ma, Y., Benz, J. P., Tian, C., (2015). Functional analysis of two L-arabinose transporters from filamentous fungi reveals promising characteristics for improved pentose utilization in *Saccharomyces cerevisiae*. *Applied and Environmental Microbiology* **81** (12)**,** 4062–4070.

Li, Y.-J., Wang, M.-M., Chen, Y.-W., Wang, M., Fan, L.-H., Tan, T.-W., (2017). Engineered yeast with a CO_2-fixation pathway to improve the bio-ethanol production from xylose-mixed sugars. *Scientific reports* **7** (1)**,** 1-9.

Lian, J., Mishra, S., Zhao, H., (2018). Recent advances in metabolic engineering of *Saccharomyces cerevisiae*: New tools and their applications. *Metabolic Engineering* **50,** 85–108.

Liang, Z., Liu, D., Lu, X., Zong, H., Song, J., Zhuge, B., (2018). Identification and characterization from *Candida glycerinogenes* of hexose transporters having high efficiency at high glucose concentrations. *Applied Microbiology and*

Biotechnology **102,** 5557–5567.

Lim, H. G., Eng, T., Banerjee, D., Alarcon, G., Lau, A. K., Park, M., Simmons, B. A., Palsson, B. O., Singer, S. W., Mukhopadhyay, A., Feist, A. M., (2021). Generation of *Pseudomonas putida* KT2440 strains with efficient utilization of xylose and galactose via adaptive laboratory evolution. *ACS Sustainable Chemistry & Engineering* **9,** 11512–11523.

Lolkema, J. S., Poolman, B., (1995). Uncoupling in secondary transport proteins. A mechanistic explanation for mutants of *lac* permease with an uncoupled phenotype. *Journal of Biological Chemistry* **270** (21)**,** 12670-12676.

Lõoke, M., Kristjuhan, K., Kristjuhan, A., (2011). Extraction of genomic DNA from yeasts for PCR-based applications. *BioTechniques* **50,** 325-328.

Lopes, H., Rocha, I., (2017). Genome-scale modeling of yeast: chronology, applications and critical perspectives. *FEMS Yeast Research* **17** (5).

Loureiro-Dias, M. C., (1988). Movements of protons coupled to glucose transport in yeasts. A comparative study among 248 yeast strains. *Antonie van Leeuwenhoek* **54,** 331-343.

Luttik, M. A., Kötter, P., Salomons, F. A., van der Klei, I. J., van Dijken, J. P., Pronk, J. T., (2000). The *Saccharomyces cerevisiae ICL2* gene encodes a mitochondrial 2-methylisocitrate lyase involved in propionyl-coenzyme A metabolism. *Journal of Bacteriology* **182** (24)**,** 7007-7013.

Madigan, M., Martinko, J., Stahl, D., Clark, D., 2011. Brock Biology of Microorganisms. Pearson Education.

Malpartida, F., Serrano, R., (1981). Proton translocation catalyzed by the purified yeast plasma membrane ATPase reconstituted in liposomes. *FEBS letters* **131** (2)**,** 351-354.

Mans, R., Daran, J.-M. G., Pronk, J. T., (2018). Under pressure: evolutionary engineering of yeast strains for improved performance in fuels and chemicals production. *Current Opinion in Biotechnology* **50,** 47-56.

Mans, R., Hassing, J.-E., Wijsman, M., Giezekamp, A., Pronk, J. T., Daran, J.-M. G., Van Maris, A. J. A., (2017). A CRISPR/Cas9-based exploration into the elusive mechanism for lactate export in *Saccharomyces cerevisiae*. *FEMS Yeast Research* **17,** 1-12.

Mans, R., van Rossum, H. M., Wijsman, M., Backx, A., Kuijpers, N., van den Broek, M., Daran-Lapujade, P., Pronk, J. T., van Maris, A. J. A., Daran, J.-M. G., (2015). CRISPR/Cas9: a molecular Swiss army knife for simulaneous introduction of multiple genetic modifications in *Saccharomyces cerevisiae*. *FEMS Yeast Research* **15,** 1-15.

Marini, A.-M., Soussi-Boudekou, S., Vissers, S., Andre, B., (1997). A family of ammonium transporters in *Saccharomyces cerevisiae*. *17* **8** (4282-4293).

Marques, W. L., Mans, R., Henderson, R. K., Marella, E. R., Horst, J. T., Hulster, E., Poolman, B., Daran, J. M., Pronk, J. T., Gombert, A. K., van Maris, A. J. A., (2018a). Combined engineering of disaccharide transport and phosphorolysis for enhanced ATP yield from sucrose fermentation in *Saccharomyces cerevisiae*. *Metabolic Engineering* **45,** 121-133.

Marques, W. L., Mans, R., Marella, E. R., Cordeiro, R. L., Van den Broek, M., Daran, J.-M. G., Pronk, J. T., Gombert, A. K., van Maris, A. J. A., (2017). Elimination of sucrose transport and hydrolysis in *Saccharomyces cerevisiae*: a platform strain for engineering sucrose metabolism. *FEMS Yeast Research* **17,** 1-11.

Marques, W. L., Raghavendran, V., Stambuk, B. U., Gombert, A. K., (2015). Sucrose and *Saccharomyces cerevisiae*: a relationship most sweet. *FEMS Yeast Research* **16** (1).

Marques, W. L., van der Woude, L. N., Luttik, M. A. H., van den Broek, M., Nijenhuis, J. M., Pronk, J. T., van Maris, A. J. A., Mans, R., Gombert, A. K., (2018b). Laboratory evolution and physiological analysis of *Saccharomyces cerevisiae* strains dependent on sucrose uptake via the *Phaseolus vulgaris* Suf1 transporter. *Yeast* **35** (12)**,** 639-652.

McGovern, P. E., Zhang, J., Tang, J., Zhang, Z., Hall, G. R., Moreau, R. A., Nuñez, A., Butrym, E. D., Richards, M. P., Wang, C.-S., Cheng, G., Zhao, Z., Wang, C., (2004). Fermented beverages of pre- and proto-historic China. *PNAS* **101** (51)**,** 17593–17598.

Meadows, A. L., Hawkins, K. M., Tsegaye, Y., Antipov, E., Kim, Y., Raetz, L., Dahl, R. H., Tai, A., Mahatdejkul-Meadows, T., Xu, L., (2016). Rewriting yeast central carbon metabolism for industrial isoprenoid production. *Nature* **537** (7622)**,** 694-697.

Merico, A., Sulo, P., Piškur, J., Compagno, C., (2007). Fermentative lifestyle in yeasts belonging to the *Saccharomyces* complex. *FEBS Journal* **274,** 976–989.

Mishra, N. K., Chang, J., Zhao, P. X., (2014). Prediction of membrane transport proteins and their substrate specificities

using primary sequence information. *PLoS ONE* **9** (6).

Mitchell, P., (1961). Coupling of phosphorylation to electron and hydrogen transfer by a chemi-osmotic type of mechanism. *Nature* **4784,** 144-148.

Mitchell, P., (1966). Chemiosmotic coupling in oxidative and photosynthetic oxidation.

Mohsenzadeh, A., Zamani, A., Taherzadeh, M. J., (2017). Bioethylene production from ethanol: A review and techno-economical evaluation. *ChemBioEng Reviews* **4** (2)**,** 75–91.

Möller, S., Croning, M. D. R., Apweiler, R., (2001). Evaluation of methods for the prediction of membrane spanning regions. *Bioinformatics* **17** (7)**,** 646–653.

Monnard, P.-A., Deamer, D. W., 2010. Membrane self-assembly processes: Steps toward the first cellular life. In: Luisi, P. L., Stano, P., Eds.), The minimal cell: the biophysics of cell compartment and the origin of cell functionality. Springer Science+Business Media B.V., Springer Dordrecht Heidelberg London New York.

Monteiro, G. A., Supply, P., Goffeau, A., Sá-Correia, I., (1994). The *in vivo* Activation of *Saccharomvces cerevisiae* Plasma Membrane H^{+}-ATPase by Ethanol depends on the Expression of the *PMA1* Gene, but not of the *PMA2* Gene. *Yeast* **10,** 1439-1446.

Moraes, I., Evans, G., Sanchez-Weatherby, J., Newstead, S., Stewart, P. D. S., (2014). Membrane protein structure determination — The next generation. *Biochimica et Biophysica Acta* **1838,** 78–87.

Morii, M., Sugihara, A., Takehara, S., Kanno, Y., Kawai, K., Hobo, T., Hattori, M., Yoshimura, H., Seo, M., Ueguchi-Tanaka, M., (2020). The dual function of OsSWEET3a as a gibberellin and glucose transporter is important for young shoot development in rice. *Plant Cell Physiology* **61** (11)**,** 1935–1945.

Morita, K., Nomura, Y., Ishii, J., Matsuda, F., Kondo, A., Shimizu, H., (2017). Heterologous expression of bacterial phosphoenol pyruvate carboxylase and Entner-Doudoroff pathway in *Saccharomyces cerevisiae* for improvement of isobutanol production. *Journal of Bioscience and Bioengineering* **124** (3)**,** 263-270.

Mulkidjanian, A. Y., Dibrov, P., Galperin, M. Y., (2008). The past and present of sodium energetics: May the sodium-motive force be with you. *Biochimica et Biophysica Acta* **1777,** 985–992.

Mumberg, D., Müller, R., Funk, M., (1995). Yeast vectors for the controlled expression of heterologous proteins in different genetic backgrounds. *Gene* **156,** 119-122.

Mustacchi, R., Hohmann, S., Nielsen, J., (2006). Yeast systems biology to unravel the network of life. *Yeast* **23,** 227–238.

Nagle, J. F., Scott, H. L. J., (1978). Lateral compressibility of lipid mono- and bilayers. Theory of membrane permeability. *Biochimica et Biophysica Acta* **513** (2)**,** 236-243.

Narendranath, N. V., Thomas, K. C., Ingledew, W. M., (2001). Acetic acid and lactic acid inhibition of growth of *Saccharomyces cerevisiae* by different mechanisms. *Journal of the American Society of Brewing Chemists* **59,** 187-194.

Navarrete, C., Nielsen, J., Siewers, V., (2014). Enhanced ethanol production and reduced glycerol formation in *fps1Δ* mutants of *Saccharomyces cerevisiae* engineered for improved redox balancing. *AMB Express* **4** (86).

Navas, M. A., Cerdán, S., Gancedo, C., (1993). Futile cycles in *Saccharomyces cerevisiae* strains expressing the gluconeogenic enzymes during growth on glucose. *PNAS* **90** (4)**,** 1290-1294.

Navas, M. A., Gancedo, C., (1996). The regulatory characteristics of yeast fructose-1,6-bisphosphatase confer only a small selective advantage. *Journal of Bacteriology* **178** (7)**,** 1809–1812.

Nelson, N., Taiz, L., (1989). The evolution of H^{+}-ATPases. *Trends in Biochemical Sciences* **14** (3)**,** 113-116.

Nevado, J., Navarro, M. A., Heredia, C. F., (1994). Transport of hexoses in yeast. Re-examination of the Sugar Phosphorylation Hypothesis with a New Experimental Approach. *Yeast* **10,** 59-65.

Nevoigt, E., (2008). Progress in metabolic engineering of *Saccharomyces cerevisiae*. *Microbiology and Molecular Biology Reviews* **72** (3)**,** 379–412.

Niebel, B., Leupold, S., Heinemann, M., (2019). An upper limit on Gibbs energy dissipation governs cellular metabolism. *Nature Metabolism* **1,** 125–132.

Nielsen, J., (2001). Metabolic Engineering. *Applied Microbiology and Biotechnology* **55,** 263–283.

Nijkamp, J. F., van den Broek, M., Datema, E., de Kok, S., Bosman, L., Luttik, M. A., Daran-Lapujade, P., Vongsangnak,

W., Nielsen, J., Heijne, W. H. M., Klaasen, P., Paddon, C. J., Platt, D., Kötter, P., van Ham, R. C., Reinders, M. J. T., Pronk, J. T., de Ridder, D., Daran, J.-M. G., (2012). *De novo* sequencing, assembly and analysis of the genome of the laboratory strain *Saccharomyces cerevisiae* CEN.PK113-7D, a model for modern industrial biotechnology. *Microbial Cell Factories* **11** (36)**,** 1-16.

Nijland, J. G., Driessen, A. J. M., (2020). Engineering of pentose transport in *Saccharomyces cerevisiae* for biotechnological applications. *Frontiers in Bioengineering and Biotechnology* **7** (464).

Nijland, J. G., Shin, H. Y., de Jong, R. M., de Waal, P. P., Klaassen, P., Driessen, A. J. M., (2014). Engineering of an endogenous hexose transporter into a specific D-xylose transporter facilitates glucose-xylose co-consumption in *Saccharomyces cerevisiae*. *Biotechnology for Biofuels* **7** (168).

Nijland, J. G., Shin, H. Y., de Waal, P. P., Klaassen, P., Driessen, A. J. M., (2017). Increased xylose affinity of Hxt2 through gene shuffling of hexose transporters in *Saccharomyces cerevisiae*. *Journal of Applied Microbiology* **124,** 503-510.

Nijland, J. G., Vos, E., Shin, H. Y., de Waal, P. P., Klaassen, P., Driessen, A. J. M., (2016). Improving pentose fermentation by preventing ubiquitination of hexose transporters in *Saccharomyces cerevisiae*. *Biotechnology for Biofuels* **9** (158).

Nikaido, H., (2003). Molecular basis of bacterial outer membrane permeability revisited. *Microbiology and Molecular Biology Reviews* **67** (4)**,** 593–656.

Nissen, T. L., Anderlund, M., Nielsen, J., Villadsen, J., Kielland-Brandt, M. C., (2001). Expression of a cytoplasmic transhydrogenase in *Saccharomyces cerevisiae* results in formation of 2-oxoglutarate due to depletion of the NADPH pool. *Yeast* **18** (1)**,** 19-32.

Nissen, T. L., Hamann, C. W., Kielland-Brandt, M. C., Nielsen, J., Villadsen, J., (2000a). Anaerobic and aerobic batch cultivations of *Saccharomyces cerevisiae* mutants impaired in glycerol synthesis. *Yeast* **16,** 463-474.

Nissen, T. L., Kielland-Brandt, M. C., Nielsen, J., Villadsen, J., (2000b). Optimization of ethanol production in Saccharomyces cerevisiae by metabolic engineering of the ammonium assimilation. *Metabolic engineering* **2** (1)**,** 69-77.

Nissen, T. L., Schulze, U., Nielsen, J., Villadsen, J., (1997). Flux distributions in anaerobic, glucose-limited continuous cultures of *Saccharomyces cerevisiae*. *Microbiology* **143,** 203-21 8.

Nogae, I., Johnston, M., (1990). Isolation and characterisation of the *ZWF1* gene of *Saccharomyces cerevisiae,* encoding glucose-6-phosphate dehydrogenase. *Gene* **96,** 161-169.

Nogueira, K. M. V., Mendes, V., Carraro, C. B., Taveira, I. C., Oshiquiri, L. H., Gupta, V. K., Silva, R. N., (2020). Sugar transporters from industrial fungi: Key to improving second-generation ethanol production. *Renewable and Sustainable Energy Reviews* **131** (109991).

Norbeck, J., Påhlman, A.-K., Akhtar, N., Blomberg, A., Adler, L., (1996). Purification and Characterization of Two Isoenzymes of DL-Glycerol-3-phosphatase from *Saccharomyces cerevisiae*. *Journal of Biological Chemistry* **271** (23)**,** 13875–13881.

Oud, B., van Maris, A. J. A., Daran, J.-M., Pronk, J. T., (2011). Genome-wide analytical approaches for reverse metabolic engineering of industrially relevant phenotypes in yeast. *FEMS Yeast Research* **12** (2)**,** 183–196.

Overkamp, K. M., Kötter, P., van der Hoek, R., Schoondermark-Stolk, S., Luttik, M. A. H., van Dijken, J. P., Pronk, J. T., (2002). Functional analysis of structural genes for NAD$^+$-dependent formate dehydrogenase in *Saccharomyces cerevisiae*. *Yeast* **19,** 509–520.

Özcan, S., Johnston, M., (1995). Three different regulatory mechanisms enable yeast hexose transporter (*HXT*) genes to be induced by different levels of glucose. *Molecular and Cellular Biology* **15** (3)**,** 1564–1572.

Paalme, T., Vilu, R., (1992). A new method of continuous cultivation with computer-controlled change of dilution rate. *IFAC Proceedings Volumes* **25** (2)**,** 299-301.

Packer, M. S., Liu, D. R., (2015). Methods for the directed evolution of proteins. *Nature Reviews Genetics* **16,** 379–394.

Paiva, S., Devaux, F., Barbosa, S., Jacq, C., Casal, M., (2004). Ady2p is essential for the acetate permease activity in the yeast *Saccharomyces cerevisiae*. *Yeast* **21,** 201-210.

Palková, Z., Devaux, F., Řičicová, M., Mináriková, L., Le Crom, S., Jacq, C., (2002). Ammonia pulses and metabolic oscillations guide yeast colony development. *Molecular Biology of the Cell* **13,** 3901–3914.

Pao, S. S., Paulsen, I. T., Saier, M. H. J., (1998). Major Facilitator Superfamily. *Microbiology and Molecular Biology Reviews* **62** (1)**,** 1-34.

Papapetridis, I., Goudriaan, M., Vázques Vitali, M., de Keijzer, N. A., Van den Broek, M., van Maris, A. J. A., Pronk, J. T., (2018). Optimizing anaerobic growth rate and fermentation kinetics in *Saccharomyces cerevisiae* strains expressing Calvin-cycle enzymes for improved ethanol yield. *Biotechnology for Biofuels* **11** (17).

Papapetridis, I., van Dijk, M., Dobbe, A. P., Metz, B., Pronk, J. T., van Maris, A. J., (2016). Improving ethanol yield in acetate-reducing *Saccharomyces cerevisiae* by cofactor engineering of 6-phosphogluconate dehydrogenase and deletion of *ALD6*. *Microbial cell factories* **15** (1), 1-16.

Papapetridis, I., van Dijk, M., van Maris, A. J., Pronk, J. T., (2017). Metabolic engineering strategies for optimizing acetate reduction, ethanol yield and osmotolerance in *Saccharomyces cerevisiae*. *Biotechnology for biofuels* **10** (1)**,** 107.

Parisutham, V., Chandran, S.-P., Mukhopadhyay, A., Lee, S. K., Keasling, J. D., (2017). Intracellular cellobiose metabolism and its applications in lignocellulose-based biorefineries. *Bioresource Technology* **239,** 496-506.

Pasteur, L., (1857). Mémoire sur la fermentation alcoolique. *Comptes Rendus Chimie* **45,** 1032-1036.

Pasteur, L., (1860). Mémoire sur la fermentation alcoolique. *Annales de chimie et de physique* **58,** 323-426.

Paulsen, I. T., Sliwinski, M. K., Nelissen, B., Goffeau, A., Saier, M. H. J., (1998a). Unified inventory of established and putative transporters encoded within the complete genome of *Saccharomyces cerevisiae*. *FEBS Letters* **430,** 116-125.

Paulsen, I. T., Sliwinski, M. K., Saier, M. H. J., (1998b). Microbial genome analyses: Global comparisons of transport capabilities based on phylogenies, bioenergetics and substrate specificities. *Journal of Molecular Biology* **277** (3)**,** 573-592.

Paulsen, P. A., Custódio, T. F., Pedersen, B. P., (2019). Crystal structure of the plant symporter STP10 illuminates sugar uptake mechanism in monosaccharide transporter superfamily. *Nature Communications* **10** (407).

Pazdernik, N. J., Cain, S. M., Brooker, R. J., (1997). An analysis of suppressor mutations suggests that the two halves of the lactose permease function in a symmetrical manner. *Journal of Biological Chemistry* **272** (42)**,** 26110-26116.

Perli, T., Vos, A. M., Bouwknegt, J., Dekker, W. J. C., Wiersma, S. J., Mooiman, C., Ortiz-Merino, R. A., Daran, J.-M., Pronk, J. T., (2021). Identification of oxygen-independent pathways for pyridine nucleotide and coenzyme A synthesis in anaerobic fungi by expression of candidate genes in yeast. *mBio* **12** (3).

Perli, T., Wronska, A. K., Ortiz-Merino, R. A., Pronk, J. T., Daran, J. M., (2020). Vitamin requirements and biosynthesis in *Saccharomyces cerevisiae*. *Yeast* **37,** 283-304.

Persson, B. L., Lagerstedt, J. O., Pratt, J. R., Pattison-Granberg, J., Lundh, K., Shokrollahzadeh, S., Lundh, F., (2003). Regulation of phosphate acquisition in *Saccharomyces cerevisiae*. *Current Genetics* **43,** 225–244.

Petterson, N., Hagström, J., Bill, R. M., Hohmann, S., (2006). Expression of heterologous aquaporins for functional analysis in *Saccharomyces cerevisiae*. *Current Genetics* **50,** 247–255.

Pfromm, P. H., Amanor-Boadu, V., Nelson, R., Vadlani, P., Madl, R., (2010). Bio-butanol vs. bio-ethanol: A technical and economic assessment for corn and switchgrass fermented by yeast or *Clostridium acetobutylicum*. *Biomass and Bioenergy* **34,** 515-524.

Pi, J., Chow, H., Pittard, A. J., (2002). Study of second-site suppression in the *pheP* gene for the phenylalanine transporter of *Escherichia coli*. *Journal of Bacteriology* **184** (21), 5842-5847.

Pinheiro, C., Longatto-Filho, A., Azevedo-Silva, J., Casal, M., Schmitt, F., Baltazar, F., (2012). Role of monocarboxylate transporters in human cancers: state of the art. *Journal of Bioenergetics and Biomembranes* **44,** 127–139.

Pirt, S. J., (1965). The maintenance energy of bacteria in growing cultures. *Proceedings of the Royal Society of London. Series B.* **163** (991), 224-231.

Piškur, J., Langkjær, R. B., (2004). Yeast genome sequencing: the power of comparative genomics. *Molecular Microbiology* **53** (2)**,** 381–389.

Pohorille, A., Schweighofer, K., Wilson, M. A., (2005). The origin and early evolution of membrane channels. *Astrobiology* **5** (1)**,** 1-17.

Postma, E., Scheffers, W. A., Van Dijken, J. P., (1988). Adaptation of the Kinetics of Glucose Transport to Environmental Conditions in the Yeast *Candida utilis* CBS 621: a Continuous-culture Study. *Journal of General Microbiology* **134,** 1109-1116.

Postma, E., Scheffers, W. A., Van Dijken, J. P., (1989). Kinetics of growth and glucose transport in glucose-limited chemostat cultures of *Saccharomyces cerevisiae* CBS 8066. *Yeast* **5** (3)**,** 159-165.

Postma, E. D., Dashko, S., van Breemen, L., Taylor Parkins, S. K., van den Broek, M., Daran, J. M., Daran-Lapujade, P., (2021). A supernumerary designer chromosome for modular *in vivo* pathway assembly in *Saccharomyces cerevisiae*. *Nucleic Acids Research* **49** (3)**,** 1769–1783.

Postma, E. P., Verduyn, C., Kuiper, K., Scheffers, W. A., Van Dijken, J. P., (1990). Substrate-accelerated death of *Saccharornyces cerevisiae* CBS 8066 under maltose stress. *Yeast* **6** (2)**,** 149-158.

Pronk, J. T., (2002). Auxotrophic yeast strains in fundamental and applied research. *Applied and Environmental Microbiology* **68** (5)**,** 2095-2100.

Pronk, J. T., Wenzel, T. J., Luttik, M. A., Klaassen, C. C. M., Scheffers, W. A., Steensma, H. Y., van Dijken, J. P., (1994). Energetic aspects of glucose metabolism in a pyruvate-dehydrogenase-negative mutant of *Saccharomyces cerevisiae*. *Microbiology* **140,** 601-610.

Qui, B., Xia, B., Zhou, Q., Lu, Y., He, M., Hasegawa, K., Ma, Z., Zhang, F., Gu, L., Mao, Q., Wang, F., Zhao, S., Gao, Z., Liao, J., (2018). Succinate-acetate permease from *Citrobacter koseri* is an anion channel that unidirectionally translocates acetate. *Cell Research* **28,** 644–654.

Quistgaard, E. M., Löw, C., Guettou, F., Nordlund, P., (2016). Understanding transport by the major facilitator superfamily (MFS): structures pave the way. *Nature Reviews Molecular Cell Biology* **17** (123-132).

Rabitsch, K. P., Tóth, A., Gálová, M., Schleiffer, A., Schaffner, G., Aigner, E., Rupp, C., Penkner, A. M., Moreno-Borchart, A. C., Primig, M., Esposito, R. E., Klein, F., Knop, M., Nasmyth, K., (2001). A screen for genes required for meiosis and spore formation based on whole-genome expression. *Current Biology* **11** (13)**,** 1001-1009.

Radecka, D., Mukherjee, V., Quintilla Mateo, R., Stojiljkovic, M., Foulquié-Moreno, M. R., Thevelein, J. M., (2015). Looking beyond *Saccharomyces*: the potential of non-conventional yeast species for desirable traits in bioethanol fermentation. *FEMS Yeast Research* **15,** 6.

Radler, F., Schütz, H., (1982). Glycerol production of various strains of *Saccharomyces*. *American Journal of Enology and Viticulture* **33** (1)**,** 36-40.

Rasmussen, M. L., Koziel, J. A., Jane, J.-L., Pometto, A. L., (2015). Reducing bacterial contamination in fuel ethanol fermentations by ozone treatment of uncooked corn mash. *Journal of Agricultural and Food Chemistry* **63** (21)**,** 5239-5248.

Regenberg, B., Düring-Olsen, L., Kielland-Brandt, M. C., Holmberg, S., (1999). Substrate specificity and gene expression of the amino-acid permeases in *Saccharomyces cerevisiae*. *Current Genetics* **36,** 317-328.

Regueira, A., Lema, J. M., Mauricio-Iglesias, M., (2021). Microbial inefficient substrate use through the perspective of resource allocation models. *Current Opinion in Biotechnology* **67,** 130-140.

Reifenberger, E., Boles, E., Ciriacy, M., (2004). Kinetic characterization of individual hexose transporters of *Saccharomyces cerevisiae* and their relation to the triggering mechanisms of glucose repression. *European Journal for Biochemistry* **245,** 324-333.

Remize, F., Barnavon, L., Dequin, S., (2001). Glycerol export and glycerol-3-phosphate dehydrogenase, but not glycerol phosphatase, are rate limiting for glycerol production in *Saccharomyces cerevisiae*. *Metabolic Engineering* **3,** 301–312.

Renewable Fuels Association, Annual Ethanol Production. Vol. 2021, 2021.

Reznicek, O., Facey, S. J., de Waal, P. P., Teunissen, A. W. R. H., de Bont, J. A. M., Nijland, J. G., Driessen, A. J. M., Hauer, B., (2015). Improved xylose uptake in *Saccharomyces cerevisiae* due to directed evolution of galactose permease Gal2 for sugar co-consumption. *Journal of Applied Microbiology* **119,** 99-111.

Ribas, D., Sá-Pessoa, J., Soarez-Silva, I., Paiva, S., Nygård, Y., Ruohonen, L., Penttilä, M., Casal, M., (2017). Yeast as a tool to express sugar acid transporters with biotechnological interest. *FEMS Yeast Research* **17**.

Ribas, D., Soares-Silva, I., Vieira, D., Sousa-Silva, M., Sá-Pessoa, J., Azevedo-Silva, J., Viegas, S. C., Arraiano, C. M., Diallinas, G., Paiva, S., Soares, P., Casal, M., (2019). The acetate uptake transporter family motif "NPAPLGL(M/S)" is essential for substrate uptake. *Fungal Genetics and Biology* **122,** 1-10.

Riesmeier, J. W., Willmitzer, L., Frommer, W. B., (1992). Isolation and characterization of a sucrose carrier cDNA from spinach by functional expression in yeast. *The EMBO Journal* **11** (13)**,** 4705-4713.

Roca, C., Nielsen, J., Olsson, L., (2003). Metabolic engineering of ammonium assimilation in xylose-fermenting *Saccharomyces cerevisiae* improves ethanol production. *Applied and environmental microbiology* **69** (8)**,** 4732-

4736.

Roels, J. A., (1980). A simple model for the energetics of growth on substrates with different degrees of reduction. *Biotechnology and Bioengineering* **22,** 33-53.

Rogers, D. T., Szostak, J. W., Strains of yeast with increased rates of glycolysis. Vol. US 005268285A. Genetics Institute, Inc., 1993.

Rogers, P. L., Lee, K. J., Tribe, D. E., (1979). Kinetics of alcohol production by *Zymomonas mobilis* at high sugar concentrations. *Biotechnology Letters* **1** (4)**,** 165-170.

Rosa, M. F., Sá-Correia, I., (1991). *In vivo* activation by ethanol of plasma membrane ATPase of *Saccharomyces cerevisiae*. *Applied and Environmental Microbiology* **57** (3)**,** 830-835.

Ruchala, J., Kurylenko, O. O., Dmytruk, K. V., Sibirny, A. A., (2020). Construction of advanced producers of first- and second-generation ethanol in *Saccharomyces cerevisiae* and selected species of non-conventional yeasts (*Scheffersomyces stipitis*, *Ogataea polymorpha*). *Journal of Industrial Microbiology & Biotechnology* **47,** 109–132.

Russel, I., 2003. Yeast and management of fermentation. In: Jacques, K. A., Lyons, T. P., Kelsall, D. R., Eds.), The Alcohol Textbook. Nottingham University Press, Nottingham.

Russell, I., 2003. Understanding yeast fundamentals. In: Jacques, K. A., Lyons, T. P., Kelsall, D. R., Eds.), The Alcohol Textbook. Nottingham University Press, Nottingham, pp. 85-120.

Russell, J. B., Cook, G. M., (1995). Energetics of bacterial growth: Balance of anabolic and catabolic reactions. *Microbiological Reviews* **59** (1)**,** 48-62.

Sadie, C. J., Rose, S. H., den Haan, R., van Zyl, W. H., (2011). Co-expression of a cellobiose phosphorylase and lactose permease enables intracellular cellobiose utilisation by *Saccharomyces cerevisiae*. *Applied Microbiology and Biotechnology* **90,** 1373-1380.

Saier, M. H. J., (2001). Evolution of transport proteins. *Genetic Engineering* **23,** 1-10.

Saier, M. H. J., (2003). Tracing pathways of transport protein evolution. *Molecular Microbiology* **48** (5)**,** 1145–1156.

Saier, M. H. J., (2016). Transport protein evolution deduced from analysis of sequence, topology and structure. *Current Opinion in Structural Biology* **38,** 9–17.

Salazar, A. N., Gorter de Vries, A. R., van den Broek, M., Wijsman, M., de la Torre Cortéz, P., Brickwedde, A., Brouwers, N., Daran, J.-M. G., Abeel, T., (2017). Nanopore sequencing enables near-complete de novo assembly of *Saccharomyces cerevisiae* reference strain CEN.PK113-7D. *FEMS Yeast Research* **17,** 1-11.

Samyn, D. R., Persson, B. L., 2016. Inorganic phosphate and sulfate transport in *S. cerevisiae*. In: Ramos, J., Sychrová, H., Kschischo, M., Eds.), Yeast membrane transport. Advances in experimental medicine and biology. vol. 892. Springer International Publishing, Springer Cham Heidelberg New York Dordrecht London, pp. 253-269.

Sánchez, B. J., Nielsen, J., (2015). Genome scale models of yeast: towards standardized evaluation and consistent omic integration. *Integrative Biology* **7,** 846-858.

Sánchez, B. J., Zhang, C., Nilsson, A., Lahtvee, P.-J., Kerkhoven, E. J., Nielsen, J., (2017). Improving the phenotype predictions of a yeast genome-scale metabolic model by incorporating enzymatic constraints. *Molecular Systems Biology* **13** (935).

Sanchez, R. G., Karhumaa, K., Fonseca, C., Nogué, V. S., Almeida, J. R. M., Larsson, C. U., Bengtsson, O., Bettiga, M., Hahn-Hägerdal, B., Gorwa-Grauslund, M., (2010). Improved xylose and arabinose utilization by an industrial recombinant *Saccharomyces cerevisiae* strain using evolutionary engineering. *Biotechnology for Biofuels* **3** (13).

Sandberg, T. E., Salazar, M. J., Weng, L. L., Palsson, B. O., Feist, A. M., (2019). The emergence of adaptive laboratory evolution as an efficient tool for biological discovery and industrial biotechnology. *Metabolic Engineering* **56,** 1-16.

Santos, E., Rodriguez, L., Elorza, M. V., Sentandreu, R., (1982). Uptake of sucrose by *Saccharomyces cerevisiae*. *Archives of biochemistry and biophysics* **216** (2)**,** 652-660.

Santos, J., Sousa, M. J., Cardoso, H., Inácio, J., Silva, S., Spencer-Martins, I., Leão, C., (2008). Ethanol tolerance of sugar transport, and the rectification of stuck wine fermentations. *Microbiology* **154,** 422–430.

Saraceni-Richards, C. A., Levy, S. B., (2000). Second-Site Suppressor Mutations of Inactivating Substitutions at Gly247 of the Tetracycline Efflux Protein, Tet(B). *Journal of Bacteriology* **182** (22)**,** 6514-6516.

Schmidl, S., Iancu, C. V., Reifenrath, M., Choe, J.-y., Oreb, M., (2021). A label-free real-time method for measuring glucose uptake kinetics in yeast. *FEMS Yeast Research* **21** (1).

Semkiv, M. V., Dmytruk, K. V., Abbas, C. A., Sibirny, A. A., (2014). Increased ethanol accumulation from glucose via reduction of ATP level in a recombinant strain of *Saccharomyces cerevisiae* overexpressing alkaline phosphatase. *BMC Biotechnology* **14** (42).

Semkiv, M. V., Dmytruk, K. V., Abbas, C. A., Sibirny, A. A., (2016). Activation of futile cycles as an approach to increase ethanol yield during glucose fermentation in *Saccharomyces cerevisiae*. *Bioengineered* **7** (2)**,** 106-111.

Serrano, R., (1977). Energy requirements for maltose transport in yeast. *European Journal of Biochemistry* **80,** 97-102.

Sheth, K., Alexander, J. K., (1967). Cellodextrin phosphorylase from *Clostridium thermocellum*. *Biochimica et Biophysica Acta* **148** (3)**,** 808-810.

Shi, S., Choi, Y. W., Zhao, H., Tan, M. H., Ang, E. L., (2017). Discovery and engineering of a 1-butanol biosensor in *Saccharomyces cerevisiae*. *Bioresource Technology* **245,** 1343–1351.

Shi, Y., (2013). Common folds and transport mechanisms of secondary active transporters. *Annual Reviews of Biophysics* **42,** 51-72.

Sikorski, R. S., Hieter, P., (1989). A system of shuttle vectors and yeast host strains designed for efficient manipulation of DNA in *Saccharomyces cerevisiae*. *Genetics* **122** (1)**,** 19-27.

Singhvi, M., Zendo, T., Sonomoto, K., (2018). Free lactic acid production under acidic conditions by lactic acid bacteria strains: challenges and future prospects. *Applied Microbiology and Biotechnology* **102,** 5911–5924.

Sloothaak, J., Tamayo-Ramos, J. A., Odoni, D. I., Laothanachareon, T., Derntl, C., Mach-Aigner, A. R., Martins dos Santos, V. A. P., Schaap, P. J., (2016). Identification and functional characterization of novel xylose transporters from the cell factories *Aspergillus niger* and *Trichoderma reesei*. *Biotechnology for Biofuels* **9** (148).

Smits, H.-P., Smits, G. J., Postma, P. W., Walsh, M. C., van Dam, K., (1996). High-affinity glucose uptake in *Saccharomyces cerevisiae* is not dependent on the presence of glucose-phosphorylating enzymes. *Yeast* **12,** 439-447.

Snoek, I. S. I., Steensma, H. Y., (2006). Why does *Kluyveromyces lactis* not grow under anaerobic conditions? Comparison of essential anaerobic genes of *Saccharomycescerevisiae* with the *Kluyveromyces lactis* genome. *FEMS Yeast Research* **6,** 393–403.

Snoek, I. S. I., Steensma, H. Y., (2007). Factors involved in anaerobic growth of *Saccharomyces cerevisiae*. *Yeast* **24,** 1-10.

Soares-Silva, I., Ribas, D., Sousa-Silva, M., Azevedo-Silva, J., Rendulić, T., Casal, M., (2020). Membrane transporters in the bioproduction of organic acids: state of the art and future perspectives for industrial applications. *FEMS Microbiology Letters* **367** (15).

Sonderegger, M., Schümperli, M., Sauer, U., (2004). Metabolic engineering of a phosphoketolase pathway for pentose catabolism in *Saccharomyces cerevisiae*. *Applied and environmental microbiology* **70** (5)**,** 2892-2897.

Stambuk, B. U., Batista, A. S., de Araujo, P. S., (2000). Kinetics of active sucrose transport in *Saccharomyces cerevisiae*. *Journal of Bioscience and Bioengineering* **89** (2)**,** 212-214.

Stambuk, B. U., da Silva, M. A., Panek, A. D., de Araujo, P. S., (1999). Active α-glucoside transport in *Saccharomyces cerevisiae*. *FEMS Microbiology Letters* **170,** 105-110.

Stambuk, B. U., de Araujo, P. S., (2001). Kinetics of active α-glucoside transport in *Saccharomyces cerevisiae*. *FEMS Yeast Research* **1** (1)**,** 73-78.

Stambuk, B. U., de Araujo, P. S., Panek, A. D., Serrano, A., (1996). Kinetics and energetics of trehalose transport in *Saccharomyces cerevisiae*. *European Journal for Biochemistry* **237,** 876-881.

Steels, E. L., Learmonth, R. P., Watson, K., (1994). Stress tolerance and membrane lipid unsaturation in *Saccharomyces cerevisiae* grown aerobically or anaerobically. *Microbiology* **140,** 569-576.

Sterling, T., Irwin, J. J., (2015). ZINC 15 – Ligand discovery for everyone. *Journal of Chemical Information and Modeling* **55** (11)**,** 2324-2337.

Stouthamer, A. H., (1973). A theoretical study on the amount of ATP required for synthesis of microbial cell material. *Antonie van Leeuwenhoek* **39,** 545-565.

Subtil, T., Boles, E., (2011). Improving L-arabinose utilization of pentose fermenting *Saccharomyces cerevisiae* cells by

heterologous expression of L-arabinose transporting sugar transporters. *Biotechnology for Biofuels* **4** (38).

Suzuki, Y., St Onge, R. P., Mani, R., King, O. D., Heilbut, A., Labunskyy, V. M., Chen, W., Pham, L., Zhang, L. V., Tong, A. H. Y., Nislow, C., Giaever, G., Gladyshev, V. N., Vidal, M., Schow, P., Lehár, J., Roth, F. P., (2011). Knocking out multigene redundancies via cycles of sexual assortment and fluorescence selection. *Nature Methods* **8** (2), 159–164.

Swanson, W. H., Clifton, C. E., (1948). Growth and assimilation in cultures of *Saccharomyces cerevisiae*. *Journal of Bacteriology* **56** (1), 115-124.

Taherzadeh, M. J., Niklasson, C., Lidén, G., (1997). Acetic acid - friend or foe in anaerobic batch conversion of glucose to ethanol by *Saccharomyces cerevisiae*? *Chemical Engineering Science* **52** (15), 2653 2659.

Tännler, S., Decasper, S., Sauer, U., (2008). Maintenance metabolism and carbon fluxes in *Bacillus* species. *Microbial Cell Factories* **7** (19).

Thomas, K. C., Ingledew, W. M., (1992). Production of 21% (v/v) ethanol by fermentation of very high gravity (VHG) wheat mashes. *Journal of Industrial Microbiology* **10,** 61-68.

Tiukova, I. A., Eberhard, T., Passoth, V., (2014). Interaction of *Lactobacillus vini* with the ethanol-producing yeasts *Dekkera bruxellensis* and *Saccharomyces cerevisiae*. *Biotechnology and Applied Biochemistry* **61** (1), 40-44.

Tiukova, I. A., Møller-Hansen, I., Belew, Z. M., Darbani, B., Boles, E., Nour-Eldin, H. H., Linder, T., Nielsen, J., Borodina, I., (2019). Identification and characterisation of two high-affinity glucose transporters from the spoilage yeast *Brettanomyces bruxellensis*. *FEMS Microbiology Letters* **366** (17).

Trott, O., Olson, A. J., (2010). AutoDock Vina: Improving the speed and accuracy of docking with a new scoring function, efficient optimization, and multithreading. **31** (2), 455-461.

Uchida, E., Ohsumi, Y. T., Anraku, Y., (1988). Purification of yeast vacuolar membrane H$^+$-ATPase and enzymological discrimination of three ATP-driven proton pumps in *Saccharomyces cerevisiae*. *Methods in Enzymology* **157,** 544-562.

Ulbricht, R. J., Northup, S. J., Thomas, J. A., (1984). A review of 5-Hydroxymethylfurfural (HMF) in parental solutions. *Fundamental and Applied Toxicology* **4,** 843-853.

van Aalst, A. C. A., de Valk, S. C., van Gulik, W. M., Jansen, M. L. A., Pronk, J. T., Mans, R., (2022). Pathway engineering strategies for improved product yield in yeast-based industrial ethanol production. *Synthetic and Systems Biotechnology* **7,** 554-566.

van Bodegom, P., (2007). Microbial maintenance: A critical review on its quantification. *Microbial Ecology* **53,** 513-523.

van den Berg, M. A., de Jong-Gubbels, P., Kortland, C. J., van Dijken, J. P., Pronk, J. T., Steensma, H. Y., (1996). The two acetyl-coenzyme A synthetases of *Saccharomyces cerevisiae* differ with respect to kinetic properties and transcriptional regulation. *The Journal of Biological Chemistry* **271** (46), 28953–28959.

van den Broek, M., Bolat, I., Nijkamp, J. F., Ramos, E., Luttik, M. A. H., Koopman, F., Geertman, J.-M., de Ridder, D., Pronk, J. T., Daran, J.-M., (2015). Chromosomal copy number variation in *Saccharomyces pastorianus* is evidence for extensive genome dynamics in industrial lager brewing strains. *Applied and Environmental Microbiology* **81** (18), 6253-6267.

van der Rest, M. E., Kamminga, A. H., Nakano, A., Anraku, Y., Poolman, B., Konings, W. N., (1995). The plasma membrane of *Saccharomyces cerevisiae*: Structure, function, and biogenesis. *Microbiological Reviews* **59** (2), 304–322.

van Dijken, J. P., Scheffers, W. A., (1986). Redox balances in the metabolism of sugars by yeasts. *FEMS Microbiology Reviews* **32,** 199-224.

Van Leeuwen, C. C. M., Weusthuis, R. A., Postma, E., Van den Broek, P. J. A., Van Dijken, J. P., (1992). Maltose/proton co-transport in *Saccharomyces cerevisiae*. Comparative study with cells and plasma membrane vesicles. *Biochemical Journal* **284** (2), 441-445.

van Maris, A. J. A., Winkler, A. A., Porro, D., van Dijken, J. P., Pronk, J. T., (2004). Homofermentative lactate production cannot sustain anaerobic growth of engineered *Saccharomyces cerevisiae*: Possible consequence of energy-dependent lactate export. *Applied and Environmental Microbiology* **70** (5), 2898-2905.

van Rossum, H. M., Kozak, B. U., Pronk, J. T., van Maris, A. J. A., (2016). Engineering cytosolic acetyl-coenzyme A supply in *Saccharomyces cerevisiae*: Pathway stoichiometry, free-energy conservation and redox-cofactor balancing. *Metabolic Engineering* **36,** 99-115.

van Tatenhove-Pel, R. J., Zwering, E., Boreel, D. F., Falk, M., van Heerden, J. H., Kes, M. B. M. J., Kranenburg, C. I., Botman,

D., Teusink, B., Bachmann, H., (2021). Serial propagation in water-in-oil emulsions selects for *Saccharomyces cerevisiae* strains with a reduced cell size or an increased biomass yield on glucose. *Metabolic Engineering* **64,** 1-14.

van Urk, H., Postma, E., Scheffers, W. A., van Dijken, J. P., (1989). Glucose transport in Crabtree-positive and Crabtree-negative yeasts. *Journal of General Microbiology* **135,** 2399-2406.

Vanrolleghem, P. A., de Jong-Gubbels, P., van Gulik, W. M., Pronk, J. T., van Dijken, J. P., Heijnen, J. J., (1996). Validation of a metabolic network for *Saccharomyces cerevisiae* using mixed substrate studies. *Biotechnology Progress* **12,** 434-448.

Varela, J. A., Puricelli, M., Montini, N., Morrissey, J. P., (2019). Expansion and diversification of MFS transporters in *Kluyveromyces marxianus*. *Frontiers in Microbiology* **9**.

Verduyn, C., Postma, E., Scheffers, W. A., van Dijken, J. P., (1990a). Energetics of *Saccharomyces cerevisiae* in anaerobic glucose-limited chemostat cultures. *Journal of General Microbiology* **136,** 405-412.

Verduyn, C., Postma, E., Scheffers, W. A., van Dijken, J. P., (1990b). Physiology of *Saccharomyces cerevisiae* in anaerobic glucose-limited chemostat cultures. *Journal of General Microbiology* **136,** 395-403.

Verduyn, C., Postma, E., Scheffers, W. A., van Dijken, J. P., (1992). Effect of benzoic acid on metabolic fluxes in yeasts: A continuous-culture study on the regulation of respiration and alcoholic fermentation. *Yeast* **8,** 501-517.

Verduyn, C., Stouthamer, A. H., Scheffers, W. A., van Dijken, J. P., (1991). A theoretical evaluation of growth yields of yeasts. *Antonie van Leeuwenhoek* **59,** 49-63.

Verhoeven, M. D., Bracher, J. M., Nijland, J. G., Bouwknegt, J., Daran, J.-M. G., Driessen, A. J. M., van Maris, A. J. A., Pronk, J. T., (2018). Laboratory evolution of a glucose-phosphorylation deficient, arabinose-fermenting *S. cerevisiae* strain reveals mutations in *GAL2* that enable glucose-insensitive l-arabinose uptake. *FEMS Yeast Research* **18** (6).

Viegas, C. A., Sá-Correia, I., (1991). Activation of plasma membrane ATPase of *Saccharomyces cerevisiae* by octanoic acid. *Journal of General Microbiology* **137,** 645-651.

von Heijne, G., (2006). Membrane-protein topology. *Nature Reviews Molecular Cell Biology* **7,** 909–918.

Voordeckers, K., Verstrepen, K. J., (2011). Experimental evolution of the model eukaryote *Saccharomyces cerevisiae* yields insight into the molecular mechanisms underlying adaptation. *Current Opinion in Microbiology* **28,** 1-9.

Vos, T., de la Torre Cortés, P., van Gulik, W. M., Pronk, J. T., Daran-Lapujade, P., (2015). Growth-rate dependency of de novo resveratrol production in chemostat cultures of an engineered *Saccharomyces cerevisiae* strain. *Microbial Cell Factories* **14** (133).

Walker, B. J., Abeel, T., Shea, T., Priest, M., Abouelliel, A., Sakthikumar, S., Cuomo, C. A., Zeng, Q., Wortman, J., Young, S. K., Earl, A. M., (2014). Pilon: An integrated tool for comprehensive microbial variant detection and genome assembly improvement. *PLoS ONE* **9** (11).

Wallin, E., von Heijne, G., (1998). Genome-wide analysis of integral membrane proteins from eubacterial, archaean, and eukaryotic organisms. *Protein Science* **7,** 1029-1038.

Wang, C., Shen, Y., Hou, J., Suo, F., Bao, X., (2013). An assay for functional xylose transporters in *Saccharomyces cerevisiae*. *Analytical Biochemistry* **442,** 241–248.

Weusthuis, R. A., Adams, H., Scheffers, W. A., van Dijken, J. P., (1993). Energetics and kinetics of maltose transport in *Saccharomyces cerevisiae*: a continuous culture study. *Applied and Environmental Microbiology* **59** (9)**,** 3102-3109.

Weusthuis, R. A., Pronk, J. T., Van den Broek, P. J. A., van Dijken, J. P., (1994). Chemostat Cultivation as a Tool for Studies on Sugar Transport in Yeasts. *Microbiological Reviews* **58** (4)**,** 616-630.

Wieczorke, R., Krampe, S., Weierstall, T., Kreidel, K., Hollenberg, C. P., Boles, E., (1999). Concurrent knock-out of at least 20 transporter genes is required to block uptake of hexoses in *Saccharomyces cerevisiae*. *FEBS letters* **464,** 123-128.

Wiersma, S. J., Mooiman, C., Giera, M., Pronk, J. T., (2020). Squalene-tetrahymanol cyclase expression enables sterol independent growth of *Saccharomyces cerevisiae*. *Applied and Environmental Microbiology* **86** (17).

Wijsman, M., Swiat, M. A., Marques, W. L., Hettinga, J. K., van den Broek, M., de la Torre Cortéz, P., Mans, R., Pronk, J. T., Daran, J.-M., Daran-Lapujade, P., (2018). A toolkit for rapid CRISPR-*Sp*Cas9 assisted construction of hexose-transport-deficient *Saccharomyces cerevisiae* strains. *FEMS Yeast Research*.

Winge, O., Roberts, C., (1952). The relation between the polymeric genes for maltose raffinose, and sucrose fermentation in yeasts. *Comptes rendus des travaux du Laboratoire Carlsberg. Serie physiologique* **25** (2)**,** 141-171.

Wisedchaisri, G., Park, M.-S., Iadanza, M. G., Zheng, H., Gonen, T., (2014). Proton-coupled sugar transport in the prototypical major facilitator superfamily protein XylE. *Nature Communications* **5** (4521).

Wronska, A. K., van den Broek, M., Perli, T., de Hulster, E., Pronk, J. T., Daran, J. M., (2021). Engineering oxygen-independent biotin biosynthesis in *Saccharomyces cerevisiae*. *Metabolic Engineering* **67,** 88-103.

Wu, X., Staggenborg, S., Propheter, J. L., Rooney, W. L., Yu, J., Wang, D., (2010). Features of sweet sorghum juice and their performance in ethanol fermentation. *Industrial Crops and Products* **31,** 164–170.

Xia, P.-F., Zhang, G.-C., Walker, B., Seo, S.-O., Kwak, S., Liu, J.-J., Kim, H., Ort, D. R., Wang, S.-G., Jin, Y.-S., (2017). Recycling carbon dioxide during xylose fermentation by engineered *Saccharomyces cerevisiae*. *ACS synthetic biology* **6** (2)**,** 276-283.

Xu, G., Zou, W., Chen, X., Xu, N., Liu, L., Chen, J., (2012). Fumaric Acid Production in *Saccharomyces cerevisiae* by *In Silico* Aided Metabolic Engineering. *PLoS One* **7** (12).

Yan, N., (2015). Structural biology of the Major Facilitator Superfamily transporters. *Annual Reviews of Biophysics* **44** (1)**,** 257-283.

Yeagle, P. L., 2016. The membranes of cells. Elsevier Academic Press.

Yenush, L., 2016. Potassium and sodium transport in yeast. In: Ramos, J., Sychrová, H., Kschischo, M., Eds.), Yeast membrane transport. Advances in experimental medicine and biology. vol. 892. Springer International Publishing, Springer Cham Heidelberg New York Dordrecht London, pp. 187-228.

Young, E., Poucher, A., Comer, A., Bailey, A., Alper, H., (2011). Functional survey for heterologous sugar transport proteins, using *Saccharomyces cerevisiae* as a host. *Applied and Environmental Microbiology* **77** (10)**,** 3311–3319.

Yu, A.-Q., Juwono, N. K. P., Foo, J. L., Leong, S. S. J., Chang, M. W., (2016). Metabolic engineering of *Saccharomyces cerevisiae* for the overproduction of short branched-chain fatty acids. *Metabolic Engineering* **34,** 36–43.

Yuen, C. M., Liu, D. R., (2007). Dissecting protein structure and function using directed evolution. *Nature Methods* **4** (12)**,** 995-997.

Zahoor, A., Messerschmidt, K., Boecker, S., Klamt, S., (2020). ATPase-based implementation of enforced ATP wasting in *Saccharomyces cerevisiae* for improved ethanol production. *Biotechnology for Biofuels* **13** (185).

Zelle, R. M., de Hulster, E., van Winden, W. A., de Waard, P., Dijkema, C., Winkler, A. A., Geertman, J.-M. A., Van Dijken, J. P., Pronk, J. T., van Maris, A. J. A., (2008). Malic acid production by *Saccharomyces cerevisiae*: Engineering of pyruvate carboxylation, oxaloacetate reduction, and malate export. *Applied and Environmental Microbiology* **74** (9)**,** 2766-2777.

Zhang, L., Tang, Y., Guo, Z.-p., Ding, Z.-y., Shi, G.-y., (2011). Improving the ethanol yield by reducing glycerol formation using cofactor regulation in *Saccharomyces cerevisiae*. *Biotechnology Letters* **33,** 1375–1380.

Zhang, W., Cao, Y., Gong, J., Bao, X., Chen, G., Liu, W., (2015). Identification of residues important for substrate uptake in a glucose transporter from the filamentous fungus *Trichoderma reesei*. *Scientific Reports* **5** (13829).

Zhou, Y., Qu, H., Dibley, K. E., Offler, C. E., Patrick, J. W., (2007). A suite of sucrose transporters expressed in coats of developing legume seeds includes novel pH-independent facilitators. *The Plant Journal* **49,** 750-764.

Acknowledgements

Even though a PhD project can be quite individual, especially those that are not part of a larger consortium like this one, I have had the opportunity to collaborate with and be surrounded by a lot of very nice, inspiring and supporting people.

First of all, many many many thanks to my daily supervisor Robert. You are probably one of the main reasons I enjoyed this four-year job as much as I did, it is a real pleasure to collaborate with you. You have always provided a great balance between independence and support, were open to questions, a spontaneous sparring session or bad word jokes. I remember when over four years ago, I was contemplating which PhD project to choose, and I was wondering whether your 'more limited' experience with supervising PhD students would be something to consider. Clearly I had nothing to worry about, I think you did (and are still doing) an absolutely excellent job as supervisor, even during your one-year adventure in Copenhagen. Apart from that, I consider you a great friend and I hope we can still have many 'dubbeldates' in the future. Jack, my second supervisor and promotor, thank you very much for your endless enthusiasm and involvement, even in the very busy position as head of the department. Not only did I enjoy our (sometimes rather spontaneous) meetings, I especially liked our teaching sessions of Biotechnologie to the first-year LST students, your engagement as teacher is truly inspiring.

Jean-Marc, as head of the IMB section you make such an important contribution to keep the organization which we work in up and running and you manage to make it a very stimulating working environment. Pascale, of course you also make a great contribution to this atmosphere. I was happy to witness your promotion to full professor, which is very well deserved. I hope to see many more of your magnificent Inktober drawings. Rinke, you joined our group fairly recently as a new PI (although time flies, I know) and I really enjoyed your presence in the Energetics meetings. You are very eager to think along in other projects and provide a refreshing point of view. I am very curious how your future work on microbial consortia is going to develop and look forward to read about it.

I also had the pleasure to collaborate with experts from other research groups and other Universities. Ryan and Bert, thank you for engaging me in the project on Mal11 mutants. You not only taught me a great deal about the fundamentals of transport protein structures, but also provided a refreshing style of scientific writing. I think we managed to make it into a great article! And even two years later, your work on binding of maltose to Mal11 appeared to be highly relevant to our most recent work, described in Chapter 6. Maria, Isabel and Margarida,

thank you for your insights and contributions to the characterization of Ato2 and Ato3. Your input added a lot more body to this story and was definitely insightful for us 'on the Delft side'. Mickel and Walter, thank you for your input for the review on bioethanol, on the industrial and modelling 'side', respectively. Your additions were essential to take this manuscript to the next level.

Contributions of the weekly 'Energetics' meetings to the working environment cannot be overlooked. Nicolò, you were always very engaged in other's projects and provided important insights, out of the box ideas and contributions ('It's D-lactate!!!!'). I really enjoyed working with you on the lactic acid transporters, for which we now share a Chapter in our theses. Also, thank you for all your jokes, memes, pranks and cryptic pop-quizzes. Aafke, for a while, we were partners in crime as the only PhD students in the Energetics meetings, where you usually made things interesting by presenting an impressive amount of results, due to your drive to run many experiments in the fermentation lab. Your enormous contributions on redox engineering in the bioethanol review were not only essential, but also a lot of fun 🐤 and I really enjoyed working with you. Also, thank you very much for all of your efforts as one of my paranymphs. Hannes, it has been a while since we last shared an energetics meeting, but in the early days of my PhD, it was really nice to have you in these meetings. You always had such a patient way of explaining and were super well-read on anything to do with respiration. Together with Nicolò and Robert, you formed a very nice team for me to join. Nowadays, Energetics has expanded with the participation of Marieke, who has a natural tendency to think along in other projects and organize nice teambuilding activities, and Sagarika, who is, after her contributions to my project as a master student, still happy to be engaged. Thanks a lot!

A PhD project at IMB is not complete without the contribution of many Bachelor and Master students. Chiel, Laura, Gijs, Susan, Marit, Sagarika, Isabel, Eline and Evi, thank you for your interest and contributions to my research. It was really nice to have you as sparring partners, and I hope your learned as much from me as I did from you. Koen, thank you for all your help and assistance with the experiments on metabolic flux analysis in Marit's project. Although this research line did not make it into a thesis chapter, we actually learned a lot, and who knows, it might still be worked out further in future research. Aljoscha, also thank you for your input and advice on this project.

Where would I have ever been without the technicians that enrich IMB? Erik, thank you so much for your efforts that keep the fermentation lab and its equipment in the exceptional state that it is in. It is really not trivial that complicated reactor experiments can be run as faithful as in our lab. You are somebody that is challenged by novel experiments and eager to think of solutions instead of problems. Additionally, you were a very nice office mate for a long time, and I enjoyed organizing the lab retreat of 2019 together with you and Eline. It is great that you so actively participate in any activity and therefore make a great contribution to the nice atmosphere at IMB. That actually also applies to Christiaan, who has been a great help in keeping the fermentation lab up and running, you helped me a lot with the Lucullus software, not to mention setting up the remote access for the computers in the fermentation lab. Saved me quite some weekend trips to the lab! Maria, thank you for keeping a sharp eye on my (sometimes long-running) reactors, your alertness has saved the fermentation lab from quite some floods! Marijke, although I was not a frequent visitor of your analysis lab, you have been an important influence during my time at IMB. You were always super encouraging when it comes to my interest in painting and illustrating, and the workshop you organized at the

atelier of Julia Woning sparked my first interest for watercolor. I am pretty sure your 'why not?!' attitude has sparked quite some IMB creative nights! (Which, by the way, I enjoyed a lot, also due to regular participation of Charlotte, Eline, Susan, Jonna, Nicolo, Erik, Francine, Jasmijn and Laura). Pilar, Agostina, Jordi and Clara, thank you for keeping the molecular biology lab up and running. Compared to some colleagues, I did not have the typical 'molecular biology project', but of course I could not do without. It is so nice that a lab with so many contents is so well organized. Marcel, thank you for helping me at all instances where I requested you to 'run the pipeline' and with answering genomics-related questions. I also very much enjoyed your workshop on genomic data carpentry. Jolanda, thanks a lot for helping me get started with the experimental side of my PhD in my first year, including my first chemostat experiments and evolutions in small-scale bioreactors. Ladies of MSD, Jannie, Astrid and Apilena, thank you so much for all your help, support and nice chats in the lab! I think you must have autoclaved a zillion reactors and medium vessels for me, and you were always ready to think along and be flexible with scheduling. Without you, I would probably have been able to do just half the experiments that I did. Erwin from the gas team, thank you for being flexible and thinking along in the (re)placement of all of the gas bottles. Your willingness to help when 'somebody' (ahem) had emptied the calibration gas has saved quite some reactor experiments.

Nicole, thank you for being my paranymph together with Aafke. You are a really fun and honest colleague to have, I enjoyed our coffee chats, organizing Sanne's cabaret as co-paranymphs and drinks. I hope you will soon be recovered from your ankle injury so we can start organizing the second edition of the IMB surf weekend! Ewout, Robert, Teun and Diederik, thanks for providing such a nice platform to complain about anything related to PhD projects. We had lot of fun (social!) evenings and (a) great trip(s) to Stockholm, which I still hope we can repeat sometime (maybe with another destination). Ewout, you were a great office mate to have in the final year, thanks for all the coffee breaks, quick fixes and (actual) scientific discussions. Sanne, we have been friends for quite some time now, and it was really nice to be able to extend our 'co-studentship' by becoming colleagues. It was nice to have you around at the coffee breaks, but even better to relax together during our face mask evenings, as well as during the LST-afhaker activities (thanks Perry, Wilson, Buijs and Kan as well). Xavier, you were a great dance partner during the earlier part of my PhD and it was way too bad that you moved to Germany. I definitely missed our weekly Eazie meals and lessons at Wesseling. Also, I had a lot of fun being you paranymph together with Jonna. Stefan and Marije, thank you for the lovely balloon, it really got me through the final days before the end of my contract :). All of the fun activities, fancy diners and awesome wintersports holidays were very welcome distractions from PhD life.

Mom, Dad and Kornelske, thank you for all your love, support, encouragement and advice during the entire education/career pathway that preceded the completion of this thesis. Although I must be hard to follow when I try to explain my daily activities, you always kept on showing interest and I always feel very warmly welcomed in Vlaardingen.

Job, you mean the world to me and there is absolutely no way imaginable that this thesis would have turned out the same way without your endless support. As your manager Matthijs already told you, a PhD project is really something you get through together, and I am happy to have shared it with you. Thank you for all the nutritious comfort meals you cooked, late night drives to the faculty, your listening ear, advice, jokes and everything else. I can't wait to move to our new house together, get married and live happily ever after :).

Curriculum vitae

Sophie de Valk was born on April 30th 1993 in Vlaardingen, the Netherlands. After graduating in 2011 from pre-university education (VWO+) at Scholengemeenschap Spieringshoek in Schiedam, she enrolled in the Life Science & Technology Bachelor's programme at Delft University of Technology (TU Delft) and Leiden University. Sophie finalized this three-year programme with a bachelor research project at the Industrial Microbiology Section at TU Delft under the supervision of dr. Tim Vos. This project involved the engineering of ethanol-repressible promoters in *Saccharomyces cerevisiae* strains. After spending one year as full-time president of the board of Study Association LIFE (study association for Life Science & Technology students), she enrolled in the Life Science & Technology Master's programme at TU Delft, with the specializations Cell Factory and Biochemical Engineering. Sophie performed her Master Research Project in the Industrial Microbiology Section, where she worked on synthetic consortia of *S. cerevisiae* strains for simultaneous fermentation of hexose and pentose sugars in mixed-sugar media, under the supervision of dr. Maarten Verhoeven and prof. Jack Pronk. She completed her Master's programme with a six-month industrial internship at DuPont Industrial Biosciences in Leiden under the supervision of dr. Barbara Kozak and Paulien Kruithof. In February 2018, Sophie started her PhD project in the Industrial Microbiology section at TU Delft under the supervision of Robert Mans. The results of this project, which was focussed on energy coupling of metabolite transport in *S. cerevisiae*, are described in this dissertation.

List of publications

Verhoeven M.D., **de Valk S.C.**, Daran J-M.G., van Maris A.J.A., Pronk J.T. (2018). Fermentation of glucose-xylose-arabinose mixtures by a synthetic consortium of single-fermenting *Saccharomyces cerevisiae* strains. *FEMS Yeast Research* **18**(8). DOI: 10.1093/femsyr/foy075.

Henderson R.K., **de Valk S.C.**, Poolman B., Mans R. (2021). Energy coupling of membrane transport and efficiency of sucrose dissimilation in yeast. *Metabolic Engineering* **65:** 243-254. DOI: 10.1016/j.ymben.2020.11.014.

Baldi N., **de Valk S.C.**, Sousa-Silva M., Casal M., Soares-Silva I., Mans R. (2021). Evolutionary engineering reveals amino acid substitutions in Ato2 and Ato3 that allow improved growth of *Saccharomyces cerevisiae* on lactic acid. *FEMS Yeast Research* **21**(4) DOI: 10.1093/femsyr/foab033.

van Aalst A.C.A., **de Valk S.C.**, van Gulik W.M., Jansen M.L.A., Pronk J.T., Mans R. (2022). Pathway engineering strategies for improved product yield in yeast-based industrial ethanol production. *Synthetic and Systems Biotechnology* **7**(1): 554-566. DOI: 10.1016/j.synbio.2021.12.010.

de Valk S.C., Bouwmeester S.E., de Hulster E., Mans R. (2022) Engineering proton-coupled hexose uptake in *Saccharomyces cerevisiae* for improved ethanol yield. *Biotechnology for Biofuels and Bioproducts* **15**:47. DOI: 10.1186/s13068-022-02145-7.

Malubhoy Z., Bahia F.M., **de Valk S.C.**, de Hulster E., Rendulić T., Ortiz J.P.R., Xiberras J., Klein M., Mans R., Nevoigt E. (2022). Carbon dioxide fixation via production of succinic acid from glycerol in engineered *Saccharomyces cerevisiae*. *Microbial Cell Factories* **21**.

de Valk S.C., Mans R. (2022). Novel evolutionary engineering approach to alter substrate specificity of disaccharide transporter Mal11 in *Saccharomyces cerevisiae*. *Journal of Fungi* **8**(4): 358. DOI: 10.3390/jof8040358.